Rotations tectoniques et déformation de l'avant-arc des Andes centrales au cours du Cénozoïque

César Arriagada

Nº Ordre : 2825
de la thèse

THÈSE/TESIS
présentée/presentada

DEVANT L'UNIVERSITÉ DE RENNES 1 et/y ANTE LA UNIVERSIDAD DE CHILE

pour obtenir/para obtener

le grade de : DOCTEUR DE L'UNIVERSITÉ DE RENNES 1
Mention : Sciences de la Terre
et/y
el grado de: DOCTOR EN CIENCIAS, MENCION GEOLOGIA, DE LA UNIVERSIDAD DE CHILE

PAR/POR
César ARRIAGADA

Équipe d'accueil : Géosciences – Rennes
École doctorale : Sciences de la Matière
Composante universitaire U.F.R. : Structure et Propriétés de la Matière

Departamento de Geología, Facultad de Ciencias Físicas y Matemáticas, Santiago

ROTATIONS TECTONIQUES ET DÉFORMATION DE L'AVANT ARC DES ANDES CENTRALES AU COURS DU CÉNOZOÏQUE

ROTACIONES TECTONICAS Y DEFORMACION DEL ANTEARCO EN LOS ANDES CENTRALES DURANTE EL CENOZOICO

Soutenue/Examinada le 28 Avril/ el 28 de Abril 2003 devant/ante la Commission d'Examen/Comisión de Examen de Grado

COMPOSITION DU JURY/MIEMBROS DE LA COMISION

Reynaldo CHARRIER :Universidad de Chile – Rapporteur/Integrante
Stuart GILDER : Institute de Physique du Globe, Paris – Rapporteur/Profesor Invitado
Annick CHAUVIN : Université de Rennes 1 – Examinateur/Profesor Invitado
Constantino MPODOZIS : SIPETROL – Examinateur/Integrante
Peter COBBOLD : Université de Rennes 1 - Directeur de Thèse/Profesor Guía
Pierrick ROPERCH : Universidad de Chile/IRD - Directeur de Thèse/Profesor Guía
Jean Pierre GRATIER : Université de Grenoble - Membre Invité/Profesor Invitado

Si pudiera vivir
Nuevamente la vida,
En la próxima trataría
De cometer más errores :
No intentaría ser tan perfecto,
Me relajaría más ;
Sería más tonto de lo que he sido ;
De hecho, tomaría muy pocas cosas
con seriedad…

Sería menos higiénico,
Correría más riesgos, haría más viajes,
Contemplaría más atardeceres,
Subiría más montañas…

Por si no lo saben
De eso esta echa la vida :
Solo de momentos.
No te pierdas el ahora…

Si pudiera volver a vivir,
Comenzaría a andar descalzo
A principios de la primavera
Y seguiría así
Hasta concluir el otoño….

Si tuviera otra vez
La vida por delante…

Pero ya ven,
Tengo ochenta y cinco años
Y sé que
Me estoy muriendo.

Jorge Luis Borges.

Remerciements

Ce travail en co-tutele a été réalisé dans le Departamento de Geología de la Universidad de Chile et le laboratoire de Géosciences Rennes et soutenu financièrement par l'IRD et CONICYT. SIPETROL a apporté de profils sismique du bassin d'Atacama.

Je remercie les membres du jury qui ont accepté de juger ce travail : Reynaldo Charrier (Universidad de Chile), Stuart Gilder (Institute de Physique du Globe de Paris), Annick Chauvin (Université de Rennes 1), Constantino Mpodozis (SIPETROL), Jean Pierre Gratier (Université de Grenoble) et mes directeurs de thèse, Peter Cobbold (Université de Rennes 1) et Pierrick Roperch (Universidad de Chile/IRD).

Merci à Géosciences Rennes

Je salue à toutes les thésards : Julien, Sebastien (Cab…. I), Charles (Cab…. II), Rodrigo (el otro chileno), Olivier, Blaise, Nicolas, Katia, Nicolas, Stephane, Stephanie, Florence, Katrine, Celine, Samuel, des filles étrangeres et toutes les autres. Ils m'ont accueilli au sein de leur labo et m'ont donnée son amitié et montré la belle Bretagne, le français, le français de la rue et beaucoup d'autres choses…

Annick Chauvin patiemment m'a orientée pendant le début de mon séjour à Rennes dans le laboratoire de paléomagnétisme. Delphine m'a donné les codes de son programme de restauration.

Agradecimientos

Gracias a los compañeros de terreno, Pierrick Roperch, Peter Cobbold, Constantino Mpodozis, Sergio y Alejandro. Los comentarios y correcciones de Thierry Nalpas mejoraron la calidad del texto. También agradezco a mis compañeros del laboratorio de paleomagnetismo y del IRD. Agradezco a Matilde Basso y Joaquín Cortés por las discusiones en torno a la geología del Salar y por proporcionar parte de las fotos aéreas de la segunda región. Gracias a todos quienes me ayudaron en el departamento de Geología de la escuela. *Finalmente agradezco a todos quienes siempre estuvieron durante el desarrollo de este trabajo…. Especialmente agradezco a 'la Vale' y al 'César chico', en los momentos de oscuridad, siempre fueron mi luz y fuente de energía para terminar este trabajito…*

Resumen

Los Andes Centrales son el ejemplo clásico de una cadena montañosa desarrollada a lo largo de un margen activo en un contexto de subducción. La placa oceánica de Nazca pasa en subducción ligeramente oblicua (N~75ºE) bajo el continente sudamericano. Un alto plateau, el Altiplano-Puna y el Oroclino Boliviano (el cambio en la orientación de los Andes de NW-SE a NS cerca de los 18ºS), son las características más notables de este segmento de la cadena. Según el modelo clásico de Isacks, el Oróclino Boliviano se formó a partir de una ligera curvatura inicial del margen continental, que fue acentuada por acortamiento diferencial durante en Neógeno, implicando la rotación ambos limbos.

En el cuadro del estudio de la evolución tectónica Cenozoica de la región del antearco del norte de Chile, era necesario responder a las preguntas siguientes: ¿Cuál es la edad, distribución espacial, magnitud y el origen de las rotaciones en el antearco del norte de Chile? ¿Cuál es la relación entre las rotaciones observadas en el antearco, el origen del Oróclino Boliviano y la construcción de los Andes Centrales? En este contexto, durante la elaboración de este trabajo, hemos efectuado un estudio paleomagnético detallado de la región de Antofagasta en el norte de Chile. Simultáneamente, para caracterizar el estilo estructural que controla las rotaciones observadas, hemos efectuado un estudio estructural y estratigráfico detallado de la vertiente oriental de la Cordillera de Domeyko. Este borde coincide con el borde occidental de la cuenca del Salar de Atacama.

Nuestro estudio indica que el relleno sedimentario de la cuenca de Atacama, de más de 8 km de espesor, se acumuló principalmente en un contexto compresivo desde el comienzo del Cretácico Superior, durante la inversión de las cuencas extensionales de tras arco del Mesozoico del norte de Chile. La sedimentación de la cuenca estuvo controlada por un sistema de fallas inversas vergentes al Este, arraigadas en la delgada faja de basamento de la proto Cordillera de Domeyko, que fue progresivamente alzada por pulsos sucesivos de deformación compresiva desde el Cretácico Superior al Neógeno. La historia de relleno y la evolución tectónica de la cuenca de Atacama son coherentes con la evolución geológica conocida para la Cordillera de Domeyko y otras cuencas a lo largo de la Depresión PreAndina del norte de Chile y en el Altiplano-Puna del noroeste de Argentina y sudeste de Bolivia.

El análisis de 146 sitios de muestras de paleomagnetismo, principalmente de rocas de edad Mesozoica a Paleógena en el antearco de la región de Antofagasta, entregó 118 sitios con magnetizaciones remanentes estables. Los datos obtenidos indican rotaciones horarias sistemáticas de hasta 65º. Sin embargo, la magnitud es independiente de la edad de las series estudiadas. Nuestro estudio sugiere que una zona importante de cizalle transpresivo dextral de orientación NE-NNE controló la amplitud de las rotaciones en la región de Antofagasta. La relación aparente entre las rotaciones tectónicas y la orientación de las estructuras de la región sugiere que las rotaciones se produjeron probablemente debido a diferencias en la magnitud del acortamiento EW a lo largo del margen durante la Fase Incaica del Eoceno-Oligoceno Inferior. La amplia distribución de las rotaciones en el norte de Chile implica que la deformación Incaica es un evento tectónico de importancia regional y no solamente ligado a la deformación en la Cordillera de Domeyko.

El estudio geológico y paleomagnético fue completado con la restauración numérica en planta del Oróclino Boliviano. Hemos modificado un algoritmo de restauración para incorporar en los cálculos los datos de rotación y acortamiento disponibles para los Andes Centrales. Este trabajo indica que las rotaciones observadas en el margen no pueden ser explicadas considerando solamente la deformación Miocena que afecta principalmente a la zona Subandina. Al considerar el acortamiento que ocurre principalmente de la Cordillera Oriental se observa una variación importante de la geometría del margen. Los resultados de la restauración pueden explicar las rotaciones antihorarias de ~10º al norte de Perú, entre 20-25º al sur de Perú y una rotación global horaria entre 10-20º en el margen de Chile.

Los resultados de la restauración en planta y los datos paleomagnéticos obtenidos en rocas de edad Neogena en el antearco indican que la curvatura oroclinal se formó principalmente durante la deformación que dio origen a la Cordillera Oriental.

Los resultados de rotación obtenidos a partir de la restauración en el norte de Chile son inferiores que las rotaciones paleomagnéticas. La variabilidad espacial y la gran magnitud de las rotaciones del margen de Chile sugieren dos episodios de rotación. Rotaciones horarias controladas principalmente por la tectónica en el antearco durante el Paleógeno, período de fuerte convergencia oblicua y posteriormente (o simultáneamente), una rotación global de todo el margen durante la migración de la deformación hacia el Este y el desarrollo de la Cordillera Oriental.

De esta manera, las rotaciones locales del norte de Chile aumentaron de 10-20º. Los resultados de este estudio demuestran que la deformación compresiva y las rotaciones tectónicas en el antearco son elementos claves de la deformación andina precoz y deben ser considerados en los modelos cinemáticos de la evolución de los Andes Centrales.

Palabras claves:
Andes Centrales, Oróclino Boliviano, anta arco, norte de Chile, Salar de Atacama, rotaciones paleomagnéticas, deformación Incaica.

Résumé

Les Andes Centrales sont l'exemple type d'une chaîne se développant le long d'une marge active en contexte de subduction. La plaque océanique Nazca passe en subduction légèrement oblique (~N75ºE) sous le continent sud-américain. Un haut plateau, l'Altiplano Puna et l'Orocline Bolivien (le changement du direction des Andes de NW-SE à NS près de 18°S), sont les caractéristiques les plus remarquables de ce segment de la chaîne. Selon le modèle classique d'*Isacks*, l'Orocline Bolivien s'est formé à partir d'une légère courbure initiale de la marge continentale, qui a été accentuée par raccourcissement différentiel pendant le Néogène, impliquant la rotation des deux limbes.

Dans le cadre de l'étude de l'évolution tectonique Cénozoïque de la région de l'avant arc du nord du Chili, il était nécessaire de répondre aux questions suivantes : Quelle est l'âge, la distribution spatiale, la quantité et l'origine des rotations dans l'avant arc du nord du Chili ? Quelle est la relation entre les rotations observées dans l'avant arc, l'origine de l'Orocline Bolivien et la construction des Andes Centrales ? Ainsi, pendant l'élaboration de ce travail, nous avons effectué une étude paléomagnétique détaillée de la région d'Antofagasta au nord du Chili. Simultanément, pour caractériser le style structural qui contrôle les rotations observées, on a effectué une étude structurale et stratigraphique détaillée du versant oriental de la Cordillère de Domeyko. Cette bordure coïncide avec le bord occidental du bassin du Salar d'Atacama.

Notre étude met en évidence que le remplissage sédimentaire du bassin d'Atacama, plus de 8 km d'épaisseur, s'est accumulée principalement dans un contexte compressif depuis le début du Crétacé Supérieur, durant l'inversion des bassins extensifs d'arrière arc du Mésozoïque du nord du Chili. La sédimentation dans la bassin a été contrôlé par un système de failles inverses vers l'Est, enracinés dans la mince ceinture du socle de la proto Cordillère de Domeyko, qui a été progressivement soulevé par divers pulses successifs de déformation compressive depuis le Crétacé Supérieur au Néogène. L'histoire du remplissage et l'évolution tectonique du bassin d'Atacama sont cohérents avec l'évolution géologique connu pour la Cordillère de Domeyko et des autres basins le long de la Dépression Préandine dans le nord du Chili, et l'Altiplano Puna du nord-ouest de l'Argentine et sud-est de la Bolivie.

L'analyse de 146 sites de données paléomagnétiques, principalement de roches d'âge Mésozoïque à Paléogène dans l'avant arc de la région d'Antofagasta, a livré 118 sites à aimantations rémanentes stables. Les données obtenues montrent des rotations horaires systématiques jusqu'à 65º. Cependant la magnitude est indépendante de l'âge des séries étudiées. Notre étude suggère qu'une importante zone de cisaillement transpressif dextre d'orientation NE-NNE a contrôlé l'ampleur des rotations dans la région d'Antofagasta. La relation apparente entre les rotations tectoniques et l'orientation des structures de la région suggère que les rotations se sont probablement produite dû a des différences de quantité de raccourcissement EW le long de la marge pendant la phase Incaïque d'âge Éocène-Oligocène Inférieur. La vaste distribution de ces rotations dans le Nord du Chili implique que la déformation Incaïque est un événement tectonique d'importance régionale non seulement lié à la déformation dans la Cordillère de Domeyko.

L'étude géologique et paléomagnétique de la région a été complétée par la restauration numérique en carte de l'Orocline Bolivien. Nous avons modifié un algorithme de restauration pour incorporer dans les calculs les données de rotations et de raccourcissement disponibles pour les Andes Centrales. Cette étude met en évidence que les rotations observées dans la marge ne peuvent pas s'expliquer en considérant seulement la déformation Miocène qui affecte principalement la zone Subandine. En prenant en compte le raccourcissement principalement dans la Cordillère Orientale on observe une variation importante de la géométrie de la marge. Les résultats de la restauration peuvent expliquer des rotations antihoraires de ~10º au nord du Pérou, entre 20-25º au sud du Pérou et une rotation globale horaire entre 10-20º dans la marge du Chili.

Les résultats de la restauration en carte et les données paléomagnétiques obtenus sur des roches d'âge Néogène dans l'avant arc indiquent que la courbure oroclinale s'est formé principalement durant la déformation qui a donné naissance à la Cordillère Orientale.

Les résultats de rotation obtenus à partir de la restauration dans le nord du Chili sont inférieurs que les rotations paléomagnétiques. La variabilité spatiale et la grande quantité des rotations dans la marge Chilienne suggèrent deux épisodes de rotation. Rotations horaires contrôlées principalement par la tectonique dans l'avant arc au cours du Paléogène, période de convergence très oblique et postérieurement (ou simultanément), une rotation globale de toute la marge pendant la migration de la déformation vers l'Est et la déformation qui a donné naissance à la Cordillère Orientale.

De cette manière les rotations locales du nord du Chili ont été augmentées des 10-20º. Les résultats de cette étude démontrent que la déformation compressive et les rotations tectoniques dans l'avant arc sont des éléments clef de la déformation Andine précoce, et doivent être considérées dans les modèles cinématiques de l'évolution des Andes Centrales.

Mots-clés :
Andes Centrales, Orocline Bolivien, avant arc, nord du Chili, Salar d'Atacama, rotations paléomagnétiques, déformation Incaïque.

Sommaire

Chapitre I : Introduction : Les Andes Centrales, synthèse bibliographique et présentation de la problématique.

Contexte tectonique général

La Cordillère des Andes s'étend sur presque 8.000 kilomètres le long de la marge occidentale du continent Sud-américain, depuis la mer des Caraïbes à la mer de Scotia (Figure I.1). Depuis le début de la théorie de la tectonique des plaques, les Andes ont été citées comme un exemple typique d'une zone de collision entre une croûte océanique et une croûte continentale, ou marge continentale active [*Dewey et Bird,* 1970; *James,* 1971]. L'analyse des différents secteurs des Andes montre une grande variété de processus de construction d'une chaîne de montagnes. Pour examiner ces processus, les Andes peuvent êtres divisés d'après la proposition de *Gansser* [1973] ou de *Jordan et al*. [1983] (Figure I.1). Les divisions proposées sont appropriées pour analyser l'histoire tectonique des différentes regions andines. Selon *Jordan et al*. [1983] la chaîne se décompose en trois regions principales (Figure I.1) :

(1) Les Andes Septentrionales s'étendent depuis le Venezuela au Nord (12ºN) jusqu'au Pérou au Sud (5ºS). Elles résultent de l'interaction des plaques Caraïbes, Cocos, Nazca ainsi que l'isthme de Panama. L'accrétion de fragments de croûte océanique, d'arcs insulaires est un mécanisme important de la construction des Andes Septentrionales pendant le Mésozoïque et le Cénozoïque [*Aspden et McCourt*, 1986; *Roperch et al*., 1987; *Van Thournout et al*., 1992].

(2) Les Andes Centrales s'étendent depuis le Pérou et la Bolivie au Nord (5ºS) jusqu'au Chili et en Argentine au Sud (~40ºS). Ce segment de chaîne résulte de la subduction de la plaque Nazca sous le continent Sud-américain.

(3) Les Andes Australes ou Patagoniennes s'allongent de part et d'autres des frontières Argentines et Chiliennes entre 40ºS et 55ºS. Elles résultent de la subduction des plaques océaniques Nazca et Antarctique et interagissent avec la péninsule Antarctique et la plaque de Scotia. Un arc entre la Cordillère de la Patagonie d'orientation nord-sud et la Cordillère de Darwin d'orientation est-ouest forme le bout méridional des Andes Australes (Figure I.1).

Le long des Andes, il y a des segments avec volcanisme actif séparées de segments sans volcanisme (Figure I.1). Le volcanisme actif est divisé en quatre segments [*Thorpe et al*., 1981] :

(1) Une zone volcanique dans le nord (NVZ) qui s'étend entre 5ºN et 2ºS, en Colombie et en Équateur.
(2) Une zone volcanique centrale (CVZ) qui s'étend entre 16ºS et 28ºS dans le sud du Pérou, la Bolivie, le nord du Chili, et l'Argentine.
(3) Et les zones volcaniques Méridionales et Australes (SVZ), au Sud (35ºS) dans le sud du Chili et l'Argentine.

Les Andes Centrales

Les Andes Centrales forment la region la plus grande et la plus montagneuse de la Cordillère des Andes (Figure I.1). Ce segment de ~4000 kilomètres de longueur est subdivisé en trois parties : les Andes Centrales du nord (5º-13ºS; entièrement situé au Pérou), l'Orocline Bolivien (13º-28ºS; depuis le sud Péruvien, la Bolivie, le nord du Chili et le nord-Ouest de l'Argentine), et les Andes Centrales du sud (28º-35ºS; dans la partie centrale du Chili et la partie centrale occidentale d'Argentine). Il se caractérise par une géométrie arquée, concave vers l'Ouest, dont la symétrie s'articule autour d'un axe passant par la ville de Santa Cruz (Bolivie) à l'Est, la Caleta Loa, sur la côte chilienne, et la fosse péruvo chilienne aux alentours de 20°S (Figure I.1&I.2 ; *Gephart*, 1994). Construite sur une croûte continentale, la chaîne Andine Centrale s'est en grande partie développée pendant le Cycle orogénique Andin, entre le Trias et l'actuel [e.g., *Coira et al*. 1982].

L'orocline Bolivien, la plus grande partie des Andes centrales (Figure I.1&I.2), comprend près de 1.300.000 km^2 et incorpore deux des caractéristiques les plus significatives de toute la chaîne andine : le plateau de l'Altiplano-Puna, le second plus haut plateau après le Tibet en surface et élévation moyenne [*Allmendinger et al*., 1997], et la courbure de 55º connue comme ***l'OROCLINE BOLIVIEN*** ou ***COUDE d'ARICA*** (Figure I.2). Ce coude se produit à la latitude de 18º S. Au nord de cette courbure, les structures sont orientées NW-SE, alors qu'au sud, les structures sont brusquement orientées suivant une direction NS (Figure I.2). Dans cette région, la topographie des Andes montre une symétrie bilatérale remarquable (Figure I.2 ; *Gephart*, [1994]). Suivant ce même plan, la symétrie de la morphologie de la plaque de Nazca est moins parfaite mais encore importante. Tandis que les zones nord et sud présentent une croûte d'épaisseur normale (30-50 km), les Andes Centrales présentent une croûte exceptionnellement épaisse, jusqu'à 70 km [*Götze et al*., 1994; *Wigger et al*., 1994; *Zandt et al*., 1994; *Beck et al*., 1996; *Götze et Kirchner*, 1997].

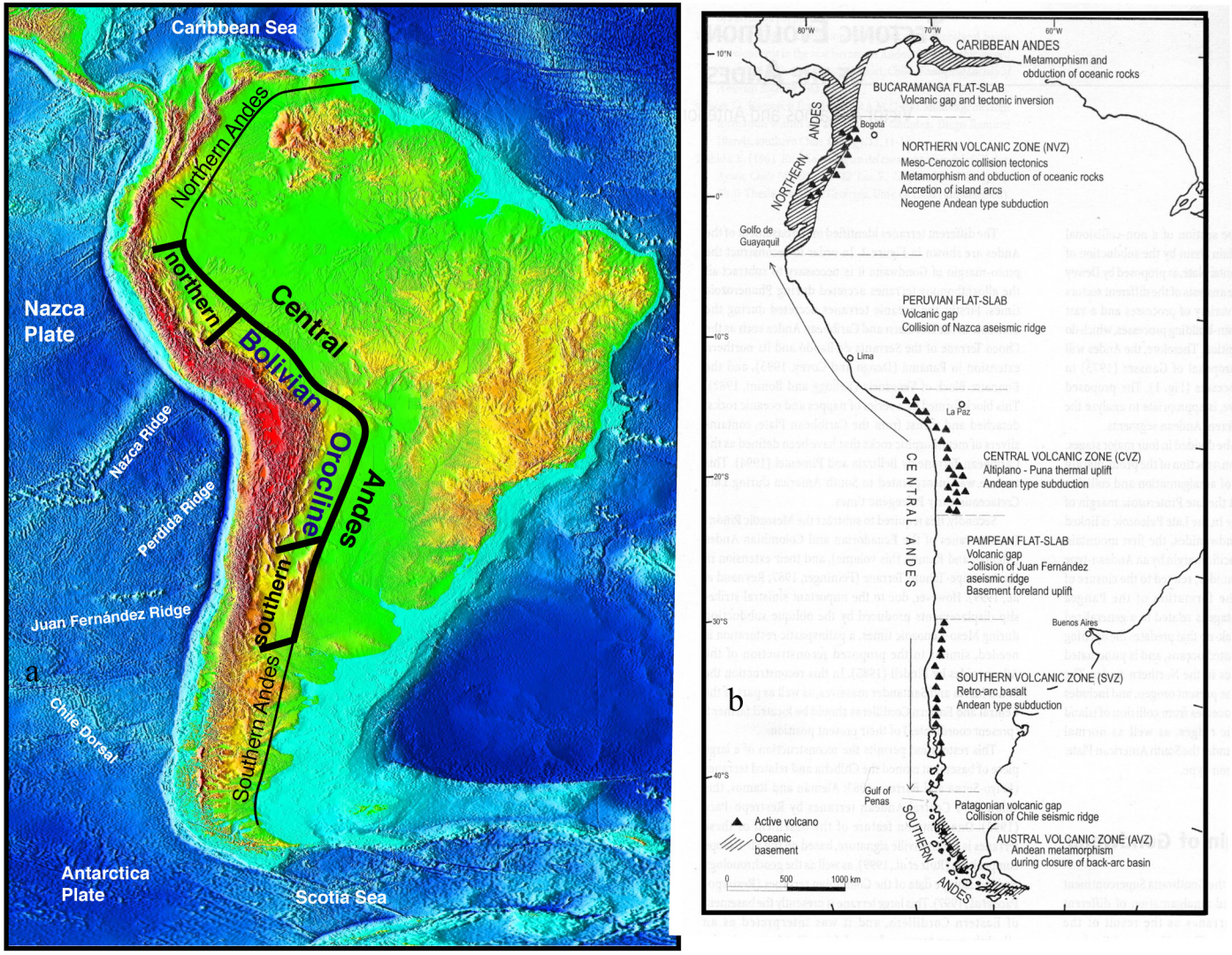

Figure I.1: Topography of the South America continent, showing main structural features on the Nazca Plate. (a) segmentation of the Andes after Jordan et al. (1983), (b) segmentation after Gansser, (1973).

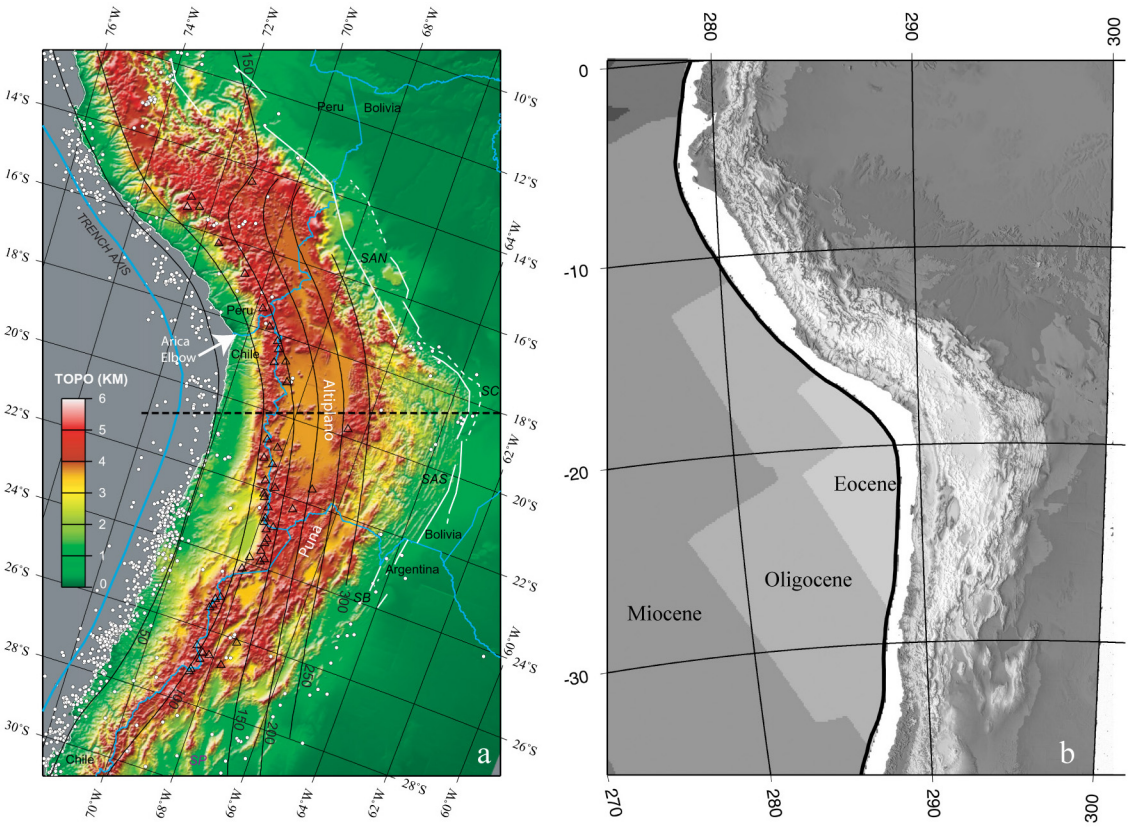

Figure I.2: a) Topography and tectonic setting of the region of Bolivian Orocline in the central Andes, in an oblique Mercator projection (After Bevis et al., 2001). The "equator" is Gephart's (1994) plane of symmetry (thick dashed black line). The light blue curve west of the coast is the trench axis. The black curves are the Cahill and Isacks (1992) depth contours (km) for the middle of the Wadati-Benioff zone. Note the "flat slab" sections of the subducted Nazca plate at the northern and southern limits of the map and the relatively steep slab underlying the central Andes. The white circles show all well-located shallow seismicity (1964–1995). The open triangles indicate the active volcanic arc, which is limited to the steep slab segment. The outermost thrusts of the back arc (foreland) region, shown in solid white lines, indicate thrust faults which break the surface, whereas dashed curves indicate buried (blind) thrusts, some of which are inferred rather than observed. Abbreviations used in the figure: SAN, the northern Subandean zone; SAS, the southern Subandean zone; SC, Santa Cruz elbow; SB, Santa Barbara belt; SP, Sierras Pampeanas. b) Age of the Nazca Plate.

Contexte Géologique

Selon *Ramos et Aleman* [2000], l'histoire andine peut-être décomposée en quatre étapes principales.

(1) La première est liée à la construction de la proto-marge de Gondwana, et se compose de l'accrétion et de la collision de différentes terranes pendant le Protérozoïque Supérieur.

(2) La deuxième étape durant le Paléozoïque Supérieur est liée à la formation des Gondwanides, la première chaîne de montagne développée le long de la marge Pacifique associée à une subduction de type Andine et l'Alleghanides, lié à la fermeture de l'océan Iapetus et à la formation du super continent de la Pangée.

(3) La troisième étape est liée à une extension généralisée pendant la rupture de la Pangée qui précède l'ouverture de l'océan Atlantique, et est ponctuée par la collision des arcs insulaires dans les Andes Septentrionales.

(4) La dernière étape ou Cycle Andin est responsable de l'orogénie actuelle, et inclut une grande variété de processus tectoniques de collision d'arcs insulaires, sismiques et asismiques, aussi bien que la subduction de la croûte océanique sous le continent sud-américain, qui définit le type Andin de subduction.

Dans la région des Andes Centrales pendant le Cycle Andin l'arc magmatique migre vers l'Est, depuis la Cordillère de la Côte à sa position actuelle dans la Cordillère Occidentale [Figure I.3, *Coira et al*., 1982; *Scheuber et Reutter*, 1992; *Allmendinger et al*., 1997; *Lamb et Hoke*, 1997]. La migration vers l'Est et aussi la non-existence de complexes de subduction (bassins d'avant arc) d'âge Mésozoïque et Cénozoïque sont expliquées par l'érosion qui se produit dans la marge lors de la subduction de la plaque océanique [*von Huene et Ranero*, 2003] ou pour des variations de l'angle de subduction [e.g. *Rutland*, 1971; *Coira et al*., 1982].

La fosse du Chili Pérou, à 80-100 kilomètres de la côte, représente l'actuelle limite entre la plaque de Nazca et la plaque sud-américaine (Figure I.2). À terre, la chaîne Andine peut être subdivisée d'Ouest en Est en un bloc d'avant-arc (constitué par la Cordillère de la Côte, la Vallée Centrale, le Précordillère du nord du Chili et la Dépression Préandine), l'arc magmatique (Cordillère Occidentale), et l'arrière arc (Altiplano-Puna, Cordillère Orientale, la chaîne Subandine, et l'avant-pays du bassin du Chaco) (Figure I.3). De -7000 m au-dessous du niveau de la mer dans la fosse, le relief atteint 2000 m dans la Cordillère de la

Côte, 4000 m dans la Précordillère et plus de 6000 m dans la Cordillère Occidentale. La Cordillère de la Côte est constituée principalement par des roches volcaniques et intrusives d'âge Jurassique à Crétacé. La Précordillère se compose principalement de roches Paléozoïques recouvertes par des roches sédimentaires et volcaniques Mésozoïques et Tertiaires et par des intrusions d'âge Paléogène [*Lamb et al*., 1997].

Les hauts sommets des volcans de l'arc volcanique actif forment la Cordillère Occidentale qui délimite la bordure occidentale du plateau de l'Altiplano-Puna. Les Cônes volcaniques Miocènes à Quaternaires, dont l'altitude peut excéder celle du plateau d'environ 2000 m, reposent sur des roches d'âge Paléozoïque à Miocène. L'arrière arc récent comporte l'Altiplano-Puna, la Cordillère Orientale et les chaînes Subandines. L'Altiplano en Bolivie et la Puna dans le nord-ouest de l'Argentine représentent un bassin intra-montagneux de plus de 200 kilomètres de large avec une altitude entre 3800 et 4500 m. Le remplissage sédimentaire Mésozoïque à Cénozoïque atteint localement une épaisseur de 10.000 m. À l'est, l'Altiplano-Puna est bordé par l'imposante Cordillère Orientale, avec des altitudes entre 5000-7000 m. Elle se compose principalement de roches d'âge Précambriennes à Paléozoïque et de sédiments Crétacés et Cénozoïques. La partie la plus orientale des Andes Centrales est la zone Subandine, une ceinture de chevauchements 'thin-skinned fold and thrust belt', de 150-200 kilomètres de large [*Kley et Monaldi*, 1998].

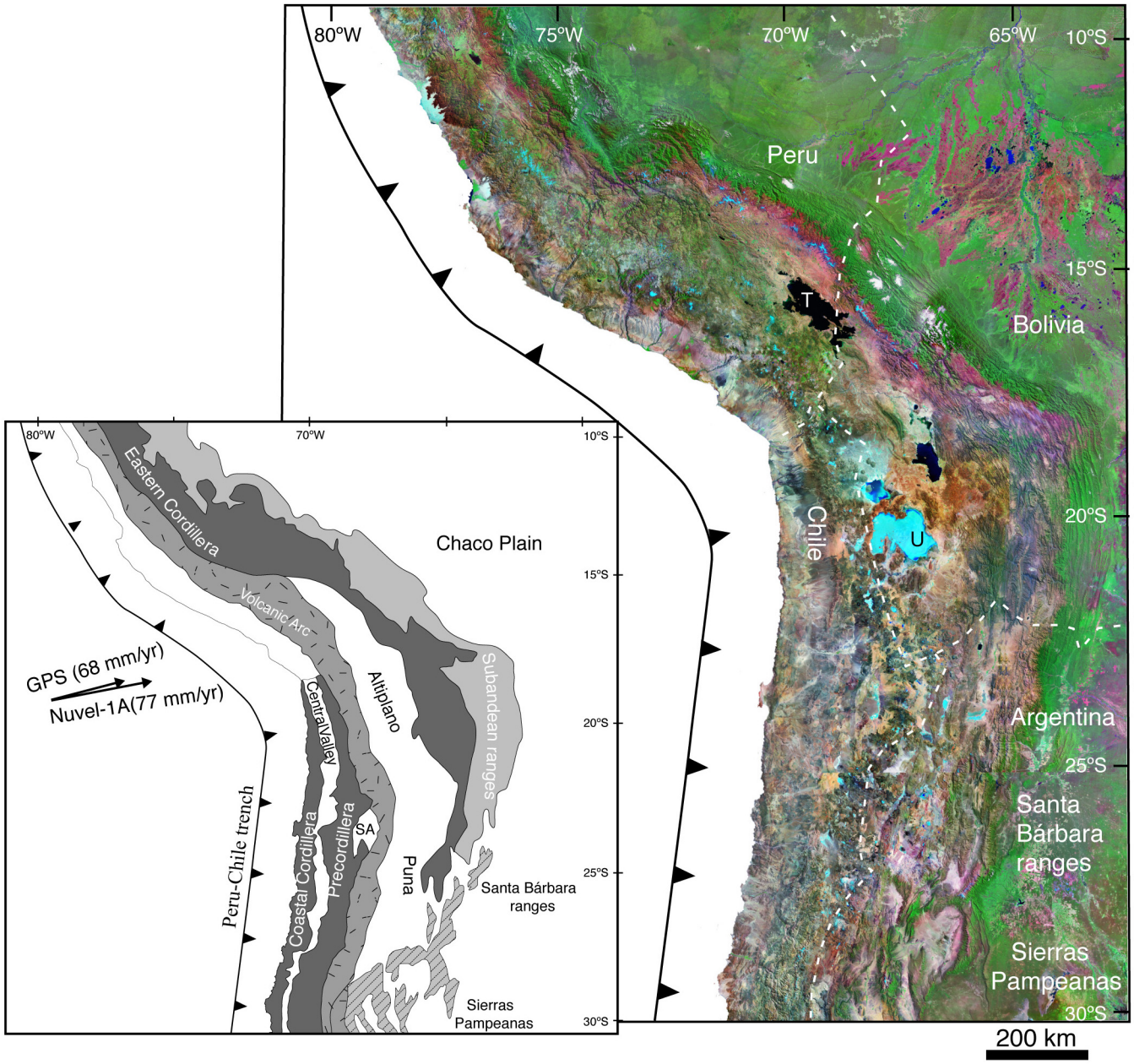

Figure I.3: From west to east, the continental margin at about 15-27ºS consists of: The Peru-Chile trench and continental slope; the Coastal Cordillera, mainly a remnant of a Mesozoic magmatic arc; the Longitudinal Valley (also called Central Depression or Pampa del Tamarugal), a modern forearc basin; the Precordillera (including Cordillera Domeyko) and Preandean Depression (including Salar de Atacama basin), that largely define the western Andean slope; the Western Cordillera, an active volcanic arc along the eastern border of Chile; the Altiplano-Puna plateau, a high-elevation hinterland plateau; the Eastern Cordillera, a rugged interior of the eastern fold-thrust belt; the Subandean Zone and Santa Barbara System, frontal active parts of the eastern fold-thrust belt; and the Beni Plain and Chaco Plain, parts of a low-elevation foreland basin underlain by the Brazilian shield.
T, Titicaca Lake. U, Salar de Uyuni.

La géométrie de la zone de subduction

Entre environ 15ºS et 27ºS, le modèle NUVEL-1A et les calculs avec le système de positionnement globaux (GPS) indiquent respectivement une convergence principalement Est-Ouest de 77 millimètres par an et de 68 millimètres par an [*DeMets et al*., 1994; *Norabuena et al*., 1998]. La direction de la convergence Nazca-Amérique du Sud a très peu changé au cours des 20 derniers Ma [*Pardo-Casas et Molnar*, 1987; *Somoza*, 1998]. Au nord et au sud de l'orocline Bolivien, la subduction de la plaque océanique est sub-horizontale. C'est au cœur de l'orocline que l'angle de subduction est le plus fort ~30º permettant ainsi le développement d'un coin d'asthénosphère entre les 2 plaques (Figure I.2; *Isacks*, [1988]). Cette géométrie de la plaque plongeante est fortement corrélée à l'âge de la croûte océanique (Figure I.2).

La présence du coin asthénosphérique affaiblit la lithosphère continentale et facilite la subduction intracontinentale du craton brésilien sous les Andes [*Barazangi et Isacks*, 1979 ; *Isacks*, 1988 ; *Cahill et Isacks*, 1992]. *Wdowinski et al*. (1989) proposent une autre conséquence de cette géométrie particulière de la plaque de Nazca. Pour ces auteurs, l'inclinaison du plan de subduction permet une convection dans le coin asthénosphérique, qui, en entraînant la base de la plaque supérieure vers la plaque de Nazca, augmente la compression latérale au niveau de la zone de contact entre les deux plaques. La morphologie de la plaque subductante exerce aussi une forte influence dans la géométrie de l'arc volcanique actif (Figure I.2) [*Barazangi et Isacks*, 1977 ; *Bevis et Isacks*, 1984]. *Barazangi et Isacks* [1979] ont attribué l'absence de volcanisme actif dans le nord, le centre du Pérou et le centre du Chili (Figure I.2) à l'absence d'un coin de manteau asthénosphérique en relation avec des subductions subhorizontales et à la superposition directe des deux plaques lithosphériques. La cause de cet angle anormal de subduction dans ces segments, a été attribuée à des effets combinés comme : la subduction de dorsales plus légères (Figure I.1), la dorsale de Nazca (au nord) et la dorsale de Juan Fernández à la latitude de Valparaiso, à une convergence rapide et à la jeunesse relative de la plaque de Nazca [*Barazangi et Isacks*, 1979 ; *Cross et Pilger*, 1982 ; *Cahill et Isacks*, 1992 ; *Yañez et al*., 2000 ; *Gutscher et al*., 2000].

Couplage entre les plaques de Nazca et Sud-américaine

La notion que les Andes modernes, en général, sont le résultat de la compression latérale dûe au fort couplage des plaques Nazca et Sud-américaine à leur interface [*Dewey et Bird*,

1970] est supporté par le caractère fortement sismogénique de cette limite de plaque. Un couplage fort entre les deux plaques dans la région de l'avant arc est également démontré par des observations de GPS le long de la marge [*Klotz et al*., 2001; *Bevis et al*., 2001]. Ces résultats montrent également que l'interface entre les plaques de Nazca et l'Amérique du Sud est fortement couplée et moins de 10% de la convergence est absorbé dans le continent comme déformation lithosphérique. Dans le nord du Chili, la déformation élastique enregistrée par l'avant-arc ne montre pas une partition de la déformation en réponse à l'obliquité de la subduction [*Bevis et al*., 1999 ; Figure I.4].

L'influence tectonique et mécanique de l'avant arc dans la construction de l'orogène est mal comprise. Les données de paléomagnétisme de *Roperch et al*. [2000] et *Somoza et al*., [2002] montrent que les rotations tectoniques, dans l'avant arc, sont antérieures au Miocène Supérieur, suggérant un comportement mécanique rigide de l'avant arc au cours des dix derniers millions d'années. Le système rigide et couplé de plaque de Nazca-avant arc peut être vu comme un indenteur, poussant vers l'Est et transférant avec une déformation minimale interne, la composante non sismique de la convergence vers l'est, en particulier les zones sub-andine [*Tassara*, 2002]. Dans le nord du Chili, les travaux de *Muñoz et Garcia*, [1996], *Garcia et al*. [1999], *Garcia* [2002] et *Charrier et al*. [2002] mettent aussi clairement en évidence la déformation compressive dans la zone de transition entre l'avant arc et l'Altiplano.

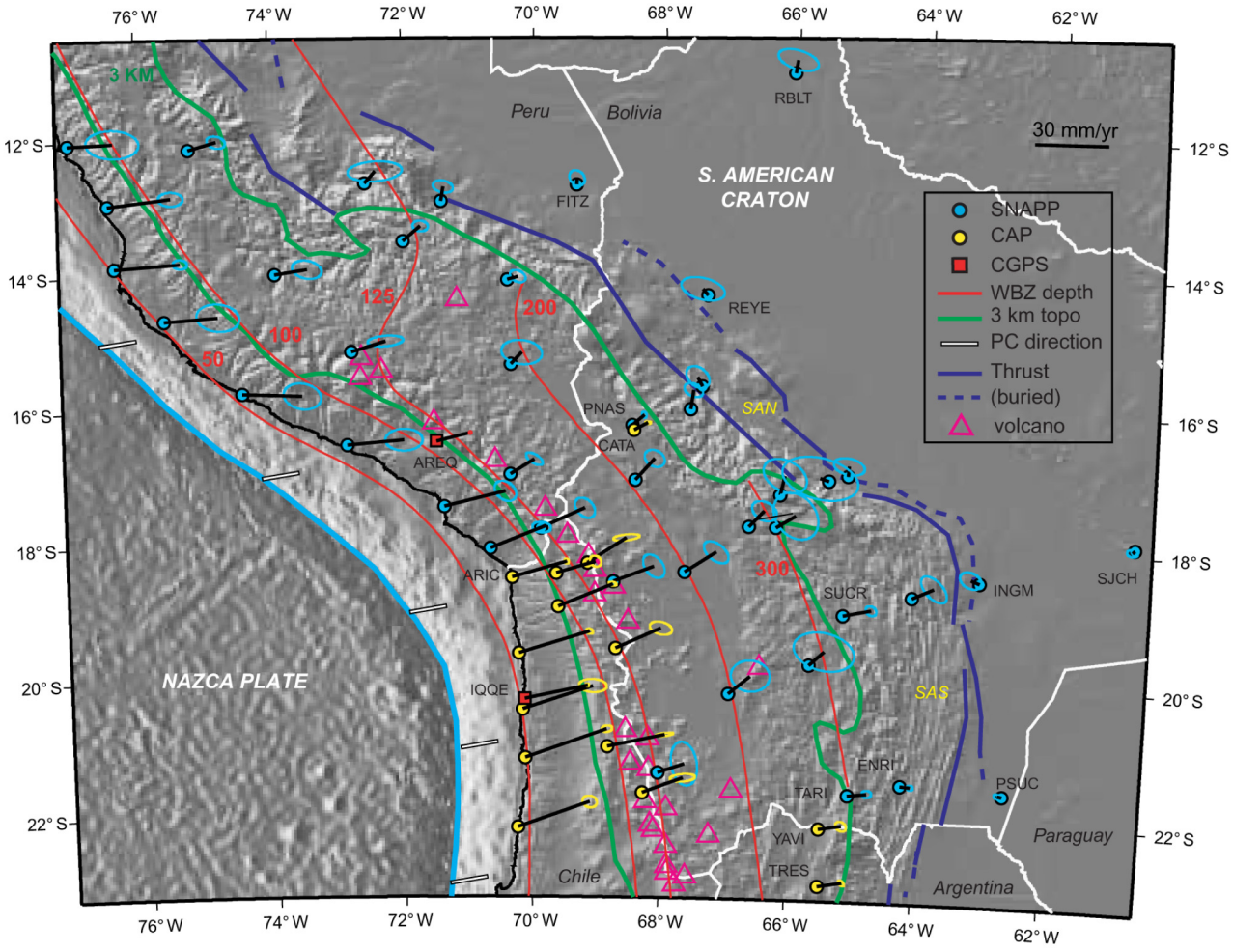

Figure I.4. Integrated crustal velocity field for the central Andes, north of 23ºS, relative to the stable core of the South American plate (After Kendrick et al., 2001). The error ellipses are nominally 95% confidence ellipses. The outermost thrusts of the back-arc (foreland) region are shown in darkblue: solid lines indicate thrust faults which break the surface, whereas dashed lines indicate buried or blind thrusts, some of which are inferred rather than observed. The open triangles indicate the active volcanic arc. Abbreviations as in the Figure I.2.

Image actuelle de la structure de la croûte des Andes centrales

Au cours des dix dernières années, plusieurs réseaux sismiques ont opéré dans le nord du Chili, le sud de la Bolivie et le nord-ouest de l'Argentine. Les ondes P et S converties et isolées de l'onde télésismique P (Receiver functions (RFs), ont été utilisées pour estimer des vitesses crustales et détecter les discontinuités dans la croûte et le manteau supérieur de la structure profonde des Andes Centrales [*Schmitz et al*., 1997; *Oncken et al*., 1999 ; *Chmielowski et al*., 1999 ; *Yuan et al*., 2000 ; *Babeyko et al*., 2002 ; *Yuan et al*., 2002]. Ces données indiquent que l'épaisseur crustale varie de 35 km dans l'avant arc jusqu'à 80 km sous le plateau. La croûte du craton brésilien a une épaisseur normale (30 km) au niveau de la plaine du Chaco (Figure I.5c). Le Moho continental est particulièrement bien reconnu entre les 40 et 75 km de profondeur (Figure I.5c). Le Moho le long de 4 sections des Andes Centrales (Figure I.5c) varie en profondeur depuis 75 km sous le Plateau à 50 km sous la Puna. Les grandes variations observées dans la profondeur du Moho sous le plateau indiquent une forte hétérogénéité dans l'épaisseur de la lithosphère. La plaque océanique (Figure I.5c, d) est aussi bien identifiée jusqu'à une profondeur de 120 km. La plupart de la sismicité profonde dans la plaque de Nazca se termine à 120 km de profondeur, suggérant que ceci a une relation avec la transformation gabbro-éclogite.

Ces études de tomographie sismique mettent en évidence deux conversions à l'intérieur de la croûte (TRAC1 et le TRAC2, Figures I.5 b,c,d) définissant une zone de vitesse réduite (ALVZ Andean low-velocity zone). L'ALVZ recoupe tout le plateau de l'Altiplano-Puna, de la Cordillère Orientale à la Cordillère Occidentale, plongeant légèrement à l'Ouest. Les 10-20 kilomètres d'epaisseur de l'ALVZ sont interprétés comme une zone de plus haute température associée à de la fusion partielle (en relation avec les plus forte conversions) et des réactions métamorphiques. Le lien direct de l'ALVZ au détachement basal sous la marge orientale du plateau suggère un important rôle dans les processus tectoniques de raccourcissement (Figure I.5d).

La faiblesse mécanique de l'ALVZ et le détachement basal de la Cordillère Orientale, confirmée par la présence des magmas et des fluides [*Babeyko et al*., 2002], suggère deux comportements de déformation de la croûte. Dans la croûte supérieure, les raccourcissements se font par des imbrications de chevauchements. Le mode de raccourcissement dans la croûte inférieure est par contre incertain. Cette interprétation de l'ALVZ est semblable, dans son aspect tectonique, à l'interprétation de la zone de vitesse

réduite dans le Tibet qui présente de fortes similitudes (profondeur, épaisseur, ampleur transversale) [*Nelson et al*., 1996; *Kind et al*., 1996]. L'existence de zones à vitesse réduite analogues pour les deux principaux plateaux suggère leur rôle fondamental dans le processus de construction de plateaux et une partition de la déformation avec des raccourcissements dans la croûte supérieur fragile et des déplacements de matière dans la croûte ductile [*Husson et Sempéré*, sous presse].

Le bassin du Salar d'Atacama

Le bassin du Salar d'Atacama est un des principaux bassins sédimentaires actifs, préservé le long de la pente ouest des Andes centrales. L'altitude du Salar d'Atacama est inférieure d'environ à 1 km à la valeur prévue par l'épaisseur de la croûte de 67 kilomètres si l'équilibre isostatique est accompli (Figure I.5e; *Yuan et al*., [2002]). Une lithosphère épaisse de 150 kilomètres pourrait expliquer cette différence mais la profondeur de la plaque subductée Nazca (100 km sous le Salar) infirme facilement cette interprétation [*Yuan et al*., 2002]. Les données de tomographie sismique montrent des vitesses sismiques élevées et une très faible atténuation dans le manteau au-dessous de ce bloc [*Yuan et al*., 2002]. Ces résultats et l'anomalie gravimétrique positive [*Götze et Krause*, 2002] sont interprétés par *Yuan et al*. [2002] comme l'évidence d'un corps à haute densité anormalement froid sous le Salar qui est mécaniquement couplé au-dessus de la plaque océanique de Nazca.

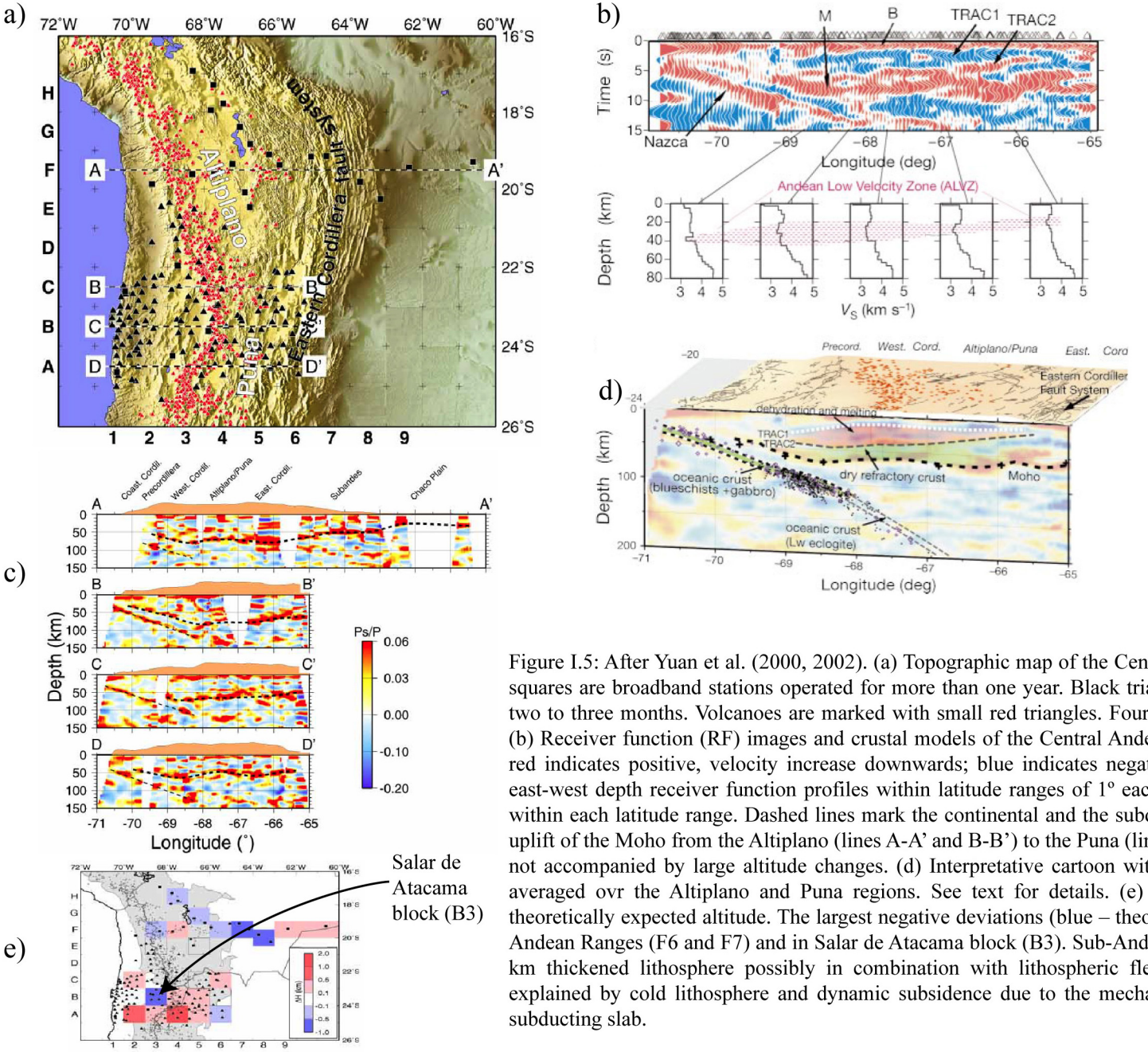

Figure I.5: After Yuan et al. (2000, 2002). (a) Topographic map of the Central Andes with seismic stations on it. Black squares are broadband stations operated for more than one year. Black triangles are short-period stations operated for two to three months. Volcanoes are marked with small red triangles. Four east-west lines mark profiles shown in (c). (b) Receiver function (RF) images and crustal models of the Central Andes along an east-west profile. In the images, red indicates positive, velocity increase downwards; blue indicates negative, velocity reduction donwards. (c) Four east-west depth receiver function profiles within latitude ranges of 1º each. The surface topography is averaged also within each latitude range. Dashed lines mark the continental and the subducted oceanic Mohos. Note that significant uplift of the Moho from the Altiplano (lines A-A' and B-B') to the Puna (lines C-C' and D-D') at the 66-68ºW, which is not accompanied by large altitude changes. (d) Interpretative cartoon with depth-migrated RF image as background averaged ovr the Altiplano and Puna regions. See text for details. (e) Difference between observed altitude and theoretically expected altitude. The largest negative deviations (blue – theoretical altitude too high) are located in Sub-Andean Ranges (F6 and F7) and in Salar de Atacama block (B3). Sub-Andean anomalies can be explained by about 50 km thickened lithosphere possibly in combination with lithospheric flexure. Salar de Atacama anomaly may be explained by cold lithosphere and dynamic subsidence due to the mechanical coupling of the cold lithosphere and subducting slab.

Les processus qui contribuent à l'épaississement de la croûte

L'épaisseur exceptionnelle de la croûte des Andes centrales a attiré l'attention depuis que son existence a été clarifiée par *James* [1971]. La formation de cette épaisse racine dans la croûte est un problème de longue date de la géologie andine. *Thorpe et al*. [1981] ont argumenté que le magmatisme avait joué un rôle important dans le soulèvement et l'épaississement de la croûte andine. *Isacks* [1988], cependant, a montré que le soulèvement Cénozoïque qui a formé le plateau de l'Altiplano-Puna d'approximativement 4 kilomètres de hauteur peut être expliqué en termes d'un modèle non unique qui implique un raccourcissement dans la croûte de 130 kilomètres, un épaississement dans la croûte de 40 à 65 kilomètres, et un amincissement thermique de la lithosphère de 140 à 70 kilomètres. Le modèle proposé par *Isacks* [1988] suggère que la courbure et le soulèvement des Andes Centrales ont été contrôlés par la géométrie de la plaque de Nazca (Figure I.2). Bien que cet amincissement thermique de la lithosphère soit associé probablement au magmatisme, *Isacks* suggère que le soulèvement et l'épaississement de la croûte Andine ne soient pas associés à des contributions magmatiques.

La marge continentale active des Andes centrales a subi un épaississement de la croûte depuis le Crétacé Supérieur [e.g., *Jaillard et Soler*, 1996]. La plupart des études considèrent que le raccourcissement total des Andes Centrales est principalement Néogène dans la Cordillère Orientale et la zone Subandine-Santa Barbara (Figure I.2) [*Isacks*, 1988; *Sempere et al*., 1990; *Schmitz*, 1994; *Gubbels et al*., 1993; *Allmendinger et al*., 1997; *Baby et al*., 1997; *Lamb et Hoke*, 1997; *Kley et al*., 1999]. La plus jeune de ces unités morpho-tectoniques est la zone Subandine, une ceinture d'ecailles tectoniques que chevauchent le bassin d'avant pays légèrement déformé [*Lamb*, 2000]. Selon *Kley et Monaldi* [1998] et *Kley* [1999], le degré de raccourcissement dans la zone Subandine et dans la large région d'arrière arc a une valeur maximum près du Coude de Santa Cruz (plan de symétrie de *Gephart*, Figure I.2) et diminue vers le sud et le nord-ouest. Les estimations de 80-140 kilomètres de raccourcissement faites à partir de coupes balancées dans la zone Subandine impliquent un raccourcissement de 8-14 millimètres par an sachant que les déformations se sont produites principalement au cours des dix derniers millions d'années. Sur la base de séries sédimentaires syn-orogéniques de l'Oligocène Supérieur et plus récentes identifiées dans l'avant pays et l'Altiplano, une valeur maximum du raccourcissement dans les Andes centrales d'environ 200-250 kilomètres est proposée par la plupart des auteurs [*Isacks*,

1988; *Sheffels*, 1990; *Sempere et al*., 1990; *Gubbels et al*., 1993; *Schmitz*, 1994; *Baby et al*., 1997; *Allmendinger et al*., 1997; *Kley et Monaldi*, 1998].

Ce raccourcissement estimé est insuffisant pour expliquer l'épaisseur dans la croûte actuelle sous l'Altiplano, l'arc moderne (Cordillère Occidentale), et la région de l'avant arc (Précordillère, vallée longitudinale et Cordillère de la Côte). Cette situation a conduit certains auteurs à proposer des mécanismes complémentaires de l'épaississement de la croûte tels qu'une accrétion de matériel sous le plaque continentale, matériel provenant de l'érosion tectonique pendant la subduction ou de l'ajout magmatique dérivé de la lithosphère océanique [*Schmitz*, 1994; *Baby et al*., 1996; *Baby et al*., 1997; *Allmendinger et al*., 1997].

Des études récentes [*McQuarrie et DeCelles*, 2001; *Müller et al*., 2002] basées sur les coupes équilibrées de l'Altiplano et de la Cordillère Orientale, proposent un raccourcissement total minimum de 340 kilomètres dans les Andes centrales. Ces nouvelles interprétations structurales suggèrent que l'épaisseur actuelle des Andes centrales puisse être expliquée seulement par l'empilement tectonique, qui s'est produit principalement au niveau de la Cordillère Orientale depuis l'Éocène Supérieur au Miocène Inférieur [*McQuarrie et DeCelles*, 2001; *Müller et al*., 2002; *Husson et Sempere*, 2003].

Plusieurs auteurs soulignent aussi l'importance de la déformation pré-Néogène dans l'histoire tectonique des Andes centrales [*Horton et DeCelles*, 1997; *Sempere et al*., 1997; *Roperch et al*., 2000; *Coutand et al*., 2001]. Les résultats de traces de fission sur apatite de *Coutand et al*. [2001] indiquent que les raccourcissements Andins ont affectés la partie nord-est de la Puna vers la fin de l'Éocène et la Cordillère Orientale adjacente vers la fin de l'Éocène ou début de l'Oligocène. Cet exhumation tardi-Paléogène est probablement une manifestation de la phase orogénique Incaïque, qui a été identifiée la première fois au Pérou par *Steinmann* [1929]. Cet événement s'est produit pendant un période de convergence rapide entre les plaques de l'Amérique du Sud et de Farallon [*Pardo-Casas et Molnar*, 1987].

Cependant, l'extension géographique d'une chaîne de montagne d'âge pré Néogène avec un système de bassin d'avant pays ainsi que l'estimation des raccourcissements pré Néogène dans la plupart des segments de l'avant arc sont incertaines.

Hormis, les déplacements verticaux et la fracturation de l'avant-arc en relation avec le cycle sismique, aucune déformation importante ne semble s'être produite dans la région de l'avant arc depuis 10 Ma. Les études structurales, de stratigraphie et de paléomagnétisme effectuées dans la région de l'avant arc mettent en évidence des déformations compressives d'âge Crétacé Supérieur - Paléogène [*Chong et Reutter*, 1985; *Bogdanic*, 1990; *Hammerschmidt et al*., 1992; *Hartley et al*., 1992; *Scheuber et Reutter*, 1992; *Charrier et Reutter*, 1994; *Somoza et al*., 1999].

Orocline Bolivien

L'origine de l'Orocline Bolivien, en relation directe avec la formation de l'Altiplano, est aussi un des sujets de controverses dans les Andes. La zone oroclinale où le changement de la direction des Andes de NW-SE au NS près de 18°S, est l'une des caractéristiques remarquables de toute la chaîne (Figure I.1 & I.2). Le concept d'orocline a été initialement formulé par *Carey* [1958]. Cet auteur a supposé la rotation dans le sens anti-horaire du segment des Andes entre la courbure d'Arica-Santa Cruz au sud et la courbure de Huancabamba au nord, essentiellement après la formation d'une chaîne Andine initialement droite. En 1988, *Isacks* a indiqué que les variations de la largeur de l'Altiplano Bolivien du Nord au Sud sont associées au raccourcissement différentiel pendant le soulèvement du plateau. Selon ce modèle, une légère courbure initiale de la marge continentale andine a été accentuée par raccourcissement différentiel pendant le Néogène, impliquant la rotation des deux limbes. Les rotations prévues sont de 5-10° horaire pour le bloque sud et de 10-15° antihoraire pour le bloque nord. Ce modèle tectonique a été vérifié par les premiers résultats de paléomagnétisme obtenus, la plupart le long de l'avant arc [*Heki et al*., 1984; *Heki et al*., 1985; *May et Butler*, 1985; *Beck*, 1988].

Au cours des dernières années, de nombreuses études de paléomagnétisme ont été effectuées dans les Andes Centrales et ont indiquées des rotations horaires au Chili et des rotations dans le sens anti-horaires au Pérou [ex.: *Kono et al*., 1985; *Roperch et Carlier*, 1992; *Macedo Sanchez et al*., 1992; *Hartley et al*., 1992; *Riley et al*., 1993; *Beck et al*., 1994; *Forsythe et Chisholm*, 1994; *Randall et al*., 1996; *Taylor et al*., 1998; *Coutand et al*., 1999; *Roperch et al*., 2000; *Somoza et Tomlinson*, 2002]. Les études de paléomagnétisme indiquent que les rotations tectoniques sont importantes dans le domaine de la Cordillère

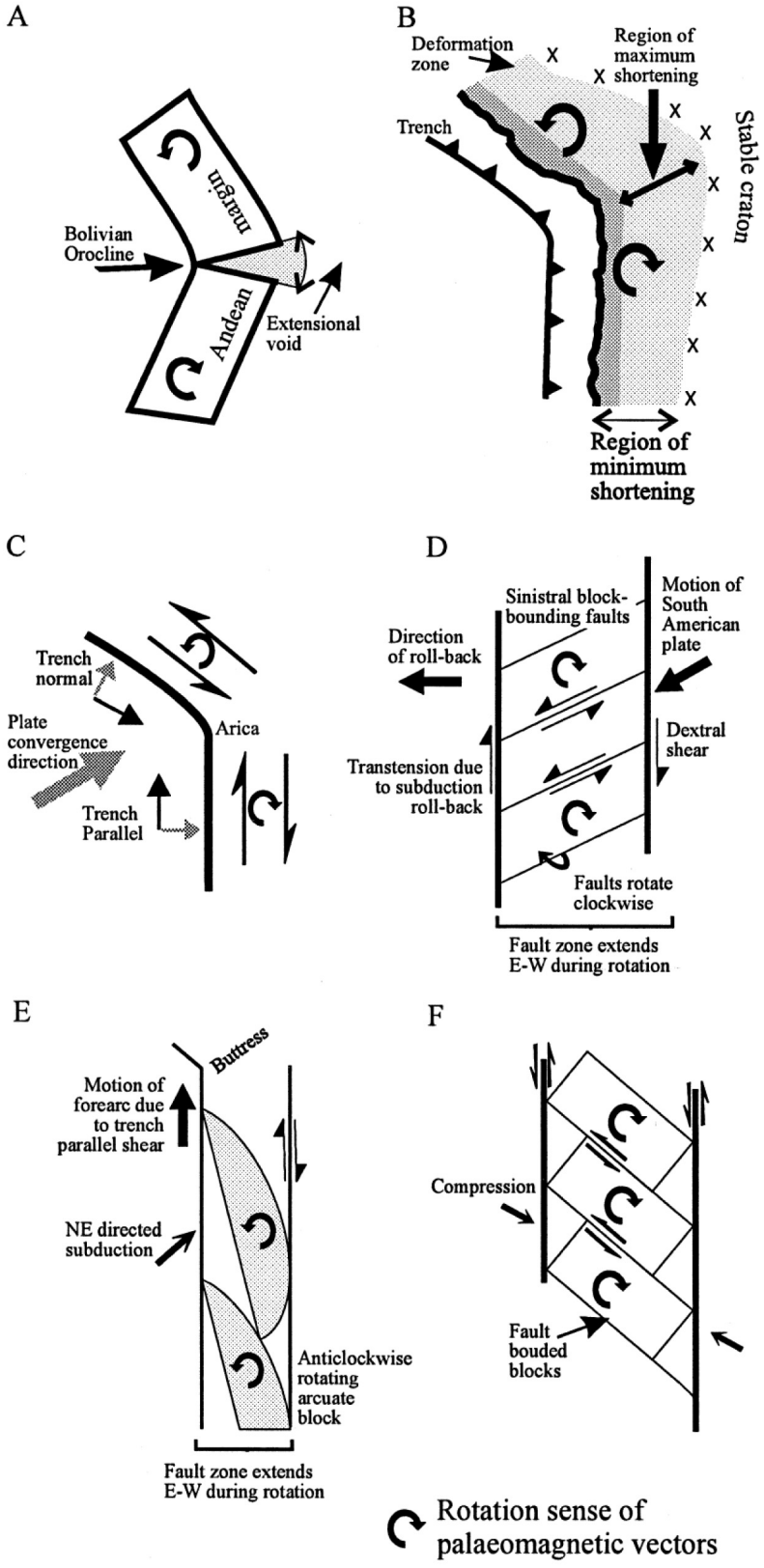

Figure I.6. Cartoons of some models proposed to explain the presence and/or pattern of rotations observed in the Andean margin (After Randall,1998). (A) Oroclinal bending (Carey, 1955). (B) Differential shortening (Isacks, 1988). (C) In situ rotation by distributed shear (Beck, 1988). (D) In situ rotation due to transtension (Hartley et al., 1988). (E) Rotation of arcuate blocks due to buttressing (Beck et al., 1993). (F) In situ block rotation due to strike-slip faulting (Randall et al., 1996).

Orientale [*Butler et al*., 1995], l'Altiplano [*MacFadden et al*., 1995; *Coutand et al*., 1999; *Roperch et al*., 2000] et l'avant arc [*Roperch et Carlier*, 1992; *Beck et al*., 1994; *Somoza et Tomlinson*, 2002; cette étude]. Bien que des modèles simples ont été avancés pour expliquer la géométrie des Andes Centrales [*Kono et al*., 1985; *Beck*, 1988; *Roperch et al*., 2000, Figure I.6] la géométrie et le style de la déformation sont très hétérogènes. Dans les paragraphes suivantes nous présenterons une synthèse des études réalisées dans l'Altiplano-Puna, le Sud du Pérou et la région d'Arica. Dans le chapitre III seront discutées les travaux conduits dans le nord du Chili au Sud d'Arica.

Rotations tectoniques dans le plateau d'Altiplano-Puna

Le modèle tectonique d'*Isacks* [1988] implique que les rotations dans les Andes Centrales devraient s'être produites pendant le Néogène. Dans le plateau d'Altiplano-Puna et la Cordillère Orientale, il y a une bonne corrélation entre le soulèvement du plateau, l'orientation des structures principales et la quantité des rotations, indiquant que ces rotations se sont produites pendant le Néogène [*MacFadden et al*., 1995; *Butler et al*., 1995; *Coutand et al*., 1999; *Roperch et al*., 2000; Figure I.7]. La corrélation entre la direction structurale et les rotations paléomagnétiques, aussi indiquée par les linéations de l'anisotropie de susceptibilité magnétique dans plusieurs sites de sédiments de l'Altiplano-Puna [*Coutand et al*., 1999], montre que ces rotations ont eu lieu pendant la derniere phase de chevauchement et non avant ou pendant le début de la déformation. La propagation vers l'Est de la déformation pendant le Néogène a provoqué la formation de la ceinture Subandine. Des rotations horaires, enregistrées par des roches Paléozoïques [*Roperch et al*., 2000] et des sédiments Oligocène-Miocène [*Lamb*, 2001] dans le sud de la ceinture sub-Andine suggèrent une rotation tectonique des directions structurales principales NNE des chevauchements pendant la phase de déformation Miocène Supérieur-Pliocène.

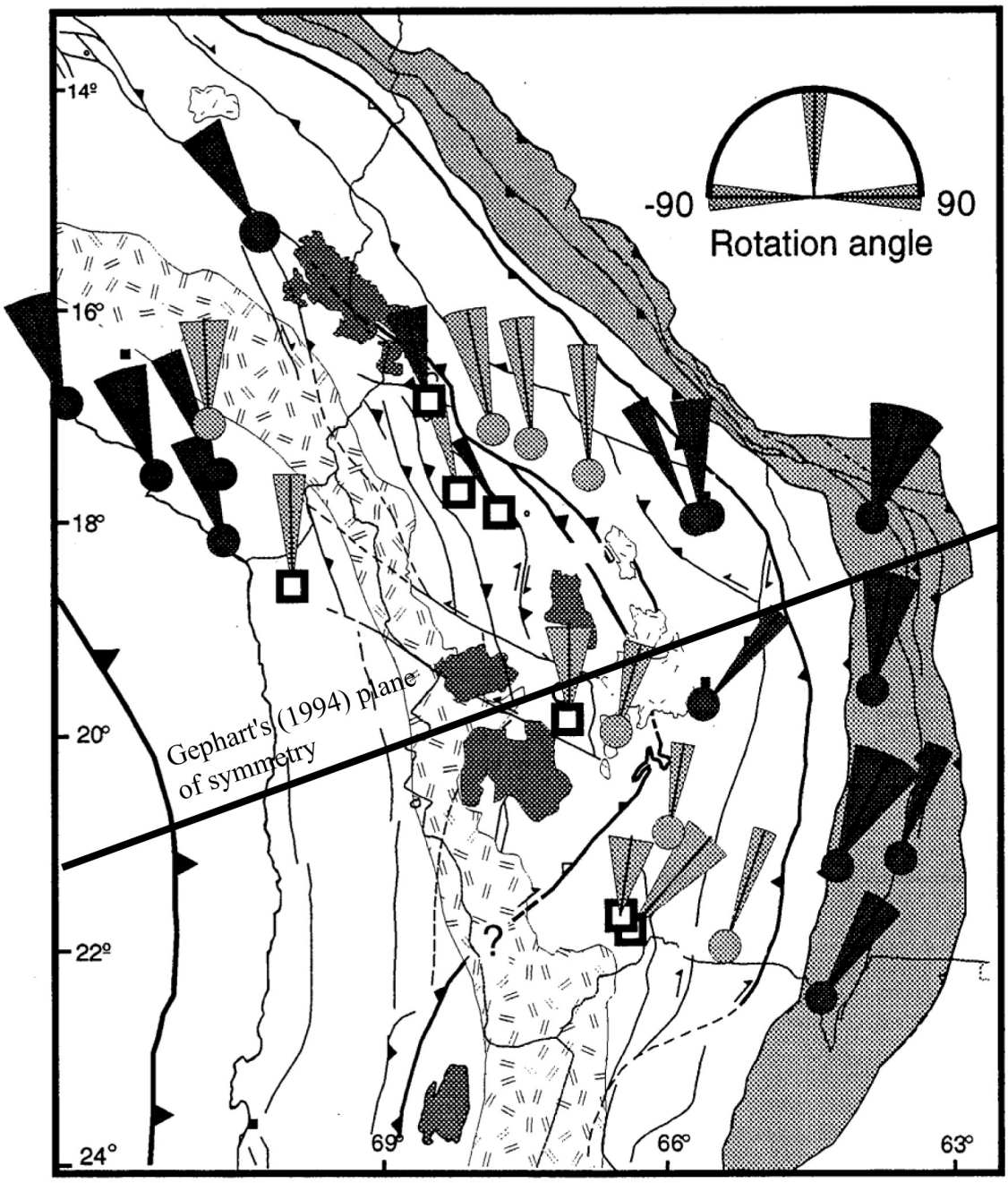

Figure I.7: Observed paleomagnetic rotations in the central Andes (After Roperch et al., 2000). Squares indicate localities from Roperch et al. (2000). Circles correspond to other studies (Roperch and Carlier, 1992; Butler et al., 1995; MacFadden et al., 1995). Rotations recorded by Miocene rocks are shown with errors at 95% highlighted by light shading, while dark shading correspond to results from older units.

Rotations tectoniques au sud du Pérou et la région d'Arica

Les résultats paléomagnétiques obtenus sur les roches volcaniques, intrusives et sédimentaires Mésozoïques et Paléocènes démontrent que l'avant arc du sud de Pérou a tourné dans le sens anti-horaire, 25º-30°, principalement comme un bloc simple qui est conforme à l'hypothèse de la courvure oroclinal [*Roperch et Carlier*, 1992; *Macedo Sanchez et al*., 1992; *Roperch et al*., 2002a, b; Figure I.8]. Aucune évidence de rotation significative n'a été trouvée immédiatement au sud de la zone de la courbure d'Arica [*Roperch et al*., 2000, 2002 a, b]. Les rotations se sont apparemment produites avant le Néogène parce que les ignimbrites d'âge Miocène Inférieur ne semblent pas enregistrer de rotation. Il faut cependant être prudent dans ces interprétations des données d'ignimbrites car le nombre relativement limité d'unités indépendantes et la présence de directions intermédiaires du champ magnétique rendent incertaine l'élimination des effets de variations séculaires. Ces nouvelles données [*Roperch et al*., 2002a, b; Figure I.8] suggèrent que la rotation principale de l'avant arc Péruvien du sud s'est produite autour de 30-25 Ma. Cette période de temps est légèrement plus jeune que celle proposée par *Roperch et al*. [1999] en associant la formation de la courbure oroclinale à la déformation de la phase Incaïque durant l'Éocène. Au lieu de cela, la rotation dans le sens anti-horaire de l'avant arc Péruvien paraît plutôt liée au début de la déformation dans la Cordillère Orientale en Bolivie. *Rousse et al*. [2002] dans un modèle alternatif de rotation pour l'avant arc du Pérou, indiquent que cette région a tourné pendant un période de déformation très courte de 2 Ma vers 8 Ma correspondant à un soulèvement rapide et à l'initiation de la déformation dans la zone Subandine pendant la phase de déformation Quechua 2. Bien que plus d'études soient nécessaires pour bien définir l'âge des rotations, la proposition d'un intervalle de temps aussi court que 2 Ma pour permettre la rotation globale de tout l'avant arc ne semble pas en accord avec les données de géologie structurale suggérant une déformation distribuée dans le temps (par exemple modèles de déformation proposés par *McQuarrie et DeCelles*, [2001]).

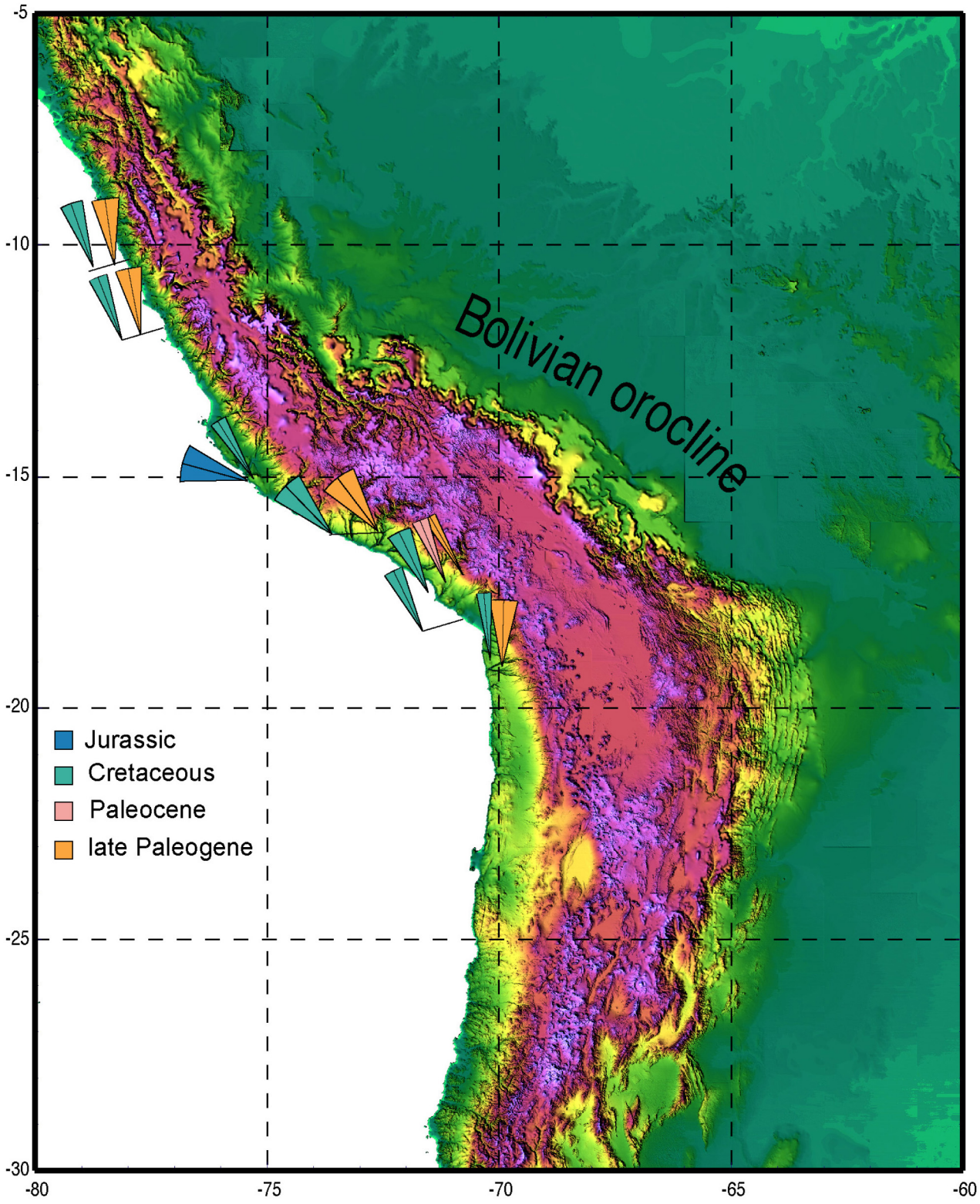

Figure I.8: Tectonic Rotations in Peru and the Arica region (after Roperch et al., 2002a, b).

Objectifs de l'étude et méthodologie

Des pages précédentes, nous pouvons déduire que l'état actuel de la connaissance des Andes Centrales, permet d'établir une vision générale, sur les processus de premier ordre, qui ont donné naissance à cette ceinture orogénique. La plupart des études tectoniques se sont concentrées autour de l'origine du plateau de l'Altiplano-Puna. Toutefois, la structure interne et l'évolution (et l'interaction entre eux) des éléments individuels qui conforment dans leur ensemble les Andes Centrales sont encore mal compris. En accord avec ce qui précède, l'objectif principal de ce travail de thèse est d'apporter, au moins en partie, de nouvelles données sur la structure de l'avant-arc du nord du Chili. De cette façon, nous essaierons d'établir quelle est l'importance de la tectonique dans cette région et sa relation dans la construction des Andes Centrales.

Dans ce contexte, pendant l'élaboration de ce travail, nous avons effectué une étude paléomagnétique et structurale détaillée dans la région d'Antofagasta au nord du Chili. L'objectif a été d'apporter des nouvelles données paléomagnétiques et structurales afin de mieux décrire et comprendre l'origine des déformations antérieures au Néogène. Notre étude inclut des roches Mésozoïques de la Cordillère de la Côte, des roches Crétacés de la Vallée Centrale, des roches Tertiaires du bord ouest de la Cordillère de Domeyko (Précordillère) et des séquences Crétacés à Paléogènes du bord oriental de la Cordillère de Domeyko.

Ainsi un vaste secteur de l'avant-arc a été étudié, et permet d'analyser les relations existantes entre les processus à l'origine des rotations horaires du nord du Chili et les processus associés à la formation de la courbure oroclinale.

Simultanément, pour caractériser le style structural qui contrôle les rotations observées dans la région d'Antofagasta, on a effectué une étude structurale et stratigraphique détaillée du versant oriental de la Cordillère de Domeyko. Cette bordure coïncide avec le bord occidental du bassin du Salar d'Atacama. Ce bassin est une caractéristique topographique de premier ordre dans le versant occidental de la Cordillère Occidentale. En même temps, le remplissage sédimentaire du bassin, permet de délimiter le temps et l'extension de la déformation produite dans l'avant-arc. Un ensemble de lignes sismiques dans le Salar d'Atacama a été mis à ma disposition par la société ENAP-SIPETROL pour cette étude.

Ces données, avec l'information de terrain, permettent de présenter un modèle de déformation pour le Crétacé-Paléogène à cette latitude de l'avant-arc.

Davantage de travail est nécessaire pour établir un modèle qui intègre toutes les données de rotations publiées des Andes Centrales. Toutefois, dans la dernière partie de cette étude on essaye d'élaborer un modèle général de l'évolution tectonique des Andes Centrales qui intègre, de manière cohérente, la déformation associée à la rotation tectonique de blocs. Dans cette partie on inclut les résultats de rotations tectoniques dans un algorithme de déformation non plane, développé par *Audibert* [1991], *Rouby et al*. [1993] et *Bourgeois et al*. [1997] pour les cas décrochant, extensif et compressif respectivement. Cet algorithme permet la restauration de la déformation d'une région. Les modifications que nous avons effectuées dans cet algorithme permettent d'introduire les résultats de rotation et la quantité de raccourcissement sur une mosaïque de blocs limités par des failles, normales ou inverses. À partir d'itérations successives qui insèrent des translations et des rotations de blocs, on obtient une mosaïque de blocs dans l'état non-déformé. Finalement, les résultats obtenus peuvent être comparés avec les modèles actuels sur l'évolution des Andes.

Chapitre II : Géologie et tectonique de l'avant arc du nord du Chili dans la région d'Antofagasta.

Introduction

Ce chapitre, présente le cadre géologique de la région d'Antofagasta. Cette présentation est une introduction générale aux études paléomagnétiques et tectoniques publiées sous forme d'articles. C'est dans la région du Salar d'Atacama que s'est concentrée la plus grande partie de mon travail sur le terrain. C'est en effet dans cette région, et plus particulièrement le long de la bordure orientale de la Cordillère de Domeyko que l'on trouve probablement les meilleurs affleurements du nord du Chili. D'autre part, la compagnie SIPETROL a mis à notre disposition un ensemble complet des lignes sismiques acquises dans la grande dépression du Salar d'Atacama. Ainsi, l'évolution tectonique de l'avant arc du nord du Chili est bien décrite pour cette région. En accord avec ce qui précède, nous avons effectué une étude détaillée de la stratigraphie et la tectonique de la région du Salar d'Atacama, qui se trouve dans la partie Publications de ce chapitre.

Contexte général

Depuis le Paléozoïque Supérieur, l'évolution de la marge occidentale de Gondwana est le résultat de l'interaction entre la plaque Sudaméricaine et les systèmes de plaques de l'Océan Pacifique. Deux grands cycles orogéniques sont reconnus pour le Phanérozoïque : le Cycle Préandin Hercynien du Paléozoïque et le Cycle Andin du Méso-Cénozoïque [*Coira et al*., 1982].

Le Cycle Préandin

Au cours de ces dernières années, l'évolution du Paléozoïque des Andes Centrales a été le sujet de considérable débats. Selon certains auteurs [*Ramos*, 1988, 1995; *Unrug*, 1996; *Astini et al*., 1995], la marge Pacifique actuelle de l'Amérique du Sud correspond à un ensemble de terrains allochtones qui ont été accrétés au Gondwana pendant le Protérozoïque et/ou pendant le Paléozoïque Inférieur à Moyen. Un scénario tectonique possible est l'échange de terrains entre les cratons de l'Amérique du Sud (Gondwana) et de l'Amérique du Nord (Laurentia) durant la collision qui a formé le super continent hypothétique de Rodinia [*Wasteneys et al*., 1995; *Tosdal*, 1996; *Dalziel*, 1997]. La séparation ultérieure a été suivie par une seconde collision entre Laurentia et Gondwana pendant l'orogenèse Famatiniene de l'Ordovicien Moyen dans les Andes et l'orogenèse Taconiene dans les Appalaches [*Dalziel et al*., 1994]. Une modification des derniers

modèles place un petit océan entre Laurentia et l'Amérique du Sud avec des arcs dans, ou en avant des marges respectives au cours de l'Ordovicien Inférieur. *Dalziel*, [1997] suggère la possible collision d'une plateforme continentale dérivée de Laurentia qui inclut la Précordillère de l'Argentine au cours de l'Ordovicien Moyen. Ces reconstructions tectoniques globales de l'histoire Paléozoïque des Andes Centrales se basent principalement sur l'interprétation du registre sédimentaire et faunistique, sur l'évolution tectono-magmatique des bassins et sur les données paléomagnétiques [*Astini et al*., 1995; *Unrug*, 1996; *Tosdal*, 1996; *Dalziel*, 1997].

D'un point de vue pétrologique, l'interprétation de l'histoire métamorphique résultante des événements d'accrétion n'est pas possible à cause du manque de données fiables. Dans les Andes Centrales, les affleurements des roches métamorphiques sont peu nombreux, mais observés depuis la Cordillère de la Côte jusqu'à la zone subandine (Figure II.1). Dans le nord du Chili, les affleurements continus n'existent pas [*Damm et al*., 1990, 1994]. En Argentine des roches métamorphiques, de basse température-haute pression, sont décrites dans la région de la Puna [*Viramonte et al*., 1993; *Miller et al*., 1994] et dans les Sierras Pampeanas [*Rapela et al*., 1990; *Miller et al*., 1994]. Ces roches appartiennent à la Formation Puncoviscana (et équivalents) du Précambrien Supérieur au Cambrien Inférieur.

Les affleurements de socle métamorphique du nord du Chili (Figure II.1) ont des caractéristiques lithologiques et les mêmes relations de contact avec les sédiments ou les roches ignées post-métamorphiques. Les métasédiments riches en quartz et les orthogneis granitiques à dioritiques sont dominants, tandis que les affleurements de métabasites correspondent à moins de 5% des affleurements de roches du socle dans le nord du Chili. Le socle est affecté d'une foliation pénétrative importante, d'orientation générale NS témoigne d'une déformation ductile, alors que les roches intrusives du Paléozoïque Supérieur ne montrent pas de déformation ductile pénétrative. Ces magmas dioritiques à granitiques ont été mis en place dans les niveaux supérieures des roches métamorphiques et sédimentaires [*Breitkreuz et al*., 1989; *Lucassen et al*., 1999].

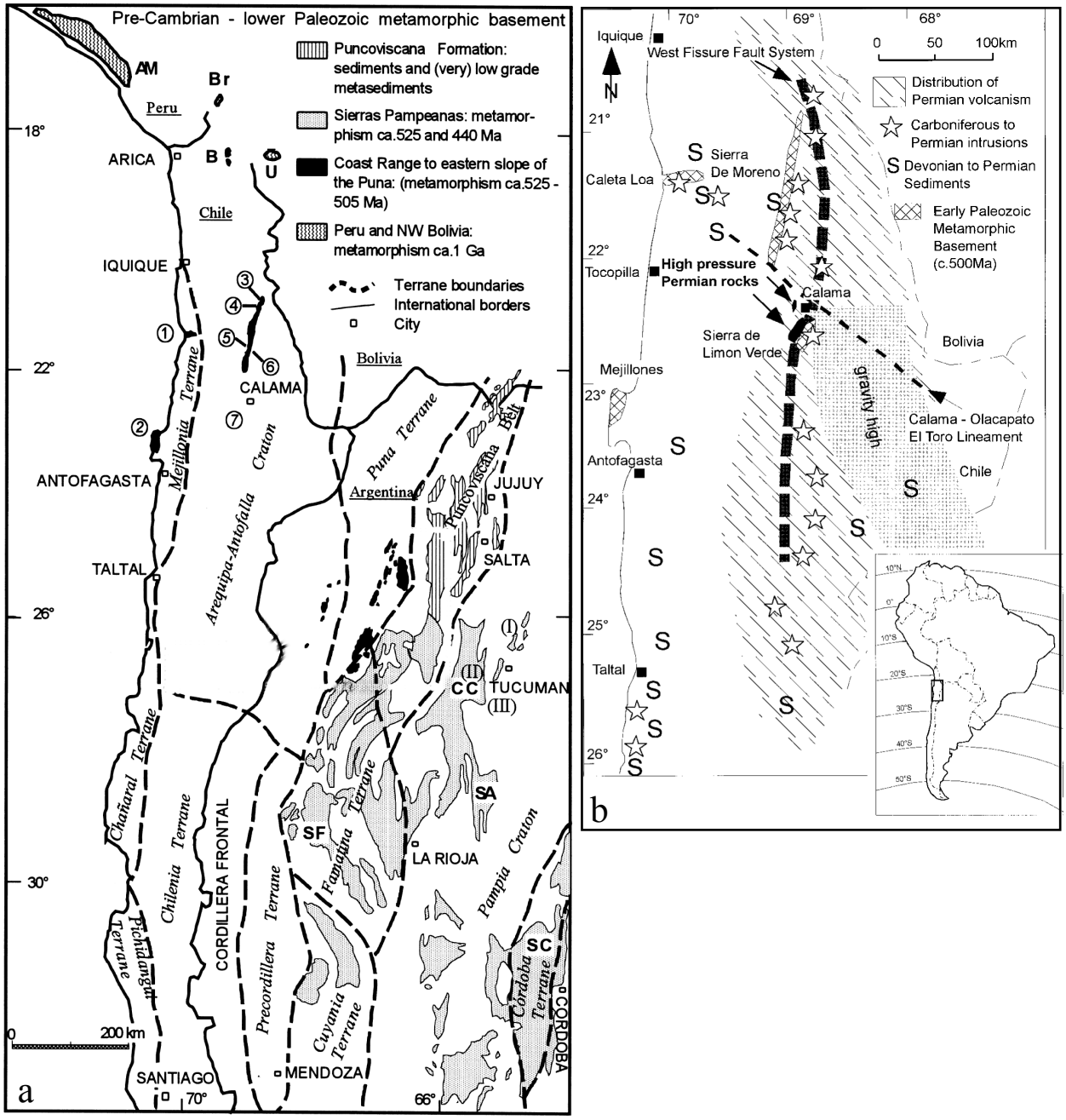

Figure II.1: a. Map of the major Precambrian to Early Paleozoic units in N. Chile and NW Argentina after Lucassen et al. [2000]: 1, Caleta Loa; 2, Mejillones; 3 to 6, Sierra de Moreno (3, Quebrada Choja; 4, Tambillo o Seca; 5, Quebrada Arcas; 6, Quebrada Quinchamale, parallels the eastern slope of southern Sierra de Moreno); 7, Sierra Limón Verde, (I)=Sierra de Medina, (II)=Cumbres Calchaquies, (III)=Las Viñas. Other locations (from N to S) are: AM, Arequipa Massif; Br, Berenguela; B, Belen-Tignamar; U, Uyarani; CC, Cumbres Calchaquies; SA, Sierra de Ancasti; SF, Sierra Fiambalá; SC, Sierras de Córdoba. Terrane boundaries (dashed lines) and terminology are from Ramos [1995]. b. Geological sketch showing the distribution of Early to Late Paleozoic rocks in northern Chile, after Lucassen et al. [1999].

La Figure II.2 montre un résumé des différents événements magmatiques et métamorphiques pendant le Protérozoïque et le Paléozoïque. Le Cycle Pampéen avec son métamorphisme de haut grade entre les 500-525 Ma a été le plus grand événement de formation de la croûte continentale [*Lucassen et al*., 2000]. Dans les roches métamorphiques de la Cordillère de la Côte, les âges K-Ar en biotite et hornblende sont rajeunis par la mise en place de l'arc Jurassique. Dans la Cordillère de Domeyko, la plupart des âges vont de 420 à 300 Ma pour les hornblendes et entre 300 à 270 Ma pour les biotites, démontrant ainsi une importante activité magmatique autour de 300 Ma [*Lucassen et al*., 1999]. Aux latitudes 21-26ºS, la similitude pétrologique et les relations d'âge pour les roches du socle de haut grade a permis de préciser les scénarios géodynamiques du Protérozoïque Supérior-Paléozoïque Inférieur pour cette ancienne marge continentale du Gondwana. Les nouvelles données isotopiques de *Lucassen et al*. [2000] indiquent un développement semblable du socle métamorphique entre le sud du Massif d'Arequipa (18ºS) et le nord de la Précordillère de l'Argentine (28ºS). Un modèle de croissance de la marge Pacifique au nord de la Précordillère de l'Argentine, par accrétion de différents terrains exotiques pendant le Paléozoïque Inférieur, n'est pas en accord avec les derniers résultats d'âges de métamorphisme obtenus. *Lucassen et al*. [2000] indiquent qu'il n'y a-t-il pas une zone claire d'accrétion dans la marge entre les 18-26ºS, et proposent un modèle de "Ceinture Mobile" pendant le Cycle Pampéen (Figure II.3). L'exhumation du socle, entre 400 et 300 Ma, est aussi associée aux discordances du Dévonien.

Du Dévonien au Carbonifère, l'activité magmatique dans le nord du Chili diminue d'intensité. Ce magmatisme et le type de bassins sédimentaires développés dans cette période ont été interprétés comme les témoins d'une marge passive [*Bahlburg et Hervé*, 1997]. Par contre, l'activité magmatique du Paléozoïque Supérieur est amplement distribuée et correspond aux intrusions de roches granitiques et à la mise en place de roches volcaniques, à partir de magmas crustaux [*Breitkreuz et al*., 1989; *Lucassen et al*., 1999]. Au Carbonifère et Permien Inférieur se sont déposés des sédiments marins carbonatés à l'ouest de l'arc de la Puna et des sédiments continentaux rouges à l'est. Du Permien au Trias, le magmatisme et le volcanisme riche en silice est surtout développé à l'ouest de l'actuelle Cordillère Occidentale. Pendant cette période se développent aussi des bassins sédimentaires en extension [*Charrier*, 1979 ; *Suarez et Bell*, 1992].

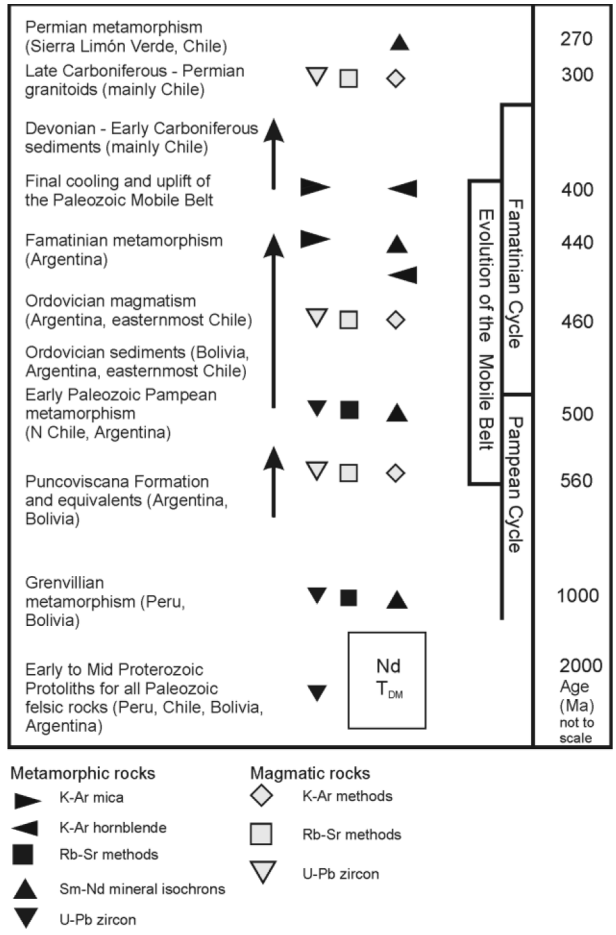

Figure II.2: Principal sedimentary, magmatic and metamorphic events known from the Premesozoic basement in the Central Andes in S. Peru, N. Chile, SW Bolivia and NW Argentina, after Lucassen et al. [2000].

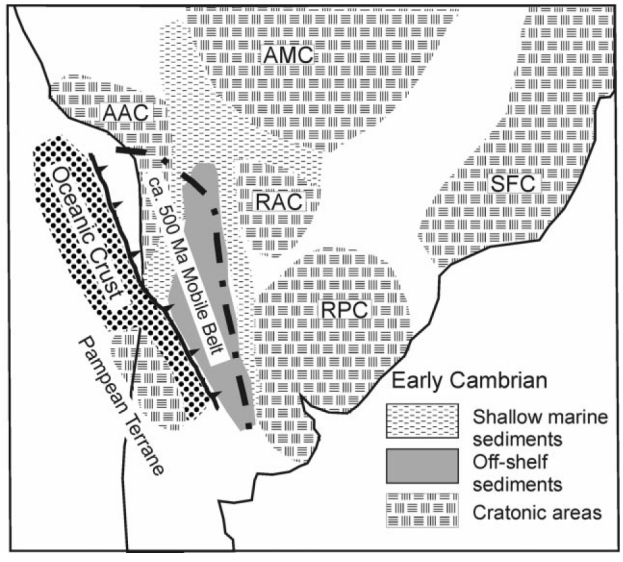

Figure II.3: Possible geodynamic scenario of the Early Cambrian, after Lucassen et al. [2000] with the distribution of cratonic areas (Grenvillian or older) and position of the later mobile belt, which formed during the Early Paleozoic and completely reworked the southern part of the hypothetical Arequipa-Antofalla craton (AAC). Shallow marine and off-shelf Early Cambrian sediments age were deposited in the Puncoviscana basin. A subduction zone and oceanic crust north of the Pampean Terrane cannot be identified and are therefore hypothetically placed west of the present coas line. Other cratonic areas are: AMC, Amazonian; RAC, Rio Apa; SFC, San Francisco; RPC, Rio de la Plata.

Cycle Andin

Pendant le Mésozoïque et le Cénozoïque, les roches de socle et les structures Paléozoïque des Andes Centrales sont fortement reprises par les événements tectoniques et magmatiques du Cycle Andin. L'importance du volcanisme Jurassique et Crétacé est en faveur de l'hypothèse d'une subduction plus ou moins continue des plaques océaniques du Pacifique Oriental sous les Andes. La connaissance des paramètres de convergence de plaque est assez incertaine pour le Jurassique et le Crétacé. Au cours du Cénozoïque, les variations de vitesse, d'obliquité et l'angle de plongement du slab sont des facteurs importants et fortement corrélés aux changements de style de déformation le long de la marge. Dans l'avant arc du nord du Chili, le magmatisme induit par subduction a été actif depuis au moins 180 Ma [*Coira et al*., 1982]. Il est possible de distinguer plusieurs étapes magmatiques (Figure II.5,6,7&8) :

- un arc Jurassique-Crétacé Inférieur (180-120 Ma) dans la Cordillère de la Côte.
- un arc Crétacé Moyen (110-85 Ma) dans la Vallée Centrale.
- un épisode volcanique dans la dépression centrale dans le Crétacé Supérieur (85-65 Ma).
- un arc principalement Paléocène (65-55 Ma) le long de la pente ouest de la Cordillère de Domeyko [*Scheuber et González*, 1999; *Marinovic et García*, 1999; *Cortés*, 2000].
- les épisodes magmatiques les plus jeunes dans la région de l'avant arc, d'âge Éocène à Oligocène Inférieur, correspondent à la mise en place d'une série de stocks superficiels le long de l'axe de la Cordillère de Domeyko, incluant certains des porphyres cuprifères géants du nord du Chili [*Cornejo et al*., 1997].

D'un point de vue tectonique, un nombre croissant de travaux stratigraphiques, structuraux et paléomagnétiques montrent l'existence de raccourcissements du Crétacé au Paléocène dans le nord du Chili [*Chong et Reutter*, 1985; *Bogdanic*, 1990; *Hammmerchschmidt* et al., 1992; *Hartley et al*., 1992; *Scheuber et Reutter*, 1992; *Charrier et Reutter*, 1994; *Mpodozis et al*., 1999; *Somoza et al*., 1999; *Arriagada et al*., 2000, 2002, 2003].

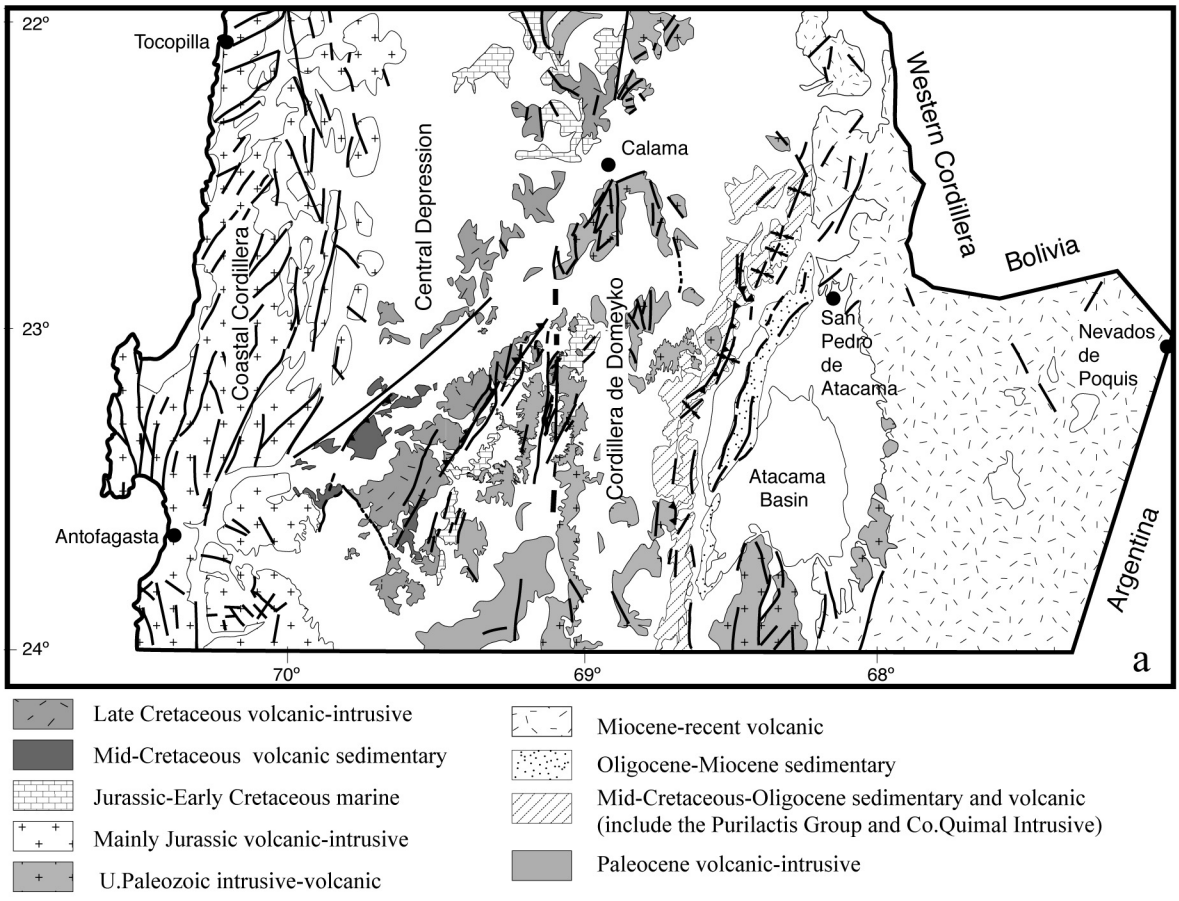

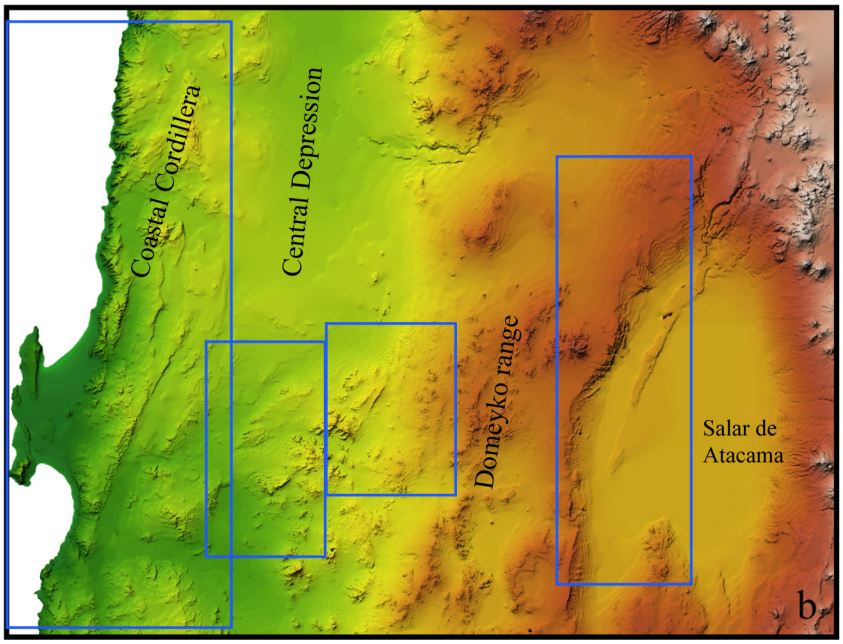

Figure II.5: a. Simplified geological map of the Antofagasta region (after Mapa Geologico (1:1000.000), SERNAGEOMIN Chile (1982); Marinovic and García, (1999); Cortez, (2000); Basso, (in prep.); this study). b. Digital elevation model of the Antofagasta region showing main morphostructuralunits and location of the figures II.6, 7,8&9.

Géologie de la Cordillère de la Côte

Stratigraphie

La géologie de la Cordillère de la Côte est principalement déterminée par des laves andésitiques et des plutons d'un arc magmatique qui a été actif du Jurassique au Crétacé Inférieur (Figures II.5&II.6). Le socle Paléozoïque composé de micaschistes et gneiss d'age 520 et 560 Ma affleure principalement dans la partie nord de la Péninsule de Mejillones (Fms. Punta Angamos y Jorgino; [*Baeza et Pichowiak*, 1988]). Dans la partie orientale de la Cordillère de la Côte (Figure II.7), des sédiments volcano-détritiques du Trias et des roches marines du Lias au Sinémurien (Formation Rencoret; [*Ferraris et Di Biase*, 1978; *Muñoz et al*., 1989]) sont recouvert d'une séquence de laves de composition basaltique à andésitique de quelque 3 à 10 km d'épaisseur (Formation La Negra). Cette relation permet donc de donner un âge maximum Jurassique Inférieur à la Formation La Negra.

Les plutons qui intrudent la séquence volcanique de la Formation La Negra sont des gabbros ou des granodiorites. Les premiers plutons commencent à se mettre en place autour des 180 Ma. Cependant, le plutonisme est surtout intense entre le Jurassique Moyen et le Crétacé Inférieur (160-120 Ma) [*Boric et al*., 1990]. Les rapports initiaux $^{87}Sr/^{86}Sr$ de l'ordre de 0.703 [*Diaz et al*., 1985; *Hervé et Marinovic*, 1989] dans les roches intrusives excluent la possibilité d'une contamination corticale significative. Les relations de contact des roches intrusives, ainsi que ses textures montrent que les profondeurs de mise en place sont faibles (< 10 km) [*Damm et Pichowiak*, 1981]. Toutefois, au sud d'Antofagasta et au sud de Mejillones, un niveau crustal plus profond d'environ 12-15 km est à l'affleurement [*Rössling*, 1988], qui consiste en des roches intrusives basaltiques et des roches métamorphiques de composition dioritique et des migmatites (Bolfin Complex, d'âge probable Jurassique Inférieur).

Au sud d'Antofagasta, la Formation La Negra est recouverte en concordance par des sédiments clastiques de la Formation Caleta Coloso et des roches marines d'âge Crétacé Inférieur (Fm. El Way, Hauterivian-Aptian, Figure II.6). Des sédiments non consolidés d'âge principalement Miocène ("Graviers du Pampas") sont en discordance sur les unités plus anciennes. Dans la Péninsule de Mejillones ces unités passent à des sédiments marins de la Formation La Portada (Miocène) et Formation Mejillones (Pliocène).

Structure Régionale

L'arc magmatique de la Cordillère de la Côte est coupée longitudinalement par le Système de Failles d'Atacama. Ce système présente une association complexe de mylonites d'orientation NS avec des zones cataclastiques et une déformation fragile visible le long de la Cordillère de la Côte du nord du Chili, entre les 22 à 29ºS [*Hervé*, 1987; *Scheuber et Adriessen*, 1990; *Grocott et al*., 1994; *Scheuber et González*, 1999]. Le Système de Faille d'Atacama a une longue histoire de déformation entre le Jurassique Inférieur et le Cénozoïque. *Scheuber et González*, [1999], ont suggéré que les structures de l'arc magmatique Jurassique à Crétacé Inférieur se sont développées suivant quatre étapes. Dans la première étape (entre 195-155 Ma), le mouvement est senestre et parallèle à l'arc. Dans la seconde étape (160-150 Ma), il y a eu une forte extension normale à l'arc. Dans la troisième (155-147 Ma), un changement du régime des contraintes est indiqué par deux générations de dikes ; la plus ancienne d'orientation NE-SW et une plus jeune d'orientation NW-SE. Les indicateurs de déplacements senestres enregistrés par la déformation ductile pendant la quatrième étape (jusqu'à ~125 Ma) ont conduit plusieurs auteurs à considérer la Faille d'Atacama comme un exemple de "trench-linked left-lateral fault". Pendant le Crétacé Supérieur et le Cénozoïque, la déformation fragile est surtout normale avec une composante décrochante dextre ou senestre suivant la relation entre l'orientation des failles et la direction d'extension [*Hervé*, 1987; *Delouis et al*., 1998].

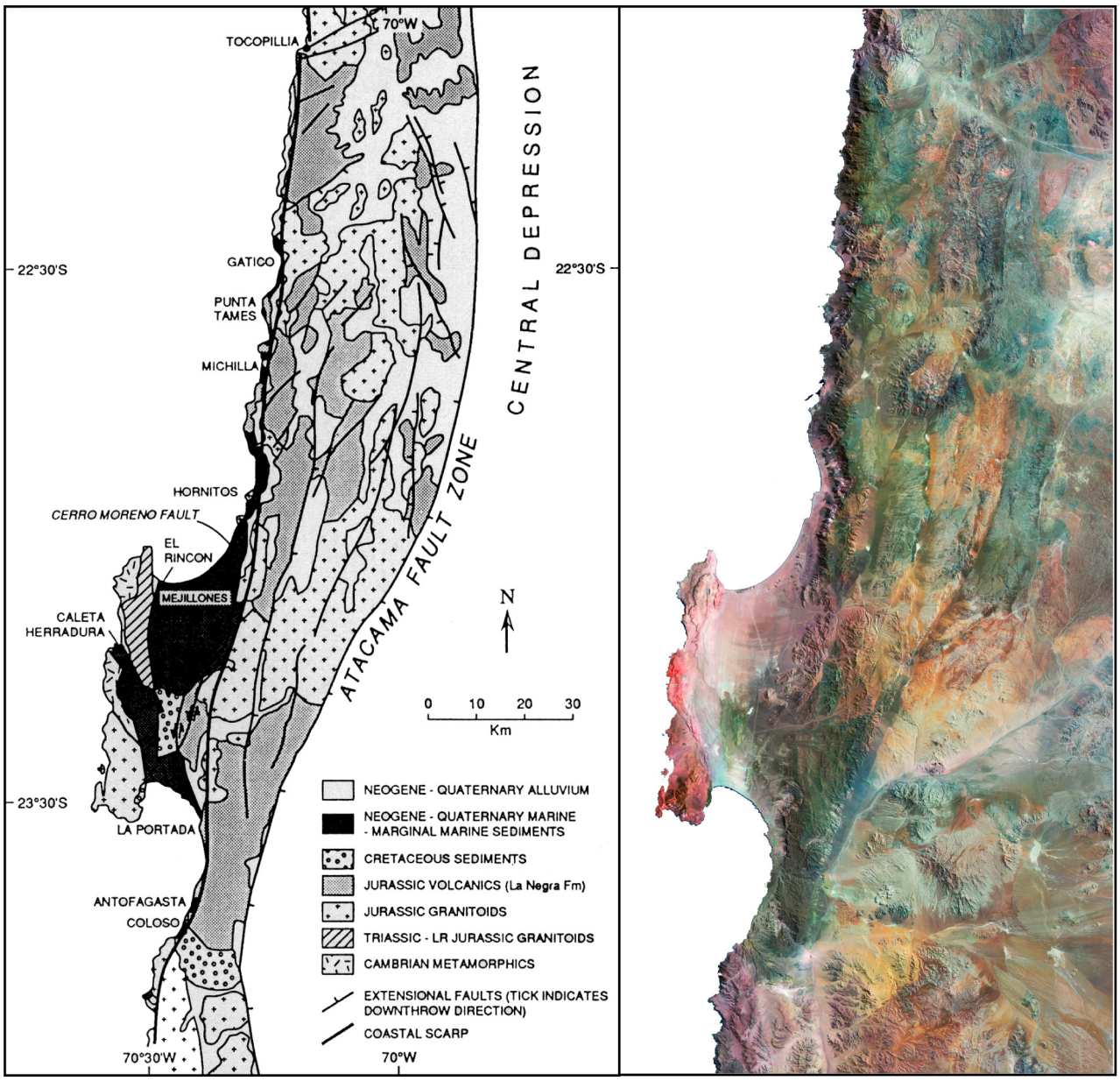

Figure II.6: Geological map and Landsat image of the Coastal Cordillera of northern Chile between 22 and 24ºS (after Hartley and Jolley, 1995).

Géologie de la Vallée Centrale dans la région d'Antofagasta

Stratigraphie

La Vallée Centrale est morphologiquement peu développée dans la région d'Antofagasta au sud de la Route d'Antofagasta-Calama (Figure II.5). Cependant, plus au nord, la région de Pampa del Tamarugal est une large dépression remplie de sédiments provenant de la Cordillère de Domeyko et la Cordillère de la Côte. Le long du bord occidental de la Vallée Centrale, les rares affleurements de roches sédimentaires du Paléozoïque Supérieur sont recouverts en discordance pour une séquence marine d'âge Triasique Supérieur à Jurassique Inférieur (Formation Rencoret, *Cortés*, [2000]; Figura II.7) avec des fossiles de l'Hetangien-Sinemurien. Ces séquences sont couvertes par des roches andésitiques de la Formation La Negra. Plus à l'Est, ces laves ne sont pas présentes, mais on trouve une séquence volcanique continentale d'age Crétacé Moyen (Formation Paradero del Desierto, *Cortés*, [2000]), sous-jacente à la Formation Quebrada Mala (voir description ci-dessous). Le long de la bordure occidentale de la Cordillère de Domeyko, une puissante séquence de sédiments Jurassiques marins (Groupe Caracoles, *Marinovic et García*, [1999]) s'est accumulée dans un bassin arrière-arc associé à l'arc Jurassique-Crétacé Inférieur de la Cordillère de la Côte (bassin de Tarapaca, *Mpodozis et Ramos* [1990]; Figure II.7,8). La partie supérieure de la séquence est constituée de sédiments continentaux rouges d'age Jurassique Supérieur à Crétacé Inférieur. Les roches du Groupe Caracoles sont recouvertes en discordance par une séquence, d'environ 3 km d'épaisseur, constituée de sédiments continentaux et de roches volcaniques (Formation Quebrada Mala), déposée entre les 85-65 Ma [*Marinovic et García*, 1999]. Le batholite de la Sierra del Buitre correspond à des monzodiorites et granodiorites avec des âges K-Ar et $^{39}Ar/^{40}Ar$ entre les 74-66 Ma [*Cortés*, 2000]. À l'Est de la Sierra del Buitre, les unités Mésozoïques sont recouvertes par quelque 500 m conglomérats, des ignimbrites et des laves andésitiques de la Formation Cinchado d'âge Paléocène (63-55 Ma ; Figure II.8). Localement la Formation Cinchado est recouverte par de faibles flux de laves et d'ignimbrites de la Formation Cerro Casado (48-45 Ma) [*Marinovic et García*, 1999]. Les deux unités sont séparées par une faible discordance angulaire.

Structure Régionale

La Vallée Centrale est traversée par plusieurs failles et linéaments d'orientation NE-NNE. La caractéristique structurale la plus importante est un grand linéament qui est parallèle à la

Route d'Antofagasta-Calama "Linéament Antofagasta-Calama" (Figure II.5, 7, 8). Vers le SE de ce linéament, la Sierra del Buitre est un bloc structurellement soulevé constitué principalement par des roches Mésozoïques. La Faille Sierra del Buitre est un système de failles imbriquées inverses, de vergence Est, qui se trouve immédiatement à l'Est de la Sierra del Buitre (Figure II.8), et fait chevaucher la Formation Quebrada Mala sur le Groupe Caracoles. Cette faille, probablement normale lors du dépôt des roches de la Formation Quebrada Mala, est ensuite réactivée en faille inverse pendant la fin du Crétacé Supérieur-Paleocène Inférieur [*Marinovic y García*, 1999].

Plusieurs épisodes de déformation affectent les roches Mésozoïques pendant le Crétacé. La déformation dans le Groupe Caracoles, particulièrement bien marquée dans les niveaux de roches calcaires et évaporites et caractérisée par des plis de grande longueur d'onde, est partiellement antérieure au dépôt de la Formation Quebrada Mala. La déformation dans la Formation Quebrada Mala se caractérise par des plis symétriques, avec des axes subhorizontaux d'orientation N10-N50ºE. Finalement, la Formation Cinchado est déformée principalement par des plis ouverts avec des amplitudes de plusieurs centaines de mètres.

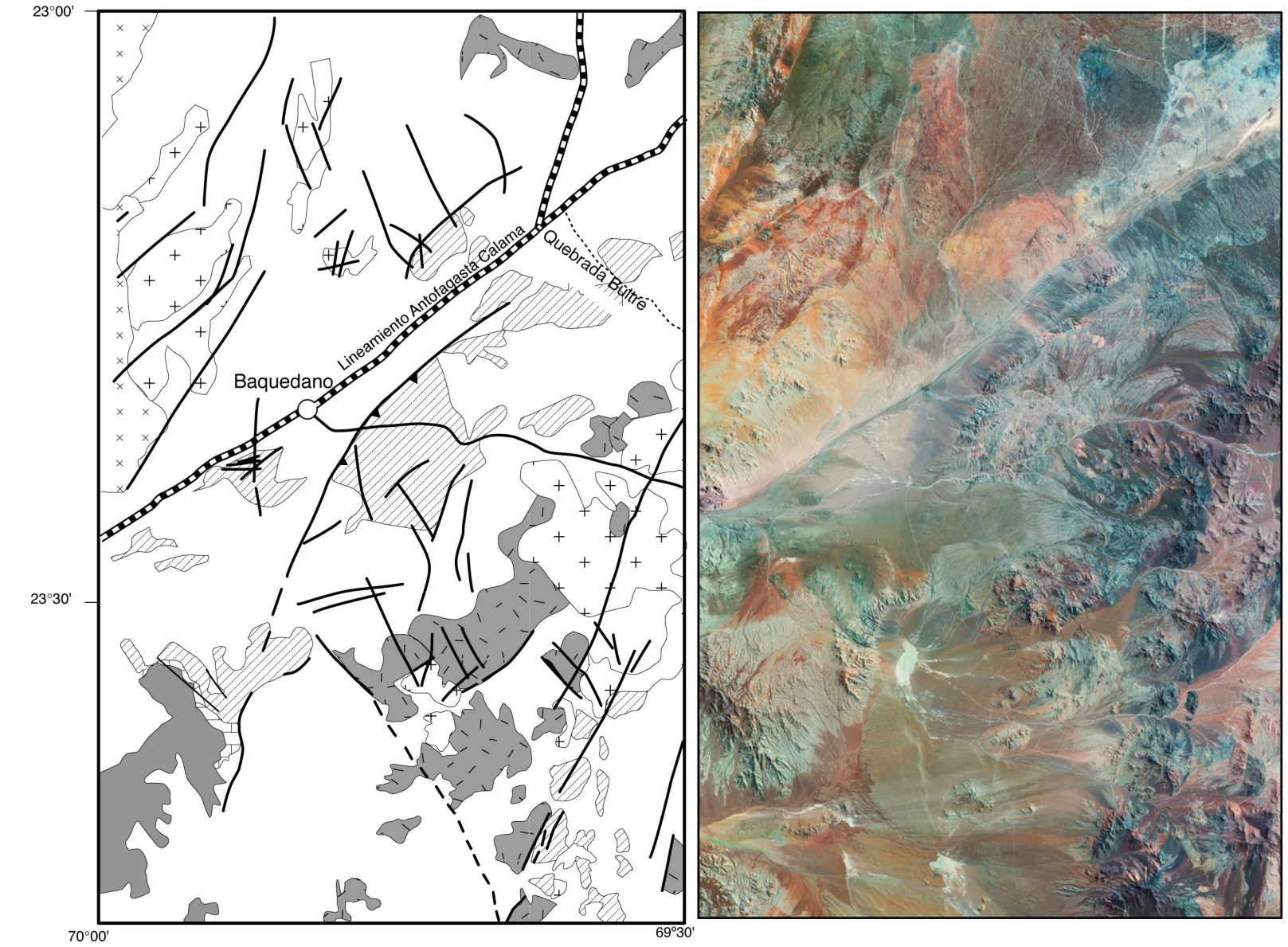

Figure II.7: Geology of the Baquedano area, western Central Valley (after Marinvic and García [1999], Cortes [2000] and this study).

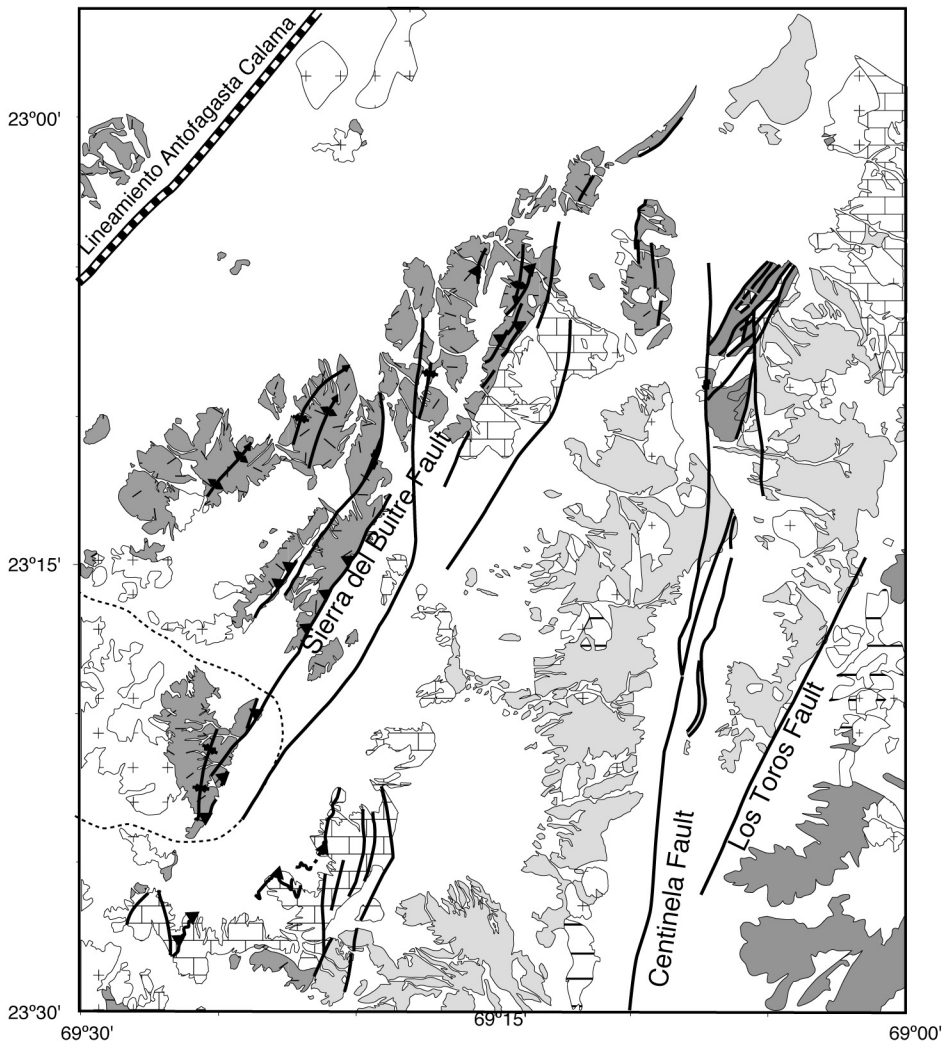

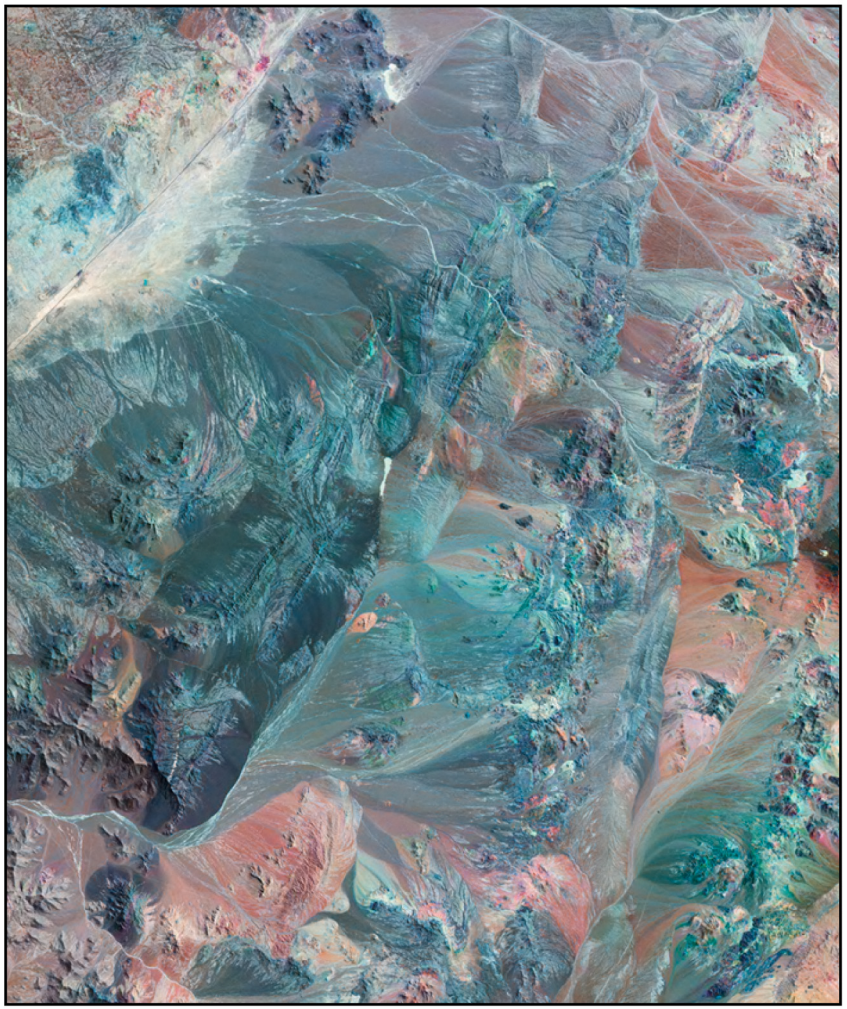

Figure II.8: Geology and Landsat image of the Sierra del Buitre area, eastern Central Valley (after Marinovic and García [1999] and this study).

Géologie de la Cordillère de Domeyko dans la région d'Antofagasta

Stratigraphie

La Cordillère de Domeyko, à l'Est de la Dépression Centrale, est séparée de la Cordillère Occidentale par la Dépression Préandine. La couverture du socle de la Cordillère de Domeyko est constituée par des roches volcaniques et des sédiments d'âge Carbonifère Supérieur à Triasique [*Coira et al*., 1982; *Reutter et al*., 1988; *Mpodozis et al*., 1993]. Dans le secteur de Limón Verde, les roches métamorphiques d'âge probable Ordovicien [*Baeza et Pichowiak*, 1988] sont intrudées par des magmas granitiques pendant le Carbonifère Supérieur et le Permien [*Pichowiak et al*., 1990]. La bordure orientale de la Cordillère de Domeyko, coïncide avec un escarpement topographique d'environ 900 m de hauteur (l'Escarpe del Bordo, Figure II.9, voir Publications ci-après). Cet escarpement (environ 120 km et d'orientation nord-sud) correspond à la bordure occidentale du bassin de Salar d'Atacama. Une épaisse séquence sédimentaire déposée entre le Crétacé Inférieur et l'Éocène est en discordance sur le socle Paléozoïque de la Cordillère de Domeyko. Cependant, dans certains secteurs (Cerro Negro par exemple), les roches du Paléozoïque sont en contact par faille inverse sur les unités Mésozoïque. Les changements de facies importants observés le long de l'escarpement (grès, conglomérats, évaporites, intercalations de coulées volcaniques) associés à des données chronostratigraphiques peu nombreuses rendent difficiles les corrélations entre les différentes descriptions de cette séquence [*Dingman*, 1963; *Ramírez et Gardeweg*, 1982; *Hartley et al*., 1992; *Flint et al*., 1993; *Charrier et Reutter*, 1994; *Mpodozis et al*., 1999]. Les nouvelles données géochronologiques obtenues au cours de ce travail nous ont permis de proposer une nouvelle interprétation des environnements de dépôts qui fait l'objet d'un projet de publication en anglais (ci dessous).

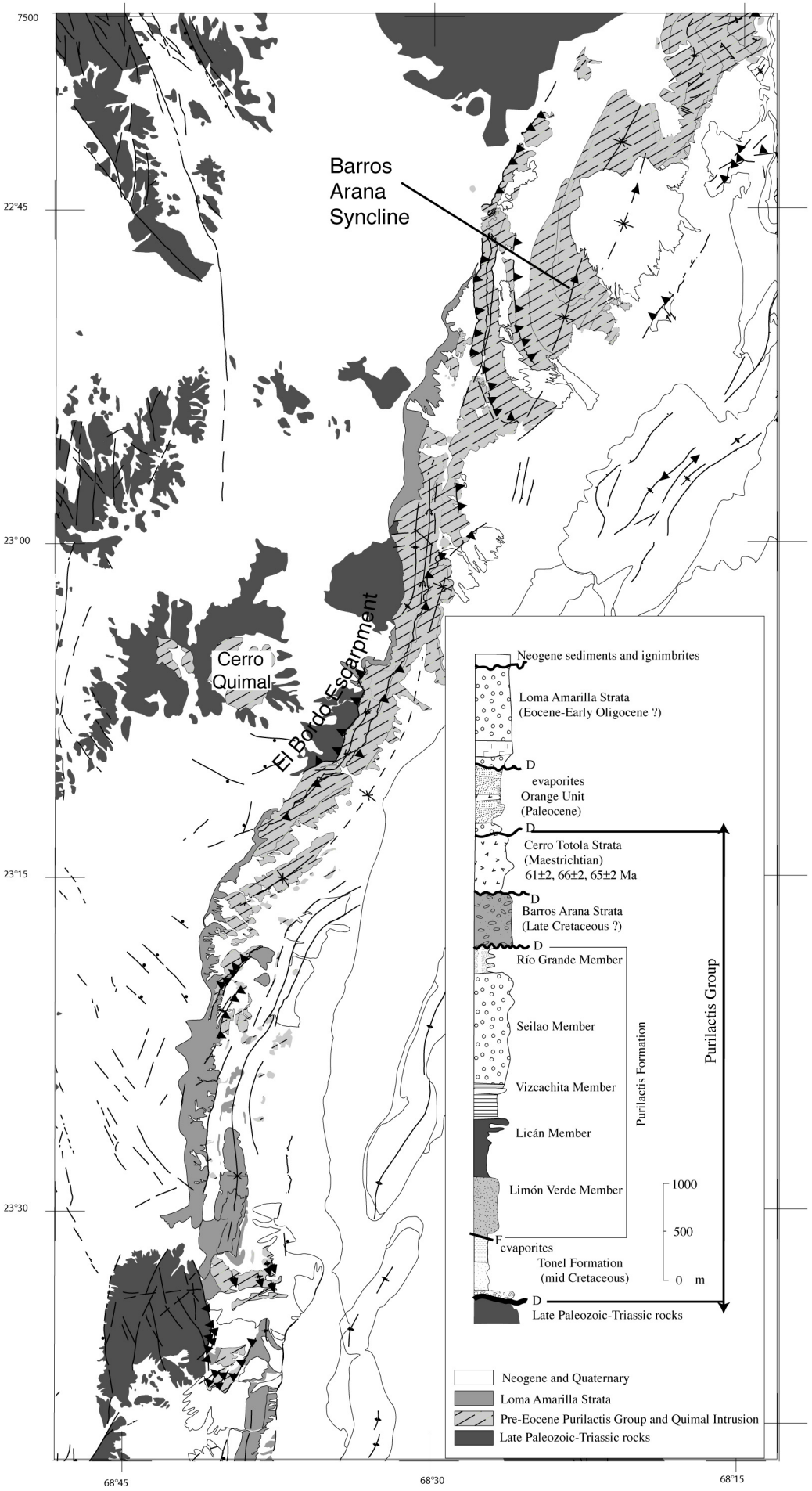

Figure II.9: Simplified geological map and stratigraphy for the western edge of the Salar de Atacama basin (see Publications for details).

Structure Régionale

La caractéristique structurale principale de la Cordillère de Domeyko est le Système de Failles de Domeyko (SFD). Les mouvements transpressifs dans le SFD ont été documentés dans l'Éocène Supérieur et probablement dans l'Oligocène Inférieur au sud de Calama, bien que le déplacement ne dépasse probablement pas les ~2 km [*Mpodozis et al*., 1993; *Tomlinson et al*., 1994]. Au sud de Calama, cependant, la déformation Éocène (Incaïque) est représentée par un ensemble de failles à vergence Ouest et Est, qui ont soulevé des blocs de socle et ne montrent pas une composant significative de déplacement décrochant [*Tomlinson et Blanco*, 1997a]. Après les ~31 Ma, une période de déplacements senestres est bien documentée pour le secteur au nord de Calama, par la mise en évidence d'un déplacement de quelques 35 km dans la région de Chuquicamata-El Abra (Falla Oeste ou West Fissure). Cette faille semble avoir été active jusqu'au Miocène Moyen [~17 Ma; *Reutter et al*., 1996; *Dilles et al*., 1997; *Tomlinson et Blanco*, 1997b]. Des systèmes imbriqués de failles inverses, des plis serrés et renversés caractérisent la déformation compressive d'âge Crétacé-Paléogène. Selon certains auteurs [*Chong*, 1977; *Scheuber et Reutter*, 1992], les déplacements accumulés sur certaines failles inverses sont supérieurs à 5 km. Bien qu'il soit encore nécessaire d'effectuer davantage d'études, les estimations préliminaires de raccourcissement de la région sont supérieures à 25% [*Scheuber et Reutter*, 1992].

Au sud du linéament Antofagasta-Calama, la Cordillère de Domeyko est limitée à l'ouest par la Faille Centinela d'orientation NS. Celle-ci a été interprétée comme une des failles principales du SFD [*Mpodozis et al*., 1993]. Des mouvements décrochantes de type senestre peuvent être générés à partir d'un duplex compressif visibles le long de la partie nord de cette faille [*Marinovic et García*, 1999]. À l'est de la Faille Centinela, la Formation Cinchado et le Groupe Caracoles sont séparés des unités paléozoïques par la Faille Los Toros (N30ºE). Cette faille a été interprétée comme une structure secondaire de la Faille Centinela [*Marinovic et García*, 1999].

Dépression Préandine, Le Salar d'Atacama

Dans le nord du Chili, le Salar d'Atacama forme la plus forte dépression Préandine séparant la Cordillère de Domeyko de la Cordillère Occidentale. Le Salar d'Atacama (Figure II.5,10) est limitée à l'Ouest par les unités du socle Paléozoïque et sédiments du Groupe Purilactis de la bordure orientale de la Cordillère de Domeyko. Le versant oriental du bassin est constitué par des ignimbrites Mio-Pliocène et quelques affleurements de roches du Paléozoïque Supérieur (Groupe Peine du *Breitkreuz et Zeil*. [1994]) et l'arc volcanique actif de la Cordillère Occidentale. Le bord sud du bassin est limité par la Cordillère Occidentale et par le Cordón de Lila. Dans ce secteur la Cordillère Occidentale est décalée d'environ 60 km vers l'Est et prend une orientation NE-SO. Le Cordón de Lila comprend des roches sédimentaires, volcaniques et plutoniques datant de l'Ordovicien au Carbonifère [*Niemeyer*, 1984; *Damm et al*., 1991]. Des âges de traces de fission dans des apatites indiquent que ce socle a été soulevé à une profondeur inférieure à 3-4 km pendant l'Éocène Supérieur [*Andriessen et Reutter*, 1994].

Le bassin d'Atacama a des dimensions approximatives d'environ 100 km en largeur (EO) et de 200 km de longueur (NS). Son altitude moyenne de 2300 m contraste avec les altitudes de 6700 m dans la Cordillère Occidentale et de 4300 m du Cerro Quimal dans la Cordillère de Domeyko. La principale structure visible dans le Salar d'Atacama est la Cordillère de la Sal, une ceinture plissée et faillée d'orientation SSO-NNE de 5-10 km de large. Cette cordillère dont la déformation est complexe, est constituée par des sédiments continentaux, des évaporites et des ignimbrites, datant de l'Oligocène au Pliocène [*Ramírez et Gardeweg*, 1982; *Flint et al*., 1993; *Wilkes et Görler*, 1994]. Ce bloc encore tectoniquement actif traverse le bassin et sépare le Salar du Llano de la Paciencia. Le Llano de la Paciencia est un sous-bassin étroit (8 km de large) rempli par des éventails alluviaux d'age Quaternaire [*Jolley et al*., 1990].

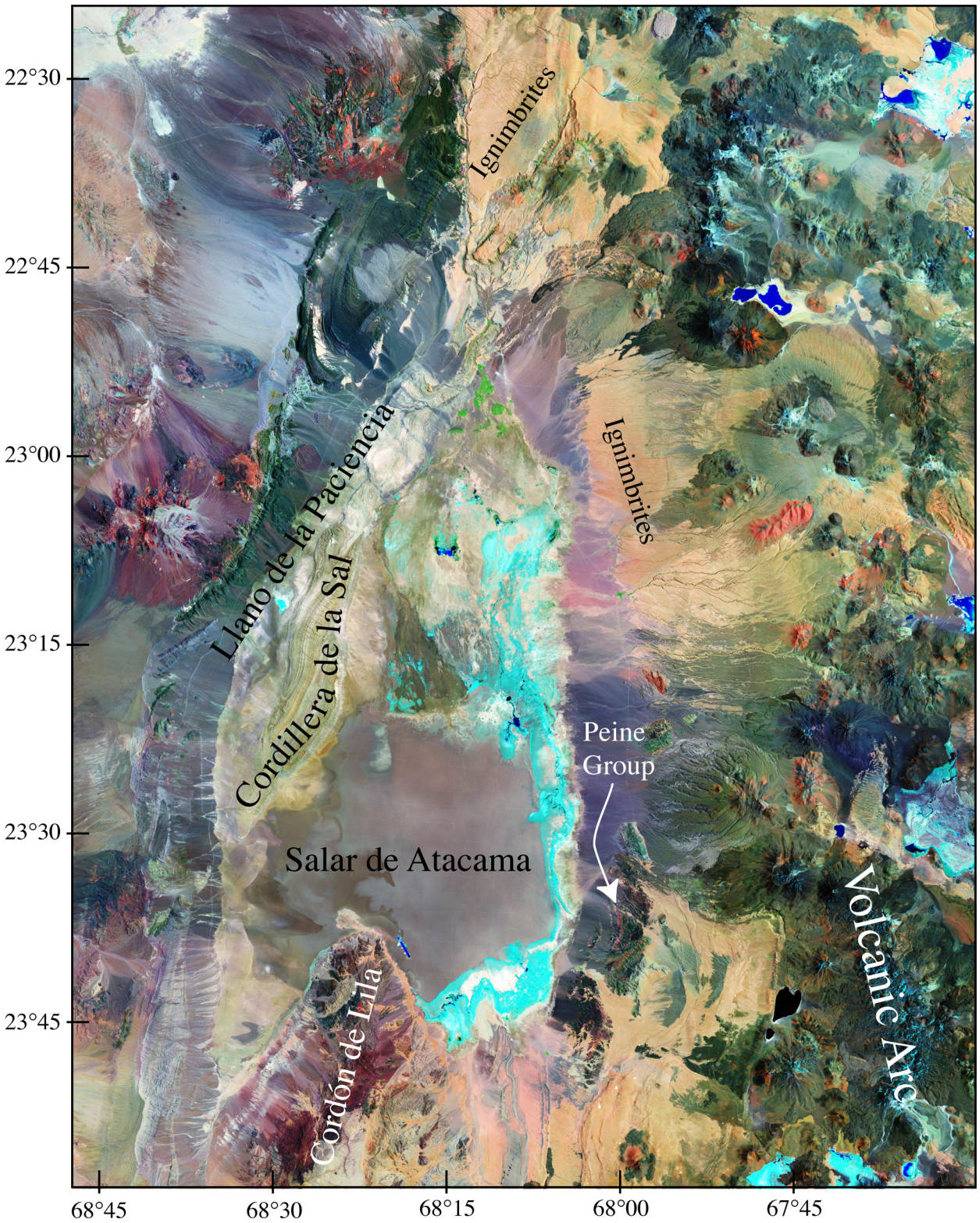

Figure II.10: Landsat Image of the Salar de Atacama basin (see Publications for details).

Manuscrip soumis : La stratigraphie Mésozoïque-Paléogène du bassin de Purilactis-Atacama, région d'Antofagasta, nord du Chili : Une approximation pour les premieres étapes de l'évolution tectonique des Andes Centrales Occidentales.

Constantino MPODOZIS, César ARRIAGADA, Matilde BASSO, Pierrick ROPERCH, Peter COBBOLD, Martin REICH

Résumé: Une section de presque 6000 m de roches sédimentaires et volcaniques d'âge Crétacé à Paléogène (Groupe Purilactis), affleure sur environ 150 km le long de l'escarpement El Bordo, une grande discontinuité topographique qui forme le bord ouest du bassin du Salar d'Atacama. Dans le bassin, les roches du Groupe Purilactis sont généralement couvertes par une épaisse séquence d'évaporites du Cénozoïque supérieur.
La succession stratigraphique du Groupe Purilactis commence, au niveau de l'escarpement El Bordo, par environ 1000 m de couches rouges continentales et d'évaporites (Formation Tonel) accumulées dans un environnement lacustre et sebhka. Les dépôts en onlap sont les témoins du début de soulèvement de la Cordillère de Domeyko pendant le Crétacé "Moyen"-Supérieur. Ces dépôts sédimentaires de type avant-pays sont couverts par quelque 3000 m de grès (Formation Purilactis) et des conglomérats fluviatiles (Formation Barros Arana) provenant de l'ouest et qui représentent la réponse sédimentaire à une nouvelle impulsion de soulèvement tectonique le long de la Cordillère de Domeyko. Des coulées volcaniques de géochimie alcaline et des ignimbrites (Formation Cerro Totola, 64-66 Ma K/Ar) intercalés avec des sédiments rouges et des conglomérats et dans une localité avec des roches calcaires marines, couvrent en discordance la Formation Purilactis dans la zone centrale/sud de l'escarpement El Bordo. En discordance sur les laves de Cerro Totola, la Formation Naranja correspond à quelque 900 m de conglomérats surmontés par des grès et des évaporites déposés pendant le Paléocène. Les grès et conglomérats de la Formation Loma Amarilla correspondent aux dépôts sinorogéniques de déformation transpressive de la phase de Incaïque.

Article soumis a *Tectonophysics*

Mesozoic to Paleogene stratigraphy of the Atacama (Purilactis) Basin, Antofagasta region, northern Chile: insights into the earlier stages of Central Andean tectonic evolution

Constantino MPODOZIS [(1)], César ARRIAGADA [(2)], Matilde BASSO [(3)], Pierrick ROPERCH [(4)], Peter COBBOLD [(5)], Martin REICH [(6)]

(1) Servicio Nacional de Geología y Minería, now at Sipetrol. SA, Santiago (cmpodozi@sipetrol.cl)
(2) Departamento de Geología, Universidad de Chile, Santiago (cearriag@cec.uchile.cl)
(3) Servicio Nacional de Geología, Santiago (mbasso@sernageomin.cl)
(4) IRD/Dep. de Geología, Universidad de Chile, Santiago, (properch@cec.uchile.cl)
(5) Géosciences-Rennes (UMR6118 du CNRS), France, (peter.cobbold@univ-rennes1.fr)
(6) Department of Geological Sciences University of Michigan (mreichm@umich.edu)

Abstract

The Atacama basin, the largest negative topographic anomaly along the western Andean slop in Northern Chile was formed in the Early Late Cretaceous as consequence of the tectonic collapse and inversion of the former northern Chile Jurassic-Early Cretaceous back arc basin. Inversion led to uplift of the Cordillera de Domeyko (CD), a thick-skinned basement range bounded by a system of reverse faults and blind thrusts with alternating polarity along strike. Syntectonic sediments were deposited in discontinuous basins both to the east and west of the CD. The almost 6000 m Late Cretaceous-Early Paleocene sedimentary (volcanic) section (Purilactis Group) infilling the Atacama basin reflects rapid local subsidence east of the CD, possibly controlled by the anomalous dense crustal body associated to the CAGH gravimetric anomaly. The oldest sequence of the Purilactis Group (Tonel Formation) is formed by more than 1000 m of continental red sandstones and evaporites, deposited as growth strata during the initial stages of CD uplift. Tonel strata are capped by of up to 3000 m of sandstones and conglomerates of western provenance, representing the sedimentary response to renewed pulses of tectonic shortening and deposited in alluvial fan, fluvial and eolian settings together with minor lacustrine mudstone

(Purilactis Formation). These are covered by c.a. 500 m of coarse, proximal alluvial fan conglomerates (Barros Arana Formation). Maastrichtian alkaline lava and minor welded tuffs and red beds (Cerro Totola Formation: 70-64 Ma K/Ar were, finally, deposited when the El Molino-Yacoraite Late Cretaceous sea covered large tracts of the Altiplano-Puna domain. Limestones interbedded with the Totola volcanics indicate that this marine incursion advanced to west to reach the eastern CD slope. Late Cretaceous CD shortening was accompanied by volcanism and continental sedimentation in fault bounded strike slip (pull-apart) basins along the north Chilean magmatic arc to the west. Oblique plate convergence during the Late Cretaceous, seems to have been resolved into a highly partitioned strain system where margin-parallel displacements along the thermally weakened arc coexisted with margin-orthogonal shortening associated to syntectonic sedimentation in the Atacama (Purilactis) basin in the back arc.

Introduction

The Salar de Atacama (or Atacama) basin is the largest negative topographic anomalies occurring along the generally "smooth" western slope of the Central Andes in northern Chile (Isacks, 1988; Gephart, 1994, Figures 1, 2). The basin overlaps the prominent Central Andean Gravity High (CAGH), a first order, oblique, NW trending feature of the residual gravity field (Götze and Kirchner, 1997; Götze and Krause, 2002). The Atacama basin has been a long-lived subsiding region since the Paleozoic (Ramírez and Gardeweg, 1982; Breitkreutz at al., 1992; Hartley et al., 1992a; Flint et al., 1993; Muñoz et al., 1997, 2002) and is now filled by more than 8 km of sediments (4 sec TWT, Macellari et al., 1991). One of the key elements of the basin fill (Fill Unit 2 of Flint et al., 1993) is a sedimentary (volcanic) Cretaceous to Paleogene unit, almost 6 km-thick, described, generally in the literature, as the "Purilactis Group". The understanding of the stratigraphy, age, facies and sedimentary history of the Purilactis Group is key to any model trying to get an hold on the Cretaceous to Paleogene tectonic evolution of the Central Andes, as the Purilactis Group has been frequently compared with the sediments of the Salta Rift in Argentina (Salfity et al , 1985; Salfity and Marquillas, 1994, 1999; Galliski and Viramonte 1988; Coutand et al., 2001) or the sedimentary Cretaceous to Tertiary sequences of southwestern Bolivia (Welsink et al., 1995; Sempere et al., 1997; Horton et al., 2001; McQuarrie et al., 2003). Purilactis strata crop out, along the western margin of the Atacama basin along the El Bordo

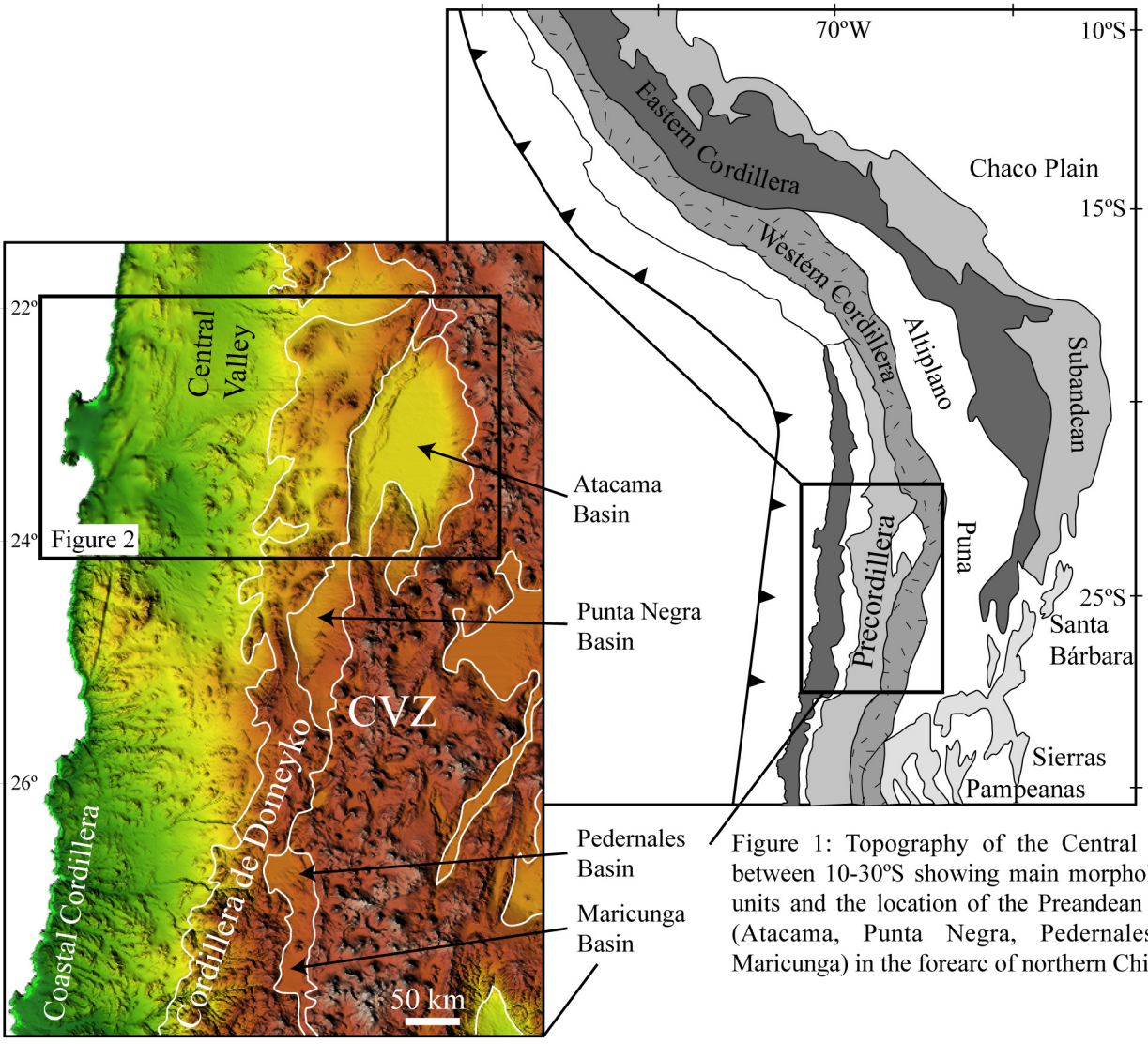

Figure 1: Topography of the Central Andes between 10-30ºS showing main morphological units and the location of the Preandean basins (Atacama, Punta Negra, Pedernales and Maricunga) in the forearc of northern Chile.

Escarpment, a NNE trending 120 km long, 800 m high, cliff, which bounds the basin to the west, and define the eastern edge of the Cordillera de Domeyko (Mpodozis et al., 1993a,b; Maksaev and Zentilli, 1999). Purilactis strata has been imaged by industry seismic lines at the subsurface in the Atacama basin and tested at the Toconao 1 deep exploration oil well (Muñoz et al., 1997; Muñoz and Charrier, 1999; Muñoz et al., 2002).

Numerous authors have studied the stratigraphy of the Purilactis Group (Brüggen, 1934, 1942, 1950; Dingman 1963; Ramírez and Gardeweg 1982; Marinovic and Lahsen 1984; Hartley et al., 1988, 1992a; Flint et al., 1989; Charrier and Reutter, 1990, 1994; Hammerdschmidt et al., 1992; Arriagada , 1999; Mpodozis et al., 1999). In spite of this, important disagreements about the stratigraphy and age of the Purilactis Group persist, which is no surprise considering the non-fossiliferous nature of the sequence and the scarcity of interbedded tuffs or volcanic horizons suitable for dating. Consequently, different and even conflicting models about the tectonic evolution of basin have been proposed. These discrepancies have made difficult to validate probable regional correlations with southwestern Bolivian and northwestern Argentine sequences and, in turn, has led to incomplete or faulty regional tectonic synthesis for this critical period of the Central Andean history.

In this contribution we intend to present a reassessment of the stratigraphy and age of the Purilactis Group and discuss its implications for regional tectonic models. Detailed mapping carried out during 1997-2000 permitted us to collect a set of samples from previously undated volcanic horizons from which we obtained 10 new K-Ar ages. These ages, the recognition of major structural discontinuities, the study of lateral facies changes and the revision of all previously published age-significant data serve the starting point to build in the new stratigraphy system we here propose.

Geological Framework of the Atacama Basin

The Atacama basin is a low lying region, 200 km (N-S) long by 100 km (E-W) width, at an average altitude of about 2300 m which extends in the modern Andean fore arc of northern Chile between 22º30` and 24º30`S, with its center occupied by the active Salar (salt pan) de Atacama (Figures 1, 2). The basin is found directly west of a sharp bend in the present

Central Andean arc (Western Cordillera) which, in this particular area retreats 60 km eastwards from its regional north/south trend (Figure 1). The basin is bounded to the west by the Cordillera de Domeyko (or Precordillera), a basement range, uplifted during Cretaceous and Eocene tectonic events, which reach an average altitude of 3000 m.a.s.l. (Ramírez and Gardeweg, 1982; Flint et al., 1993; Charrier and Reutter, 1990, 1994; Mpodozis et al., 1993a,b, 1999).

Main morphological features of the western Atacama basin and eastern Cordillera de Domeyko region include, from west to east, the Cordillera de Domeyko, El Bordo Escarpment, Llano de La Paciencia, the Cordillera de la Sal and, finally, the active Atacama salt pan (Figure 2). The Cordillera de Domeyko is formed by Late Carboniferous to Early Permian rhyolitic ignimbrites and domes, associated to volumetrically minor basaltic to andesitic lavas and intruded by granitoid plutons which have yield K-Ar, Rb/Sr and U/Pb (zircon) ranging between 300-200 Ma (Davidson et al., 1985; Mpodozis et al., 1993a; Breitkreutz and van Schmus, 1996). The top levels of the volcanic succession include, north of Cerro Quimal (Figure 3,4) 1200 m of fossiliferous, plant-bearing lacustrine, sediments which, recently has been attributed a Triassic age (Basso and Mpodozis, in prep). The eastern border of the Cordillera de Domeyko coincides with the 'El Bordo' Escarpment where, unconformably overlying the Paleozoic (Triassic) basement, a thick succession of Cretaceous to Miocene continental sediments, including the Purilactis Group, is exposed (see below). Further east the Llano de la Paciencia is a narrow 80 km long N-S, and 8 km wide sub/basin filled by a complex coalescing quaternary alluvial fans (Jolley et al., 1990) secluded from the main, Atacama basin by the Cordillera de la Sal, a still tectonically active north-south ridge of complexly deformed Oligocene-Pliocene, evaporite-rich, continental sediments and ignimbrites (Ramírez and Gardeweg, 1982; Flint et al., 1993; Wilkes and Görler, 1994, Kape, 1996; Mpodozis et al., 2000; Blanco et al., 2000). The older and best exposed sequences of the Mesozoic to Cenozoic Atacama basin fill basin occur in a series of major E/W to NW/SE trending canyons, cutting trough El Bordo Escarpment. Further to the east, but however, unexposed, also form the lower section of the Llano de la Paciencia and the Atacama Basin sedimentary fill (Macellari et al., 1991; Muñoz et al., 1997).

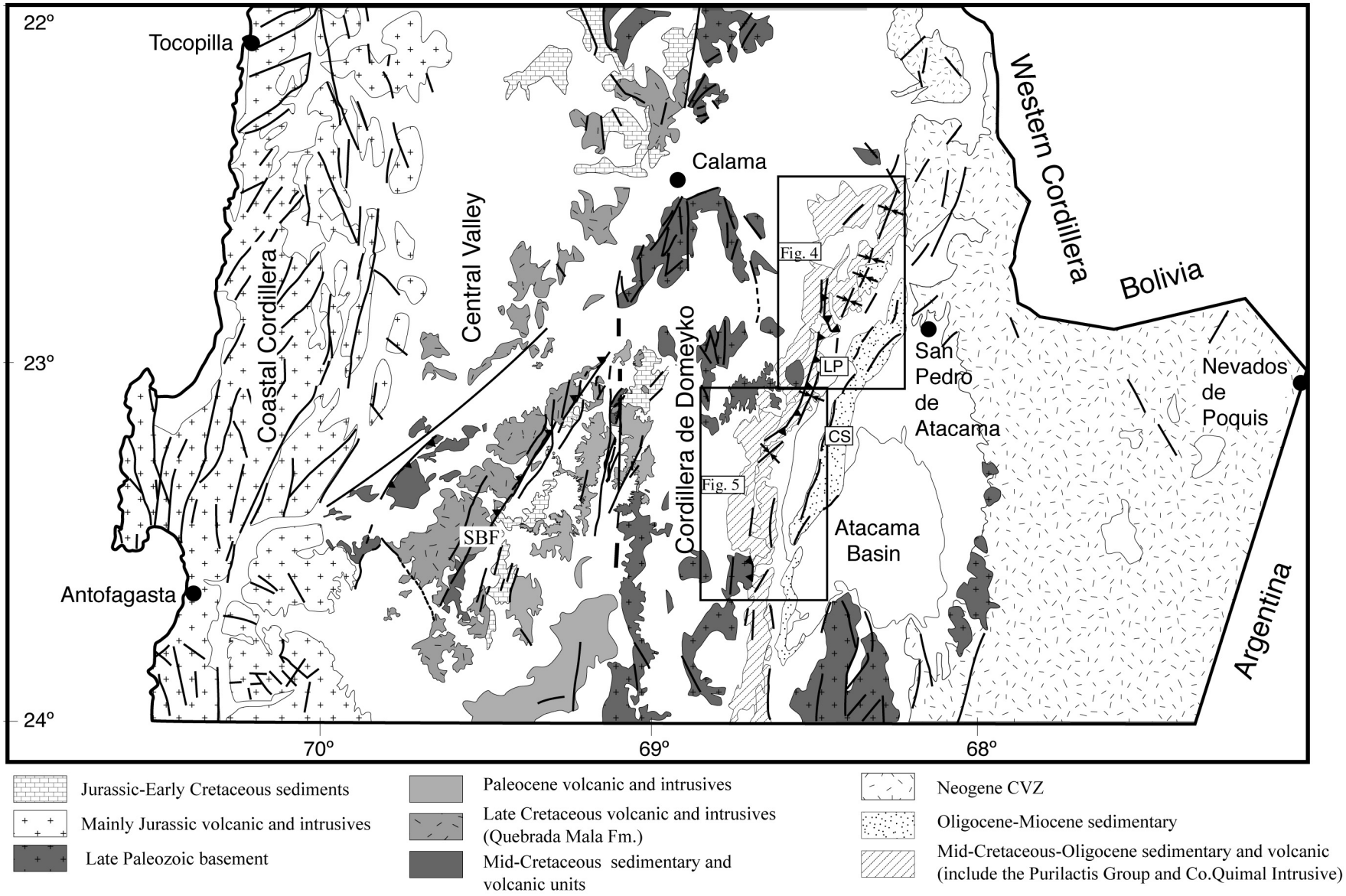

Figure 2: Simplified geological map of the Antofagasta region and location of figures 4&5. CS, Cordillera de la Sal, LP, Llano de la Paciencia, SBF, Sierra El Buitre Fault. (after Mapa Geologico (1:1000.000), SERNAGEOMIN Chile (2002); Marinovic and García, (1999); Cortés, (2000); Basso, (in prep.)).

Stratigraphy and structure of the El Bordo Escarpment area

Recent regional 1:50.000 and 1:100.000 mapping along the El Bordo Escarpment (Arriagada, 1999; Mpodozis et al., 1999; Arriagada et al., 2002; Basso and Mpodozis, in prep.) allowed the identification of seven major stratigraphic sequences, probably spanning the Late Cretaceous-Oligocene time interval. Mpodozis et al. (1999) embodied the lowermost five within the Purilactis Group and briefly described their main stratigraphic characteristics. However, after recognizing the importance of the regional unconformity between Paleocene-Eocene and the older strata we here prefer to limit the Purilactis Group to the lowermost four units, which share an interrelated evolution and history. The renamed Purilactis Group comprise (bottom to top) the Tonel, Purilactis, Barros Arana and Totola Formations (Figures 3,4, 5). During the Neogene the basin continued to evolve showing a complex history of Neogene sedimentation, volcanism and deformation (see Wilkes and Görler, 1994; Blanco et al., 2000; Kappe, 1996; Mpodozis et al., 2000), to be discussed elsewhere.

The main structure affecting the Cretaceous sedimentary sequences along the El Bordo Escarpment is a very large (up to 15 km wavelength) syncline (Barros Arana Syncline) which extends for more than 80 km between Cerro Totola and Pampa Vizcachita (Figures 4, 5). Fold geometry changes from tight-chevron in the south (east of Cerro Quimal) to open-concentric to the north (Cuesta de Barros Arana) while the trend of its axial surface shifts form N60ºE (Cerro Totola) to NNE (Barros Arana). The syncline is bounded to the west by outcrops of Paleozoic to Triassic intrusives and (mainly) volcanics forming the easternmost ranges of the Cordillera de Domeyko. Contact relations between basement and cover are not easy to investigate, as in most places it is cover by Tertiary (Eocene-Miocene) gravel-rich sequences (Figure 4). Only around Cerro Quimal a complete structural section can be investigated. There, immediately west of the Purilactis Syncline (Barros Arana Syncline), Triassic (?) sediments and volcanics underlying the Tonel Formation along the eastern edge of the Cordillera de Domeyko block are deformed in a, east verging, overturned growth anticline (Quimal Anticline: Figure 4). Cretaceous Purilactis Group sediments form the external, discordant, eastern, sedimentary envelope of the anticline, cored by Late Paleozoic lavas, which appears to be a fault propagation fold associated to a blind thrust rooted to the west in the Cordillera de Domeyko basement. All the Cretaceous units (Tonel, Purilactis, Barros Arana and Totola) are folded.

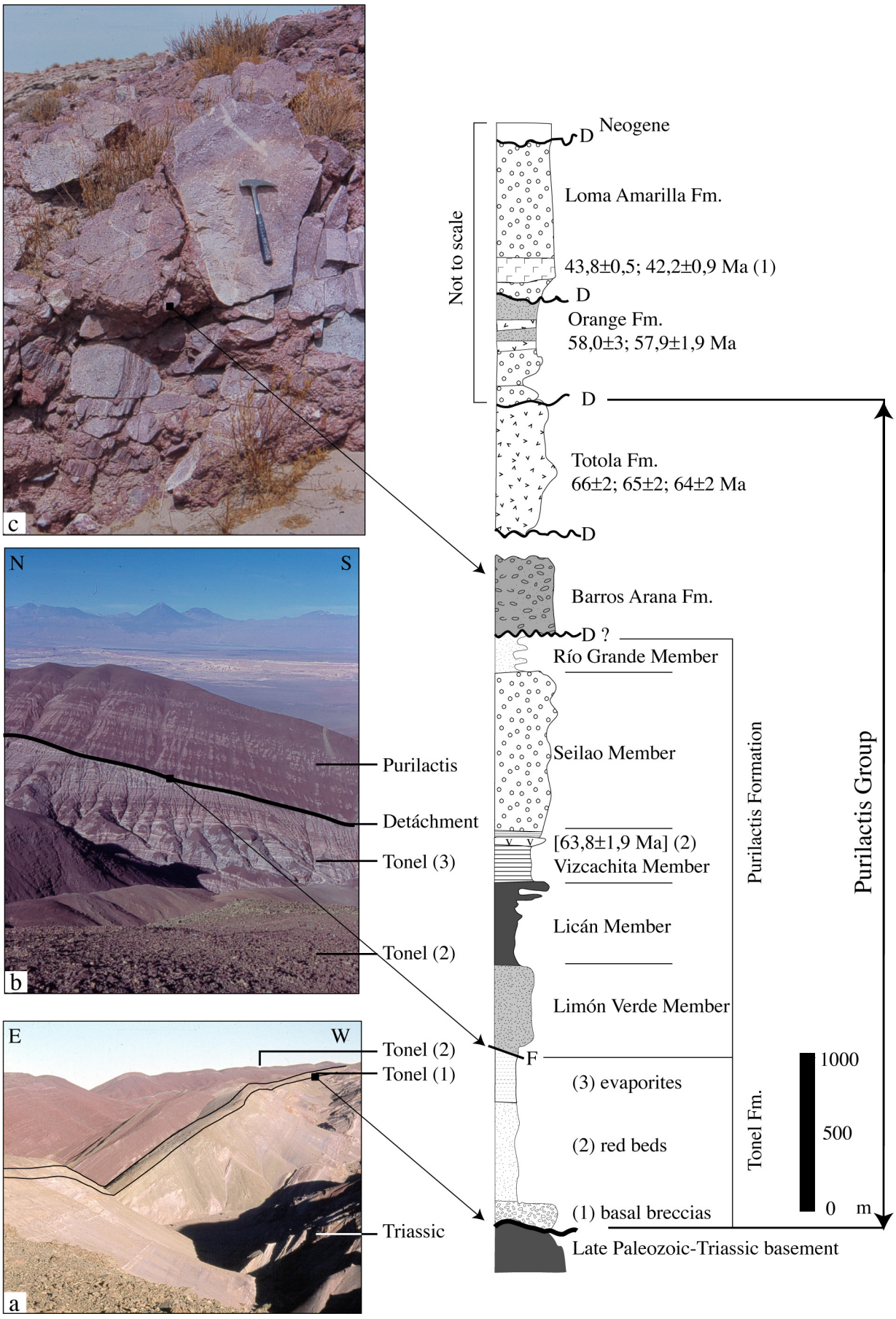

Figure 3: Synthetic stratigraphic section of the Purilactis Group and Paleogene strata outcropping along the El Bordo Escarpment.

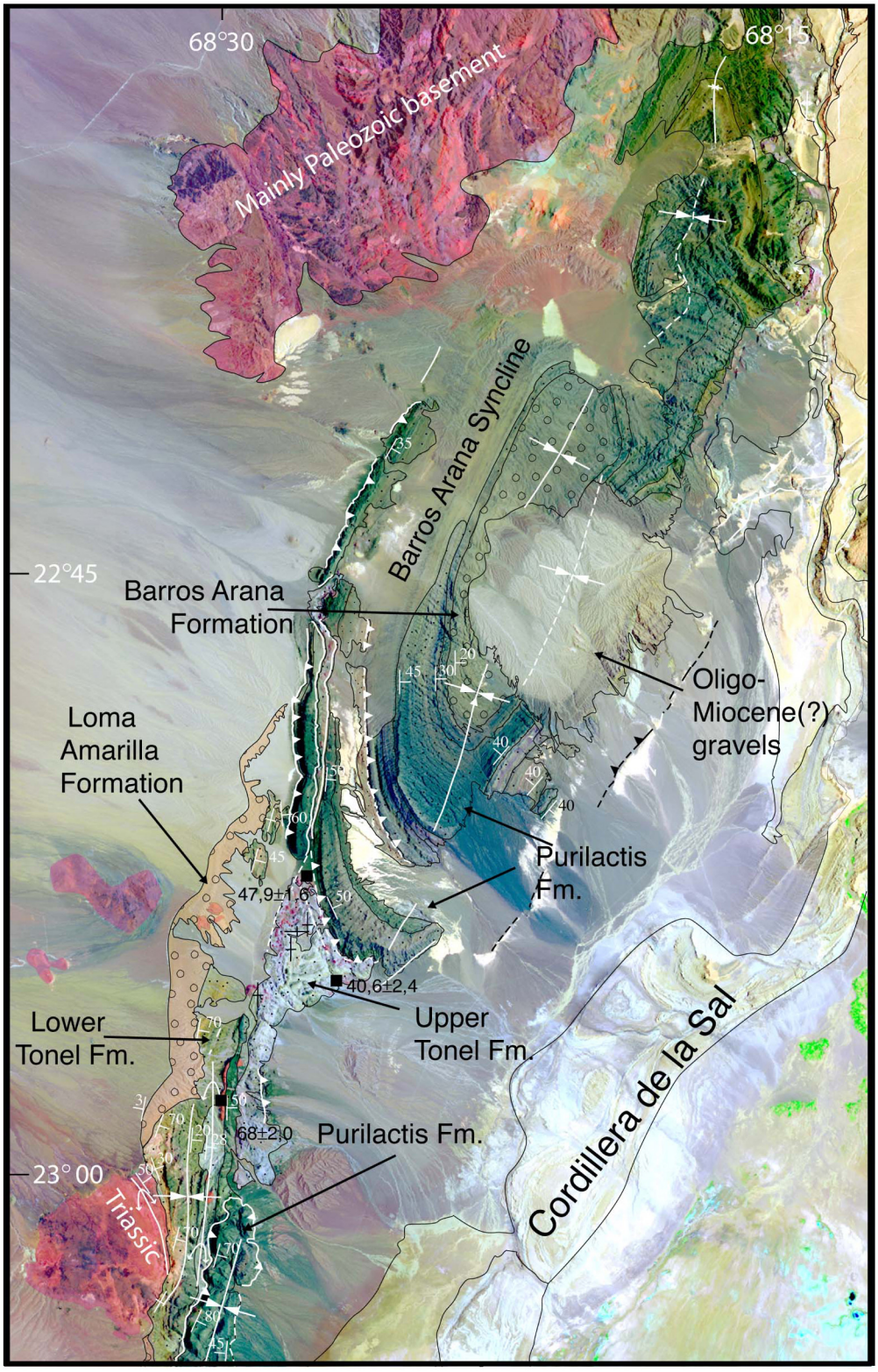

Figure 4: Geological map of the Barros Arana area.

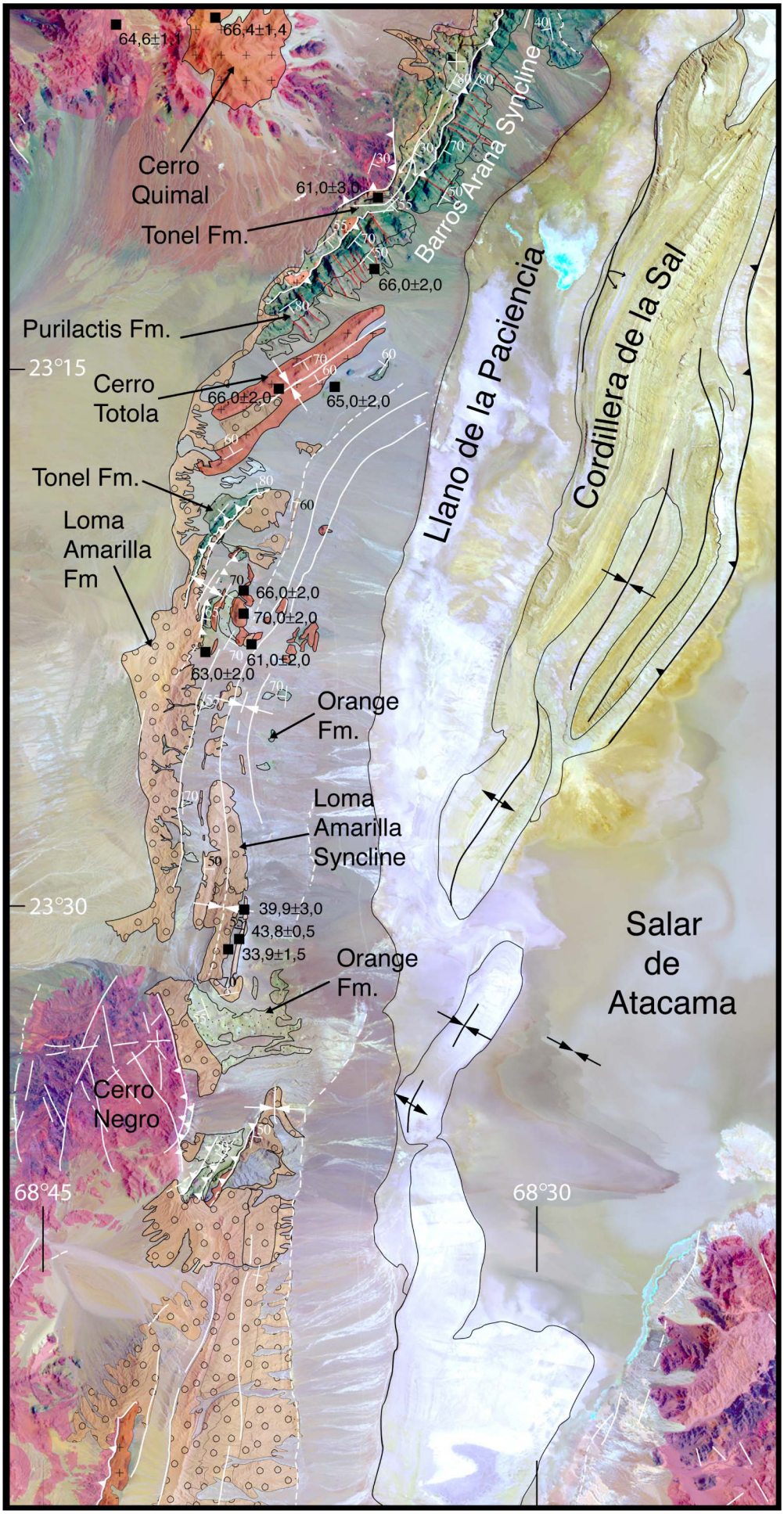

Figure 5: Geological map between Cerro Quimal and Cerro Negro area

A remarkable angular unconformity between the "Orange Formation" (Figure 3) and the Purilactis Group south of Cerro Totola clearly indicates that, Quimal-Barros Arana fold system was already formed by the earliest Paleocene although its original geometry was later modified during the Incaic (Eocene) and other, Neogene, deformation episodes (see Arriagada et al, 2000). Late stage reactivation can be seen along the western limb of the Barros Arana Syncline at Cerros de Purilactis where a detáchment separating the Purilactis Formation from the upper evaporites of the Tonel Formation acts as the décollement level for a west verging back-thrust (Purilactis Fault) carrying westwards Purilactis strata on top of Miocene gravels (Figure 4). Secondary west verging back thrusts tectonically repeat Purilactis beds along the western limb of the syncline.

Folding of the axis of the Barros Arana Syncline around the Cerro Quimal basement block (Figures, 4, 5) is considered by Arriagada et al (2002, 2003) to be a consequence o the clockwise rotation of crustal locks during the Eocene Incaic deformation. The effects of the Incaic episode seems to be specially important in the Cerro Negro area (Figure 5) where discrete basement blocks are thrusted eastwards over the Purilactis Group, post Purilactis Paleocene-Eocene ("Orange" formation) and syntectonic Eocene- Oligocene strata (Loma Amarilla Formation). Deformation is particularly important in the thrust's footwalls where the Orange Formation show a complex array of tight, hectometric scale isoclinal to chevron folds with sub vertical axial surfaces.

Lower Purilactis (Late Cretaceous?): Tonel, Purilactis and Barros Arana Formations

The lowermost, sedimentary, units of the redefined Purilactis Group are, essentially the same originally recognized by Brüggen (1942). The Tonel Formation was first described by Brüggen's as the Salina de Purilactis Formation and was renamed as the Tonel Formation by Dingman (1963). The Purilactis Formation was also first described by Brüggen ("Porphyritic" Purilactis Formation). Finally, the Barros Arana Formation (Barros Arana Strata in Arriagada, 1999 and Mpodozis et al., 1999) which is exposed at the core of the Barros Arana Syncline (Figure 4) is equivalent to the Conglomerados de Purilactis Formation of Brüggen's. It was also recognized as an independent unit by Hartley et al.

(1992a) and Flint et al. (1993) although they included this unit as a part of the Cinchado Formation (*sensu* Ramírez and Gardeweg, 1982).

Tonel Formation

This sequence, corresponds to a succession of red beds and evaporites deposited in smooth angular unconformity over late Triassic and volcanics and sedimentary rocks outcropping along the eastern edge of the Cordillera de Domeyko, northeast of Cerro Quimal (Figure 4). Its outcrops extends for more than 60 km along the El Bordo Escarpment (Cordón de Barros Arana to Cerro Oscuro.. The lower beds of the Tonel Formation are formed by 60 m of medium grained breccias and conglomerates with basement-derived andesitic, rhyolitic and sedimentary clasts (alluvial fan facies, deposited in a proximal alluvial fan/valley fill environment, Hartley et al., 1992a). Middle Tonel, by contrast, is formed by 400 to 1000 m. finely bedded, laminated red-brown sandstones, some of them displaying planar cross bedding, and gypsum nodules. In some places, the sandstones alternate with thin (centimeter-thick) gypsum layers. At Cerros de Tonel, massive and complexly deformed anhydrite deposits of unknown total thickness form the top of the formation (Figures 3, 4). According to Hartley et al. (1992a) this sequence represents a playa/shabka facies association accumulated in playa mudflat and fringing sandflat environment. Paleocurrent measurements generally indicate a western source provenance. Numerous, disrupted lamproitic blocks, ("hornblendites" Dingman, 1963) several meters in diameter, and clearly visible, as "red specks" in the TM images, come out embedded into the upper anhydrite complex. These coarse porphyritic rocks, possible parts of a dismembered dyke swarm, show, in the field, a typical green color and large (1-4 mm) amphibole, pyroxene and plagioclase phenocrysts.

Purilactis Formation

A faulted (detached) contact over the Tonel Formation marks an abrupt upwards transition to the Purilactis Formation in the Barros Arana Syncline (Figure 4). The Purilactis Formation as a whole form a sequence of almost 3000 m of sandstones, red mudstone and minor conglomerate in which the detrital fraction is dominated by andesitic to rhyolitic volcanic material, quartz and abundant potassium feldspar. Fragments of the mafic hornblende-rich dykes, which intrude the Tonel Formation, and fossil bearing, Jurassic limestone clasts, are also present (Brüggen, 1942; Dingman, 1963; Ramírez and Gardeweg,

1982). Paleocurrent data indicate a western source for the sediments (Hartley et al., 1988, 1992a).

Hartley et al. (1992a) divided the Formation into five members of regional extent. The lowermost (Limón Verde) includes 400 m of fine to coarse, reddish, cross-bedded sandstones, conglomerates, and, thin, red, mudstone deposited as sheet floods in an alluvial fan setting (Hartley et al., 1992a). 700 m of red sandstones, mudstones, minor conglomerate and evaporites (Licán Member), which represent canalized and sheet flood sediments accumulated in a medial/distal alluvial fan and playa environment follow. Continuing upwards (Figure 3) , the Vizcachita Member, is formed by almost 300 m of light-green, cross-bedded, eolian (dune) sandstones and structureless fluvial sands which, near the top, in Quebrada Seilao include 40 m thick, strongly altered, porphyritic andesitic lava. Vizcachita sandstones gradually merge upwards with more than 1000 m coarse conglomerates and sandstones (Seilao Member, Figure 3) with volcanic clasts up to 30 cm in diameter, which accumulated as sheet flood and canalized sandstones during repeated cycles of alluvial fan progradation from the west (Hartley et al., 1992a). Finally, the top of the Formation in the Barros Arana area Cerros de Purilactis area corresponds to a sequence of 250 m of "varved" black mudstones and sandstones (Río Grande Member) which Hartley et al. (op cit) considered to have been deposited in a shallow lake environment.

Barros Arana Formation

The upper member of the Purilactis Formation (Río Grande) is overlain by a sequence of 550 m of coarse-grained conglomerates, which outcrop at the core or the Barros Arana Syncline (Figures 3, 4). The reddish, well cemented conglomerates and associated sandstones from laterally extensive beds, up to 50 m thick with sub-rounded and moderately sorted clasts up to 20 cm in diameter, composed mainly by Paleozoic granitoids and rhyolites and a minor andesite and limestones. Imbrications indicate a western provenance. According to Hartley et al. (1992a), this unit corresponds to an association of facies accumulated as proximal sheet and channel conglomerates and high-density flood and debris flows deposited in a proximal alluvial fan setting.

Similar rocks are also exposed at Cerros de Ayquina, approximately 45 km to the north of Cerros de Purilactis (Marinovic and Lahsen, 1984). When compared to the underlying Purilactis Formation clasts The Barros Arana (and the Ayquina conglomerates) shows a

noticeable larger volume of basement-derived granitoid clasts which may indicate deep exhumation of the Cordillera de Domeyko during an increasing period of erosion and uplift as its is also reflected by the much more energetic depositional environment. The fact that the Ayquina conglomerates rest directly on top of the basement suggest the probable existence of an unconformity between the Purilactis and Barros Arana Formations.

Age constraints

One of the main difficulties in relation to the Purilactis, Tonel and Barros Arana formations concerns its poorly constrained age. No hard data about the age of the Tonel Formation is available although the formation is doubtless post Triassic as indicated by a new ^{240}U/Pb age obtained for underlying volcanics (dacitic tuffs) near Cerro Quimal (Basso and Mpodozis, in prep). Two K/Ar whole rock dates of the altered, dismembered lamproitic dykes associated to the upper Tonel Formation (PC-1 and PC-22, Table 1) we collected south of Cordón de Barros Arana (Figure 4) gave ages of 40,6Å2,4 and 47,9Å1,6 Ma. Macellari et al. (1991) obtained an older, whole rock, age of 63,6±2,8 Ma for the same hornblende-rich dykes at Quebrada Los Cóndores even though they admit that this may represent a minimum age considering the "deep weathering of the rocks in the area". We concur and believe that these results represent only resetted values as an andesitic dyke intruding the middle member of the Tonel Formation, yield a K/Ar age of ca 68 Ma (see below). These numbers only allow the Tonel to be placed in the general Jurassic-Cretaceous interval.

A shorter "permitted range" exists, however, for the Purilactis Formation. The occurrence of reworked mid Jurassic marine fossils (*Vaugonia v. l. gottschei* (Moericke), *Perisphinctes* sp, Ramirez and Gardeweg (1982) and the fact that part of the strata are unconformably covered by the 66-65 Ma volcanics of the Totola Formations (Figures 4, 5) as well as intruded by a late Cretaceous complex of dykes and stocks dated (K/Ar) between 70 –61 Ma (see below) constraints the age of the Purilactis formation to the Late Jurassic-Cretaceous interval. Flint et al. (1989) reported a ^{39}Ar/^{40}Ar date from a lava flow interbedded on the middle part of the Purilactis Formation (Seilao Member) at Quebrada Seilao, which yield an "age" of 63,8Å1,9 Ma (Figure 3). Nevertheless, the extremely disturbed Ar release spectra, the strongly altered nature of the sampled rocks and the very

low K content of the analyzed clinopyroxene indicate that this, is a questionable "minimum" value inconsistent with the regional stratigraphic relations.

Arriagada et al. (2000) carried out a detailed paleomagnetic survey on the Tonel and Purilactis Formations sampling 10 sites in the middle member of the Tonel Formation and other 20 sites mainly the lower part of the Purilactis Formation (Limón Verde and Licán). Results indicate that all these samples acquired its characteristic magnetization during a normal polarity interval. This observation and the Late Cretaceous age of the overlying volcanic rocks of Cerro Totola Strata (which, in contrast, show both normal and reverse polarities) led Arriagada et al. (2000) to suggest that deposition and magnetization of the lowermost units of the Purilactis Group occurred during the Cretaceous normal polarity superchron, between 119-84 Ma (Cande et al., 1988; Besse and Courtillot, 1991). Hartley et al. (1991, 1992b) also report paleomagnetic data for the Purilactis Formation in the Barros Arana area (Figure 4) . Samples came, apparently, from higher stratigraphic levels and exhibit both normal and reverse polarities which its consistent with its younger age, although Arriagada et al. (2000) draw attention to the fact that these may be secondary magnetizations and not primary values.

Tectonic controls on sedimentation

Flint et al. (1989), studying the outcrops along the Barros Arana region suggested that the Purilactis basin was formed following a compressive deformation event which led to the emergence of the Proto-Cordillera de Domeyko in the "mid Cretaceous". However, the study of some of the ENAP (Chilean National Oil Company) seismic lines which seemingly show that the Purilactis Group strata thickens westwards led Flint et al. (1993), later to suggest that the tectonic environment during deposition of the Purilactis was dominantly extensional. Macellari et al. (1991) suggested that the Purilactis Fault may have been formed in the Early Cretaceous, as an east dipping listric normal fault with at least 4 km of vertical throw normal fault which originally delineated the western boundary of the Purilactis basin and was reactivated as inverse during the Tertiary.

However, and unlike these views, our observations near Cerro Quimal indicate that the Lower units of the Purilactis Group (Tonel Formation) were deposited under a compressional regime instead. The sandstones of the Tonel middle member, exposed along the eastern limb of the east-verging Quimal Anticline, form part of a panel which exhibit

progressive internal unconformities as shown by a systematic decrease in dip from very steep (80ºE) to gentle (30ºE) when moving away (eastwards) from the basement-cover contact. Individual bed thickness increases from west to east (see Figure 6) while the strata are deformed by second-order upwards attenuated synclines, following a pattern described elsewhere as typical for syntectonic growth strata deposited in an active compressional environment (Riba , 1976; Barrier, 2002). Growth structures and compressional folding led us to infer that, the lower and middle section of the Tonel Formation accumulated in a compressional context during the growth of the Quimal Anticline during the Late(?) Cretaceous (Arriagada et al., 2002).

The evaporites of the Upper Tonel may well indicate a period of relative tectonic quiescence and subdued fold "growth" which culminated with the emplacement of the Tonel mafic dyke swarm (hornblendites). The occurrence of "hornblendite" clasts in the basal layers of the Purilactis Formation seems even to indicate according to Dingman (1963) a period of no deposition-erosion. The drastic facies change of the evaporites of Tonel Formation to sandstones and conglomerates of alluvial fan, and eolian-lacustrine facies of Purilactis Formation show an important increase in the sedimentary energy, triggered by renewed uplift and shortening in the Cordillera de Domeyko. Finally, the conglomeratic Barros Arana Formation can be considered an independent unit which progrades, probably, from the west into to the Purilactis basin although its age is yet to be better constrained. The large volume of Paleozoic granitoid clasts in the Barros Arana Formation (Hartley et al., 1992a), which are almost absent in the Purilactis Formation, indicate deep erosion and the unroofing of Paleozoic intrusive complexes, that today constitute most of the exposed rocks in the Cordillera de Domeyko.

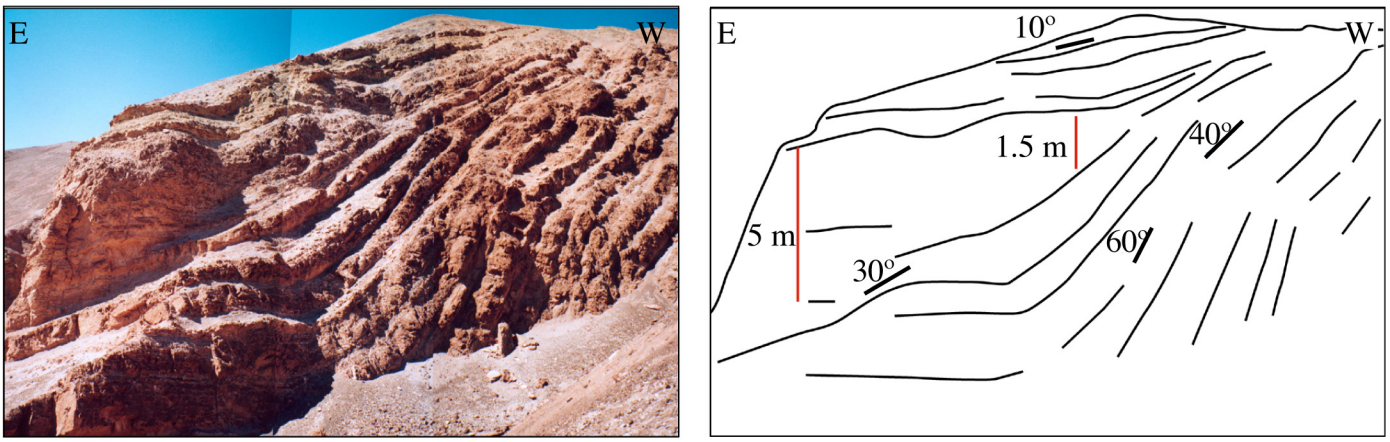

Figure 6: Syntectonic growth strata in the middle member of the Tonel Formation, east of the Cerro Quimal.

Upper Purilactis (Campanian -Lower Paleocene) :Totola Formation and related intrusives

To the south-east of Cerro Quimal, playa and alluvial playa fan facies of the Licán Member of the Purilactis Formation and red beds of the Tonel Formation are unconformably overlain by a volcanic-sedimentary sequence, first described as an independent unit by Arriagada (1999) and Mpodozis et al., (1999). This unit was previously attributed by Ramírez and Gardeweg (1982) to the Cinchado Formation and considered by Charrier and Reutter (1994) to be part of their "Purilactis" Formation. The sequence, at the core of the Barros Arana Syncline, is constituted by an 800 m thick succession of andesitic, andesitic-basaltic and minor dacitic lava flows, interbedded with welded rhyolitic ignimbrites, and, at its base, coarse red, volcaniclastic conglomerates and sandstones. 60 km south of Cerro Totola, at Cerro Pintado, another, small outcrop of the Totola Formation can be found. Its base is not exposed and , to the west is overthrusted by a mafic Paleozoic lavas. This outcrop is specially interesting because there, 100 m of andesitic to basaltic flows are capped by 150 m of red conglomerates and calcite-cemented sandstones which alternate with gray limestone beds up to 5 m thick and composed mainly by sparry calcite but including some bioclastic material which point to an organic (marine) origin.

Equivalent units are also probably present in the subsurface of the Salar, forming the oldest units recognized in the Toconao 1 well. According to Muñoz et al. (1997) at 2980 m below the subsurface, the well penetrated red claystone and siltstone and minor shallow water marine carrying foraminifera and pollen of Senonian age. Although this strongly folded, unit was considered by Muñoz et al. (1997) to unconformably cover a "Paleozoic basement" unit of andesitic lavas, tuffs and sandstones and minor limestone intercalations. The review of the seismic lines and original wells reports doesn't permit to discern any definitely unconformity and, contrary to described, any Paleozoic diagnostic fossil assemblage.

The Cerro Totola basalts and basaltic andesites are porphyritic rocks with idiomorphic plagioclase and clinopyroxene phenocrysts. Groundmass, pilotaxitic in part, include plagioclase microlites, pyroxene and opaque minerals. The intermediate portion of the lava flows is massive fresh, while the flow tops exhibit quartz and zeolite-filled vesicles. The andesitic lavas include albitized plagioclase, amphibole and biotite phenocrysts embedded in

a microgranular array of plagioclase and opaque minerals. Calcite occurs in fractures and veins throughout the flows. Dacites are also porphyritic with albitized plagioclase phenocrysts immersed in a devitrified glassy groundmass with plagioclase microlites and opaque minerals. Finally, the ignimbrites are rhyolitic, biotite-amphibole rich, welded tuff, with stretched pumice fragments, and andesitic lithic fragments in a devitrified groundmass.

Totola-related intrusives

At Cerro Totola the lavas are intruded by a swarm of sub vertical basaltic to dacitic dikes, less than 10 m thick which also cut the Tonel and Purilactis formations southeast of Cerro Quimal where they seem to form a radial array around the Cerro Quimal stock, a Late Cretaceous granodiorite stock, 5 km in diameter emplaced in Triassic volcanics of the Cordillera de Domeyko basement. North of Quebrada El Salto the dykes trend N60ºW and N30-40º W. These dykes are, probably feeders of the Totola volcanics as they share the same chemistry and age. Irregular, smaller size, stocks, hundredths of meters of maximum length also intrude the Totola and Tonel formations around Quebrada Tonel, near Quebrada El Salto and southeast of Cerro Pichungo (Figure 5). The large (25 km^2) Cerro Quimal stock is formed by medium-grained amphibole-biotite granodiorite but also small (1 km^2) pyroxene bearing diorite stock occur also west and south of Cerro Quimal. Dacitic stocks and dykes, further east display a porphyritic texture, albitized plagioclase amphibole and a small percentage of clinopyroxene (< 2%) while the basaltic andesitic to andesitic dykes, outcropping in the same general area, are also porphyritic, with plagioclase and pyroxene phenocrysts including biotite in the less acidic facies.

Age

We have acquired four new K/Ar ages for the, previously undated, Totola lavas and also, 5 ages for related dykes and intrusives (Table 1). Two of these correspond to concordant K/Ar whole rock ages of 66,0±2,0 and 65,0±2,0 Ma from lava flows forming part of the eastern limb of the Totola Syncline (samples PC 26, PC 27, Figure 5) while another age of 64,0±2,0 was recently obtained by Basso and Mpodozis (in prep). These ages are older than other K/Ar (whole rock), 61,0±2,0 Ma value we got for a basaltic-andesitic lava flow sampled further south, near Cerro Oscuro (PC 28, Figure 5). Yet, we interpret this number as a minimum value because one andesitic dyke (PC 29) intruding the Totola lavas nearby yield an 66,0 ±2,0 Ma (whole rock) age. Other K/Ar (biotite) ages from dykes intruding the

Tonel Formation north of Quebrada Tonel (PC 39= 68,0±2,0 Ma) and the Purilactis Formation southeast of Cerro Quimal (PC 33=66,±2,0 Ma) fall in the same general range indicating the main period of volcanism and dyke emplacement occurred , most probably, during the Maastrichtian to earliest Paleocene interval. Only one andesitic dyke (PC 40) intruding the middle member of the Tonel Formation at the Quebrada el Salto turned out to be younger (61,0±3,0 Ma, whole rock, see Figure 5). The largest intrusive bodies also gave similar ages to the Totola Formation. Ramírez and Gardeweg (1982) reported two (biotite) ages of 66,4±1,4 and 64,4±1,4 Ma for the monzonite to granodiorite Cerro Quimal stock for which Andriessen and Reutter (1994) obtained a slightly younger (biotite) age of 63,3±0,7 Ma. We produced two other hornblende ages of 70,2±2,0 and 63,0±2,0 Ma from andesite porphyries (PC 17, PC 52) outcropping 10 km to the south of Cerro Totola and another (K/Ar) biotite age of 68±2 Ma for diorites outcropping southeast of Cerro Quimal (Basso and Mpodozis, in prep).

Rocks equivalent to those the Totola Formation outcrop also further north along strike with the structural axis of the Barros Arana Syncline, some 100 km. NNE of Cerro Quimal where they has been described as the Lomas Negras Formation (Lahsen, 1969, Marinovic and Lahsen, 1984). This unit (base unexposed) outcrops in an erosional window below Miocene-Pliocene volcanics and includes 500 m of "andesitic" lavas, interbedded with multicolored conglomerates, sandstone, mudstone and thin beds (1-3 m) of marine, fossiliferous, (oolitic) limestones including bivalves (Brachiodonte sp?), foraminifera, fish bones, trace fossils and plant remains (Marinovic and Lahsen, 1984). It can be considered a direct equivalent to the Totola Formation as shown by a $^{39}Ar/^{40}Ar$ (biotite) plateau age of 66,6± 1,2 Ma for a lapilli tuff near the base of the Formation reported by Hammerdschmidt et al. (1992).

Table 1 – Radioisotopic ages

Sample	UTM N, Lat	Coordinates (E, Long)	Geological Unit	Method	Material	% K	Ar rad. (nl/g)	%Ar Atm.	Age (Ma)	Error (2 Sig)
PC-1	7465998	557760	Dismembered lamproitic dykes	K/Ar	Whole rock	0,565	0,901	59	40,6*	2,4
PC-22	7469772	555538	Dismembered lamproitic dykes	K/Ar	Whole rock	2 658	5 015	24	47,9*	1,6
KP3L (1)	7476621	565866	Lava in Vizcachita Member	Ar/Ar	Clinopyroxene				64,0**	10,0
PC-26	7428249	540074	Totola Formation	K/Ar	Whole rock	0,944	2 429	20	65,0	2,0
PC-27	7428898	535909	Totola Formation	K/Ar	Whole rock	3 704	9 695	10	66,0	2,0
PC-28	7414484	535575	Totola Formation	K/Ar	Whole rock	1 597	3 863	26	61,0	2,0
									64	2,0
PC-29	7418040	536420	Dyke (intruding Totola Fm)	K/Ar	Whole rock	3,28	8 604	26	66,0	2,0
PC-33	7434314	542265	Dyke (intruding Purilactis Fm)	K/Ar	Biotite	5 712	14 872	13	66,0	2,0
PC-39	7460116	551591	Dyke (intruding Tonel Fm)	K/Ar	Biotite	7 018	19 017	36	68,0	2,0
PC-40	7437536	542930	Dyke (intruding Tonel Fm)	K/Ar	Whole rock	2 203	5 315	58	61,0	3,0
PC-17	7415123	534538	Dyke Intruding Purilactis Fm)	K/Ar	Amphibole	1 372	3 391	11	63,0	2,0
PC-52	7416397	536318	Porphyritic stock	K/Ar	Amphibole	1 038	2,88	23	70,0	2,0
MAF-306 (2)	7446800	534900	Cerro Quimal stock	K/Ar	Biotite	7 598	19 967	22	66,4	1,4
MAF-325-C (2)	7446500	529500	Cerro Quimal stock	K/Ar	Biotite	7 071	18 055	15	64,6	1,1
Pu-1(3)	7390991	537328	Loma Amarilla Fm	Ar/Ar	Biotite				43,8	0,5
Pu-13(3)	7419224	536576	Loma Amarilla Fm	Ar/Ar	Biotite				42,2	0,9
To-432 (2)	7398000	535500	Loma Amarilla Fm	K/Ar	Plagioclase	0,362	0,567	76	39,9	3,0
PC-13	7398993	535322	Loma Amarilla Fm	K/Ar	Amphibole	0,355	0,473	54	33,9*	1,5

(1) Flint et al. (1989), (2) Ramírez and Gardeweg, (1982), (3) Hammerdschmidt et al., (1992), * Minimun age, ** Value of unknown significance

Geochemistry

9 selected whole-rock major and trace element analysis of samples of mafic lavas from the Cerro Totola Formation and associated dykes are presented in Table 2. Silica content varies from 46 to 51 % SiO_2. All the rocks show high Na_2O+K_2O values which allow them to be classified as and alkaline suite according to the various criteria summarized in Rollinson (1993). Chemically the lavas are trachybasalts and basaltic according to the TAS classification of Lemaitre et al. (1989). The dykes (44 to 52 % SiO_2) show a slightly higher alkali content as two of the samples (PC 33, PC 40) fall in the tephrite-basanite, and tephriphonolite fields of the TAS classification diagram. Despite the fresh appearance in hand-specimen and thin section of the analyzed rocks, the moderate to high loss on ignition values (LOI>2 wt%) suggests some alkali remobilization by alteration. However, the alkaline affinity of the lavas and dykes is confirmed considering their relative high TiO_2 and P_20_5 content as it's shown in discrimination diagrams for basalts of Winchester and Floyd [1976, Figure 7). The lavas and dykes are enriched in incompatible elements (K, Ba, Rb, Sr), when compared to MORB values (Figure 8). The chondrite-normalized REE patterns present a gentle slope (La/Yb= 7-13) and no Eu anomalies. Light REE are only slightly enriched in relation to the heavy's (La /Sm= 3-6, Sm/Yb= 2-3, Figure 9).

Table 2 – Representative major and trace element whole-rock analyses.

	Lavas						Dykes		
Sample:	PC-49	PC-26	PC-28	PC-53	PC-45	PC-27	PC-40	PC-41	PC-33
SiO_2	46.42	46.49	49.53	50.30	53.13	56.46	44.81	47.99	51.69
Al_2O_3	17.50	17.66	17.32	17.26	19.84	20.49	15.04	16.16	17.92
TiO_2	1.21	1.25	0.93	0.92	0.68	0.48	1.05	0.79	0.77
Fe_2O_3	8.77	9.14	8.95	7.04	4.25	3.16	6.11	5.55	4.50
FeO	2.16	2.27	1.04	1.37	1.21	0.72	5.10	3.60	2.01
CaO	8.37	8.65	9.48	7.55	4.29	3.92	9.32	6.91	5.19
MgO	4.66	4.36	3.99	4.68	1.74	1.07	6.47	5.89	2.77
MnO	0.18	0.18	0.18	0.18	0.17	0.14	0.25	0.17	0.18
Na_2O	4.43	4.35	3.34	4.33	4.94	5.78	2.99	4.25	4.10
K_2O	1.63	1.41	2.57	2.39	5.35	5.02	3.37	3.03	5.79
P_2O_5	0.7	0.66	0.7	0.37	0.53	0.29	0.57	0.62	0.48
LOI	3.67	3.44	1.95	3.16	3.58	2.38	4.71	4.85	4.91
Total	99.69	99.86	99.98	99.55	99.71	99.92	99.8	99.82	99.91
Ba	1500	1500	615	645	2000	1400	852	1000	1800
Rb	27	13	61	57	60	91	73	59	118
Sr	1200	1400	944	718	1300	1600	534	699	407
Y	23	19	24	21	18	18	19	20	21
Ni	15	13	7	15	-	-	26	22	-
Cr	23	29	19	54	6	6	52	95	7
Nb	10	6	5	8	15	12	-	-	10
Zr	115	102	104	115	165	199	67	96	157
La	22	25	18.6	18.9	26	24	11	16.5	27
Ce	51	49	43	42	55	51	25	39	53
Pr	6	5.7	5.2	4.9	6.1	5.10	3.1	4.7	-
Nd	27	25	25	23	25	21	15.8	23	26
Sm	6	5.6	5.8	5	4.9	4.3	4.2	5.3	5.38
Eu	1.87	1.67	1.74	1.59	1.43	1.31	1.41	1.58	1.61
Gd	5.5	5.1	5.5	4.7	4.2	3.7	4.4	4.9	4.91
Tb	0.82	0.77	0.81	0.67	0.62	0.6	0.71	0.78	0.79
Dy	4.3	4	4.6	3.9	3.5	3.10	3.7	3.9	3.99
Ho	0.84	0.74	0.85	0.80	0.68	0.59	0.71	0.75	0.73
Er	2.2	2.1	2.5	2.2	1.7	1.77	2	2	2.12
Tm	0.29	0.26	0.32	0.29	0.26	0.23	0.24	0.25	0.28
Yb	1.98	1.89	2.3	2.1	1.94	1.85	1.65	1.79	2.01
Lu	0.29	0.28	0.32	0.31	0.29	0.27	0.24	0.26	0.29

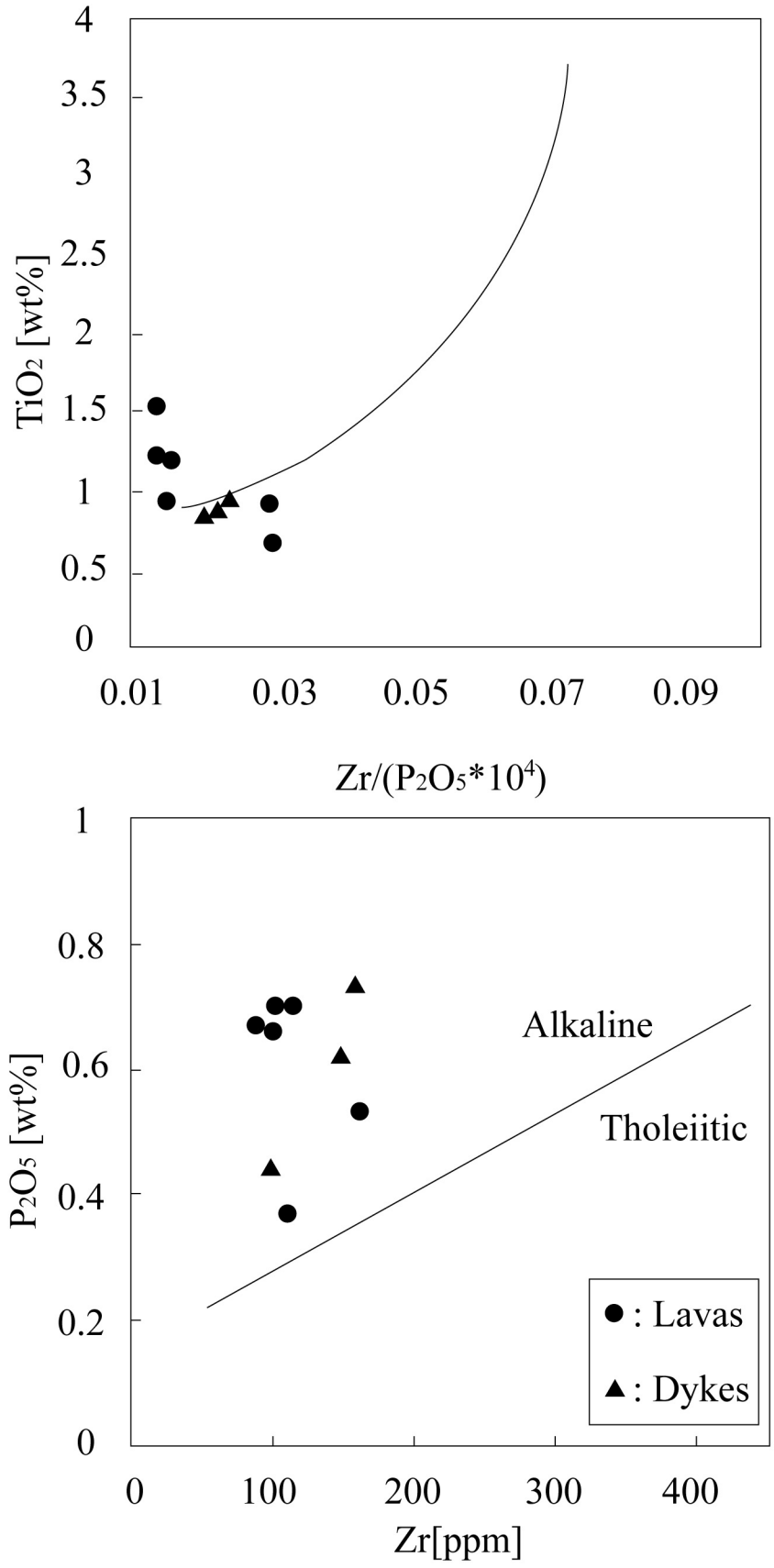

Figure 7: Discriminates diagrams of basalts [Winchester and Floyd, 1976] from lavas and related dykes of the Totola Formation.

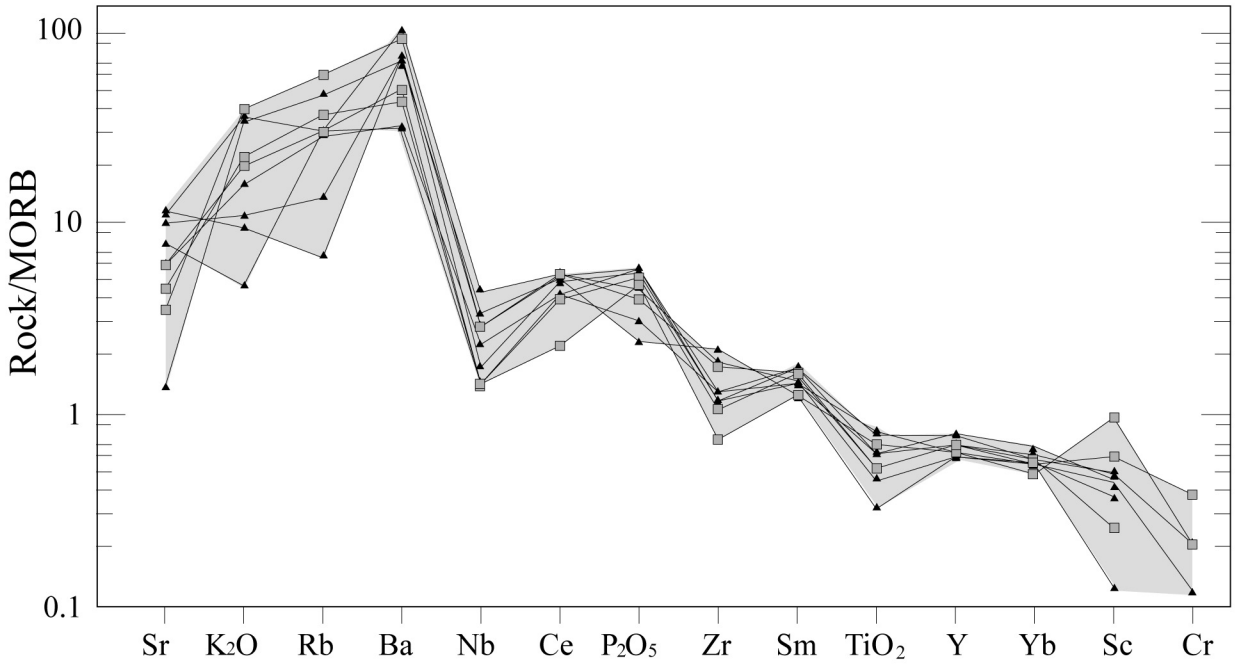

Figure 8. MORB normalized spider diagram from Trace Elements/MORB from lavas and related dykes of the Totola Formation.

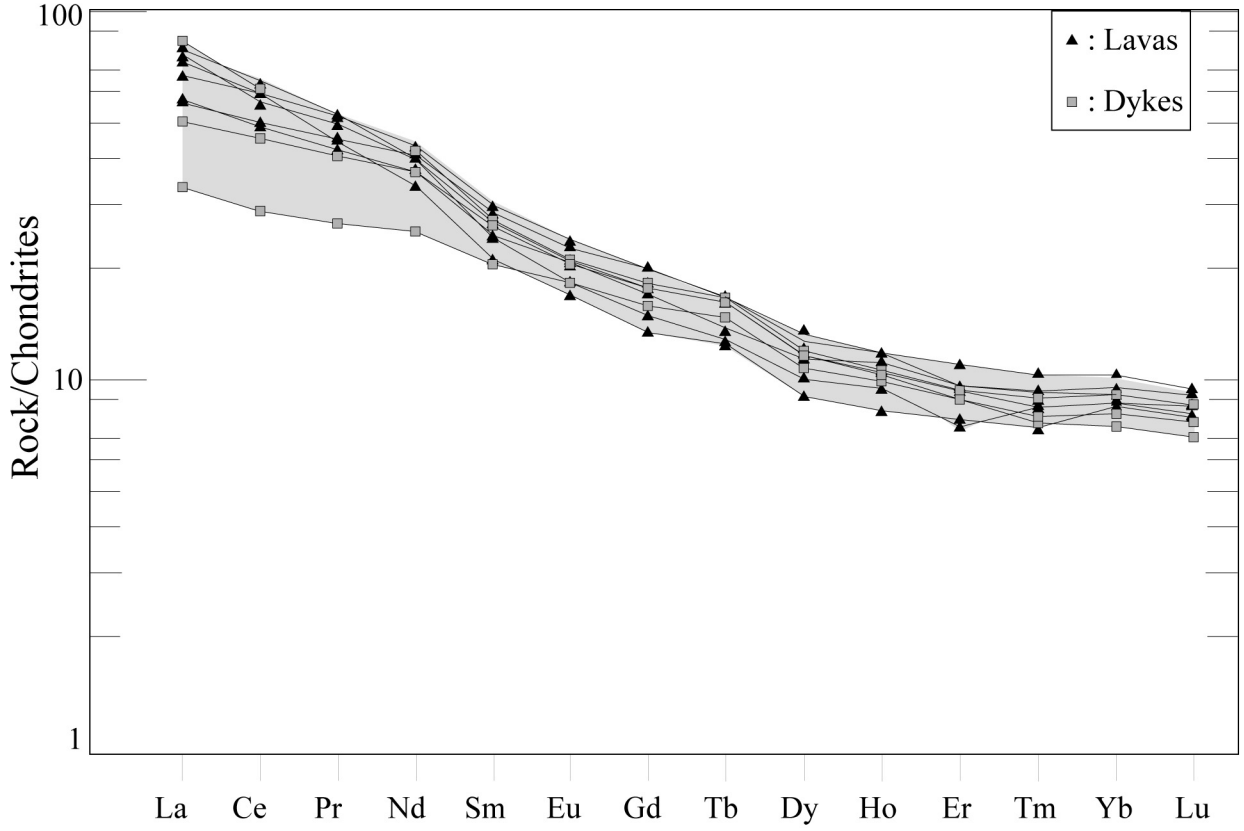

Figure 9. Chondrite normalized REE patterns from lavas and related dykes of the Totola Formation.

Post Purilactis Paleogene sequences.

The Paleocene -Eocene ÅgOrangeÅhFormation

Folded Mesozoic units of Purilactis Group and volcanic of the Cerro Totola Formation, (and associated intrusives) forming part of the Barros Arana Syncline are cover, in strong, angular unconformity by a clastic sequence up to 900 m thick, with a characteristic orange color ("Orange" Formation). The sequence mainly outcrops to the south of Cerro Totola and in the area around Cerro Negro where it deformed in turn by a complex set of tight (tenths to hundredths m wavelength) upright folds (Figure 5). This tinning upwards sequence, with an exposed minimum thickness of around 900 m, was proposed as an independent unit by Arriagada (1999) and Mpodozis et al. (1999). The lowermost levels the formation are constituted by a proximal alluvial fan facies association. roughly 400 m thick, formed by of coarse red conglomerates with clasts up to 1 m in diameter which intermingle with coarse reddish, laminated cross bedded, arcosic sandstones. Clasts are mainly derived from the Cordillera de Domeyko basement (granitoids, rhyolitic porphyries, mafic lavas) but dacitic and porphyritic andesite clasts similar to the Late Cretaceous and Paleocene volcanics outcropping west of the Cordillera de Domeyko (Cinchado and Quebrada Mala formation, Montaño 1976; Marinovic and García,1999) are also found. The conglomeratic lower member grades upwards into a sequence of 500m of "orange" channelized and sheet-flood medium to fine grained sandstones showing both planar an cross bedded stratification which alternate with thin mudstone layers and evaporites (gypsum) which became increasingly important towards the upper levels of the formation (saline lake and/or playa facies association).

Age and tectonic setting. The Orange Formation is equivalent to a thick (up to 100 m) sedimentary sequence (Unit H, Jordan et al., in prep) which in the Salar subsurface onlap over folded Late Cretaceous strata and fills the intervening synclinal depressions. In the Toconao 1 borehole Unit H is formed by volcanoclastic sandstones interbedded with conglomerates and claystones (Muñoz et al., 1997, 2002; Jordan et al., in prep). 70 km south of Cerro Quimal (Pan de Azúcar, region) andesitic lava horizons interbedded in the Formation have been dated at 57,9±1,9 and 58,0±3 Ma (K/Ar, whole rock, Gardeweg et al., 1994), data suggesting a Late Paleocene age. At Loma Amarilla (Figure 5) it's unconformably covered by Eocene-Oligocene strata (Loma Amarilla Formation, Figure 3). The strong angular unconformity at the base of the Orange Formation and the rapid upwards change from proximal alluvial fan to playa lake facies is consistent with the unit being a post tectonic sedimentary sequence which accumulated after a brief pulse of compressional deformation which probably occurred during the lower Paleocene (see discussion bellow).

The Eocene-Early Oligocene Loma Amarilla Formation

The volumetrically most important unit along the El Bordo Escarpment and specially south of Cerro Quimal, is a thick sequence of mostly unconsolidated, coarse, reddish to gray, gravels and conglomerates which form most of the El Bordo ridgeline from Cuesta de Barros Arana to Cerro Negros (Figures 4, 5). Earlier workers considered most of this sequence to be of Miocene age (Ramírez and Gardeweg, 1982, Marinovic and Lahsen, 1984, Hartley et al, 1992a). The Loma Amarilla gravels are filling a very irregular topography carved in the Cretaceous and Paleocene-Eocene sequences; to the west of the El Bordo ridgeline, they are sculptured by a gently west dipping pediplain surface where remains of Late Miocene (10-8 Ma) ignimbrites are found (Naranjo et al, 1994, Mpodozis et al 2001). North of Cerro Quimal, sub horizontal Loma Amarilla strata onlap over Paleozoic and Purilactis outcrops although the same gravels are seen to be dipping up to 80° east of the El Bordo ridgeline. Progressive internal unconformities indicate the syntectonic character of the sequence. The exposed thickness of the Loma Amarilla formation can surpass the 2500 m; its lower levels include (Loma Amarilla-Cerros Negros area) up to 200 m of white tuffs, coarse conglomerates with tuffaceous matrix, and reworked coarse pyroclastics flows with abundant, porphyritic dacitic clasts (Figure 3). The thick upper beds are a monotonous succession of massive, poorly bedded coarse conglomerates, mainly unconsolidated gravels, and minor sandstone. Conglomerates contain clasts from 5 to 50 cm in diameter, including sub rounded boulders of Paleozoic granitoids, rhyolites, dacite and andesite. According to Hartley et al (1992a), who carefully studied a detailed section south of Cerro Negro, they represent an association of proximal alluvial fan facies including hyper concentrated debris flow deposits.

Age and tectonic setting The only horizon suitable for dating in the gravel-rich Loma Amarilla Formation correspond to its tuffaceous basal horizon where Ramírez and Gardeweg (1982) first obtained a K/Ar plagioclase age of 39,9±3,0 Ma (Late Eocene). This age was later confirmed and refined by Hammerdschmidt et al. (1992) who obtained two $^{39}Ar/^{40}Ar$ plateau (biotite) ages of 43,8±0,5 (Pu-1) and 42,2±0,9 Ma (Pu-13). At the same time we acquired an K/Ar age of 59,1±2 Ma (BF-451) for a volcanic (amphibole bearing andesite) clast in the same volcanoclastic layer. This age is similar to the ages obtained for the lavas interbedded within the "Orange Formation" (Gardeweg et al, 1994) and also fall in the 63-55 Ma K/Ar age range reported for lavas of the volcanic Cinchado Formation exposed west of Cordillera de Domeyko (Marinovic and García, 1999) a fact that indicates the sedimentary reworking of

Paleocene volcanic units. Another (porphyritic) clast from volcanoclastic conglomerates, 100 m above the basal contact of the Formation yield a younger (K/Ar, hornblende) age of 33,9±0,3 Ma although, the very low potassium content (0,36% K_2O) of the analyzed material cast doubt about its meaning. Even so it's worth to mention that this value fall in the range of the total degassing age $^{39}Ar/^{40}Ar$ ages of Hammerdschmidt et al. (1992), Pu-1 and Pu-13 biotite samples (32,05+0,6; 36,4±1,0 Ma) which may well indicate a regional event or Ar loss during the Oligocene.

Studies of seismic lines in the Salar allows Loma Amarilla strata to be compared to seismic sequence J in the salar subsurface (Jordan et al. in prep) which in the Toconao 1 borehole is formed by 600 m of multicolored sandstone and conglomerates (Muñoz et al., 1997). Sequence J overlie (Paleocene-Eocene?) sequence H though a prominent erosional unconformity and it's covered by seismic sequence K which can be correlated with the Oligocene-Early Miocene Paciencia Group. This unit which forms large outcrops in the Cordillera de La Sal (Figure 4) includes thin ash layers which has been dated between ca 28 and 20 Ma (Marinovic and Lahsen, 1984, Mpodozis et al, 2000). These age constraints seem to indicate that the Loma Amarilla formation was deposited during the Late Eocene-Oligocene interval being no older than 42 Ma and no younger than 28 Ma. The Loma Amarilla Formation can be considered as a thick sedimentary blanket syntectonic to the Eocene "Incaic" deformation that affected large tracts of Northern Chile approximately between 45 to 35 Ma.

Discussion

Origins: What kind of basin?

Initiation of compressional uplift associated to east verging high angle reverse fault an fault-propagation folding along the eastern edge of the Cordillera de Domeyko in the El Bordo Escarpment region triggered sedimentation in the Purilactis basin with the accumulation of the syntectonic sediments of the Tonel Formation. Our new findings seems to disapprove the extensional hypothesis presented by Macellari et al. (1991); Hartley et al. (1992a) and Flint et al. (1993) and better support more contraction-dominated models. Charrier and Muñoz (1994) and Muñoz et al. (1997) considered that the Purilactis basin formed as a foreland basin related to Cretaceous thrusting to the west while McQuarrie et al. (2003)

suggested that during the Cretaceous "a fold-thrust belt existed in the western portion of the Central Andes as early as Cretaceous to early Paleocene time". According to these models east directed thrusting (along the Cordillera de Domeyko) should have produced a thrust-loaded fore deep in which sediments of the lower Purilactis Group may have been deposited (see also Horton et al., 2001).

The Cordillera de Domeyko deformation zone is not, however, and cannot be considered a thin skinned thrust belt. Detailed regional mapping (Mpodozis et al.,1993a; Marinovic et al., 1995; Cornejo and Mpodozis 1996; Tomlinson et al., 2001) indicates that this tectonic element which runs N-S for more than 800 km between 21Åã and 28ÅãS, (including its northern prolongation, Sierra de Moreno-Sierra del Medio , Figures 1, 2, 10) is a complexly deformed basement ridge formed mainly by Late Paleozoic volcanics and intrusives that was first uplifted during the Late Cretaceous inversion of the Jurassic-Early Cretaceous backarc basin of Northern Chile (Mpodozis and Ramos, 1990; Amiblia et al., 2000, Tomlinson et al, 2001). Since then it has been a positive element that was reworked by Tertiary episodes of deformation (Paleocene, Eocene-Oligocene, Miocene) including the transpressional Eocene-Oligocene ÅgIncaicÅh event which formed the Domeyko Fault System (Maksaev, 1990; Reutter et al., 1991; Tomlinson et al., 1994, 1997; Tomlinson and Blanco,1997; Cornejo et al., 1997; Maksaev and Zentilli, 1999).

Late Cretaceous compressional deformation has also been documented at Sierra de Moreno-Sierra del Medio (Figure 10) even if the large scale geometry of the system is different if compared to the Salar de Atacama segment. In the northern domain a system of west verging high angle reverse faults along the western edge of the Cordillera de Domeyko block (Sierra de Moreno Fault system, SMFS, Tomlinson et al, 2001) brings a Paleozoic basement block on top of deformed Jurassic continental and marine sediments (Ladino et al, 1997, Tomlinson et al, 2001, Figure 10). Solid evidences about the age of the inception of uplift and shortening, has been presented for the Sierra de Moreno by Ladino et al. (1997, 1999 and Tomlinson et al, 2002) who, studying the relations between syntectonic intrusives and regional faults along the at Quebrada Barrera demonstrate that west verging thrusting initiated there between 109-83 *Ma.*

Syntectonic continental sediments of eastern provenance (Tambillos Formation) equivalent to the Lower Purilactis sequence, accumulated, in a "foreland" position unconformable on top of deformed Jurassic sediments on the SMFS footwall (Bogdanic, 1990, Tomlinson et al, 2001) while, at same time continental conglomerates and sandstones (Tolar formation) accumulated in piggyback basins in the hanging wall block of the SMF (Figure 10). Paleocurrent analysis (Bogdanic, 1991, Tomlinson et al, 2001) indicate an eastern provenance for the Tambillos clastics and a western provenance for the Tolar. A 109Å}4 Ma (K/Ar, biotite) age obtained for an andesitic clast from the basal conglomerates of the Tolar Formation (Sierra del Medio) and another (biotite) age of 77 Å}3 Ma for a tuff 460 m above the base (Quebrada Quinchamale) back up the Late Cretaceous age of the sequence (Ladino et al., 1997; Tomlinson et al., 2001).

Thrust load and associated lithospheric flexure cannot be then invoked as the main reason for the creation of accommodation space. The Atacama basin has been a subsiding region not only during the Cretaceous, but also during most of the Cenozoic (see Flint et al., 1993). Even today the basin is topographically more than 1 km below the theoretical altitude to be expected if the local crustal column were in isostatic equilibrium (Yuan et al., 2002). Götze and Krause (2002) speculate that the unusual CAGH gravimetric anomaly outlines an early Paleozoic (?), mafic to ultramafic rock body to be found at mid crustal (10-38 km) levels below to the Atacama basin and which may well be one of the key factors explaining the protracted history of basin subsidence.

Interactions with the Late Cretaceous intra-arc basins of northern Chile

The Late Cretaceous sequences deposited in the Preandean basins are not, the only units of that age known in northern Chile. West of the Cordillera de Domeyko, volcanic and sedimentary units such as the Cerro Empexa Formation west of the Sierra de Moreno block (Tomlinson et al, 2001), the Quebrada Mala Formation, west of the Atacama basin (Montaño, 1976; Marinovic et al., 1996; Marinovic and García 1999; Cortés, 2000) or the LLanta Formation, further south, west of the Pedernales basin (Cornejo et al., 1993, 1996) accumulated in a north south string of, discontinuous, fault bounded basins (Figure 10). The Quebrada Mala Formation which unconformably overlies Late Jurassic-Early Cretaceous sediments and early Late Cretaceous (98-94 Ma) volcanics is a very thick (3700 m) unit of conglomerates and sandstones, interbedded with calc-alkaline andesitic lavas and welded

tuffs dated (K/Ar) between 86 to 66 Ma (Williams, 1992; Marinovic and García, 1999; Cortés, 2000). It was deposited in a small rhomb shaped basin bounded to the east by a NNE trending, west dipping, high angle fault (Sierra El Buitre Fault) formed in the Late Cretaceous as a normal fault along the southeastern basin edge (Marinovic and García, 1999; Figures 2, 10).

It's certainly difficult to match hinterland "extension" with coeval shortening in the Cordillera de Domeyko. Nevertheless, the discontinuous nature of the intraarc basins, thick volcanic and sedimentary fill, and the orientation of related faults is consistent with the basins being formed in a (right lateral?) strike slip setting as Arévalo et al. (1994) and Arévalo (1999) suggested for the Late Cretaceous Hornitos basin in the Copiapó (26-27ÅS) region. Coexistence of zones of margin-parallel strike slip faulting and margin perpendicular shortening is not, however, rare, in active continental margins where plate convergence is oblique as it has been discussed in recent tectonic models for the Late Cenozoic southern Andes (i. e. Cembrano et al., 2002; Folgera et al., 2003). Theoretical model such as of Saint BlanquantÅLs et al. (1998) show that oblique plate convergence along active margins may produce, a strain-partitioned transpressional structural array characterized by arc-parallel strike slip faults, which may be associated to local pull-apart basins, along the thermally weakened arc. Strike slip motion may coexist with arc-orthogonal shortening and thrusting in the back-arc region (Åg magma facilitated strike-slip partitioningÅh). This proposal, which has been verified for the active Sumatra arc (see Mount and Suppe, 1992; Tikoff and Teyssier 1994) may well be a good example for the tectonic conditions prevailing in Northern Chile during the Late Cretaceous as it is shown in Figure 10

Connections with the Salta Rift Basins and the Huaytiquina High

The Atacama (Purilactis Basin) is located at the western slope of the vast Altiplano-Puna plateau where a thick sequence of sediments was deposited during the Cretaceous and Tertiary, both in Bolivia (Sempere et al., 1997; Horton et al., 2001) and Northwestern Argentina (Allmendinger et al., 1997; Salfity and Marquillas, 1999, Coutand, et al., 2001). Studies on the timing, distribution and provenance of sediments has led to some authors to suggest a western source for the Cretaceous sediments outcropping in southwestern Bolivia (Sempere et al., 1997; Horton et al., 2001; McQuarrie et al., 2003). The Cordillera de Domeyko needs to be part of this western source terrain while the Atacama basin and the

string of "preandean" basins which extends further south in Chile, up to the Pedernales-Maricunga basin (26-27ÅãS, Mpodozis and Clavero, 2002, Figure 1) correspond to the more proximal depocenters of the eastern basin system. However, as the connection between the northern Chile depocenters and the rest of the Altiplano-Puna basins was cut short by the onset of volcanism along the Western Cordillera at 26 Ma (Coira et al., 1982; Jordan and Gardeweg, 1988; Kay et al., 1999) correlations between the now two separated domains has been difficult to establish.

Directly east of the El Bordo Escarpment, chronologically equivalents units of the Lower Purilactis Group has not been found in the deep (more than 5000 m) Toconao 1 well drilled at the center of the Atacama basin. Only a volcanic sequence, likely comparable with the Totola Formation, carrying thin layers of shallow water marine limestones bearing Late Cretaceous (ÅgSenonianÅh) foraminifera was found near the well termination at depth (Muñoz et al., 1997; Muñoz and Townsend, 1997). The well was drilled over the northern extension of the Cordón de Lila, a basement ridge formed by Ordovician granitoids, Late Devonian-Early Carboniferous sediments and Permian igneous complexes which protrudes as a peninsula at the southern end of the Salar de Atacama (Ramírez and Gardeweg, 1982, Figure 2). South of the Salar, at Cerros Colorados and Quebrada Guanaqueros, the Paleozoic units are unconformably covered by 500 m of fine-grained red sandstones and shales interbedded with thin limestones layers carrying Campanian to Maastrichtian dinosaur (Titanosauridade) bones (Pajonales Formation, Salinas et al., 1991). Such observations show that Lower Purilactis Group accumulated in a narrow NS trending depocenter between the Cordillera de Domeyko and a basement massif (Huaytiquina High) which separated the basin from the Cretaceous depocenters of the Salta rift System to the east (Salfity et al, 1985, see Figure10).

The oldest Mesozoic sequences known over the Huaytiquina High, in Chile, correspond to a section, marine sandstones oolitic limestones and tuffs (Quebrada Blanca de Poquis Formation, Gardeweg and Ramirez, 1985) carrying Late Cretaceous foraminifera (Hedbergella) which rest unconformably on top of Ordovician strata in the Poquis-Zapaleri region, near the triple boundary between Chile, Argentina and Bolivia (Figure10). Further south in the vicinity of the Chile-Argentine frontier at Huaytiquina (Figure. 10) 100 m of Late Cretaceous carbonate cemented sandstones, conglomerates and impure limestones

attributed to the Yacoraite Formation (Marquillas and Salfity, 1988; Salfity and Marquillas, 1994, 1999) also rest on top of Ordovician sediments (Donato and Vergani, 1987; Marquillas et al, 1997). Yacoraite limestones seems to be an important component of the basement of the Late Cenozoic CVZ volcanic arc as carbonate skarn xenoliths, with geochemical signatures akin to the Yacoraite limestones, have been found in recent lavas erupted from the Lascar volcano (Matthews et al., 1996, 1997). The westernmost extension of this marine incursion is to be found in the marine sediments of the Lomas Negras Formation (Salfity et al., 1985) and the limestones interbedded with the alkaline volcanics of the Totola Formation which seems to have covered a large stretch of the Purilactis basin (Figure 10).

The latest Cretaceous marine incursion over the Huaytiquina High, linked, for the fist time, the Purilactis basin to the Salta rift system of northwestern Argentina (Marquillas and Salfity, 1988; Comínguez and Ramos, 1995; Salfity and Marquillas, 1999). Volcanism seems to have terminated in the Chilean intra arc basins near the end of the Cretaceous while the alkaline nature of the Totola lavas points to more extensional conditions in the Purilactis basin favoring the incursion of the Yacoraite-El Molino sea over the former basement highs (see Figure 10). Yet, models presented for the Salta rift speculate that Yacoraite limestones accumulated during the thermal subsidence stage of the Rift System (Comínguez and Ramos 1995), a disputable hypothesis as the onset of rifting occurred more than 60 Ma before the deposition of the Maastrichtian limestones. The oldest fill unit of the Salta basins is the Pirgua Subgroup (Figure 11) which Salfity et al. (1985), considered as a counterpart of the Tonel and Purilactis formations. This is not totally true, however, as the oldest Pirgua unit, the coarse, proximal alluvial-fan, synrift, conglomerates of the La Yesera Formation, are undoubtedly older than the Tonel formation as K/Ar ages of interbedded alkaline lavas range between 128 and 96 Ma (Viramonte and Escayola, 1999; Viramonte et al., 1999). The Salta rift system seems to have formed during an event of Mid Cretaceous extension associated to continental-scale processes leading to the opening of the South Atlantic (Uliana and Biddle, 1988; Salfity and Marquillas, 1994; Viramonte et al., 1999). This extensional episode coincides with a generalized period of intra-arc extension, in Chile (Aberg et al., 1984; Mpodozis and Allmendinger, 1993) that affected large areas of the Andean margin (Ramos and Alemán, 2000) well before initiation of sedimentation in the Purilactis basin.

The Upper Pirgua sequences (Los Blanquitos and Las Curtiembres formations and the 78-76 Ma Las Conchas basalt, Salfity and Marquilllas, 1999; Viramonte et al.,1999) are time-equivalents to the Lower Purilactis succession (Figure 11). The abrupt facies change from the coarse alluvial fan conglomerates of the La Yesera synrift to the fine-grained lower energy facies of the Las Curtiembres and Los Blanquitos sediments which accumulated Ågon a subtler relief due to the filling of the basin and to less active tectonicsÅh (Comínguez and Ramos 1995) guide Salfity and Marquillas (1999) to propose that ca. 89 Ma the Salta basins were affected by a tectonic episode (cessation or slow-down of active rifting ?) which may well be a far-field effect of the initiation of compression in the Cordillera de Domeyko.

Links to other Chilean Preandean Basins and the Bolivian Altiplano

Continental Cretaceous basins that can be compared with the Atacama (Purilactis) basin also occur south of the Salar de Atacama between and 27ÅS (Punta Negra and Pedernales-Maricunga basins, Figure 1). These are located, as the Atacama between the Cordillera de Domeyko and the CVZ arc to the east. In the Punta Negra basin the thick Tertiary volcanic and sedimentary cover preclude the observation of the older parts of the sedimentary fill. Nevertheless, in the Maricunga-Pedernales basin (Figure 1) a thick sequence of continental clastics (Leoncito Formation) accumulated on strong angular unconformity over Early Cretaceous sandstones (Quebrada Monardes Formation) is exposed at the surface (Cornejo et al., 1993, 1998; Mpodozis and Clavero 2002) and its lower levels are formed by more than 2000 m of fine grained laminates sandstones (Tonel equivalent?, Figure 11) which grade upwards to 800 m sandstones an coarse conglomerates (proximal alluvial fan facies) with reworked Jurassic fossils, limestone clasts and Paleozoic granitoid boulders more that 1 m in diameter. The exposed top of the Formation is formed by 150-200 m of vesicular mafic lavas. Mafic dykes, though to be feeders of the volcanics has been dated (K/Ar) at 64 Ma (Cornejo et al., 1993, 1998). The Leoncito sedimentary episode reflects the onset of uplift and unroofing of the Cordillera de Domeyko during the Late Cretaceous (Mpodozis and Clavero, 2002) and its basal unconformity on top of Early Cretaceous sediments permit to better constrain the age of beginning of sedimentation in the preandean basins of northern Chile.

Northwest of the Salar de Atacama, the NNE active deformed zone of the El Bordo Escarpment and Cordillera de La Sal (Figure 1) pass below the NNW trending active Andean arc to emerge in Bolivia in the Uyuni-Khenayani Fault Zone (Baby et al.,1990; Welsink et al., 1995; Elger and Onken, 2002). There, and also further to the northeast (Sevaruyo region), Cretaceous to Paleogene sediments of the Puca Group (Lohman and Branisa, 1962; Cherroni, 1974; Sempere, 1995; Sempere et al., 1990, 1997; Welsink et al., 1995) unconformably overlie Paleozoic sediments. The Kimmeridgian-Albian Lower Puca is a sequence of continental conglomerates and red sandstones, including eolian facies, accumulated, as the Lower Pirgua subgroup, in an extensional (rift) setting (Welsink et al., 1995; Moretti et al., 1995; Sempere et al., 1997) to culminate with a Cenomanian-Turonian marine episode (Miraflores Formation, Figure11). The Upper Puca Cycle started at 89 Ma with the deposition of the red-mudstones, fine grained laminated sandstones, evaporites (gypsum beds) and pink-brown gypsiferous mudstones (Aroifilla Formation, latest Turonian-Coniacian) deposited, as the Tonel Formation, in a distal alluvial o salt lacustrine (playa lake) environment (Sempere et al., 1997). The overlying Santonian-Campanian, (86-73 Ma) Chaunaca Formation inaugurated by a short-lived restricted marine episode, is also an association of playa lake facies dominated by red-brown mudstones which in the Central Altiplano domain possibly intermingle to the west with more proximal sandstones and mudstones of western provenance (Coroma Formation) which may be compared with the Purilactis Formation.

The Upper Puca cycle terminates with the 100 to 500 m thick Maastrichtian-Danian (73-60 Ma) El Molino Formation whose shallow to restricted marine facies (carbonates, black shales and mudstones) alternate with tuffaceous horizons dated ($^{39}Ar/^{40}Ar$) at 71,6 and 72,5 Ma (Sempere et al., 1997). As in Northern Chile, the ingression advanced over the high ground the east of the basin axis. In the Vilque-X1 well (Figure 10) to the east of the Uyuni-Khenayani fault zone El Molino limestones are found directly on top of Silurian? sediments (Welsink et al., 1995).

Sempere et al. (1997), suggest that at 89 Ma (Late Turonian - Early Coniacian), the Early Cretaceous extensional conditions prevailing in the southern Altiplano, began to change towards a more compressional setting and consider that the accumulation of the younger Upper Aroifilla and Chaunaca formations occurred in a distal foreland basin related to

compression occurring to the west, in Chile. Horton and DeCelles, (1997) and McQuarrie et al. (2003) propose, as well, that Late Cretaceous sedimentation in the Altiplano took place in an early foreland basin related to initial Andean shortening. A more complex model has been presented by McQuarrie et al. (2003) envisaging that the upper Puca sedimentation occurred to the east of an elevated forebulge which separated the Bolivian basin from a western "foredeep" close to the zone of active deformation where Purilacts Group equivalents may have (hypothetically) been deposited (see also Horton et al., 2001). We, however, don`t see conclusive evidences for the existence of a forebulge as the Tonel Formation outcrops directly along strike with the Upper Puca sequences (Aroifilla-Chaunaca) of the Uyuni-Khenayani Fault zone (Figure 10). An alternative proposition may be that, the Bolivian basins were, during the Coniacian-Campanian times connected along strike with the Purilactis depocenter and further south, possibly with the Pedernales basin. This western realm bounded to the west by the Cordillera de Domeyko block, was separated by the Huaytiquina High from the Salta Rift system. Only during Maastrichtian when the Balbuena-El Molino sea advanced over the basements highs and the two domains became finally connected (Figure 10).

Post Purilactis Paleogene tectonics

The major tectonic unconformity at the base of the "Orange" Formation marks the end of accumulation of the Purilactis Group and the beginning of the Cenozoic history on the Atacama basin. The ÅgOrangeÅhFormation is the main Cenozoic sedimentary body that recognized at the subsurface of basin (Muñoz et al., 2002; Jordan et al., in prep), where it cover in strong angular unconformity and onlaps over a system of folds affecting rocks equivalents to the Totola Formation. We interpret this fining upward sequence, whose facies change from coarse conglomerates to sandstones and evaporites, as a sedimentary wedge post-dating a strong pulse of deformation which affected large expanses of northern Chile in the earliest Paleocene an produced renewed uplift in the Cordillera de Domeyko. An apatite fission track age of 64,5±0,9 Ma for the Cerro Quimal intrusive reported by Andriessen and Reutter (1994) seems to trace fast uplift and exhumation shortly after pluton emplacement. Further west, in the Central Depression, the Quebrada Mala basin (Figure 2) was inverted during the earliest Paleocene, before the accumulation of Paleocene volcanics (Cinchado Formation) which rest unconformably on top of deformed Jurassic-Lower Cretaceous to the east of the inverted late Cretaceous basin (Marinovic et al., 1996;

Marinovic and García, 1999). Further south, in the El Salvador-Copiapó region, a strong unconformity between Paleocene volcanics and Late Cretaceous ("Hornitos" and LLanta formations) has been described by Cornejo et al. (1993, 1999), Arévalo et al.,(1994) and Iriarte et al.,(1996). Also Geochemical data indicate that the continental Andean crust in northern Chile grew thicker after this deformation episode as Paleocene-Eocene magmas evolved at higher pressures in a crust already able to stabilize hornblende (Cornejo et al,1999; Cornejo and Matthews, 2001).

The earliest Paleocene deformation seems, to be have affected the mainly the western Andean domain as in the Zapaleri region the continental sandstones of the Chofjias formation (Gardeweg and Ramírez, 1985) possible distal equivalents of the "Orange" Formation rest in concordance over the Late Cretaceous marine strata. Reduced sediment thickness and the presence of numerous paleosol horizons characterize the Paleocene in the southern Bolivian Altiplano, (Santa Lucia, lowermost Potoco and Impora formations, Sempere et al., 1997) indicating a period of very low sedimentation rates. This is also recorded in the thin Paleocene lacustrine sequences of the Paleocene Santa Barbara Subgroup (Mealla and Maíz Gordo formations) which concordantly overlie the Yacoraite limestones in the western Puna and the Salta basins (Salfity and Marquillas 1999).

During the Eocene-Early Oligocene synorogenic Loma Amarilla conglomerates where shed to the east from the Cordillera de Domeyko, into the Salar basin. The Loma Amarilla represents a pulse of synorogenic sediments associated to the Eocene "Incaic" deformation (Coira et al., 1982) when the whole Cordillera de Domeyko was affected by left-lateral transpression which led to localized thrusting, strike-slip faulting, clockwise block rotations, mayor uplift and porphyry copper emplacement (Maksaev, 1990; Reutter et al., 1991; Cornejo et al., 1997; Mpodozis at al., 1993; Arriagada et al., 2000). Very fast uplift and important erosion was suggested by Alpers and Brimhall (1988) when studied the relation between porphyry copper emplacement and supergene enrichment at La Escondida. Maksaev and Zentilli (1999), modeling fission track (apatite) data indicate that at least 4 to 5 km of rocks were exhumed form the Cordillera de Domeyko at rates as high as 100 to 200 m/my during the "Incaic" deformation episode between 50 to 30 Ma.

The onset of the Incaic deformation concur with the beginning of a period of very high oblique convergence rates between the Farallon and South American plates at a 45 Ma (Pilger, 1984; Pardo-Casas and Molnar, 1987) and the eastward migration of the magmatic front from the Central Depression to the Cordillera de Domeyko axis. However, and contrary to the Paleocene, when extensive volcanism took place under extensional conditions in the Central Depression (Cornejo and Matthews, 2000, 2001), Eocene volcanism is almost absent and magmatism is represented only by discontinuous clusters of, small volume, shallow levels stocks, associated including porphyry coppers of emplaced between 42 to37 Ma along the fault traces of the Domeyko Fault System (Maksaev, 1990; Sillitoe, 1992; Cornejo et al., 1997,1999). Extreme compressional (transpressional) conditions prevailing during this period seem to have prevented easy magma ascent, favoring the pounding of magmas at the base of the crust, leading, in turn to ductile failure of the lower crust and localized tectonic thickening below the Cordillera de Domeyko (Mpodozis et al., 1993, Yañez et al., 1994; Tomlinson et al., 1997; Arriagada et al, 2000).

Steep REE patterns of Eocene-Early Oligocene intrusives (Maksaev, 1990; Cornejo et al, 1999 ; Richards et al., 2001) indicate the progressive stabilization of garnet in the source region of the Eocene magmas which is consistent with the formation of a significant crustal root bellow the Cordillera de Domeyko at that time (Cornejo et al., 1999). Rapid isostatic rebound triggered by the creation of the crustal root may explain the fast uplift recorded in the Cordillera de Domeyko during Eocene-Early Oligocene times. The regional distribution of the Loma Amarilla Formation indicate that sedimentation was controlled by a the formation of a short wavelength, high amplitude regional uplift centered along the topographic axis of the Cordillera de Domeyko (Maksaev and Zentilli, 1999) from which sediments where shed to the west and east to almost completely conceal the previous structural landscape along the El Bordo Escarpment (Mpodozis et al., 2000; Arriagada et al., 2002, Figures 4, 5)

Thick (up to 6000 m) Late Eocene to Oligocene continental sequences also have cover large tracts of the southern Altiplano in Bolivia (i.e. Potoco, Tihuanacu formations, Sempere et al., 1997; Lamb and Hoke, 1997; Horton et al., 2001; Rochat, 2002) and the Puna, in Argentina (Geste and Quiñoas formations, Jordan and Alonso, 1987; Allmendinger et al., 1997; Kraemer et al., 1999; Coutand et al, al, 2001; Voss, 2003). Provenance studies and the

discontinuities existing between depocenters indicate that sedimentation was associated not only to uplift in the western Andes but also to the uplift of the Eastern Cordillera block in Bolivia (Lamb and Hoke, 1997) and discrete mountain blocks in the Argentine Puna (Boll and Hernández, 1986; Kraemer et al., 1999; Coutand et al., 2001). The distributed nature of the deformation which affected a very wide swath of the central Andes, including the westernmost Sierras Pampeanas at 27ºS (Coughlin et al, 1998) may be an indication that the Eocene (Incaic) orogeny was associated to a shallowing of the subducting slab as it has been suggested for southern Peru (Sandeman et al. 1995; James and Sacks (1999).

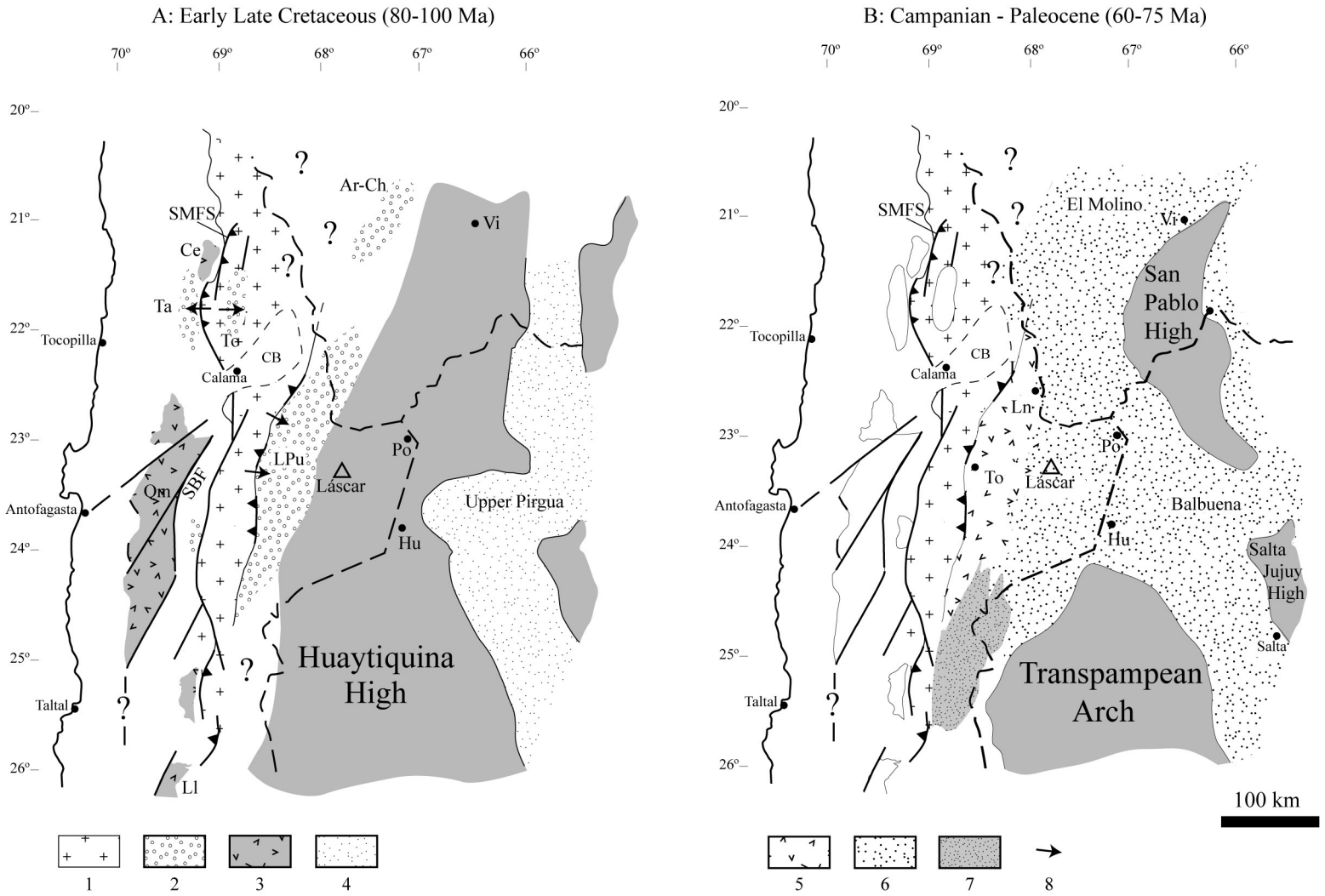

Figure 10: Late Cretaceous – Early Tertiary paleogeography and tentative elements of the Western Central Andes (21-26ºS). (1) Cordillera de Domeyko basement, (2) Late Cretaceous syntectonic deposits, (3) Arc volcanics and intraarc basin sediments, (4) Continental sediments of the Salta Rift Basin, (5) Alkaline mafic lavas of the Totola Formation, (6) Shallow marine deposits of the El Molino – Yacoraite sea, (7) Continental sequences of the Sierra de Almeida region, (8) Sediment provenance direction. Ce: Cerro Empexa Fm. Ta: Tambillos Fm. To: Tolar Fm. Qm: Quebrada Mala Fm. Ll: Llanta Fm. LPu: Lower Purilactis Group. Ar-Ch: Airofilla – Chaunaca formations. SMFS: Sierra de Moreno Fault System. SBF: Sierra El Buitre Fault. CB: Calama basin. Po: Poquis. Hu: Huaitiquina. Vi: Vilque well. Ln: Lomas Negras. To: Cerro Totola. Discussion in text.

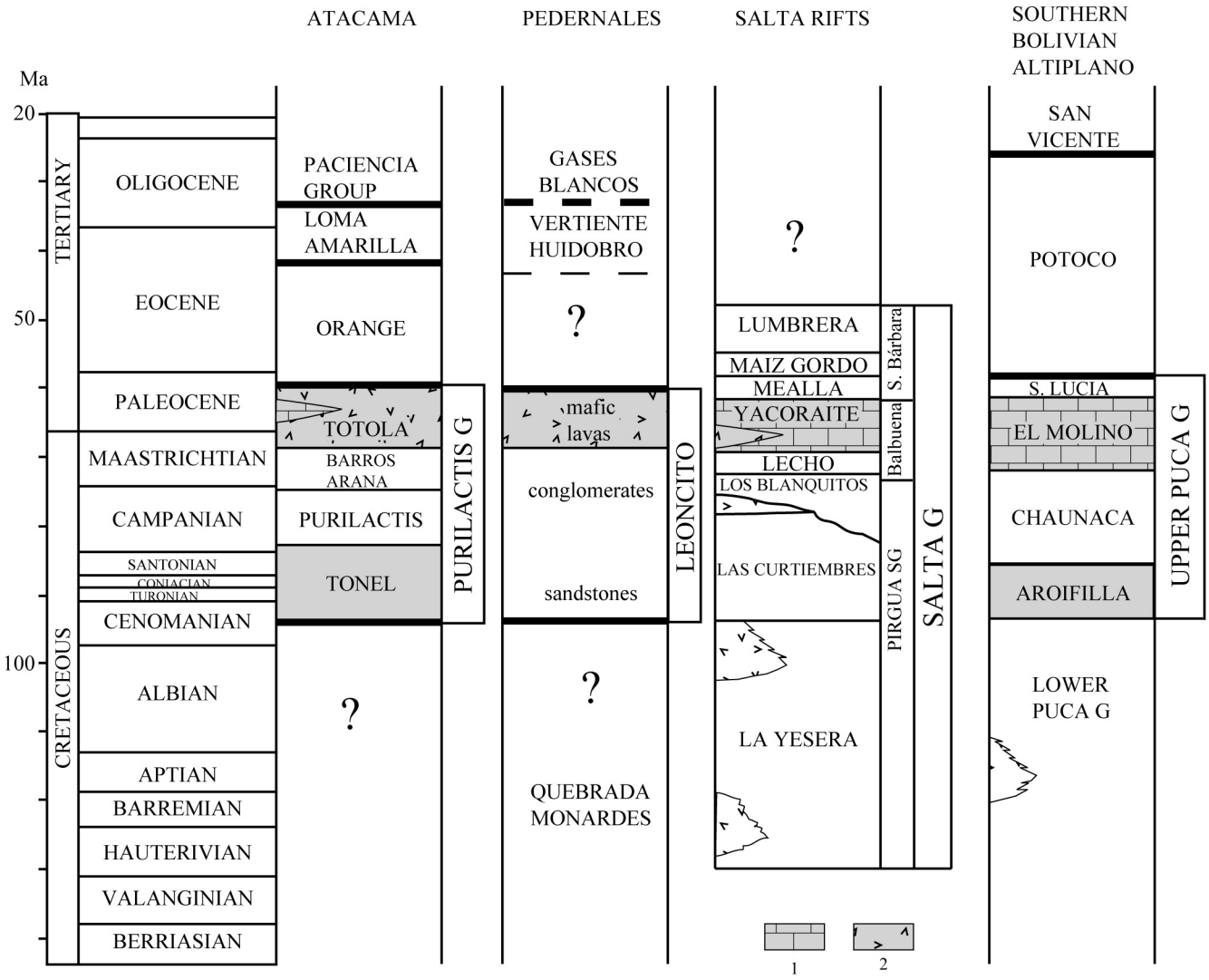

Figure 11: Correlation table of Cretaceous-Paleogene units from Southwestern Central Andes. Thick black lines represent regionally important unconformity. (1) Limestone. (2) Volcanics.

Conclusions

The Atacama basin is a deep depocenter with exhibits an unusually well preserved Mesozoic to Cenozoic sedimentary record of the earlier tectonics events leading to the formations of the Central Andes. New field and geochronological support the presentation of an updated stratigraphic system for the earlier (Early Late Cretaceous. Paleocene-Eocene) basin fill (Purilactis Group) we use to formulate an improved model about the basin tectonic history. Unlike previous previous hypothesis we consider that the basin was formed not as an extensional basin, nor a classic foreland basin produced by lithospheric flexure. It was created in the Early Late Cretaceous as a consequence of tectonic collapse and inversion of the Mesozoic back-arc basin of northern Chile. Inversion led to the formation of the proto Cordillera de Domeyko as a narrow, thick skinned, basement range bounded by high angle reverse faults and blind thrusts, which shift vergence along strike. Syntectonic sediments where deposited in basins both to the west (Tambillos Formation) and east of the Cordillera de Domeyko (Purilactis Group in the Atacama Basin). The extremely thick Cretaceous to Paleogene fill of the Atacama (Purilactis) basin seems to be related to an inherited (Paleozoic) anomalously dense crustal body which originated the CAGH anomaly which may have controlled rapid subsidence and creation of accommodation space. Repeated episodes of uplift related to shortening in the Cordillera de Domeyko led to the accumulation of syntectonic sediments of the Tonel, Purilactis and Barros Arana formations during the Late Cretaceous. During the same time interval, volcanism and sedimentation occurred in strike-slip of pull-apart basins along the active Andean arc in the central part of the Antofagasta region .

The prevalent tectonic regime during the Late Cretaceous in Northern Chile seem to have been controlled by oblique plate convergence with led to the partitioning of regional strain into a margin parallel component, along the arc, and a margin -perpendicular component in the back arc. Back arc compression favored the inversion of the former Jurassic-Early Cretaceous back arc basin and the accumulation of syntectonic sediments in the Atacama basin.

The basin is the westernmost depocenter of the Cretaceous. Paleogene Altiplano Puna domain and events recorded in its sedimentary fill are consistent with the reported history of more distal areas of northwestern Argentina and southeastern Bolivia. Nevertheless the comparison with the Salta Rift System (SR) of northwestern Argentina show that the SR was formed during a period of generalized by Early Cretaceous extension, also recorded in Bolivia (Lower Puca) and along the Chilean active margin. Far-field effects of the Early Late Cretaceous inversion of the northern Chile back-arc basin and initial uplift of the Cordillera de Domeyko have been recognized both in the southern Bolivian Altiplano and the SR system.

Acknowledgements

Research funds provided by FONDECYT, Chile (grants 1970002, 199009) a cooperative program IRD/ Departamento de Geología, Universidad de Chile and the Servicio Nacional de Geología y Minería. Discussions with Teresa Jordan, Nicolás Blanco, Moyra Gardeweg and Andy Tomlinson greatly helped us to develop the ideas we presented in this paper.

References

Åberg, G., Aguirre, L., Levi, B., Nystrom, J. O., 1984. Spreading-subsidence and generation of ensialic marginal basin: an example from the Early Cretaceous of Central Chile. Geol. Soc. London, Spec. Pub. 16, 185-193.

Allmendinger, R. W., Jordan, T. E., Kay, S. M., Isacks, B.L., 1997. The evolution of the Altiplano-Puna Plateau of the Central Andes. An. Rev. Earth Planet. Sci. 25, 139-174.

Alpers, C.N.,. Brimhall, G. H., 1988. Middle Miocene climatic change in the Atacama Desert, northern Chile; evidence from supergene mineralization at La Escondida, Geol. Soc. Am. Bull. 100, 1640-1656.

Amilibia, A., Sabat, F., Chong, G., Muñoz, J. A., Roca, E., Gelabert, B., 2000. Criterios de inversión tectónica: ejemplos de la Cordillera de Domeyko (II Región de Antofagasta). Proc. IX Congr. Geol. Chileno 2, 548-552.

Andriessen, P. A., Reutter, K. J., 1994. K-Ar and fission track mineral age determinations of igneous rocks related to multiple magmatic arc systems along the 23ºS Latitude of Chile and Argentina. Tectonics of the Southern Central Andes, Springer-Verlag, Berlin, 141-154.

Arévalo, C., 1999. The Coastal Cordillera/Precordillera boundary in the Tierra Amarilla area of Northern Chile and the structural setting of the Candelaria Cu-Au deposit. PhD. thesis, Kingston University, 1-204.

Arévalo, C., Rivera, O., Iriarte, S., Mpodozis, C, 1994. Cuencas extensionales y campos de calderas del Cretácico Superior-Terciario Inferior en la Precordillera de Copiapó (27°-28ºS), Chile. Proc. VII Congr. Geol. Chileno 2, 1288-1292.

Arriagada, C., 1999. Geología y Paleomagnetismo del Borde Oriental de la Cordillera de Domeyko entre los 22Åã45' y 23Åã30' latitud Sur, II Región, Chile. . thesis, Univ. Chile, 1-176.

Arriagada, C., Cobbold, P. R., Mpodozis, C., Roperch, P., 2002. Cretaceous to Paleogene compressional tectonics during the deposition of the Purilactis Group, Salar de Atacama. Proc. V IRD-ISAG, Tolouse, 41-44.

Arriagada, C., Roperch, P., Mpodozis, C., 2000. Clockwise block rotations along the eastern border of the Cordillera Domeyko, northern Chile (22º45'-23º30' S). Tectonophysics 326, 153-171.

Arriagada, C., Roperch, P., Mpodozis, C., Dupont-Nivet, G., Cobbold, P.R., Chauvin, A., Cortés, J., 2003. Paleogene clockwise tectonic rotations in the fore-arc of Central Andes, Antofagasta region, Northern Chile. J. Geophys. Res. 108 (B1)

Baby, P., Sempere, T., Oller, J., Barrios, L., Hérail, G., Marocco, R., 1990. A late Oligocene-Miocene intermountain foreland basin in the southern Bolivian Altiplano. C. R. Acad. Sci. Paris, Ser. II, 311, 341-347.

Barrier, L., 2002. Interactions déformations-sédimentation dans les systemes compressifs supracrustaux: Examples numériques et modelisátion analogique. PhD. thesis, Univ. Rennes, 1-181

Basso, M. Mpodozis, C. (in prep.). Hoja Cerro Quimal. Serv. Nac. Geol. Min., Mapas Geológicos (1:100.000).

Besse, J., Courtillot, T, V., 1991. Revised and synthetic apparent polar wander paths of the African, Eurasian, North American and Indian plates and true polar wander since 200 Ma. J. Geophys. Res. 96, 4029-4050.

Blanco, N., Mpodozis, C., Gardeweg, M., Jordan, T.E., 2000. Sedimentación del Mioceno Superior-Plioceno en la cuenca del Salar de Atacama. Estratigrafía de

la Formación Vilama, II Región de Antofagasta. Proc. IX Congr. Geol. Chileno 1, 446-450

Bogdanic, T., 1991. Evolución paleogeográfica del Cretácico-Terciario Inferior, entre los 21Åã23ÅãS, Región de Antofagasta, Chile. Proc. VI Congr. Geol. Chileno 1, 857-861,

Boll, A., Hernández, R. M., 1986. Interpretación estructural del área Tres Cruces. Bol. Inf. Petrol., Buenos Aires, 7, 2-14

Breitkreutz, C., Helmdach, F.F., Kohring, R., Mosbruger, V., 1992. Late Carboniferous Intra-arc sediments in the North Chilean Andes: Stratigraphy, Paleogeography and Paleoclimate. Facies 26, 67-80.

Breitkreutz, C., van Schmus, W.R., 1996. U-Pb geochonology and significance of Late Permian ignimbrites in Northern Chile. J. South Am. Earth Sci. 9 (5/6), 281-293.

Brüggen, J., 1934. Las Formaciones de Sal y Petróleo de la Puna de Atacama. Bol. Min. Petr., Santiago, 32, 105-122.

Brüggen, J., 1942. Geología de la Puna de San Pedro de Atacama y sus formaciones de areniscas y arcillas rojas. Proc. Congr. Pan. Ing. Min. Geol., Santiago,.2, 342-367.

Brüggen, J., 1950. Fundamentos de la Geología de Chile. Inst. Geog. Militar, Santiago, 1-374

Cande, S.C., La Brecque, J.L., Haxby, W.F., 1988. Plate kinematics of the South Atlantic: Chron C34 to Present. J. Geophys. Res. 93, 13479-13492.

Cembrano, J., Lavenu, A., Reynolds, P., Arancibia, G., López, G., Sanhueza, A., 2002. Late Cenozoic transpressional ductile deformation north of the Naza-South-America- Antarctica triple junction. Tectonophysics 354, 289-314.

Charrier, R., Muñoz, N., 1994. Jurassic-Cretaceous paleogeographic evolution of the Chilean Andes at 23Åã24Åãouth latitude: A comparative analysis. Tectonics of the Southern Central Andes, Springer-Verlag, Berlin, 141-154.

Charrier, R., Reutter, K.J., 1990. The Purilactis Group of Northern Chile: Link between arc and backarc during Late Cretaceous and Paleogene. Proc. I ORSTOM-ISAG, Grenoble, 249-252.

Charrier, R., Reutter, K.J. 1994. The Purilactis Group of Northern Chile: Boundary Between Arc and Back arc from Late Cretaceous to Eocene. Tectonics of the Southern Central Andes. Springer-Verlag, Berlin, 189-202

Cherroni, C. 1974. Geología de la región Corocoro. Rev.Téc.YPFB, Santa Cruz, 4(3), 125-154

Coira, B., Davidson, J., Mpodozis,.C., Ramos, V. A., 1982. Tectonic and magmatic evolution of the Andes of northern Argentina and Chile. Earth Sci. Rev. 18, 303-332

Comínguez, A.H., Ramos, V. A., 1995. Geometry and Seismic expression of the Cretaceous Salta Group. Am Assoc. Petrol Geol. Mem. 62, 325-340.

Cornejo, P., Matthews, S. J., 2000. Relación entre magmatismo-tectónica y su implicancia en la formación de pórfidos cupríferos: yacimiento El Salvador, III Region, Chile. Proc. IX Congr. Geol. Chileno 1, 184-188

Cornejo, P., Matthews, S. J 2001. Evolution of magmatism from the uppermost Cretaceous to Oligocene and its relationship to changing tectonic regime. Proc. III South Am. Symp. Isotop. Geol., Santiago, 558-561.

Cornejo, P., Mpodozis, C., 1996. Geología de la Región de Sierra Exploradora (25°-26°S): Serv. Nac. Geol. Min., Informe Registrado IR-96-09, 1-330.

Cornejo, P. Mpodozis, and C., Ramírez, C. F., Tomlinson., 1993. Estudio Geológico de la Región de El Salvador y Potrerillos. Serv. Nac. Geol., Min. Informe Registrado IR-93-1, 1-258.

Cornejo, P., Mpodozis, C., Tomlinson, A., 1998. Hoja Salar de Maricunga. Serv. Nac. Geol. Min., Mapas Geológicos, 7 (1:100.000).

Cornejo, P., Mpodozis, C., Matthews, S., 1999. Geología y Evolución Magmática del Distrito Indio Muerto y Yacimiento El Salvador. Serv. Nac. Geol. Min. Informe Registrado IR-98-14, 1-99

Cornejo, P., Tosdal, R., Mpodozis, C., Tomlinson, A. J., Rivera, O., Fanning, M., 1997. El Salvador Porphyry Copper revisited: Geologic and geochronologic framework. Int. Geol. Rev. 39, 22-54.

Cortés, J., 2000. Hoja Palestina, Región de Antofagasta., Serv. Nac.Geol. Min., Mapas Geológicos, 19 (1:100.000).

Coughlin, T. J., O'Sullivan, B., Kohn, B. P., Holcombe, R. J., 1998. Apatite fission-track thermochronology of the Sierras Pampeanas, central western Argentina:

Implications for the mechanism of plateau uplift in the Andes. Geology 26 (11) 999-1002.

Coutand, I., Cobbold, P.R., de Urreiztieta, M., Gautier, P., Chauvin, A., Gapais, D., Rossello, E., Gamundi. O. L., 2001. Style and history of Andean deformation, Puna plateau, northwestern Argentina. Tectonics 20 (2), 210-234.

Davidson, J., Ramírez, C.F., Brook, M., Pankhurst, R., 1985. Calderas del Paleozoico superior-Triásico inferior y mineralización asociada. Comunicaciones, Dep. Geol. Univ. Chile. 35, 53-57.

Dingman, R. J. 1963. Cuadrángulo Tulor. Inst. Invest. Geol., Carta Geol. Chile, 11(1:50.000), 1-35

DeCelles, P.G., Horton, B. K, 2003. Early Tertiary foreland basin development and the history of Andean crustal shortening in Bolivia. Geol. Soc. Am. Bull. 115 (1), 58-77.

Donato, E., Vergani, G., 1987. Estratigrafía de la Formación Yacoraite (Cretácico) en Paso Huyatiquina, Salta, Argentina. Proc. IX Congr. Geol. Argentino 1, 263-266.

Elger, K., Onken, O. 2002 The pattern of deformation related to growth of the southern Altiplano plateau (Bolivia). Proc. V IRD-ISAG, Tolouse, 203-206.

Flint, S., 1985. Alluvial fan and playa sedimentation in an Andean arid closed basin: the Paciencia Group, Antofagasta Province, Chile. J. Geol. Soc. London 142, 533-546.

Flint, S., Hartley, A., Rex, D., Guise, P., Turner, P., 1989. Geochronology of the Purilactis Formation, Northern Chile: An insight into Late Cretaceous/Early Tertiary basin dynamics of the Central Andes. Rev. Geol. Chile 16, 241-246

Flint, S., Turner, P., Jolley, E., Hartley, A., 1993. Extensional tectonics in convergent margin basins: An example from the Salar de Atacama, Chilean Andes. Geol. Soc. Am. Bull. 105, 603-617.

Folgera., A., Ramos, V., Melnik, 2003. Partición de la deformación en la zona del arco volcánico de los Andes neuquinos (36°-39°S) en los últimos 30 millones de años. Rev. Geol. Chile 29 (2), 227-240.

Galliski, M.A., Viramonte, J.G., 1988. The Cretaceous paleorift in northwestern Argentina: A petrologic approach. J. South Am. Earth Sci., 1(4), 329-342.

Gardeweg M., Ramírez C. F., 1985. Hoja Río Zapaleri, Región de Antofagasta. Serv. Nac. Geol. Min., Carta Geol. Chile, 66 (1:250.000) 1-89.

Gardeweg, M., Pino, H., Ramírez, C. F., Davidson, J., 1994. Mapa Geológico del area de Imilac y Sierra Almeida, Región de Antofagasta. Serv. Nac. Geol. Min., Doc. Trabajo 7 (1:100.000).

Gephart, J., 1994. Topography and subduction geometry in the central Andes: Clues to the mechanics of a non collisional orogen, J. Geophys. Res., 99, 12279-12288.

Götze, H-J., Kirchner, A., 1997. Interpretation of Gravity and Geoid in the Central Andes between 20° and 29°S. J. South Am. Earth Sci. 10 (2) 179-188.

Götze, H-J., Krause, S., 2002. The Central Andean Gravity High, a relic of an old subduction complex?. J. South Am. Earth Sci, 114(8), 79-811.

Hammerschmidt, K., Doebel, R., Friedrichsen, H., 1992. Implication of $^{40}Ar/^{39}Ar$ dating of early Tertiary volcanic rocks from the North-Chilean Precordillera. Tectonophysics 202, 55-58.

Hartley, A., Flint, S., Turner, P., 1988. A proposed lithostratigraphy for the Cretaceous Purilactis Formation, Antofagasta Province, northern Chile. Proc. V Congr. Geol. Chileno, 3, H83-H99.

Hartley, A., Jolley, E., Turner, P., Flint, S., 1991. Preliminary paleomagnetic results from the Late Cretaceous Tonel Formation (Purilactis Group), Precordillera of Northern Chile: Constraints on thrust sheet rotation. Proc. VI Congr. Geol. Chileno, 1-15.

Hartley, A., Flint, S., Turner, P., Jolley, E.J., 1992a. Tectonic controls on the development of a semi-arid, alluvial basin as reflected in the stratigraphy of the Purilactis Group (Upper Cretaceous-Eocene), northern Chile. J South Am. Earth Sci. 5 (3/4), 275-296.

Hartley, A.J., Jolley, E. J., Turner, P., 1992b. Paleomagnetic evidence for rotation in the Precordillera of northern Chile: structural constraints and implications for the evolution of the Andean fore-arc. Tectonophysics 205, 49-64.

Horton, B.K., DeCelles, P.G., 1997. The modern foreland basin system adjacent to the Central Andes. Geology 25, 895-898.

Horton, B.K., Hampton, B.A., Waanders S. G.L., 2001. Paleogene synorogenic sedimentation in the Altiplano plateau and implications for initial mountain building in the Central Andes. Geol. Soc. Am. Bull. 113, 1387-1400.

Iriarte, S., Arévalo, C., Mpodozis, C., Rivera, O., 1996. Mapa Geológico de la Hoja Carrera Pinto. Serv. Nac. Geol. Min., Mapas Geológicos, 3 (1:100.000).

Isacks, B.L., 1988. Uplift of the central Andean plateau and bending of the Bolivian orocline. J. Geophys. Res. 93, 3211-3231.

James, D.E., Sacks, I.S., 1999. Cenozoic formation of the Central Andes: a geophysical Perspective. Soc. Ec. Geol., Spec. Pub., 7, 1--25

Jolley, E.J., Turner, P., Williams, G.D., Hartley, A.J., Flint, S., 1990. Sedimentological response of an alluvial system to Neogene thrust tectonics, Atacama Desert, northern Chile. J. Geol. Soc. London 147, 769-784.

Jordan, T. E., Alonso, R. N., 1987. Cenozoic stratigraphy and basin tectonics of the Andes Mountains, 20°-28° south latitude. Am. Assoc. Petrol. Geol. Bull. 7, 49-64.

Jordan, T. E; Gardeweg, M., 1988. Tectonic evolution of the Late Cenozoic Central Andes (20°-33°S). Oxford Monograph Geol. Geophys. 8, 193-207.

Jordan, T. E., Muñoz, N., Mpodozis, C., Blanco, N., Pananont, P., Gardeweg, M. (in prep). Cenozoic subsurface stratigraphy and structure of the Salar de Atacama basin, northern Chile.

Kape, S. J., 1996. Basin Analysis of the Oligo-Miocene Salar de Atacama, Northern Chile. PhD. thesis, Univ. Birmingham, 1-256

Kay, S., Mpodozis, C., Coira, B., 1999. Neogene magmatism, tectonism and mineral deposits of the Central Andes (22°-33°S Latitude). Soc. Ec. Geol., Spec. Publ.7, 27 - 59.

Kraemer, B., Aldeman, D,. Alten, M., Schnurr, W., Erpstein, K., Kiefer, E., van den Bogaaard, P., Görler, K., 1999. Incorporation of the Paleogene foreland into the Negene Punaplateau: The Salar de Antofalla area, NW Argentina: J. South Am. Earth Sci. 12 (2), 157-182.

Ladino, M., Tomlinson, A., Blanco, N. , 1997. Nuevos antecedentes para la edad de la deformación cretácica en Sierra de Moreno, región de Antofagasta, Chile: Proc. VIII Congr. Geol. Chileno 1, 103-107

Ladino, M., Tomlinson, A., Blanco, N., 1999. New constrains for the age of Cretaceous compressional deformation in the Andes of Northern Chile (Sierra de Moreno 21º-22º10'S). Proc. IV IRD-ISAG, Götttingen,407-410.

Lamb, S.H., Hoke, L., 1997. Origin of the high plateau in the Central Andes, Bolivia. South America, Tectonics 16, 623-649.

Lahsen, A.,1969. Geología del área comprendida entre El Tatio y los cerros de Ayquina. Comité Geotérmico CORFO (internal report), 1-75

Lemaitre, , R. W., Bateman, P., Dudek, A., Keller, J., Lameyre Le Bas, M. J., Sabine, P. A., Shmid, R., Sorensen, H., Streckeisen, A. Wooley, A. R., Zanettin, B., 1989. A Classification of igneous rocks and glossary of terms, Blackwell, Oxford

Lohman, H. H., Branisa, L. 1962, Estratigrafía y Paleontología de Grupo Puca en el sinclinal de Miraflores, Potosí, Petrol. Boliv., 4, 9-16.

Macellari, C.E., Su, M., Townsend, F., 1991. Structure and seismic stratigraphy of the Atacama Basin, Northern Chile. Proc. VI Congr. Geol. Chileno, 133-137.

Maksaev, V, 1990. Metallogeny, geological evolution and thermocronology of the Chilean Andes between Latitudes 21Åã and 26Åã South, and the origin of major porphyry copper deposits. PhD. thesis, Dalhousie University, 1-544.

Maksaev, V., Zentilli, M., 1999. Fission track thermochronology of the Domeyko Cordillera, northern Chile; implications for Andean tectonics and porphyry copper metallogenesis. Explor. Min. Geol. 8, 65-89.

Marinovic, N., García, M.,1999. Hoja Pampa Unión. Región de Antofagasta. Serv. Nac. Geol. Min. Mapas Geológicos, 9 (1:100.000).

Marinovic, N., Smoje, I., Hervé, M., Mpodozis, C. , 1995. Hoja Aguas Blancas. Serv. Nac. Geol. Min., Carta Geol. Chile, 70 (1.250.0000), 1-150.

Marinovic, N., Lahsen, A., 1984. Hoja Calama. Serv. Nac.,Geol. Min, Carta Geol. Chile, 58 (1:250.000), 1-140.

Marinovic, N., Cortés, J., García, M., 1996. Estudio geológico regional de la zona comprendida entre Sierra del Buitre y Pampa San Román, Serv. Nac. Geol. Min., Informe Registrado IR-96-8, 1- 140.

Marquillas, R., Salfity, J.A., 1988. Tectonic framework and correlations of the Cretaceous-Eocene Salta Group, Argentina. The Southern Central Andes, Springer-Verlag .....

Marquillas, R., Salfity, J., González, R., Matthews, S., Battaglia, R., 1997. Geología del Grupo Salta (Cretácico-Eoceno) en la comarca de Huaytiquina, Puna Argentina. Proc. VIII Congr. Geol. Chileno 1, 139-143.

Matthews , S. J., Marquillas, R. J., Kemp, A. J., Grange, F. K., Gardeweg, M. C., 1996. Active skarn formation beneath Lascar volcano, northern Chile Chile: a petrographic and geochemical study of xenoliths in eruption products. J. Metam. Geol. 14, 509-530.

Matthews, S. J., Marquillas, R., Kemp, J., 1997. The lateral extent of the Yacoraite Formation (Maastrichtian) beneath the Tertiary-Recent volcanic deposits of NE Chile and NW Argentina at 23º S. Proc. VIIII. Congr. Geol. Chileno 2, 534-536.

McQuarrie, N., Horton, B., Zandt, G., Beck S., DeCelles, P., 2003. Lithospheric evolution of the Andean fold-thrust belt, Bolivia and the origin of the central Andean plateau, Tectonophysics.(submitted)

Montaño, J. M., 1976. Estudio geológico de la zona de Caracoles y áreas vecinas, con énfasis en el sistema Jurásico, Provincia de Antofagasta, II Región, Chile. Memoria de Título, Univ. Chile, 1-168.

Moretti, I., Baby, P., Araníbar, O., Rochat, P., 1995. Evaluación del Potencial Petrolero del Altiplano de Bolivia. YPFB (unpublished report), 1-30

Mount, V. S., Suppe, J., 1992. Present-day stress orientation adjacent to active strike-slip faults: California and Sumatra. J. Geophys. Res. 97, 1195-12013.

Mpodozis, C., Allmendinger, R. W., 1993. Extensional tectonics, Cretaceous Andes, northern Chile (27°S). Geol. Soc. Am. Bull. 105, 1462-1477.

Mpodozis, C., Clavero, J., 2002. Tertiary tectonic evolution of the southwestern edge of the Puna plateau: Cordillera Claudio Gay (26Åã27Å8), Northern Chile. Proc. V IRD-ISAG, Tolouse, 445-448.

Mpodozis, C.,. Ramos, V. A.,. 1990. The Andes of Chile and Argentina. Geology of the Andes and Its Relation to Hydrocarbon and Mineral Resources. Circum-Pac. Counc. En. Min. Res., Earth Sci. Ser., 59-90.

Mpodozis, C., Marinovic, N., Smoje, I., Cuitiño, L., 1993a. Estudio Geológico-Estructural de la Cordillera de Domeyko entre Sierra Limón Verde y Sierra Mariposas, Región de Antofagasta. Serv. Nac. Geol. Min. Informe Registrado IR-93-04, 1- 282.

Mpodozis, C., Marinovic, N., Smoje, I. 19933b. Eocene Left Lateral Strike Slip Faulting and Clockwise Block Rotations in the Cordillera de Domeyko, West of the Salar de Atacama, Northern Chile. Proc. II ORSTOM-ISAG, Oxford, 225-228.

Mpodozis, C., Arriagada, C., Roperch, P., 1999. Cretaceous to Paleogene geology of the Salar de Atacama basin, northern Chile: A reappraisal of the Purilactis Group stratigraphy. Proc. IV IRD-ISAG, Göttingen, 523-526.

Mpodozis, C., Blanco, N., Jordan, T., Gardeweg, M.C., 2000. Estratigrafía y deformación del Cenozoico Tardío en la región norte de la Cuenca del Salar de Atacama: la zona de Vilama-Pampa Vizcachitas. Proc. IX Congr. Geol. Chileno 2, 598-603.

Muñoz, N., Charrier, R., 1999. Interactions between the basement and the cover, Salar de Atacama basin, northern Chile. Proc. Thrust Tectonics Conf., Univ. London, 278-281

Muñoz, N., Townsed, F.,1997. Estratigrafía de la cuenca Salar de Atacama, Resultados del pozo exploratorio Toconao 1. Implicancias Regionales. Proc VIII Congr. Geol. Chileno 1, 555-558.

Muñoz, N., Charrier, R., Jordan, T. E., 2002. Interactions between basement and cover during the evolution of the Salar de Atacama Basin, Northern Chile. Rev. Geol. Chile 29 (1), 55-80.

Muñoz, N., Charrier, Reutter, K. J., 1994. Evolución de la Cuenca del Salar de Atacama: Inversión tectónica y relleno de una cuenca de antepaís de retroarco. Proc. VIII Congr. Geol. Chileno 1, 5-199.

Naranjo, J.A., Ramírez, C. F., Paskoff. R., 1994. Morphostratigraphic evolution of the northwestern margin of the Salar de Atacama basin (23ºS-68ºW). Rev Geol. Chile 21(1), 91-103.

Pardo-Casas, F., Molnar, P., 1987. Relative motion of the Nazca (Farallon) and South American plates since late Cretaceous time. Tectonics, 6, 233-248.

Pilger, R. H., 1984. Cenozoic plate kinematics., subduction and magmatism: South American Andes. J. Geol. Soc. London 141, 793-802.

Ramírez, C. F., Gardeweg, M.C., 1982. Hoja Toconao, Región de Antofagasta. Serv. Nac. Geol. Min., Carta Geol. Chile 54 (1:250.000), 1-122.

Ramos. V. A., Alemán, A., 2000. Tectonic Evolution of the Andes. Tectonic Evolution of South America. 31th Int. Geol. Cong. (Rio de Janeiro), 635-685.

Reutter, K., Scheuber, E., Helmcke, D., 1991. Structural evidence of orogen-parallel strike-slip displacements in the Precordillera of Northern Chile. Geol. Rundsch. 80 (1), 135-153.

Richards, J.P., Boyce, A. J., Pringle, M. S., 2001. Geological evolution of the Escondida area , northern Chile: A model for spatial and temporal localization of porphyry Cu mineralization. Ec. Geol. 96, 271–305.

Riba, O., 1976. Syntectonic unconformities of the alto Cardener, Spanish Pyrenees: a genetic interpretation. Sed. Geol., 15, 213-233.

Rochat, Ph., 2002. Structures et Cinématique de l'Altiplano Nord-Bolivien au sein des Andes Centrales. Lab. Geol. Univ. Grenoble, Mem H.S. 38, 1-193

Rollinson, H., 1993. Using geochemical data: evaluation, presentation, interpretation. Longman, 1-352..

Saint Blanquant, M., Tikoff, B., Teyssier, C., Vigneresse, J. L., 1998. Tranpressional kinematics and magmatic arcs. Geol. Soc. London, Spec. Pub. 135, 327-340

Salfity, J. A., Marquillas, R., 1994. Tectonic and sedimentary evolution of the Cretaceous-Eocene Salta Group Basin, Argentina, Friedr. Vieweg & Sohn, p. 266-315.

Salfity, J. A., Marquillas, R. A, 1999, La Cuenca Cretácica-terciaria del Norte Argentino. Geología Argentina, Inst. Geol. Rec. Nat., Anales, 29 (19), 613-626.

Salfity, J. A., Marquillas, R., Gardeweg, M. C., Ramírez, C.F., Davidson, J., 1985. Correlaciones en el Cretácico superior del norte de la Argentina y Chile. Proc. IV Congr. Geol. Chileno 1, 654-1 667.

Salinas, P., Sepúlveda, P., Marshall, L., 1991. Hallazgo de restos óseos de dinosaurios (Saurópodos) en la Formación Pajonales (Cretácico Superior), Sierra de Almeida, Región de Antofagasta, Chile: Implicancia Cronológica. Proc. VI Congr. Geol. Chileno, 534-537.

Sandeman, H.A., Clark, A.H., Farrar, E. 1995. An integrated tectono-magmatic model for the evolution of the southern Peruvian Andes (13-20º S) since 55 Ma. Int. Geol. Rev. 37, 1039-1073.

Sempere, T., 1995. Phanerozoic evolution of Bolivia and adjacent regions. Am. Assoc. Petrol. Geol. Mem. 62, 207-230.

Sempere, T., Hérail, G., Oller, J., Bonhomme, M.G., 1990. Late Oligocene-early Miocene major tectonic crisis and related basins in Bolivia. Geology 18, 946-949.

Sempere, T., Butler, R.F., Richards, D.R., Marshal, L.G., Sharp, W., Swisher, C.C., 1997. Stratigraphy and chronology of late Cretaceous-early Paleogene strata in Bolivia and northern Argentina. Geol. Soc. Am. Bull. 109, 709-727.

Sillitoe, R. H., 1992. Gold and Copper Metallogeny of the Central Andes - Past, Present and Future Exploration Objectives. Ec. Geol. 87, 2205-2216.

Tikoff, B., Teysier, B., 1994. Strain modeling of displacement field partitioning in trasnspressional orogens. J. Struct. Geol. 16, 1575-1588.

Tomlinson , A. J., Blanco N., Maksaev, V., Dilles, J., Grunder, A. L., Ladino, M., 2001 Geología de la Precordilera Andina de Quebrada Blanca-Chuquicamata, Regiones I y II (20Å ã30'-22Åã30'S). Serv. Nac. Geol. Min., Informe Registrado IR-01-20

Tomlinson, A.J., Blanco, N., 1997. Structural evolution and displacement history of the West Fault System, Precordillera. Proc. VIII Congr. Geol. Chileno 3, 1973-1882.

Tomlinson, A. J., Mpodozis, C., Cornejo, P., Ramírez, C. F., Dimitru, T., 1994. El Sistema de Fallas Sierra Castillo-Agua Amarga: transpresión sinistral eocena en la Precordillera de Potrerillos-El Salvador. Proc. VII Congr. Geol. Chileno 2, 1459-1463.

Uliana, M., Biddle, K. T., 1988. Mesozoic-Cenozoic paloegeographic evolution of Southern South America. Rev. Bras. Geociencias 18, 172-190.

Viramonte, J., Escayola., M., 1999. El Magmatismo Cretácico-Paleógeno del Noroeste Argentino. XIV Congr. Geol. Argentino, Relatorio, 284-291.

Viramonte, J. G., Kay, S. M., Becchio, R., Escayola, M., Novitki, I., 1999. Cretaceous rift related magmatism in central-western South America. J. South Am. Earth Sci. 12, 109-121

Welsink, H. J., Martínez, E., Araníbar, O., Jarandilla, J., 1995. Structural inversion of a Cretaceous rift basin, southern Altiplano, Bolivia. Am. Assoc. Petrol. Geol. Mem. 62, 305-324.

Wilkes, E., Görler, K., 1994. Sedimentary and Structural Evolution of the Salar de Atacama Depression. Proc. V Congr. Geol. Chileno 1, A117-A188.

Williams, W. C., 1992. Magmatic and structural controls on mineralization in the Paleocene magmatic arc between 22°40' and 23°45' south latitude, Antofagasta region, Chile. PhD. thesis, University of Arizona, 1-182.

Winchester, J. A, Floyd, P. A., 1976. Geochemical magma type discrimination: application to altered and metamorphosed igneous rocks. Earth Planet. Sci. Lett. 28, 459-469.

Voss., R., 2003, Cenozoic stratigraphy of the southern Salar de Antofalla region, northwestern Argentina. Rev. Geo. Chile (29(2), 167-189

Yañez, G., Mpodozis, C., Tomlinson, A., 1994. Eocene dextral oblique convergence and sinistral shear along the Domeyko fault System: a thin viscous sheet approach with asthenospheric drag at the base of the crust. Proc. VII Congr. Geol. Chileno 2, 1478-1482.

Yuan, X., Sobolev, S., Kind, R., 2002. Moho topography in the central Andes and its geodynamic implications. Earth Planet.Sci.Lett.199, 389-402.

Figure captions

Fig. 1. Topography of the Central Andes between 10-30ºS showing main morphological units and the location of the Preandean basins (Atacama, Punta Negra, Pedernales and Maricunga) in the forearc of northern Chile.

Fig. 2. Simplified geological map of the Antofagasta region and location of figures 4&5. CS, Cordillera de la Sal, LP, Llano de la Paciencia, SBF, Sierra El Buitre Fault. (after Mapa Geológico (1:1000.000), SERNAGEOMIN Chile (2002); Marinovic and García, (1999); Cortés, (2000); Basso, (in prep.)).

Fig. 3. Synthetic stratigraphic section of the Purilactis Group and Paleogene strata outcropping along the El Bordo Escarpment.

Fig.4. Geological map of the Barros Arana area.

Fig.5. Geological map between Cerro Quimal and Cerro Negro area.

Fig.6. Syntectonic growth strata in the middle member of the Tonel Formation, east of the Cerro Quimal.

Fig.7 Discriminates diagrams of basalts [Winchester and Floyd, 1976] from lavas and related dykes of the Totola Formation.

Fig. 8. MORB normalized spider diagram from Trace Elements/MORB from lavas and related dykes of the Totola Formation.

Fig. 9. Chondrite normalized REE patterns from lavas and related dykes of the Totola Formation.

Fig.10. Late Cretaceous – Early Tertiary paleogeography and tentative elements of the Western Central Andes (21-26ºS). (1) Cordillera de Domeyko basement, (2) Late Cretaceous syntectonic deposits, (3) Arc volcanics and intraarc basin sediments, (4) Continental sediments of the Salta Rift Basin, (5) Alkaline mafic lavas of the Totola Formation, (6) Shallow marine deposits of the El Molino – Yacoraite sea, (7) Continental sequences of the Sierra de Almeida region, (8) Sediment provenance direction. Ce: Cerro Empexa Fm. Ta: Tambillos Fm. To: Tolar Fm. Qm: Quebrada Mala Fm. Ll: Llanta Fm. LPu: Lower Purilactis Group. Ar-Ch: Airofilla – Chaunaca formations. SMFS: Sierra de Moreno Fault System. SBF: Sierra El Buitre Fault. CB: Calama basin. Po: Poquis. Hu: Huaitiquina. Vi: Vilque well. Ln: Lomas Negras. To: Cerro Totola. Discussion in text.

Fig.11. Correlation table of Cretaceous-Paleogene units from Southwestern Central Andes. Thick black lines represent regionally important unconformity. (1) Limestone. (2) Volcanics.

Table 1. Geochronological data.

Table 2. Geochemical analysis.

Projet de Publication : Tectonique compressive du Crétacé au Paléogène dans le bassin de Salar d'Atacama.

Résumé: Le bassin du Salar d'Atacama dans la dépression Préandine du nord du Chili est une caractéristique de premier ordre des Andes Centrales. Des données structurales de terrain et l'interprétation des lignes sismiques suggèrent que le développement du bassin a été contrôlé par une déformation de la couverture et du socle dans un environnement tectonique d'avant-pays. Des strates de croissance dans plusieurs niveaux du bassin fournissent la preuve d'une sédimentation contemporaine de la déformation de la Cordillère de Domeyko pendant le Crétacé Moyen, Paléogène et Néogène. Bien que, davantage de travail soit nécessaire pour obtenir une bonne évaluation du raccourcissement qui s'est produit dans le bassin, nos résultats suggèrent qu'un important épaississement et raccourcissement pre-Néogène peut avoir affecté la dépression Préandine et probablement de grands secteurs des proto-Andes Centrales. Ainsi, les modèles qui expliquent l'épaisseur actuelle des Andes Centrales devraient considérer dans leurs estimations le raccourcissement du Crétacé Supérieur-Paléogène. Une subsidence flexurale induite par la charge tectonique de la Cordillère de Domeyko et un corps rémanent, dense et froid sous le bassin expliquent la longue durée de fonctionnement de ce basin et son importante anomalie topographique.

Cretaceous to Paleogene compressional tectonics of the Salar de Atacama basin

Abstract

The Salar de Atacama basin in the pre-Andean depression of northern Chile is a first-order feature of the Central Andes. The sedimentary fill of this basin constraints the timing and extent of crustal deformation for the forearc. Structural field data and deep seismic-reflection profiles suggest that the development of the basin was controlled by both thin and thick-skinned fold-thrust deformation in a foreland tectonic setting. Growth strata in several levels of the basin fill provide evidence for sedimentation contemporaneous with motion of fold-thrust structures during mid Cretaceous, Paleogene and Neogene time. Although, further work is needed to have a well estimation of the shortening occurred in the Salar de Atacama basin, our results suggest that important pre-Neogene thickness and shortening may have affected the pre-Andean depression and probably large areas of the proto-Central Andes. Thus, models that explain the actual thickness of the Central Andes should consider in their estimations Late Cretaceous and Paleogene shortening. Flexural subsidence induced by the tectonic loading of Cordillera de Domeyko basement range, and a remnant ancient cold and dense body under the basin are probably the main causes to explain the long lived and the actual low topography of this particular basin.

Introduction

The Andean Cordillera extends for ~8000 km along the western margin of South America continent, making it the longest sub-aerial mountain chain on Earth. Since the early days of the plate tectonics, the Andes has been cited as the type example of an ocean-continent collision zone, or active continental margin [Dewey and Bird, 1970]. The Altiplano-Puna physiographic province, a high continental plateau second only to the Tibetan plateau in its area and average elevation [Allmendinger et al., 1997], and the ~55º bend known as the Bolivian Orocline or Arica elbow are the most striking features in the entire Andean mountain belt (Figure 1). The exceptionally thick crust, up to 70 km in central Andes has commended attention since its existence was clarified by James [1971]. The formation of this thick crustal root is thought to be primarily the result of tectonic shortening and thickening associated with the Andean fold-thrust belt [Isacks, 1988; Sheffels, 1990; Schmitz, 1994; Lamb and Hoke, 1997]. Most studies consider total central Andean shortening to be approximated by Neogene shortening in the Eastern Cordillera and Subandean-Santa Barbara Zone [Isacks, 1988; Sempere et al., 1990; Schmitz, 1994; Gubbels et al., 1993; Allmendinger et al., 1997; Baby et al., 1997; Lamb and Hoke, 1997; Kley et al., 1999], but shortening may have started as early as Late Cretaceous-Early Paleocene time [Coney and Evenchick, 1994; Sempere, 1995; Sempere et al., 1997; Horton and DeCelles, 1997; Horton et al., 2001; Coutand et al., 2001; McQuarrie and DeCelles, 2001; Müller et al., 2002].

Although, apparently no important deformation has occurred in the forearc region since 10 Ma, is still poorly understood what is the tectonic influence of the forearc in the construction of the orogen. Pre-Neogene deformation may have played an important role in the tectonic history of the central Andes and if pre-Neogene mountain building occurred in regions west of the eastern fold-thrust belt, most models underestimate not only the duration but also the total amount of crustal shortening across the orogenic belt. Structural, stratigraphic and paleomagnetic data suggest a deformation episode across all the forearc in northern Chile, probably, during the Late Cretaceous to Paleogene time [Chong and Reutter, 1985; Hammerschmidt et al., 1992; Hartley et al., 1992; Scheuber and Reutter, 1992; Charrier and Reutter, 1994; Somoza et al., 1999; Arriagada et al., 2000; Randall et al., 2001; Somoza and Tomlinson, 2002; Arriagada et al., 2003].

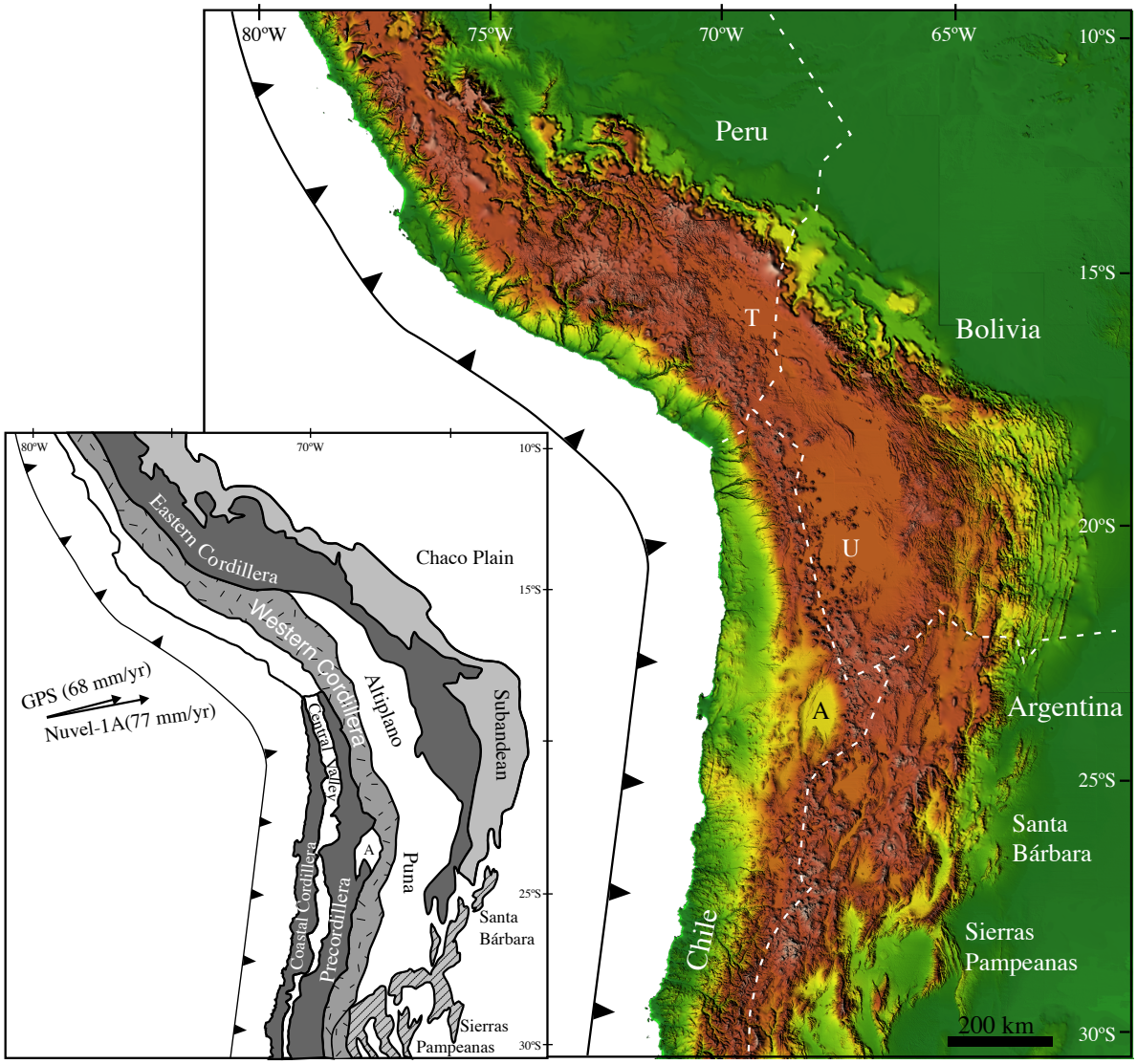

Figure 1: From west to east, the continental margin at about 15-27ºS consists of: The Peru-Chile trench and continental slope; the Coastal Cordillera, a remnant of a Mesozoic magmatic arc; the Longitudinal Valley (also called Central Depression or Pampa del Tamarugal), a modern forearc basin; the Precordillera (including Cordillera Domeyko) and Preandean Depression (including Salar de Atacama basin), that largely define the western Andean slope; the Western Cordillera, an active volcanic arc along the eastern border of Chile; the Altiplano-Puna plateau, a high-elevation hinterland plateau; the Eastern Cordillera, a rugged interior of the eastern fold-thrust belt; the Subandean Zone and Santa Barbara Zone, frontal active parts of the eastern fold-thrust belt; and the Beni Plain and Chaco Plain, parts of a low-elevation foreland basin underlain by the Brazilian shield. A, Salar de Atacama. T, Titicaca Lake. U, Salar de Uyuni. Nazca-South America convergence is represented by NUVEL-1A vector (DeMets et al., 1994) and GPS vector (Norabuena et al., 1998).

However, the extent of any pre-Neogene mountain belt and associated foreland basin system, as well as the total amount of pre-Neogene shortening, remains poorly understood.

Of particular interest is the Salar de Atacama basin, one of the major active sedimentary basins in the central Andes, which is surrounded by excellent exposures of Paleozoic to Tertiary strata and igneous rocks (Figure 1&2). Contrasting with the height average elevation of the Puna (~4400 m) and the Western Cordillera (up to 6500 m), the Salar de Atacama basin, with an average elevation of 2300 m, is a major negative topographic anomaly in the generally "smooth" western slope of central Andes [Isacks, 1988; Gerphart, 1994; Götze and Krause, 2002; Yuan et al., 2002]. The large dimensions of the low imply an origin that is at the scale of a major crustal or lithospheric feature. Seismic tomographic and residual gravity field data suggest that the lithosphere in this region is abnormally cold and dynamically subsided, due possibly to coupling with the subducting Nazca plate [Götze and Krause, 2002; Yuan et al., 2002].

The geology of this area has been the subject of several studies, its structure and tectonic setting for the up to ~8 km of sediments contained in the basin are still not completly understood. Along the western margin of the basin, almost 5 km thick, sedimentary and minor volcanic, deposited between the Cretaceous to Paleogene time, constitute one of the key elements of the basin fill (Figures 2&3). Deposition is generally assumed to have occurred during extensional tectonics in an arc or back-arc setting, even if syn-sedimentary extensional faults have not been described [Hartley et al., 1992; Flint et al., 1993; Charrier and Reutter, 1994]. Similarly, Oligo-Miocene evolution of the basin has been attributed to a stage of relaxation, following Late Eocene compressional tectonics [Götze et al., 2002]. New detailed mapping of the western border of the basin [Arriagada, 1999; Mpodozis et al., 1999; Arriagada et al., 2000; Arriagada et al., 2002; Mpodozis et al., submitted; this work], have allowed an improvement of the structural setting and the surface stratigraphy of the area. Moreover, a complete set of migrated seismic reflection lines over much of the Salar de Atacama and an exploration oil well in the center of the basin (Figure 2), permit us discuss de tectonic evolution of the Atacama basin. Several works have indicated that the geometry of the basin may be controlled by the inversion of Cretaceous extensional faults [Macellari et al., 1991; Muñoz et al., 1997; Muñoz et al., 2002], our observations, in

agreement with Muñoz et al. [1997; 2002], suggest that the Salar de Atacama basin was developed in a compressional foreland setting, from mid-Cretaceous to Paleogene times as it did also in Neogene to recent times.

Geological Setting

The Salar de Atacama is situated in the pre-Andean Depression of northern Chile. The basin is bounded to the west by the Cordillera de Domeyko (Precordillera), which exposes Paleozoic and Mesozoic rocks (Figures 1&2). This range with an average altitude of 3000 m.a.s.l, was uplifted mainly during the Eocene "Incaic" tectonic event [Ramírez and Gardeweg, 1982; Charrier and Reutter, 1994; Mpodozis et al., 1993; Maksaev and Zentilli, 2000]. To the east, it is bounded by the Andean slope, constituted by Miocene and Pliocene ignimbrites, a few Late Paleozoic rocks (Peine Group of Breitkreuz and Zeil., 1994) and the active volcanic arc of the Western Cordillera. The southern border of the basin is delineated by the Western Cordillera, which here retreats around 60 km eastwards from its regional NS trend, adopting a NE-SW trend, and the Cordón de Lila Paleozoic basement range (Figures 1&2). The Cordón de Lila comprises Ordovician to Carboniferous sedimentary and volcanic/plutonic rocks [Niemeyer, 1984; Damm et al., 1991]. Apatite fission track ages of 38.6±5.6 Ma indicate that this basement range was situated at a depth of at least 3-4 km during the Late Eocene [Andriessen and Reutter, 1994].

The basin has approximated dimensions of 100 km wide (EW) and 200 km length (NS). Its 2300 m altitude contrasts with heights of up to 6700 m in the Western Cordillera and 4278 m (Co. Quimal) in the Cordillera de Domeyko (Figure 2). The basin displays in its interior, the Cordillera de la Sal, a SSW-NNE trending fold and thrust belt, 5-10 km wide, which rises about 200 m above the basin level. This is constituted by complexly deformed Oligocene-Pliocene, evaporite-rich, continental sediments and ignimbrites [Ramírez and Gardeweg, 1982; Flint et al., 1993; Wilkes and Görler, 1994]. This still tectonically active ridge traverses the basin and separates the Salar de Atacama flat plain from the Llano de la Paciencia (Figure 2). The Llano de la Paciencia is a narrow 80 km long NS, and 8 km wide subbasin filled by a complex coalescing Quaternary alluvial fans [Jolley et al., 1990].

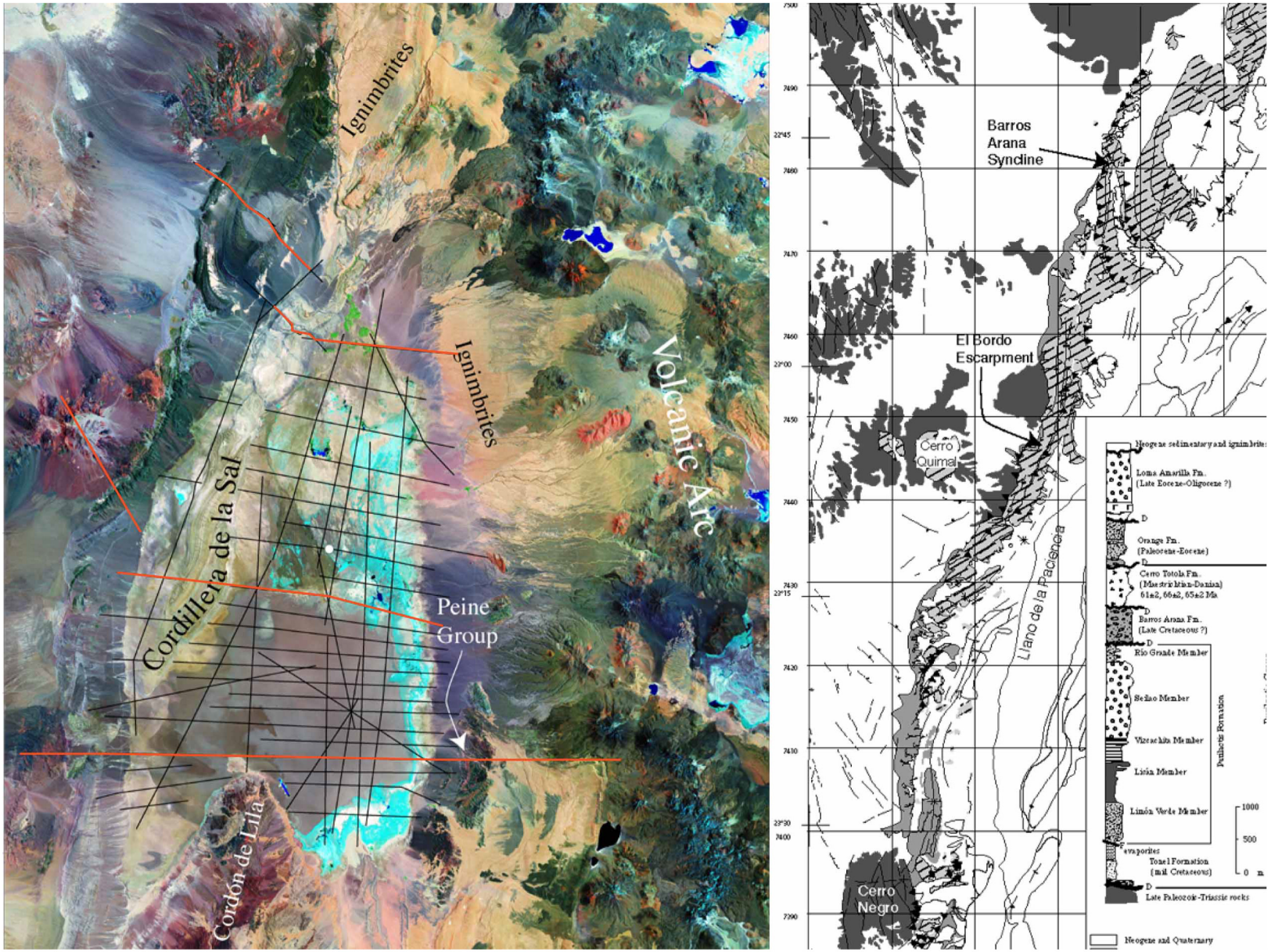

Figure 2: General geological setting of the Salar Atacama basin. a) LANDSAT image showing main topographic and geologic units. Location of the available seismic lines for this study and the position of the Toconao 1 exploration well (white circle in the center of the basin) are also displayed. Red lines show the location of the profiles in the figure 15. b) Simplified geological map and stratigraphy for the western edge of the Salar de Atacama basin.

The eastern border of the Cordillera de Domeyko, coincides with a steep 900 m high topographic scarp (El Bordo Escarpment, Figure 2), which extends for more than 120 km along the western margin of the basin. The older and best exposed sequences of the Mesozoic to Cenozoic Atacama basin fill occur in a series of major E/W to NW/SE trending canyons, cutting trough El Bordo Escarpment (Figures 2, 3&4). Sedimentary and volcanic rocks, of the Purilactis Group, the Orange and Loma Amarilla formations constitute more than 5 km thick [Dingman, 1963; Ramírez and Gardeweg, 1982; Naranjo et al., 1994; Flint et al., 1993; Charrier and Reutter, 1994; Mpodozis et al., 1999; Mpodozis et al., submitted]. Further to the east, although not exposed, these sequences also form the lower section of the Llano de la Paciencia and the Atacama basin sedimentary fill [Macellari et al., 1991; Muñoz et al., 1997; Muñoz et al., 2002].

Cretaceous-Paleogene stratigraphy of the western edge of the basin

The lower portion of the Purilactis Group, the Tonel Formation, is a sequence of red sandstone and evaporite finely bedded and laminated, accumulated in a playa-lake environment of 400-1000 m thick (Figures 2, 3, 4&5). The Tonel Formation rests in a smooth unconformity over Triassic lacustrine and volcanic rocks (Figure 5a&b), which overlie the Late Paleozoic volcanic and intrusive rocks of the Cordillera de Domeyko. The Tonel Formation is covered by almost 3000 m of fluvial, alluvial, lacustrine red sandstone and mudstone beds of the Purilactis Formation (Figure 5c). Paleomagnetic data suggest that the deposition and magnetization of the Tonel Formation and the lower portion of the Purilactis Formation occurred during the mid Cretaceous normal polarity superchron (119-84 Ma, Arriagada et al., 2000). Over the Purilactis Formation, 500 m of coarse fan conglomerate beds of alluvial setting of the Barros Arana Formation were deposited during Late Cretaceous time (Figure 3). Finally, 800 m of basaltic to rhyolitic lava flows with minor limestone beds of the Cerro Totola Formation constitute the upper portion of the Purilactis Group. The age of the Cerro Totola Formation is well defined for 11 K/Ar ages in lava flows and related intrusions (Cerro Quimal Intrusive is also included), ranging from 66 to 61 Ma [Mpodozis et al., submitted]. A strong angular unconformity separates the Purilactis Group of the Orange and Loma Amarilla formations (Figure 2,3,4&5b). The Orange Formation is constituted by up to 900 m thick conglomerate in the lower portion and sandstone and evaporite beds in the upper levels. The Orange Formation, is covered by

a tuff horizon and coarse conglomerate beds with internal crosscutting and onlapping relationship of the basal portion of the Loma Amarilla Formation, which is mainly constituted by up to 1000 m of coarse conglomerate beds. A Late Eocene age of the basal volcanic of this formation is well defined by K/Ar (39.9±3 Ma, Ramírez and Gardeweg, 1982) and $^{40}Ar/^{39}Ar$ (43.8±0.5 and 42.2±0.9, Hammerdschmidt et al., 1992). The upper portion of this succession, poorly dated was deposited probably during Early Oligocene time [Mpodozis et al., submitted].

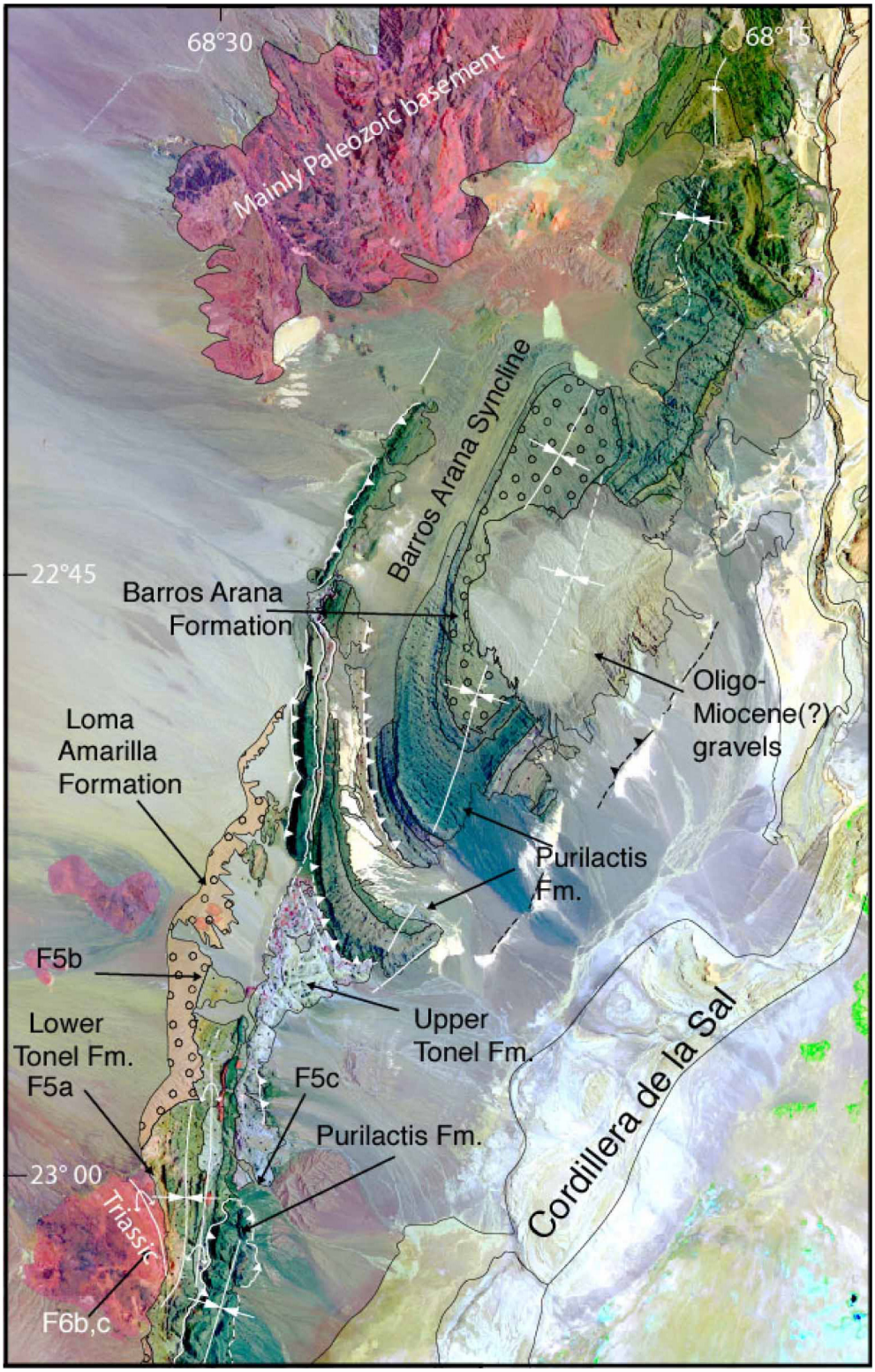

Figure 3: Geological map in LANSAT image of the north El Bordo Escarpment. F6b,c indicate the location of the photos for the Figures 5&6.

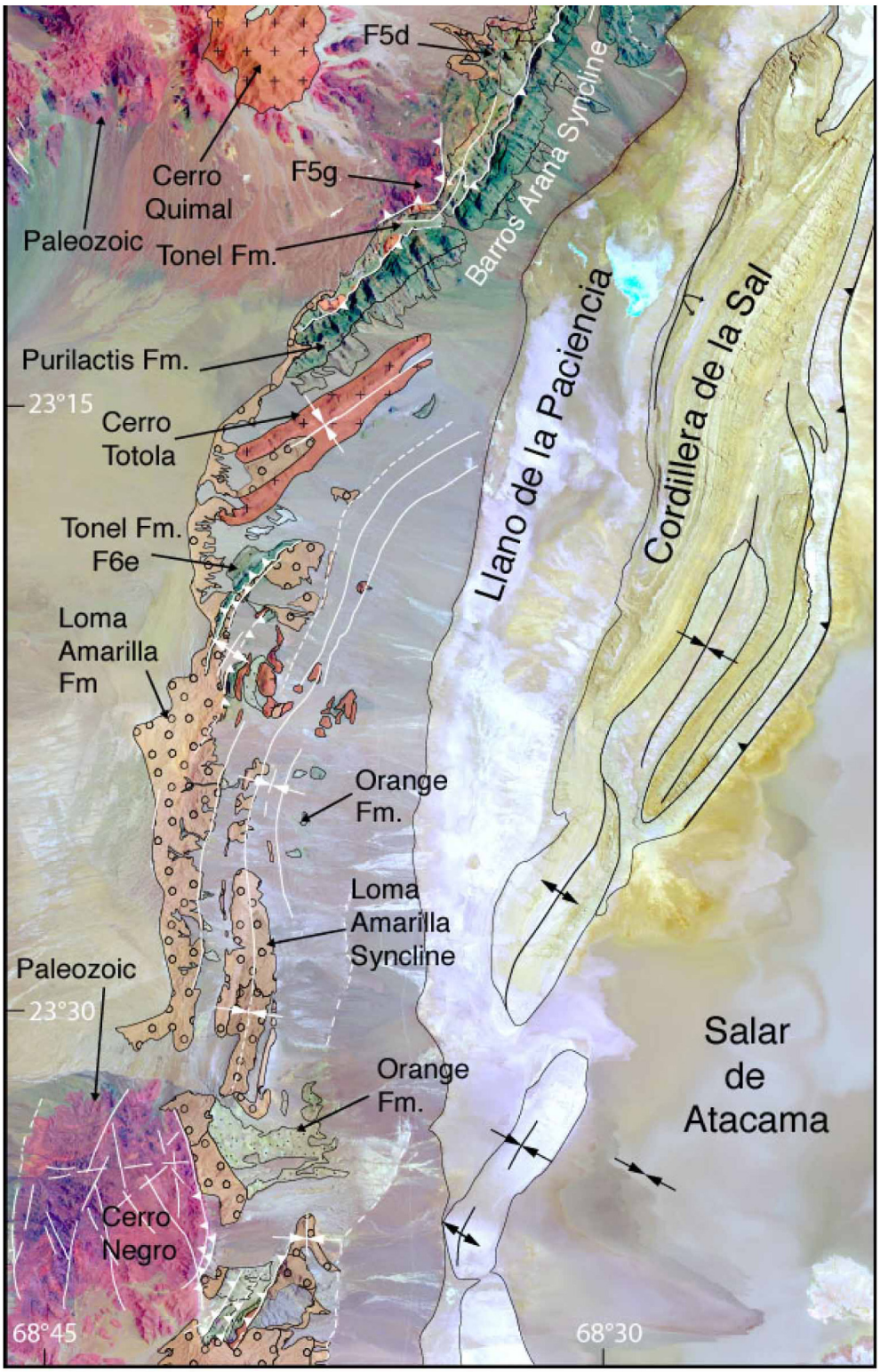

Figure 4: Geological map in LANSAT image of the south El Bordo Escarpment. F6b,c indicate the location of the Figures 5&6.

Surface structure of the western border of the Salar de Atacama

In the northwest part of the basin, on the western limb of the large cylindrical Barros Arana syncline, a westward-verging back-thrust has detached the Purilactis Formation (in the hanging wall) from evaporites of the Tonel Formation (in the footwall). The back-thrust can be traced all along the El Bordo escarpment (Figures 2, 3, 4&5c). In the central part of the area (Cerro Quimal), the syncline becomes tighter, adopting a chevron style with its axial plane dips westward (Figure 2&4). The trend of its axial surface shifts form N60º E (Cerro Totola) to NNE (Barros Arana). In the footwall of the detachment between Purilactis and Tonel formations is an anticline, overturned to the east, which appears to be a fault-propagation fold, above a east verging thrust front that roots into the eastern edge of Cordillera Domeyko (Figure 4&6). About 1 km to the SE, a syncline and adjacent anticline mark the lower part of the Tonel Formation, whereas no folds are visible in the upper part (Figures 4&6). Another 5 km to the S, the basal section of the Tonel Formation shows growth strata (Figure 5d). These were deposited over pre-growth strata, which form kink folds. Further S, on the eastern side of Cerro Quimal, Late Paleozoic (and early Triassic?) volcanic rocks are overthrusting the Tonel Formation above an eastward-verging footwall syncline (Figure 4&5g).

To the south of Cerro Totola, there is an important change in the structure of the western edge of Salar de Atacama. In this region disappears the Barros Arana Syncline and is a complex zone of deformation. More to the south, there is another conspicuous Syncline (Loma Amarilla Syncline). Contrasting with the Barros Arana Syncline, which is constituted by the Purilactis Group, the Loma Amarilla Syncline, NS trending, is constituted by the Paleocene-Eocene deposits of the Orange and Loma Amarilla formations (Figure 4&6e). In the zone of deformation that separates both synclines, the Orange and Loma Amarilla formations are overthrusted by red beds of the Tonel Formation of the east limb of the Barros Arana Syncline (Figure 4&6e). Growth strata in the conglomerate beds of the Loma Amarilla Formation, to account for syn-tectonic sedimentation, during the uplift of the Cordillera de Domeyko, and the eastward movement of the Barros Arana Syncline over the Paleocene-Eocene (Oligocene?) sediments (Figure 4&6e). Reverse faults also affect Quaternary gravels, indicating that compressive deformation is still active (Figure 6e). More to the south, in the zone of Cerro Negro, the Orange and Loma Amarilla

formations are overthrusted by the basement. This east verging thrust, has deformed intensely the evaporitic-rich facies of the upper portion of the Orange Formation and the upper Loma Amarilla Formation.

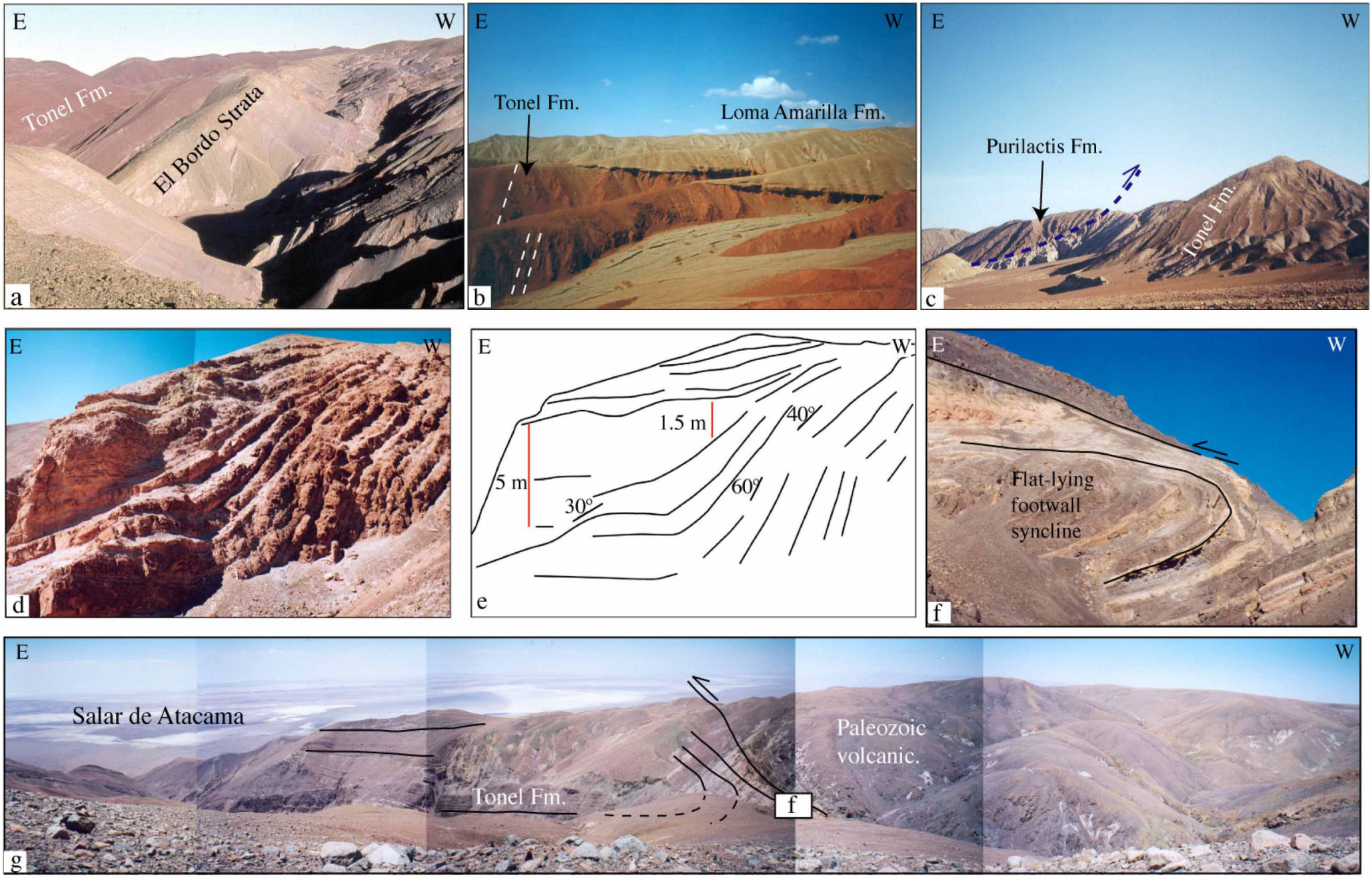

Figure 5: Structures at selected localities (see Figures 3&4). a. Smooth angular unconformity between Tonel Formation and Triassic lacustrine sediments. b. Large angular unconformity between Purilactis Group (red beds of Tonel Formation are an inclination between 70 to 80º E, see white lines) and upper Loma Amarilla Formation (gently dipping to the west). c. Purilactis Formation detached of the evaporite beds of the Tonel Formation. d. Growth strata in lower Tonel Formation. e. Sketch of Figure 5d. f. Footwall syncline in the lower Tonel Formation (see Figure 5g for location). g. Thrust front at eastern edge of Cordillera de Domeyko.

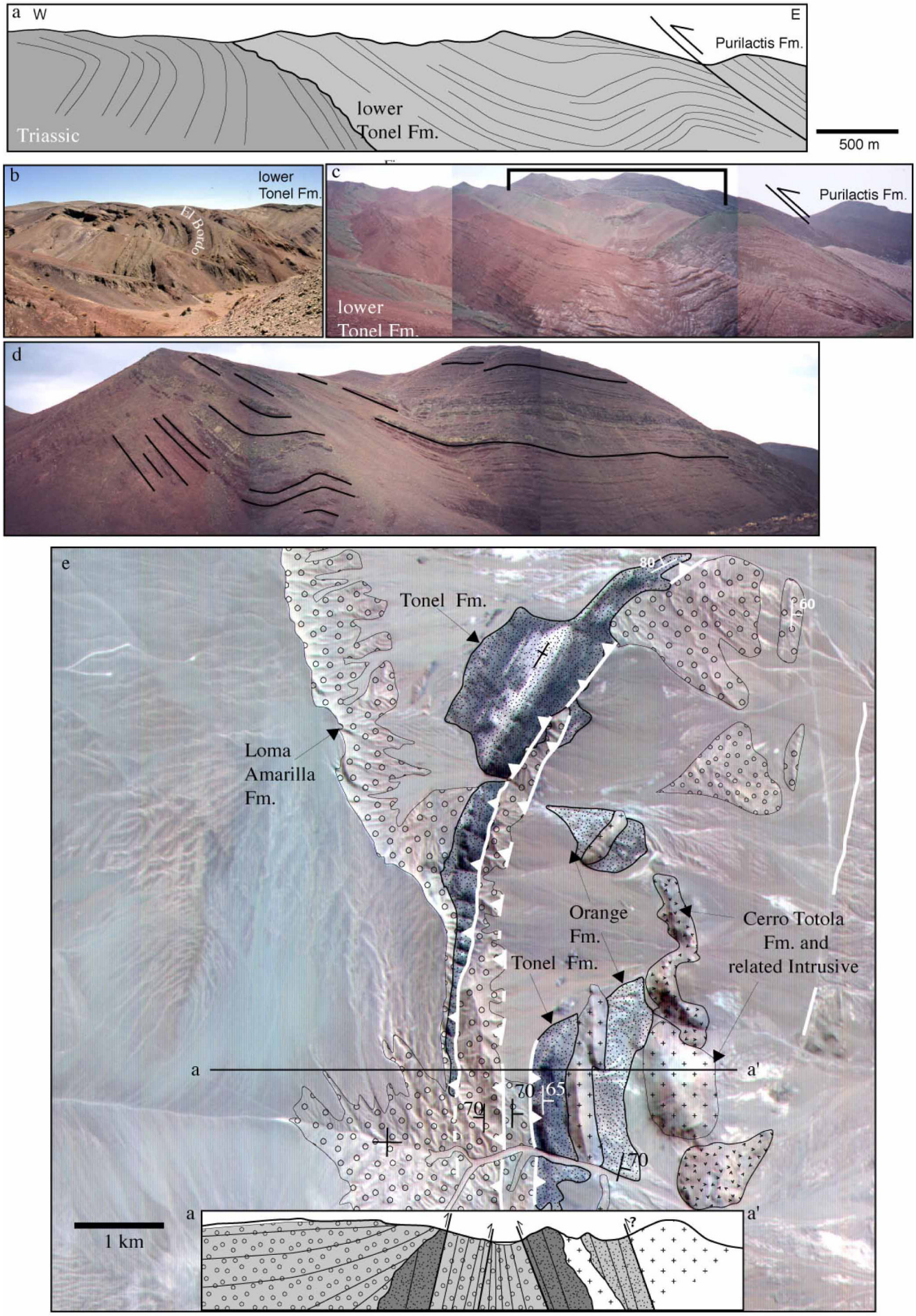

Figure 6: Evidences of compressional deformation. a. Sketch of Figures 6b&c. b. Growth anticline overturned to the east in Triassic and lower Tonel Formation. c. Growth syncline in red beds of the lower Tonel Formation. d. Detail of the Figure 6c, while the lower portion is forming a syncline, the upper portion is no showing the syncline geometry. e. ASTER image, with geological data and an EW section of the transition zone between the Barros Arana Syncline and the Loma Amarilla Syncline (see Figure 4), accounting for Eocene to recent compressional tectonics.

Basin Subsurface Structure

Stratigraphic relation between the El Bordo Escarpment and the Toconao 1 exploration well

A detailed description of the stratigraphy of the Toconao well may be found in Muñoz et al. [1997, 2002]. In this sub-section we correlate the surface stratigraphy of the El Bordo Escarpment with the subsurface stratigraphy recognized in center of the basin. The Toconao 1 exploration well shows a stratigraphic section of around 5500 m (Figures 2&7). A well-defined seismic unit between 2895 and 3900 m of depth is constituted by sandstone, marine limestone, anhydrite and claystone beds and was deposited in a marine related setting during Maastrichtian time [Muñoz et al., 1997, 2002]. The marine facies of the Toconao 1 well has been correlated with the Yacoraite Formation, which is well exposed in the Puna and Eastern Cordillera. The Yacoraite Formation has been related to the Atlantic opening and related marine transgression occurred in Late Cretaceous to Paleocene time [Salfity et al., 1985; Gallisky and Viramonte, 1988; Marquillas and Salfity, 1994]. These deposits have a similar age range than the volcanic rocks of the Cerro Totola Formation. Although, other names have been used for the units founded in the Toconao 1 well [Muñoz et al., 1997, 2002; Jordan et al., 2002], we prefer for simplicity use a similar terminology that in the El Bordo Escarpment. Thus, we correlate the Late Cretaceous deposits of the Toconao 1 well as Cerro Totola Formation (Figure 7). The lower part of the Toconao 1 well, under the Cerro Totola Formation, is constituted by 1500 m of sandstone, siltstone and limestone levels interbedded with volcanic rocks. This section traditionally has been described as the Peine Group as part of basement rocks. Nevertheless, there are no chronological data to establish a precise age for these levels. Moreover the seismic data do not allow identify a clear discordant contact between the sedimentary Cretaceous sequences and any Paleozoic basement. We considered that the lower section, of the Toconao 1 well (lower Cerro Totola Formation in Figure 7), at least in part might be equivalent to the Cerro Totola Formation (or lower units of the Purilactis Group). However, due to the low quality of the seismic data in the lower levels of the basin, it is not possible to establish a lateral continuity from the western edge towards the center of the basin. Therefore, until now, we do not know if there are equivalent deposits of the other facies of the Purilactis Group to the east of the Salar de Atacama.

The Cerro Totola Formation in the Toconao 1 well is unconformably covered by about 800 m of volcaniclastic sandstone and volcaniclastic conglomeratic beds. The top of the sequence can be traced until the western border of the basin, and coincide with the top of the Orange Formation (see below). It unit is covered unconformably by about of 500 m thick of continental coarsening upward sequences of sandstone beds, with frequent interbeds of claystone and volcanic conglomerate with minor sandstone [Muñoz et al., 2002]. This unit can be considered as an distal equivalent unit of the Eocene-Oligocene Loma Amarilla Formation. Over this unit, Neogene to Recent continental deposits constituted mainly by claystone, sandstone and evaporitic beds and interbedded ignimbrite constitute the more recent basin fill [Muñoz et al., 1997, 2002; Jordan et al., 2002].

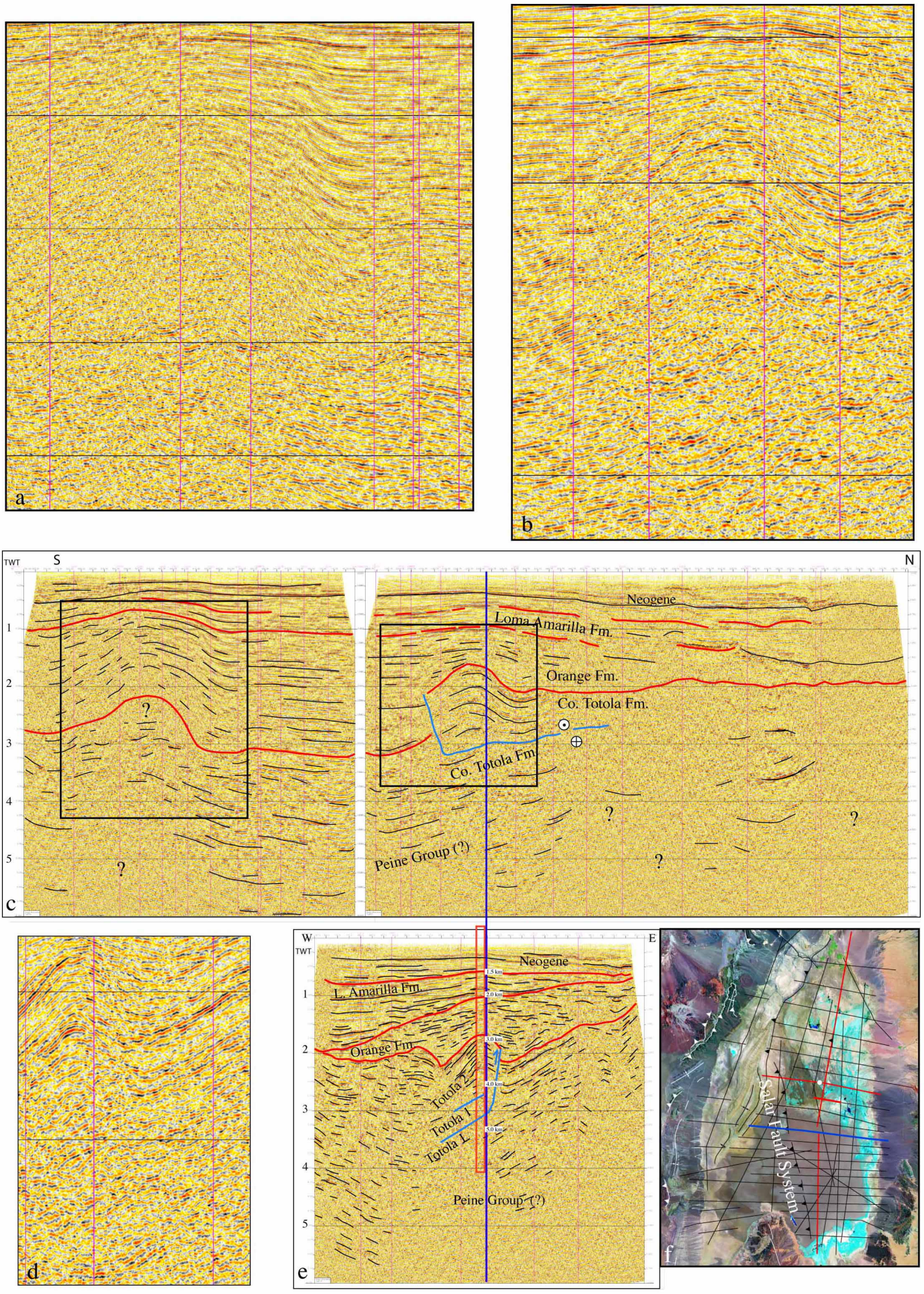

Figure 7: Seismic time sections through the Salar de Atacama basin. a. Zoom of the southern anticline showed in c. b. Zoom of the northern anticline showed in c (Toconao 1 anticline). c. NS section. d. Zoom of the Toconao 1 anticline showed in e. e. EW section (perpendicular to c) in the Toconao 1 dome anticline. f. Location of the Salar Fault System and sections (red lines are location of section showed in c & e; blue line is the location of seismic section of figure 8. The Toconao 1 well is located in the EW section (red rectangle). Red lines in c & e are showing the main stratigraphic boundaries. The blue line in c & e shows the intersection of both sections. Note the dome geometry of the northern anticline bounded to the south by a dextral lateral ramp related to a

Subsurface structure to the east of the Cordillera de la Sal

A complete set of migrated seismic reflection lines over much of the Salar de Atacama was acquired by ENAP (Figure 2). To the east of the Cordillera de la Sal, a high angle verging to the east thrust fault (Salar Fault System, [Muñoz et al., 2002]) and a NS symmetrical geometry in the eastern side of this fault are the main structural features (Figure 7). Two anticlines and a large basin between them constitute the symmetrical geometry (Figure 7). The northern anticline, with dome geometry, is where the Toconao 1 well was done (Figure 7). The anticline is faulted by an east verging ramp-flat thrust, with a detachment level located into the Cerro Totola Formation. To the south, a dextral lateral ramp connected with the detachment level is bounding the anticline (Figure 7). Several works suggest that this anticline may be related with an inverted normal fault, rooted in the basement [Muñoz et al., 1997, 2002]. The normal displacement, according to this interpretation might have occurred during the accumulation of the Cerro Totola Formation. Despite the low quality of the seismic information between 3 to 6 seconds in the figure 7, the general structure under the Toconao 1 Anticline appears to be a syncline with the detachment level in its center. The lateral ramp is not affecting the Peine Group and no evidences of variation in the thickness for the sediments of the Cerro Totola Formation in both, one or another side of the faults (lateral or frontal ramp) were found (Figure 7). Thus, although, other works have suggested a thick-skinned tectonics to explain the Toconao 1 Anticline, our observation point to a thin-skinned tectonics origin. This interpretation is supported by similar structural styles observed more to the south (see below, Figure 8).

Between the two anticlines shown in figure 7a, a large depocenter related to the Salar Fault System is observed (Figures 7c, 8). The Cerro Totola Formation shows an anticline (hanging wall)-asymmetric syncline (footwall) structure, which is displaced by the Salar Fault System. Internal unconformities and deformation occur in the Orange Formation, related to vergent to the east detachment levels, rooted in the Cerro Totola Formation (Figures 7&8). Whereas the thickness of the Cerro Totola Formation is similar in both, footwall or hanging-wall of the Salar Fault System, the thickness of the Paleogene and Neogene units shows important variation (Figure 8). The Orange Formation has the more contrasting variation of its thickness. In the footwall of the Salar Fault System, is showing large growth strata while on the crest of the anticline (in the hangingwall) shows a very

reduced thickness. This fact, to account for an important period of uplift with sedimentation (in the footwall) and erosion (in the hangingwall) during Paleocene-Eocene time. The southern anticline (figure 7) is located to the east of the Cordon de Lila basement range. It has dome geometry constituted mainly by the Orange and Loma Amarilla formations (Figure 9). A rapid variation in the thickness of the sedimentary wedge for the Orange Formation is observed (Figures 7, 8 & 9). The Cerro Totola Formation can be traced all along the NS seismic section and under the anticline. While the northern Toconao 1 anticline affects the Cerro Totola Formation, in this area the anticline, also with dome geometry is constituted mainly by the Orange and Loma Amarilla formations and no deformation (related to the anticline) is observed in the Cerro Totola Formation. This suggests a detachment level between the Orange and Cerro Totola formations.

A seismic profile in the southern edge of the basin shows the Cordón de Lila basement range and basins in each side. In the eastern side of the basement the Salar Fault System has a smaller vertical displacement than in the central area (Figures 8&10). Despite of a less displacement of the Salar Fault System, intense deformation is observed more to the east. Here, the deformation front has been displaced to the east of the Salar Fault System, and the shortening is resolved by at least 3 verging to the east, imbricate panels, with syn-tectonic related sedimentation, which are affecting the Paleogene to Neogene levels of the basin (Figure 9, 10 &11). The east verging sheets are in agreement with the surface structure observed in the southeastern margin of the basin. Detailed structural mapping of Ramírez and Gardeweg, [1982] and Kuhn, [2002], revealed the presence of east verging thin-skinned fold and thrust belt affecting Oligocene-Pleistocene rocks.

Despite the low quality in the deeper parts of the section in the figure 10, a detailed revision of the seismic data permit to trace the strongest reflections under the Cordón de Lila (Figure 12). The geometry of reflection events in the footwall probably reflects velocity pullup due to the shorter traveltimes through higher velocity basement rocks at the surface. Even though, the Cerro Totola Formation and the Peine Group appear to be overthrusted by the Cordón de Lila basement. Thus, if our interpretation is correct, the horizontal compression has been more important than previously thought.

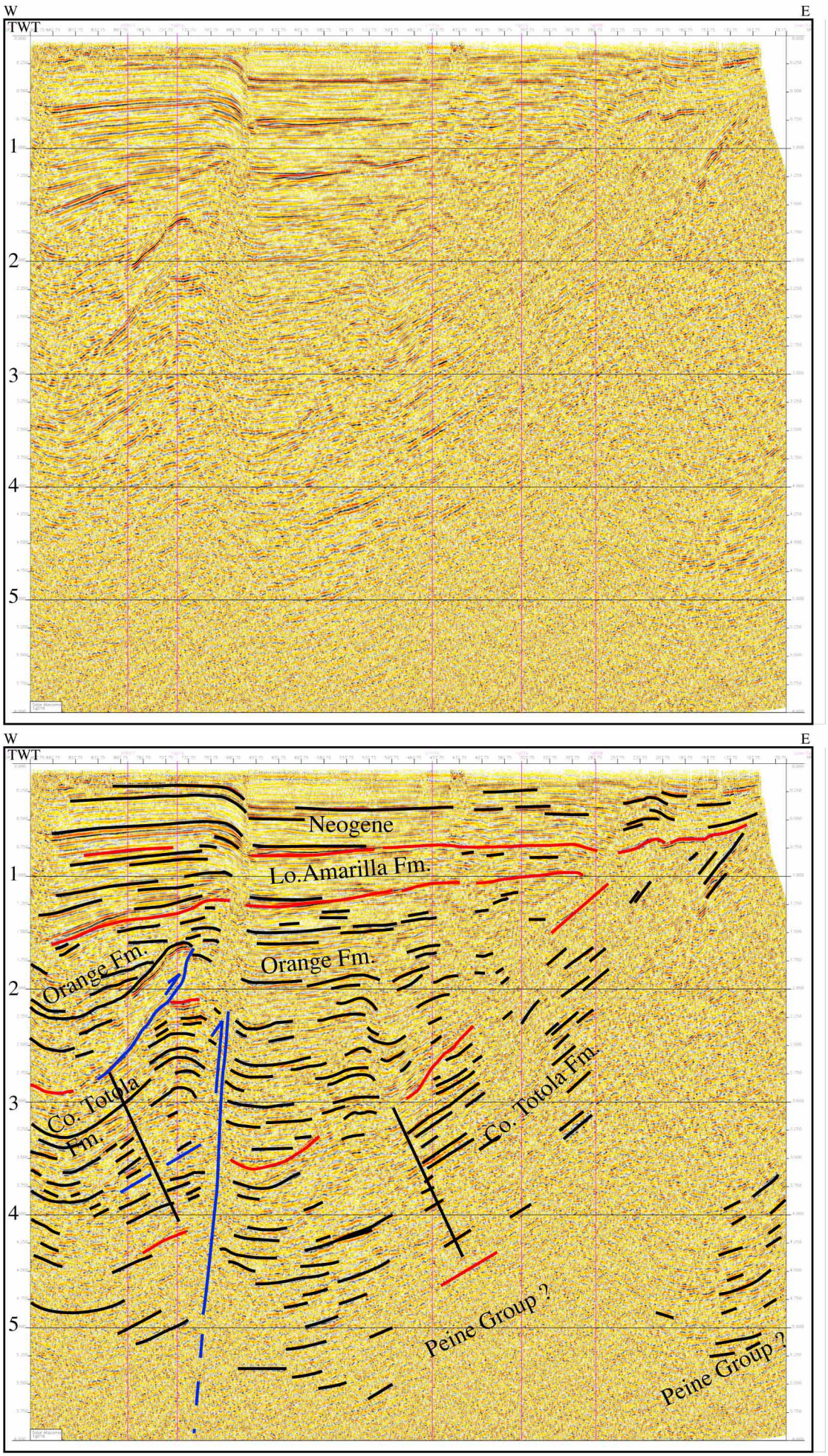

Figure 8: EW seismic time section to the south of Toconao 1 anticline (see Figure 7f for localization). 2 Black lines perpendicular to the stratification in the Co. Totola Fm. have the same longitude showing that no variation occur in the thickness for this unit in both sides of the Salar Fault System.

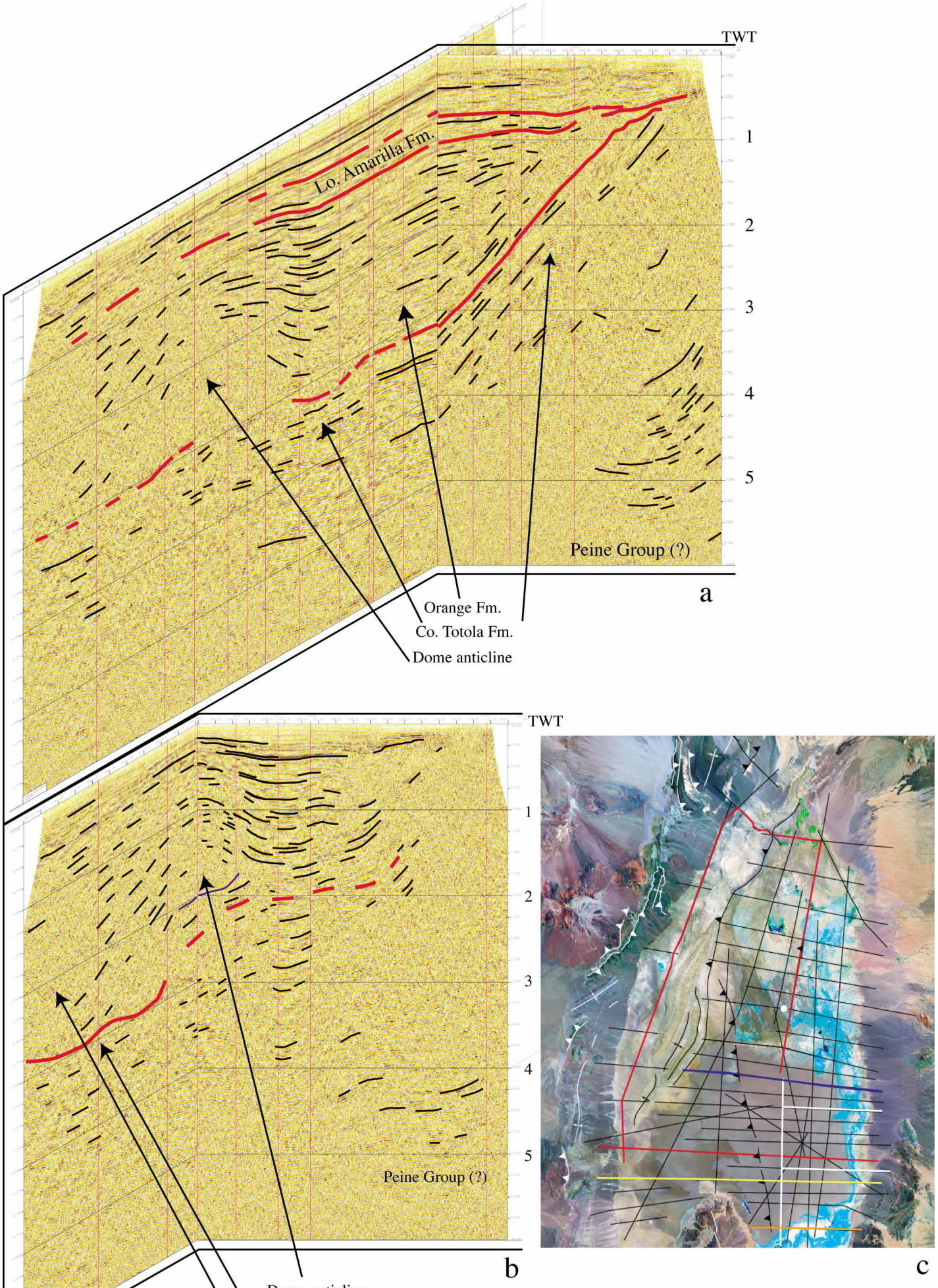

Figure 9: a & b, 3D block diagram in the northern anticline that occur to the east of Cordón de Lila, showing the NS variation in the structural style to the east of the basement range. c. Location of sections. White lines for this figure, blue line for the figure 8, yellow line for the figure 10, orange line for figure 11, red lines for the figure 13.

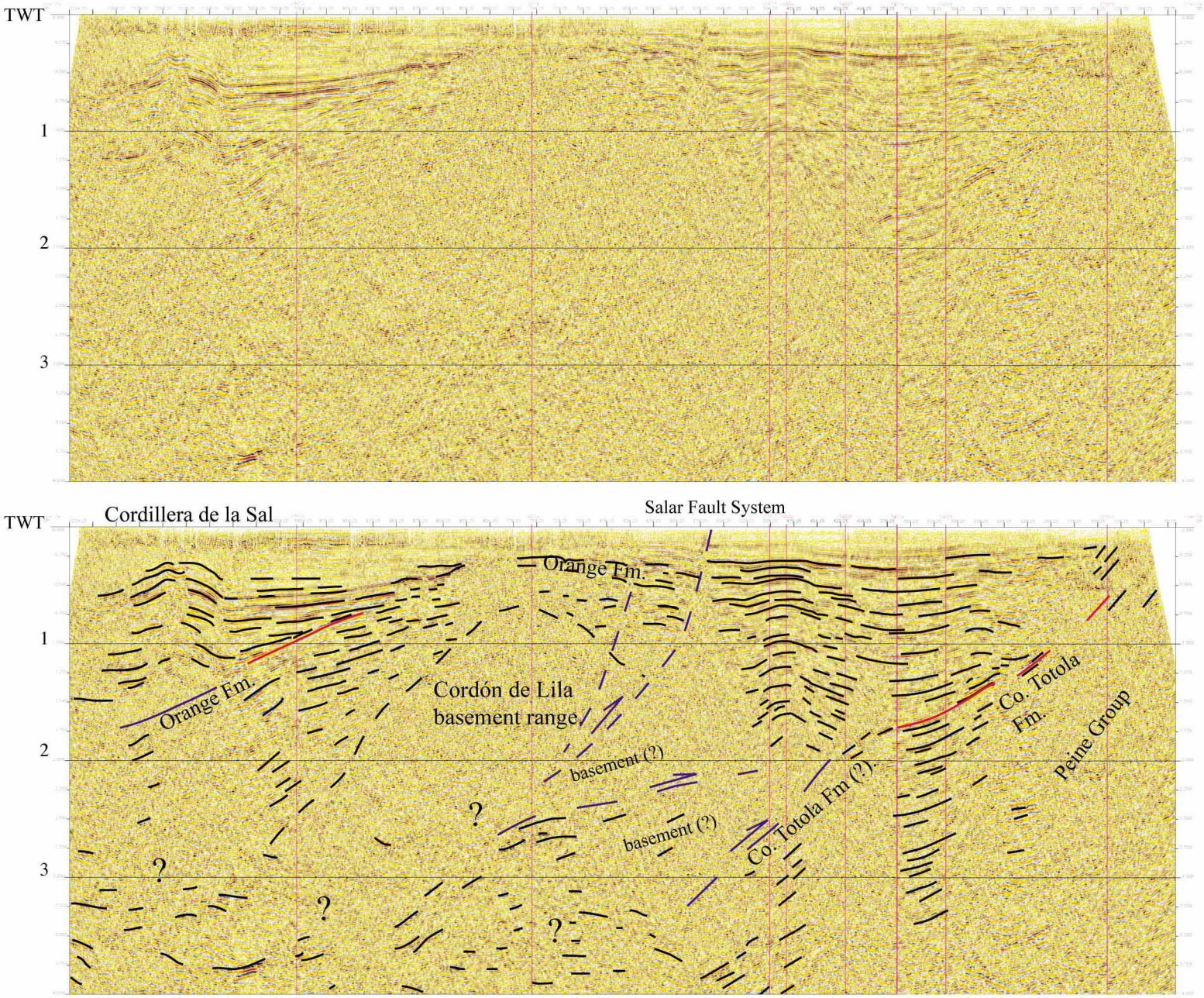

Figure 10: EW Seismic section in the southern edge of the Salar de Atacama basin. Although, further work is needed, the Cordón de Lila basement range appears overthrust the Cerro Totola Formation, if this is the case, an important amount of shortening can occurs in this area. (Location in Figure 9c).

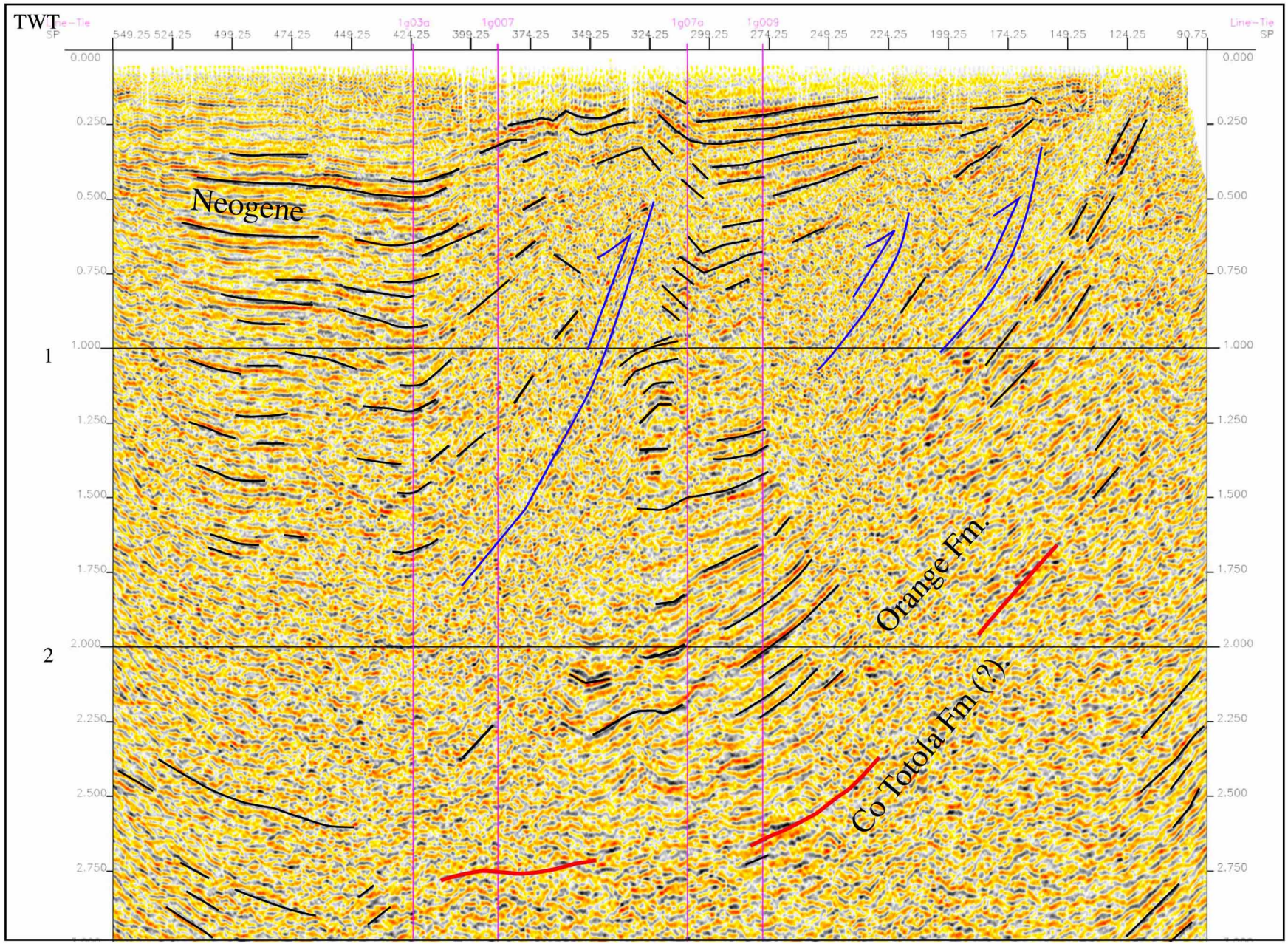

Figure 11: EW seismic section to the southeastern edge of the basin showing the structural style in the upper units (location in Figure 9c). At least 3 verging to the east imbricate sheets account for Neogene to recent compressive tectonics. The detachment level is rooted in the Orange Formation.

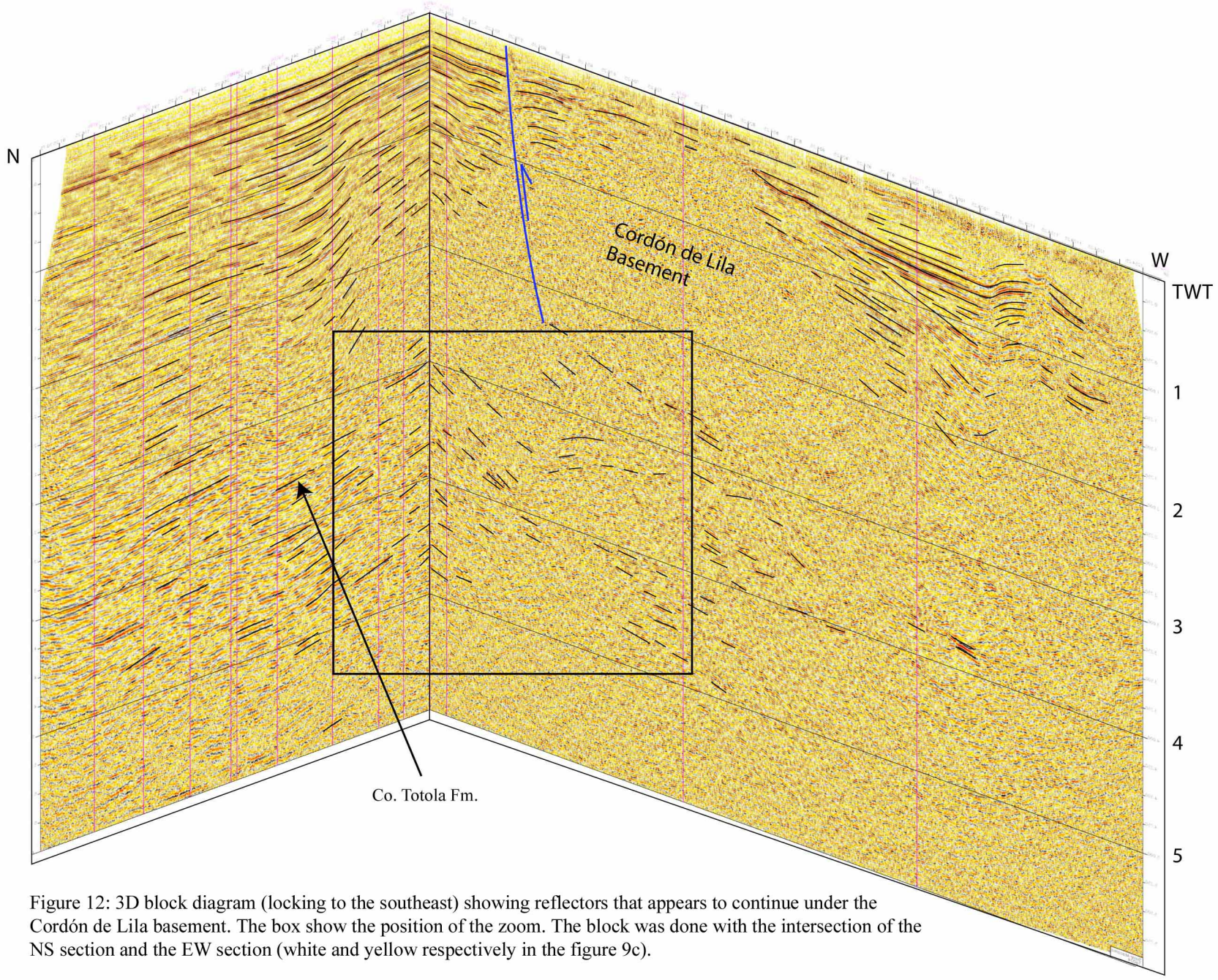

Figure 12: 3D block diagram (locking to the southeast) showing reflectors that appears to continue under the Cordón de Lila basement. The box show the position of the zoom. The block was done with the intersection of the NS section and the EW section (white and yellow respectively in the figure 9c).

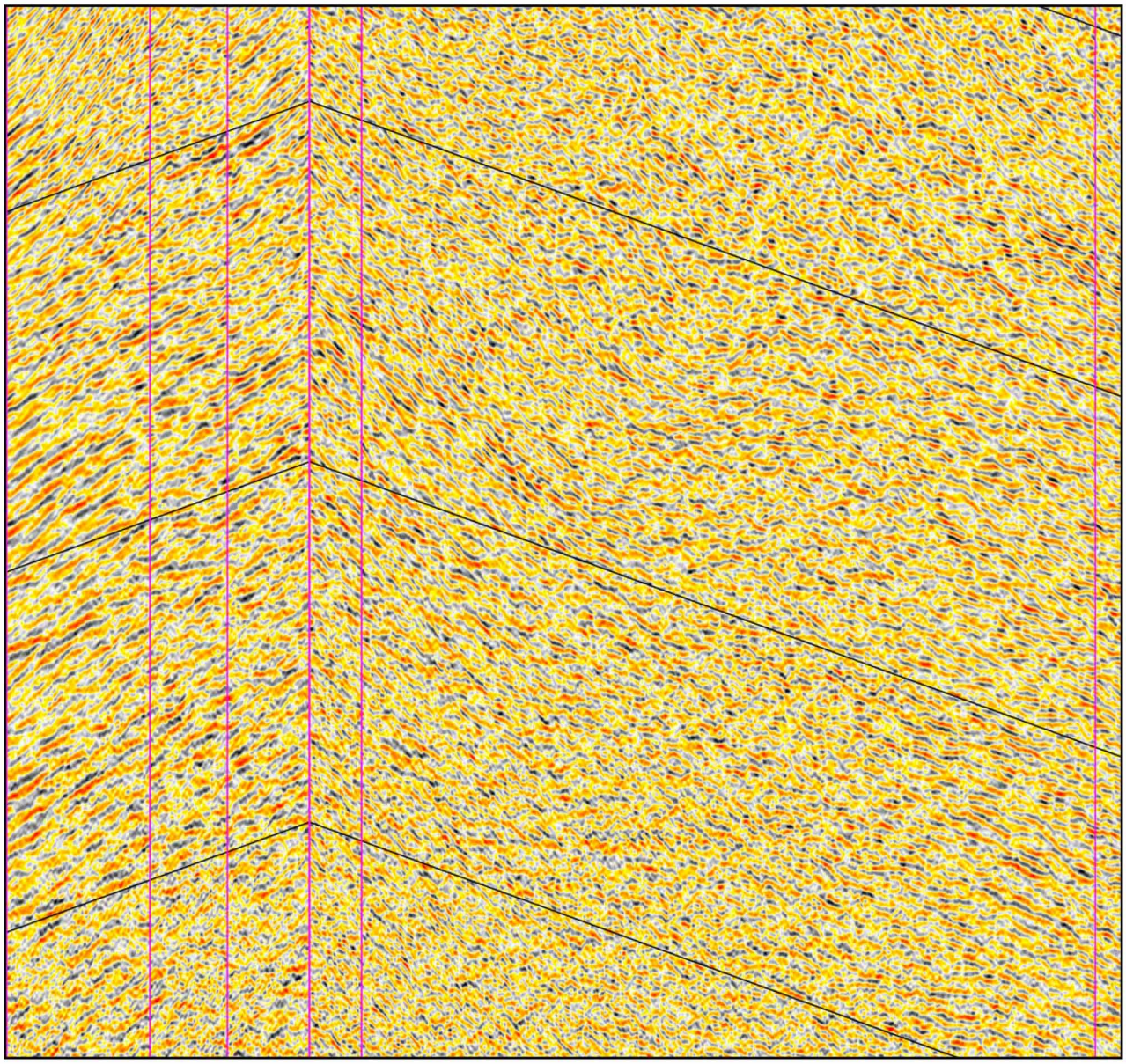

Figure 12 cont.

Subsurface structure to the west of the Cordillera de la Sal

Muñoz et al. [1999, 2002] have indicated that the fold-thrust belt of the Cordillera de la Sal, in the southern Atacama basin, is a thin-skinned tectonics feature. This is clearly observed in the figure 13. The detachment level can be continued for most of the basin and correspond to the upper Orange Formation. This is in agreement with the field observations in the western edge of the basin, where the upper Orange Formation is constituted mainly by evaporite-rich sediments. Towards the north, this level is deeper than in the south reaching up to 3 TWT. Contrasting with the south zone, in the north zone two reflectors are observed under the Cordillera de la Sal (Figure 13, see below).

Despite of the low quality of the subsurface data from the western edge of the Salar de Atacama, a detailed revision shows first order features, which can be constrained by the field observations of the El Bordo Escarpment. Although it is not possible to observe its internal structure, the Barros Arana Syncline is clearly observed in the seismic data. A strong reflector occurs under the Barros Arana Syncline, which has anticline geometry. Based with the good exposures in the Cerro Quimal area, the anticline is constituted by the Lower Tonel Formation. Thus, the Barros Arana Syncline is detached of the evaporitic beds of the upper Tonel Formation (see figures 5, 6&14). A second strong reflector, also with anticline geometry is observed between 2,5 and 3 s. This level can be interpreted as the limit between the lower Tonel Formation and the top of the lacustrine Triassic sedimentary rocks. In the upper part of the Purilactis Group, a clear unconformity in the core of the Barros Arana Syncline mark the base of the Oligocene-Miocene gravels (Figures 3&14). Thus, although, with less amount of shortening, the cross section in the north Barros Arana Syncline appears to be similar to the structure of the Cerro Quimal area (see Figures 3, 4, 5, 6 & 14).

The Barros Arana Syncline and the Tonel Formation are over the reflector, shown in figures 13&14. A geometry of anticline immediately over this level suggest that this reflector is a detachment level, where the Barros Arana Syncline the Tonel Formation and perhaps the Triassic sediments are overthrusting the Paleocene-Neogene units. This interpretation is in agreement, with the east verging sheet thrust affecting Neogene sediments and ignimbrites to the east of the Barros Arana area described by Jolley et al. [1990]. Jolley et al. [1990],

suggested an east verging mayor thrust fault (the Frontal Domeyko Thrust), which uplifted the Purilactis Group over Neogene sediments in the Barros Arana area. Probably, the east verging sheet thrust system observed in the north area, are related to the thrust fault system observed to the south of Cerro Totola area, where the Loma Amarilla Syncline is overthrusted by the Barros Arana Syncline.

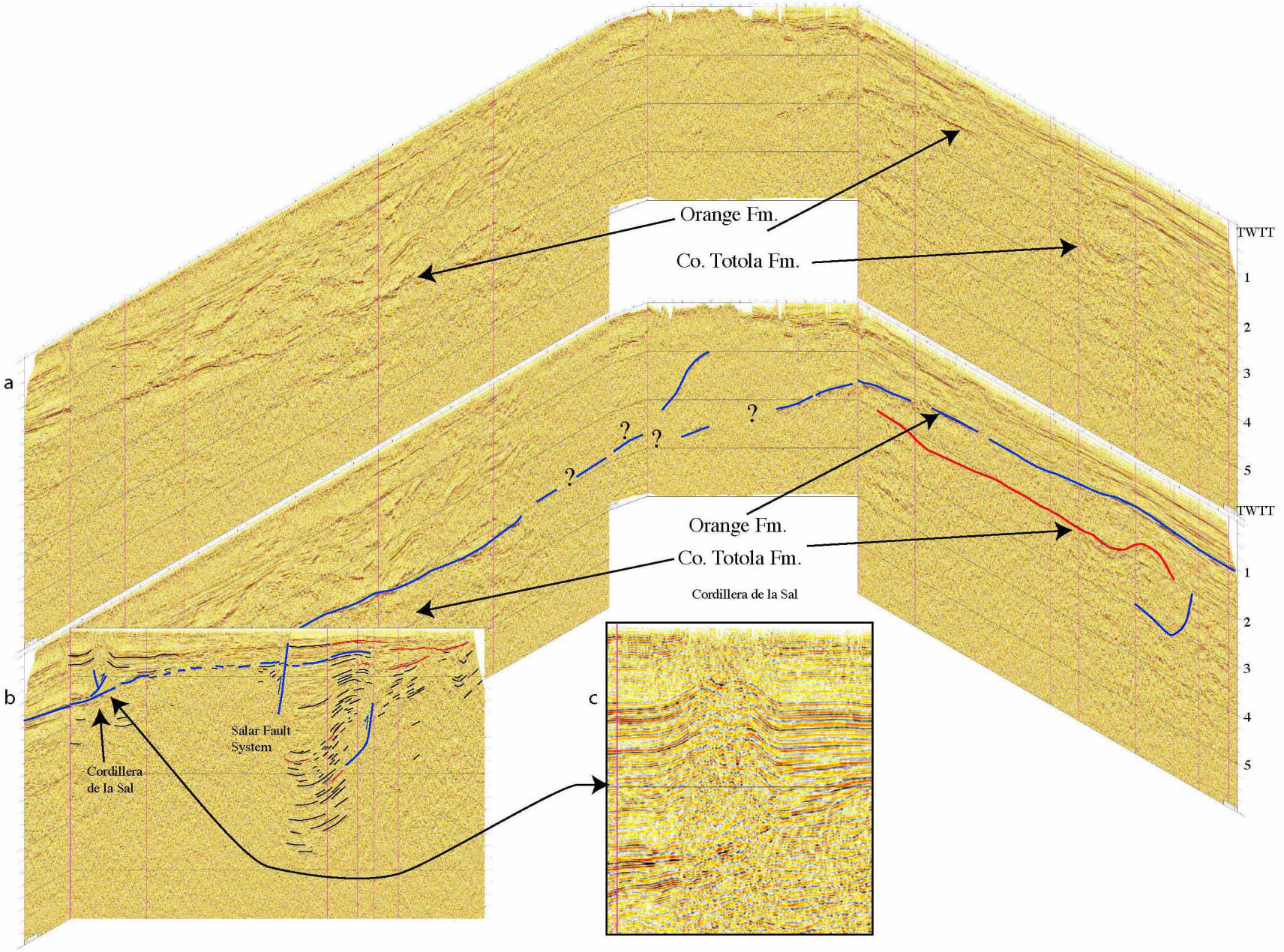

Figure 13: a. Uninterpreted 3D block diagram showing the lateral extension and variation in depth of the top of the Orange Formation. b. Interpreted 3D diagram of a, showing also the lateral continuity of the Orange Formation under the southern side of the Cordillera de la Sal. The clear detachment level in the south (zoom of b showed in c), support the interpretation in the northern side. Location of the sections in Figure 9c.

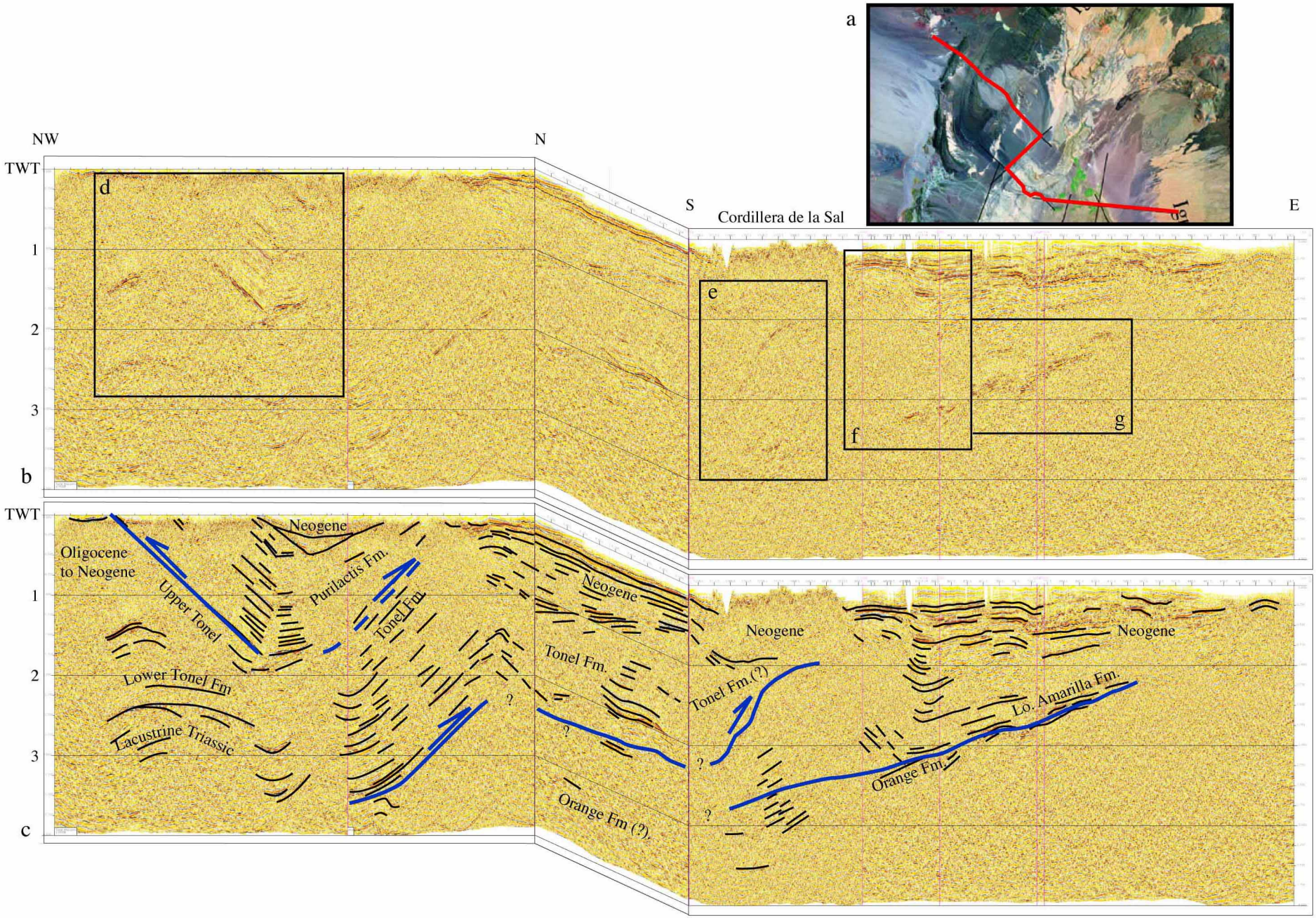

Figure 14: Composed seismic section in the Barros Arana Syncline (located in a). b. Uninterpreted section with the location of zoom of figures d, e, f and g. c. Interpreted section showing the Purilactis Group (and perhaps the lacustrine Triassic sediments) overthrusting to the east, Paleogene and Neogene units (see text for details). The reflectors showed in e, f and g are the same showed in the Figure 13a&b. The zoom in f (showing the deformation in the east edge of the Cordillera de la Sal, correspond to a seismic section parallel to the section here showed but some kms more to the south).

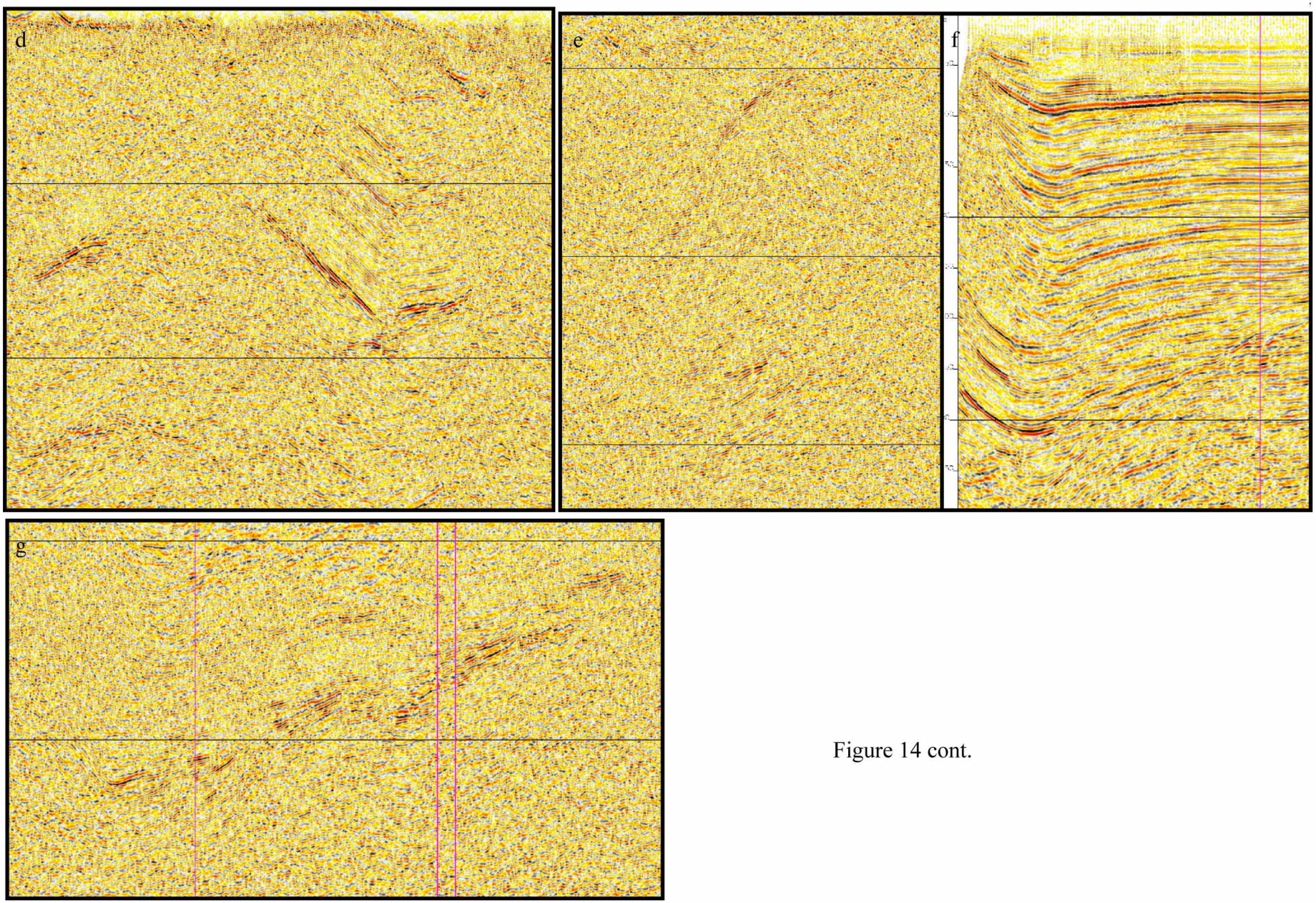

Figure 14 cont.

Discussion

Based in the field and seismic information, we have constructed 3 structural sections (Figure 15). Excepting the detachment level between the Purilactis and Tonel formations in the Barros Arana Syncline, the structural style is characterized by east verging thrusting. The intensity of the deformation increases when the basement is directly involved. If the Cordón de Lila basement is overthrusting the Cerro Totola Formation, clearly the amount of shortening increases toward the south. Due to large tectonic rotations that affect this region of the forearc [Arriagada et al., 2000, 2003], a classical method of seismic profiles restoration don't provide a good estimation of the shortening occurred in the region.

The comparison between the field data of the western border of the Atacama basin, the published data for the exploratory well Toconao1 [Muñoz et al., 1997; 2002] and the subsurface seismic data, shows a similar stratigraphy for the Late Cretaceous-Neogene units. However, Cretaceous units of the Purilactis Group (Tonel and Purilactis formations) are not clearly evidenced in the center of the basin. Important longitudinal variations in the thickness of Paleogene sediments are observed. The maximum thickness in the Paleogene units are between the Toconao 1 well and the Cordón of Lila range (Figure 8). The structural styles and growth strata in the Tonel Formation suggest that at least the lower section of the Purilactis Group was accumulated in a compressional context controlled by a east verging thrust system. Further work is needed to find field evidences for a tectonic setting of deposition for upper levels of the Purilactis Group. Fission track ages for the Cerro Quimal intrusive indicate fast uplift at about 63 Ma (Andriessen and Reutter, 1994). They thus account for Paleocene alluvial facies of the Orange Formation, deposited along all the basin, with large growth strata related mainly to the Salar Fault System in the eastern side of the basin. Probably, the main tectonic event in the area was probably the Late Eocene Incaic phase, which accounted for deposition of more than 1000 m of proximal alluvial facies (Loma Amarilla Formation), large clockwise tectonic rotations, uplift and eastward overthrusting of Cordillera Domeyko and Cordón de Lila basement range [Mpodozis et al., 1993; Charrier and Reutter, 1994; Andriessen and Reutter, 1994; Maksaev and Zentilli, 2000; Arriagada et al., 2000, 2003]. During the Neogene compressional deformation was also active as is evidenced by the field observations in the western edge of the Atacama basin, the Salar Fault System, the related deformation to the

east in the basin and more to the east in the boundary with the Western Cordillera [Ramírez and Gardeweg, 1982; Kuhn, 2002].

The Salar de Atacama basin can be understood as a long-lived basin developed in a foreland tectonic setting, active since the mid-Cretaceous to the Neogene. Thus, the tectonic setting that affected the Salar de Atacama area might be similar in all the pre-Andean depression, indicating that pre-Neogene compressional tectonics can be a fundamental element in the construction of the actual central Andes. However, traditionally, models propose that the main structural style between the forearc and the Western Cordillera is controlled by a verging to the west thrust system [Isacks, 1988; Muñoz and Charrier, 1996]. This is in fact the case more to the north in the Arica region [Muñoz and Charrier, 1996], when west vergent thick-skinned thrust tectonics support the western monocline flexure to the west of the Altiplano [Isacks, 1988]. An important boundary can be between the vergent to the west structural domain in most northern Chile and the vergent to the east structural domains observed in the Salar de Atacama basin.

Although the structural style observed is similar to the "classic" foreland basins, due to the small dimensions of the Salar, the generation of space and the long-lived of the basin cannot be explained only by flexural subsidence induced by loading of the Cordillera de Domeyko basement. Recent geophysical surveys have indicated the presence of a positive anomaly in the isostatic residual gravity [Götze and Krause, 2002] which is well correlated with the low topographic of the Salar de Atacama and Pipanaco (northwestern of Argentina) basins. Moreover, tomographic data shows under the Salar de Atacama an abnormally cold lithospheric mantle which can be mechanically coupled with the top of the subducting Nazca plate [Yuan et al., 2002]. A high density Ordovician ultrabasic and/or remnants ophiolites or the root of the Cambrian-Ordovician magmatic arc (Cordón de Lila in northern Chile) could cause the observed anomaly [Götze and Krause, 2002], and dynamically induce the subsidence of the Salar de Atacama basin during its long history.

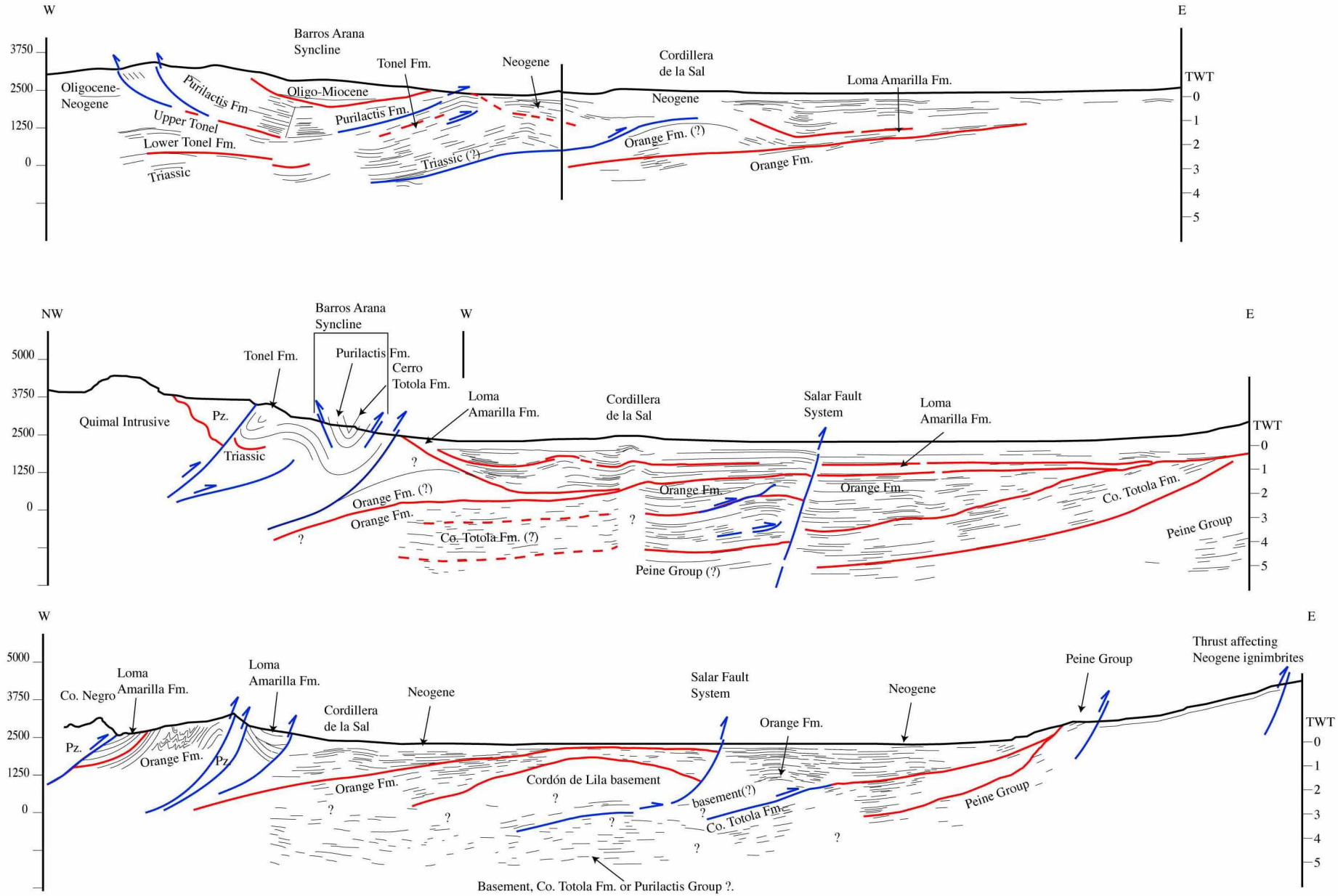

Figure 15: EW cross sections based in our field and seismic observations, and for the south eastern edge of the basin after Ramírez and Gardeweg, [1982] and Kuhn, [2002]. (see location in figure 2).

References

Allmendinger, R. W., T. E. Jordan, S. M. Kay, and B. L. Isacks, The evolution of the Altiplano-Puna plateau of the central Andes, Annu. Rev. Earth Planet. Sci., 25, 139‹174, 1997

Andriessen, P. A. M and K-J. Reutter, K-Ar and fission track mineral age determinations of igneous rocks related to multiple magmatic arc systems along the 23ºS Latitude of Chile and Argentina. In Tectonics of the Southern Central Andes. (Reutter, K-J.; Scheuber, E.; Wigger, P,; editors). Springer-Verlag, p. 141-154. Berlin, 1994

Arriagada, C. Geología y Paleomagnetismo del Borde Occidental del Salar de Atacama. M.Sc. Thesis, University Chile, Dep. Geol., Santiago, 1999

Arriagada, C., P. Roperch, and C. Mpodozis, Clockwise block rotations along the eastern border of the
Cordillera de Domeyko, northern Chile, Tectonophysics, 326, 153‹171, 2000

Arriagada, C., Cobbold, P., Mpodozis, C., Roperch, P. Cretaceous to Paleogene compressional tectonics during deposition of the Purilactis Group, Salar de Atacama. Fifth International Symposium on Andean Geodynamics, Toulouse, Extended abstracts, Ed. IRD. 2002

Arriagada, C., Roperch, P., Mpodozis, C., Dupont-Nivet, G., Cobbold, P.R., Chauvin, A., Cortés, J. Paleogene clockwise tectonic rotations in the fore-arc of Central Andes, Antofagasta Region, Northern Chile. Journal of Geophysical Research, (in press).

Baby, P., P. Rochat, G. Mascle, and G. Herail, Neogene shortening contribution to crustal thickening in the back arc of the central Andes, Geology, 25, 883–886, 1997.

Breitkreuz, C., and W. Zeil, The late Carboniferous to Triassic volcanic belt in northern Chile, in Tectonics of the Southern Central Andes, edited by K.-J. Reutter, E. Scheuber, and P. Wigger, pp. 277–292, Springer-Verlag, New York, 1994.

Charrier, R. and Reutter, K.J., The Purilactis Group of Northern Chile: Boundary between Arc and Backarc from Late Cretaceous to Eocene. edited by K.-J. Reutter, E. Scheuber, and P. Wigger, pp. 277–292, Springer-Verlag, New York, pp. 189-202, 1994.

Chong, G., and K.J. Reutter. Fenómenos de tectónica compresiva en las Sierras de Varas y de Argomedo, Precordillera Chilena, en ámbito del Paralelo 25º sur, IV Congreso Geológico Chileno, Actas, 2, 219-238. 1985

Coney, P.J., Evenchick, C.A. Consolidation of the American Cordilleras. J. S. Am. Earth Sci. 7, 241-262. 1994

Coutand, I., Cobbold, P.R., de Urreiztieta, M., Gautier, P., Chuvin, A., Gapais, D., Rossello, E., and O.L., Gamundi. Style and history of Andean deformation, Puna plateau, northwestern Argentina. Tectonics, Vol. 20, 2,pp. 210-234 2001

Damm, K.-W., S. Pichowiak, C. Breitkreuz, R. S. Harmon, W. Todt, and M. Buchelt, The Cordon de Lila Complex, central Andes, northern Chile: An Ordovician continental volcanic province, in Andean Magmatism and Its Tectonic Setting, edited by R. S. Harmon and C. W. Rapela, Geol. Soc. Am. Spec. Pap, 265, 1–309, 1991.

DeMets, C., R. G. Gordon, D. F. Argus, and S. Stein, Effect of recent revisions to the geomagnetic reversal time scale on estimates of current plate motions, Geophys. Res. Lett., 21, 2191–2194, 1994

DeMets, C., R. G. Gordon, D. F. Argus, and S. Stein, Effect of recent revisions to the geomagnetic reversal time scale on estimates of current plate motions, Geophys. Res. Lett., 21, 2191–2194, 1994

Dingman, R.J., 1963. Cuadrángulo Tulor. Inst. Invest. Geol. Carta Geol. Chile 11 (1:50 000).

Flint, S., P. Turner, E. J. Jolley, and A. J. Hartley, Extensional tectonics in convergent margin basins: An example from the Salar de Atacama, Chilean Andes, Geol. Soc. Am. Bull., 105, 603–617, 1993.

Galliski, M.A. and Viramonte, J.G. The Cretaceous paleorift in northwestern Argentina: A petrologic approach. J South Am Earth Sci, v 1 (4), p. 329-342. 1988

Gephart, J., Topography and subduction geometry in the central Andes: Clues to the mechanics of a noncollisional orogen, J. Geophys. Res., 99, 12,279-12,288, 1994.

Götze, H-J., and S. Krause. The Central Andean gravity high, a relic of an old subduction complex?, J. S. Am. Earth Sci. 14, 799-811. 2002

Gubbels, T., B. Isacks, and E. Farrar, High-level surfaces, plateau uplift, and foreland development, Bolivian Central Andes, Geology, 21, 695-698, 1993.

Hammerschmidt, K., Döbel, R., Friedrichsen, H. Implication of 40Ar/39Ar dating of Tertiary volcanics rocks from the north-Chilean Precordillera. Tectonophysics 202, 55–81. 1992

Harley, A.J., Flint, S., Turner, P., Jolley, E. J. Tectonic controls on the development of a semiarid, alluvial basin as reflected in the Stratigraphy of the Purilactis Group (upper Cretaceous-Eocene), northern Chile. J. S. Am. Earth Sci. 5, 275-296. 1992

Horton, B.K., DeCelles, P.G. The modern foreland basin system adjacent to the Central Andes. Geology 25, 895-898. 1997

Horton, B.K., Hampton, B.A., Waanders, G.L. Paleogene synorogenic sedimentation in the Altiplano Plateau and implications for initial mountain building in the Central Andes. Geol. Soc. Am. Bull. 113, 1387-1400. 2001

Isacks, B. L., Uplift of the central Andean plateau and bending of the Bolivian orocline, J. Geophys. Res., 93, 3211–3231, 1988.

James, D. Andean Crustal and Upper Mantle Structure, J. Geophys. Res, 76/14. 1971

Jolley, E. J., P. Turner, G. D. Williams, A. J. Hartley, and S. Flint, Sedimentological response of an alluvial system of Neogene thrust tectonics, Atacama Desert, northern Chile, J. Geol. Soc. London, 147, 769–784, 1990.

Jordan, T., Muñoz, N., Hein, M., Lowenstein, T., Godfrey, L., and J. Ju. Active faulting and folding without topographic expression in an evaporite basin, Chile. GSA Bulletin, v. 114, 11, p. 1406–1421; 2002

Kley, J., Geologic and geometric constraints on a kinematic model of the Bolivian orocline, J. S. Am. Earth Sci., 12, 221–235, 1999.

Kuhn, D. Fold and thrust belt structures and strike-slip faulting at the SE margin of the Salar de Atacama basin, Chilean Andes. Tectonics, VOL. 21, NO. 4, 2002

Lamb, S., and L. Hoke, Origin of the high plateau in the Central Andes, Tectonics, 16, 623–649, 1997

Macellari, C. E., M. J. Su, and F. Townsend, Structure and seismic stratigraphy of the Atacama Basin, northern Chile, paper presented at the VI Congreso Geologico Chileno, Vina del Mar, 1991.

Maksaev, V., and M. Zentilli, Fission track thermochronology of the Domeyko Cordillera, northern Chile: Implications for Andean tectonics and porphyry copper metallogenesis, Explor. Min. Geol., 8, 65–89, 1999

Marquillas, R. y Salfity, J.A. Relaciones estratigráficas regionales de la Formación Yacoreite (Cretácico Superior), norte de la Argentina. VII Congreso Geológico Chileno, V. I, pp. 479-483. 1994

McQuarrie, N., and DeCelles, P.G. Geometry and Structural Evolution of the Central Andean Backthrust Belt, Bolivia. Tectonics 17, 203-220. 2001

Mpodozis, C., N. Marinovic, and I. Smoje, Eocene left-lateral strike slip faulting and clockwise block rotations in the Cordillera de Domeyko, west of Salar de Atacama, northern Chile, paper presented at Symposium International Géodynamique Andine ISAG 93, Inst. Fr. de Rech. Sci. pour le Dév. en Coop. (ORSTOM), Oxford, UK, 1993.

Mpodozis, C., Arriagada, C., Roperch, P. Cretaceous to Paleogene geology of the Salar de Atacama basin, northern Chile: A reappraisal of the Purilactis Group stratigraphy. Proc. III. (ORSTOM) ISAG Göttingen, pp. 523-526. 1999

Mpodozis et al., submitted

Müller, J. P., Kley, J.; Jacobshagen, V. Structure and Cenozoic kinematics of the Eastern Cordillera, southern Bolivia (21°S). Tectonics, VOL. 21, NO. 5, 2002

Muñoz, N., and R. Charrier, Uplift of the western border of the altiplano on a west-vergent thrust system, Northern Chile, J. S. Am. Earth Sci., 9, 171–181, 1996.

Muñoz, N., Charrier, R. y Reutter, J.K. Evolución de la Cuenca del Salar de Atacama: Inversión tectónica y relleno de una cuenca de antepaís de retroarco. Proc. VIII Congreso Geológico Chileno, 1: pp. 195-199. 1997

Muñoz, N., Charrier, R., y Jordan, T. Interactions between basement and cover during the evolution of the Salar de Atacama Basin, northern Chile. Rev. geol. Chile, vol.29, no.1, p.55-80. 2002

Naranjo, J.A., Ramírez, C.F. y Paskoff, R. Morphostratigraphic evolution of the northwestern margin of the Salar de Atacama basin (23ºS-68ºW). Revista Geológica de Chile, v 16, Nº 1, p 91. 1994

Niemeyer, H., La megafalla Tucucaro en el extremo sur del Salar de Atacama: Una antigua zona de cizalle reactivada en el Cenozoico, Comun. Dep. Geol., 34, pp. 37–45, Univ. de Chile, Santiago, 1984.

Norabuena, E., L. Leffler-Griffin, A. Mao, T. Dixon, S. Stein, I. S. Sacks, L. Ocala, and M. Ellis, Space geodetic observations of Nazca-South America convergence along the central Andes, Science, 279,
358–362, 1998.

Ramírez, C. F., and M. Gardeweg, Hoja Toconao, Región de Antofagasta-Carta Geológica de Chile, 121 pp., scale 1:250,000, Serv. Nac. de Geol. y Minera de Chile, Santiago, 1982.

Randall, D., A. Tomlinson, and G. Taylor, Paleomagnetically defined rotations from the Precordillera of northern Chile: Evidence of localized in situ fault-controlled rotations, Tectonics, 20, 235–254, 2001

Salfity, J. A., Lineamentos transversales al Rumbo Andino en el noroeste Argentino, IV Congreso Geologico Chileno, Univ. del Norte, Antofagasta, 1985.

Scheuber, E., and K.-J. Reutter, Magmatic arc tectonics in the central Andes between 21° and 25°, Tectonophysics, 205, 127–140, 1992

Schmitz, M., A balanced model of the southern central Andes, Tectonics, 13, 484–492, 1994

Sempere, T., G. Herail, J. Oller, and M. Bonhomme, Late Oligocene-early Miocene major tectonic crisis and related basins in Bolivia, Geology, 18, 946–949, 1990.

Sempere, T., R. F. Butler, D. R. Richards, L. G. Marshall, W. Sharp, and I. C. C. Swisher, Stratigraphy and chronology of Late Cretaceous-early Paleogene strata in Bolivia and northwest Argentina, Geol. Soc. Am. Bull., 109, 709–727, 1997.

Sempere, T., Phanerozoic evolution of Bolivia and adjacent regions, in Petroleum Basins of South America, edited by A. J. Tankard, R. Suarez Soruco, and H. J. Welsink, AAPG Mem., 62, 207–230, 1995.

Sheffels, B. M., Lower bound on the amount of crustal shortening in the central Bolivian Andes, Geology, 18, 812–815, 1990

Somoza, R., and A. Tomlinson, Paleomagnetism in the Precordillera of northern Chile (22°30S): implications for the history of tectonic rotations in the Central Andes, Earth Planet. Sci. Lett., 94, 369–381, 2002.

Somoza, R., S. Singer, and A. Tomlinson, Paleomagnetic study of upper Miocene rocks from northern Chile: Implications for the origin of late Miocene–Recent tectonic rotations in the southern central Andes, J. Geophys. Res., 104, 22,923–22,936, 1999.

Wilkes, E. and Görler, K. 1994. Sedimentary and Structural Evolution of the Salar de Atacama Depression. In: Reutter, K.-J., Scheuber, E. & Wigger, P.: Tectonics of the Southern Central Andes. Springer-Verlag Berlin.

Yuan, X. Sobolev, S.V. Kind, R. Moho topography in the central Andes and its geodynamic implications. Earth and Planetary Science Letters 199, 389-402. 2002

Chapitre III : Rotations tectoniques dans l'avant arc du nord du Chili. Région d'Antofagasta

Introduction

Au moment de commencer cette étude, la grande partie des études paléomagnétiques au nord du Chili avaient été faites principalement sur les roches volcaniques et intrusives d'âge Jurassique et Crétacé Inférieur exposées le long de la Cordillère de la Côte [*Forsythe et Chisholm*, 1994; *Riley et al*., 1993; *Randall et al*., 1996; *Taylor et al*., 1998] et certains des sédiments du Crétacé Inférieur [*Turner et al*., 1988]. Contrairement à l'hypothèse proposée par *Heki et al*. [1985], la plupart des nouvelles études publiées au cours des années 90 ont généralement cherché à associer les rotations horaires observées dans la Cordillère de la Côte comme une conséquence des mouvements senestres d'âge Crétacé Inférieur le long du Système de Faille d'Atacama [*Forsythe et Chisholm*, 1994; *Randall et al*., 1996; *Taylor et al*., 1998]. Même s'il n'y avait aucune contrainte sur l'âge de la rotation, les résultats ont été expliqués au moyen de modèles de domino très simples et discutables (Figure I.6). Des études plus récentes ont démontré que des rotations horaires sont trouvées, non seulement dans la Cordillère de la Côte, mais également à travers tout l'avant arc [*Randall et al*., 2001; *Somoza et Tomlinson*, 2002; *Taylor et al*., 2001; *Fernández et al.,* 2000]. Un manque de rotation dans les strates Miocènes Inférieures non déformés [*Somoza et Tomlinson*, 2002] suggère que le nord du Chili n'ait pas subi une rotation significative pendant le Cénozoïque Supérieur. Ainsi, les travaux les plus récents semblent indiquer que les rotations horaires qui affectent les roches Mésozoïques et Tertiaires du nord du Chili se sont produites avant le Néogène et sont probablement associées aux épisodes tectoniques Paléogènes pendant une période de forte convergence oblique.

Dans le cadre de l'étude de l'évolution tectonique Cénozoïque de la région de l'avant arc du nord du Chili, il nous est apparu nécessaire de mener une campagne d'échantillonnage paléomagnétique en vue de caractériser le champ de rotation à travers cette région afin de compléter le jeu de données à l'échelle de l'orogène et de répondre des questions suivantes :

1) Quelle est l'âge, la distribution spatiale et la quantité des rotations dans l'avant arc du nord du Chili ?
2) Quelle est l'origine des rotations tectoniques horaires de l'avant arc du nord du Chili?

3) Quelle est l'importance de la partitionne de la déformation dans un régime de subduction oblique dextre pour l'origine de rotations ?
4) Le mécanisme qui contrôle les rotations est déterminé par des forces horizontales ou des forces exercées dans la base de la croûte ?
5) Quelle est la relation entre les processus qui ont été à l'origine des rotations horaires et de ceux associés à la formation de l'Orocline bolivien ?

Publication : Rotations tectoniques horaires d'âge Paléogène dans l'avant arc des Andes Centrales, région d'Antofagasta, nord du Chili.

César Arriagada, Pierrick Roperch, Constantino Mpodozis, Guillaume Dupont-Nivet, Peter Cobbold, Annick Chauvin, Joaquin Cortés

Résumé : Dans la Vallée Centrale du nord du Chili (région d'Antofagasta), l'analyse de 108 sites de données paléomagnétiques, principalement de roches d'âge Mésozoïque à Paléogène, a livré 86 sites à magnétisations rémanentes stables. À partir de ces données, on déduit des rotations tectoniques en sens horaire jusqu'à 65º dans l'avant arc des Andes Centrales. La relation apparente entre les rotations tectoniques et l'orientation des structures suggère que les rotations se sont produites principalement pendant l'événement orogénique Incaïque d'âge Éocène-Oligocène Inférieur. Certains résultats paléomagnétiques obtenus sur des roches d'âge Néogène ne montrent pas de preuves de rotation horaire. Par conséquent, la construction de l'Orocline bolivien pendant le Néogène Supérieur ne peut s'expliquer par une simple flexure de toute la marge. Ces résultats démontrent que les rotations tectoniques dans l'avant arc sont des éléments clef de la déformation Andine précoce, et devraient être considérées dans les modèles cinématiques d'évolution des Andes Centrales.

Article publié au *Journal of Geophysical Research*, v. 108, B1, 2003

Paleogene clockwise tectonic rotations in the forearc of central Andes, Antofagasta region, northern Chile

César Arriagada,[1,2] Pierrick Roperch,[1] Constantino Mpodozis,[3,4]
Guillaume Dupont-Nivet,[5] Peter R. Cobbold,[2] Annick Chauvin,[2] and Joaquin Cortés[3]

Received 24 October 2001; revised 5 May 2002; accepted 20 May 2002; published 21 January 2003.

[1] For the Central Valley of northern Chile (Antofagasta region), a paleomagnetic analysis of data from 108 sites, mainly in Mesozoic and Paleogene volcanic rocks, has yielded stable remanent magnetization directions for 86 sites. From these data, we infer clockwise tectonic rotations of up to 65° within the forearc domain of the central Andes. The apparent relationship between tectonic rotations and structural trends suggests that rotations occurred mainly during the Incaic orogenic event of Eocene–early Oligocene age. A few paleomagnetic results obtained in Neogene rocks do not show evidence of clockwise rotations. Hence the development of the Bolivian orocline during late Neogene time cannot be explained by simple bending of the whole margin. These results demonstrate that tectonic rotations within the forearc and pre-Cordillera are key elements of early Andean deformation, which should be taken into account by kinematic models of mountain building in the central Andes. *INDEX TERMS:* 1525 Geomagnetism and Paleomagnetism: Paleomagnetism applied to tectonics (regional, global); 8110 Tectonophysics: Continental tectonics—general (0905); 8102 Tectonophysics: Continental contractional orogenic belts; 1599 Geomagnetism and Paleomagnetism: General or miscellaneous; 9360 Information Related to Geographic Region: South America; *KEYWORDS:* paleomagnetism, tectonic rotations, central Andes, northern Chile, Paleogene

Citation: Arriagada, C., P. Roperch, C. Mpodozis, G. Dupont-Nivet, P. R. Cobbold, A. Chauvin, and J. Cortés, Paleogene clockwise tectonic rotations in the forearc of central Andes, Antofagasta region, northern Chile, *J. Geophys. Res.*, *108*(B1), 2032, doi:10.1029/2001JB001598, 2003.

1. Introduction

[2] The Bolivian Orocline, or change in trend of the Andes from NW-SE to N-S near 18°S, is one of the most conspicuous large-scale features of the entire Andean chain. The orocline concept was originally formulated by *Carey* [1958] who envisaged counterclockwise rotation of that segment of the Andes between the Arica–Santa Cruz bend and the Huancabamba bend in the north, essentially after formation of an initially straight Andean chain. *Isacks* [1988] indicated that along-strike variations in the width of the Bolivian Altiplano were associated with differential shortening during plateau uplift. According to this model, a slight original curvature of the Andean continental margin was enhanced by differential shortening during Neogene time, implying rotation of both limbs. The expected rotations are of 5°–10° for the southern limb and 10°–15° for the northern limb. This tectonic model was verified by early paleomagnetic results obtained mostly along the forearc [*Heki et al.*, 1984, 1985; *May and Butler*, 1985; see also review by *Beck*, 1988].

[3] During the last decade numerous new paleomagnetic data have been obtained. They demonstrate that vertical axis rotations are important components of deformation in the central Andes [*Macedo Sanchez et al.*, 1992; *Butler et al.*, 1995; *MacFadden et al.*, 1995; *Randall and Taylor*, 1996; *Randall et al.*, 2001; *Aubry et al.*, 1996; *Somoza et al.*, 1999; *Coutand et al.*, 1999; *Roperch et al.*, 2000; *Arriagada et al.*, 2000; *Somoza and Tomlinson*, 2002]. Most of the new paleomagnetic studies indicate variable amounts of rotation whose magnitudes often exceed those predicted by oroclinal bending associated with uplift of the Altiplano–Puna plateau (see also review by *Beck* [1998]). In situ block rotations, in response to oblique convergence [*Beck*, 1987] and tectonic shortening [*Coutand et al.*, 1999; *Roperch et al.*, 2000], are thus needed to explain the observed spatial variability in the magnitude of rotations.

[4] The suggested relation between plateau uplift and oroclinal bending [*Isacks*, 1988] implies that most of the rotations should have occurred during Neogene time. For the Altiplano–Puna plateau, a good correlation exists between Plateau uplift, deformation and tectonic rotations [*Coutand et al.*, 1999; *Roperch et al.*, 2000]. Within the forearc and the pre-Cordillera of northern Chile (Domeyko Cordillera, Figure 1), the situation is different. There, large rotations are observed in Paleocene rocks [*Hartley et al.*, 1992; *Arriagada et al.*, 2000] but no evidence of late Neogene rotations has been found [*Somoza et al.*, 1999; *Somoza and Tomlinson*, 2002]. In addition, although the tectonic uplift of the 3000–5000 m high ranges of the

[1]Departamento de Geología, IRD, Universidad de Chile, Santiago, Chile.
[2]UMR 6118 du CNRS, Géosciences-Rennes, Rennes, France.
[3]Servicio Nacional de Geología y Minería, Santiago, Chile.
[4]Now at SIPETROL, Santiago, Chile.
[5]Department of Geosciences, University of Arizona, Tucson, Arizona, USA.

0148-0227/03/2001JB001598$09.00

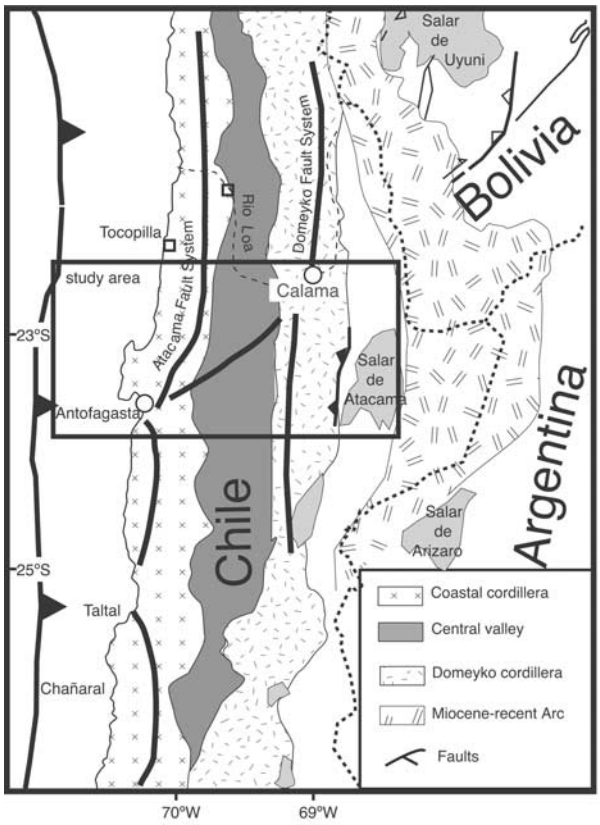

Figure 1. Simplified sketch of the Andes of northern Chile showing the principal morphologic units and main structural features. The large rectangle indicates the main study area further described in Figure 2. The small squares indicate the Tocopilla and Rio Loa sampling localities not shown in Figures 2, 4, and 5.

Domeyko Cordillera in northern Chile has been previously assumed to be mostly Miocene in age, fission track thermochronology [*Maksaev and Zentilli*, 1999] indicates that tectonic uplift and erosion were mainly active during the Eocene–early Oligocene, when at least 4–5 km of rocks were eroded during exhumation of tectonic blocks of the Domeyko Cordillera between ca. 45 and 30 Ma.

[5] In the Antofagasta region (Figure 1), most of the published paleomagnetic data have been obtained in upper Mesozoic rocks from the Coastal chain [*Turner et al.*, 1984; *Tanaka et al.*, 1988; *Forsythe and Chisholm*, 1994]. Here we report new paleomagnetic results based on extensive sampling in mostly volcanic rocks with occasional sedimentary, intrusive rocks, and semiconsolidated continental sediments across the forearc of the Antofagasta region (22°–24°S, Figures 1 and 2). The sampling includes Mesozoic rocks from the coastal chain, Cretaceous rocks from the Central Valley and Tertiary rocks from the western edge of the Domeyko Cordillera. Our study supplements results obtained by *Arriagada et al.* [2000] along the eastern border of the Cordillera de Domeyko.

2. Geology and Tectonics of the Forearc of Northern Chile

[6] In the forearc of northern Chile, subduction-induced magmatism has been active at least since 180 Ma [*Coira et al.*, 1982]. It is possible to distinguish four magmatic stages (Figures 2 and 3): a Jurassic–Early Cretaceous arc (180–120 Ma) in the Coastal Cordillera, a mid-Cretaceous arc (110–85 Ma) in the Central Valley, a latest Cretaceous (ca. 85–65 Ma) episode of volcanism in the central depression and an essentially Paleocene arc (65–55 Ma) along the western slope of the Cordillera de Domeyko [*Marinovic and García*, 1999; *Scheuber and González*, 1999; *Cortés*, 2000]. Magmatism in the forearc essentially ended during the Eocene to early Oligocene with emplacement of a suite of shallow stocks along the axis of the Domeyko Cordillera including some of the giant porphyry coppers of northern Chile [*Cornejo et al.*, 1997].

2.1. Geology of the Coastal Cordillera of the Antofagasta Region

2.1.1. Stratigraphy

[7] In the coastal Cordillera (Figures 2 and 3), a 3000–10,000 m thick volcanic sequence (La Negra Formation), composed mainly of subaerial lava and breccias of basaltic–andesitic composition, accumulated during Early to Middle Jurassic times. Associated intrusive bodies are of gabbroic to granodioritic composition. Subduction related plutonism started around 180 Ma and reached a maximum in Middle Jurassic to Early Cretaceous times (160–120 Ma) [*Boric et al.*, 1990].

2.1.2. Regional Structure

[8] The coastal magmatic arc is longitudinally cut by the Atacama Fault System (AFS, Figure 2). The AFS is a complex association of NS trending mylonitic and cataclastic zones and brittle faults exposed along the Coast Range of northern Chile, between 22°S and 29°S [*Hervé*, 1987; *Scheuber and Adriessen*, 1990; *Grocott et al.*, 1994; *Scheuber and González*, 1999]. The AFS has a long history of deformation spanning the Early Jurassic to Cenozoic.

[9] *Sheuber and González* [1999] suggested that structures of the Jurassic to Early Cretaceous magmatic arc formed in four stages. In Stage 1 (ca. 195–155 Ma), motion was left lateral and arc parallel. In Stage 2 (160–150 Ma), there was strong arc-normal extension. For Stage 3 (155–147 Ma), a reversal in the stress regime is indicated by two generations of dikes, an older one trending NE-SW and a younger one trending NW-SE. During Stage 4 (until ~125 Ma), left-lateral motions prevailed, the AFS originating as a left-lateral trench-linked fault. Brittle strike-slip and dip-slip movements continued intermittently along the AFS until the late Miocene [*Hervé*, 1987].

2.2. Geology of the Central Valley of the Antofagasta Region

2.2.1. Stratigraphy

[10] On the western side of the Central Valley (Figures 2, 3, and 4), scarce outcrops of upper Paleozoic sedimentary rocks are unconformably overlain by a marine sequence of Late Triassic to Early Jurassic age (Rencoret Formation) [*Cortés*, 2000] containing Hettangian–Sinemurian fossils. These sedimentary sequences are covered by andesitic rocks of the La Negra Formation. To the east, these andesitic rocks are not present but a mid-Cretaceous continental volcanic sequence (Paradero del Desierto Formation) [*Cortés*, 2000] is covered by the Late Cretaceous Quebrada Mala Formation (see below). Further east, along the western

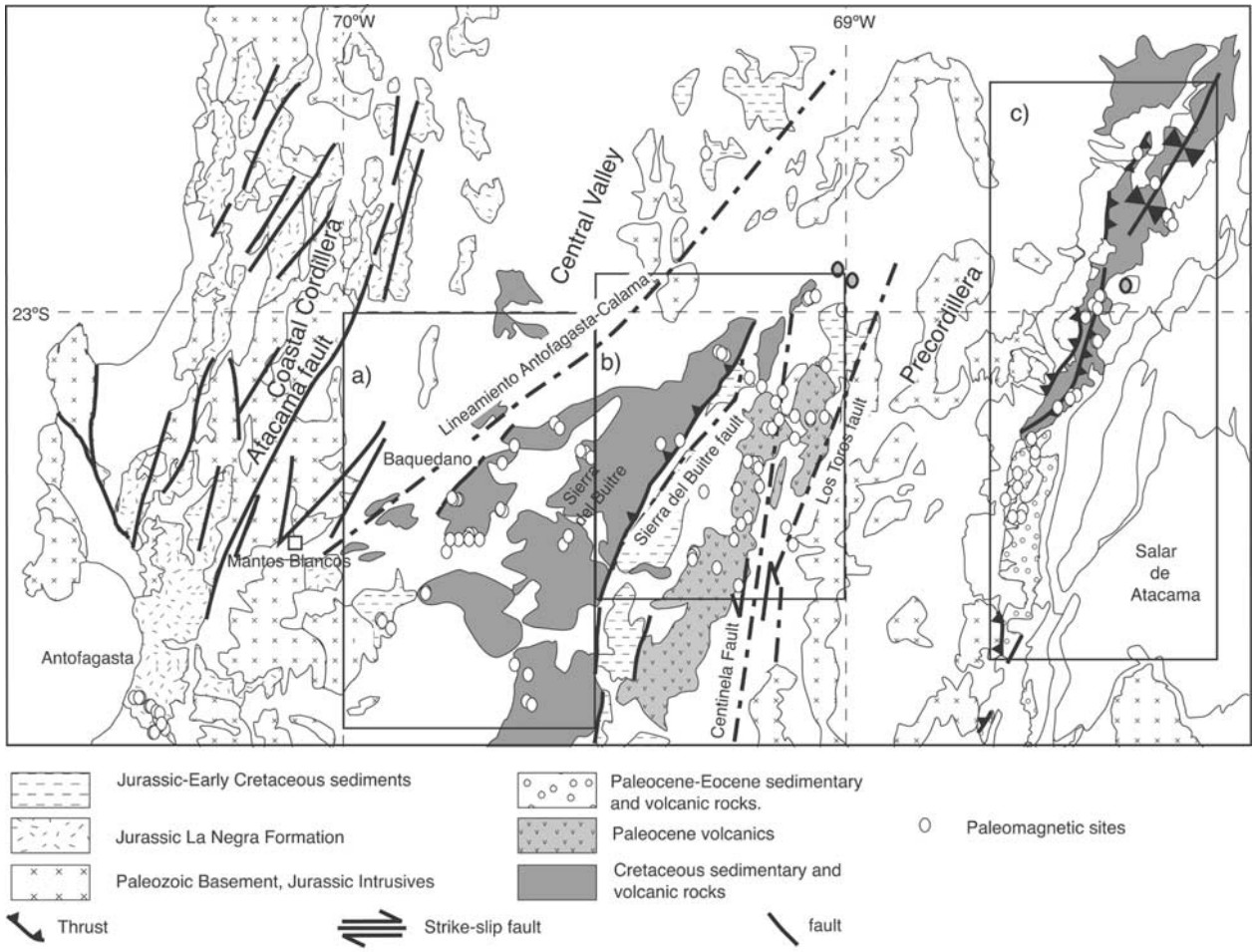

Figure 2. Geological map of the Antofagasta region showing paleomagnetic sites (modified after Mapa Geologico (1:1000.000), SERNAGEOMIN Chile) [*Marinovic and García*, 1999; *Arriagada et al.*, 2000; *Cortés*, 2000]. Rectangles a and b indicate the locations of the maps shown in Figures 4 and 5. Box c indicates the location of the paleomagnetic study previously published by *Arriagada et al.* [2000]. Circles indicate the location of the paleomagnetic sites (filled circles indicate the three sites in the Sifón Ignimbrite).

edge of the present-day Cordillera de Domeyko (Figures 2, 3, and 4), a thick sequence of Jurassic marine sediments (Caracoles Group) [*Marinovic and García*, 1999] accumulated in a long-lived back arc basin (Tarapaca basin) [*Mpodozis and Ramos*, 1990]. The upper part of the sequence consists of Upper Jurassic to Lower Cretaceous continental red beds. The Caracoles Group is overlain unconformably by continental sediments with interbedded volcanic sequences up to 3 km thick of the Quebrada Mala Formation, deposited between 85 and 65 Ma [*Marinovic and García*, 1999].

[11] In the Sierra del Buitre, the Mesozoic sequences are intruded by monzodiorites and granodiorites of the Sierra del Buitre Batholith (Figures 4 and 5). K-Ar and $^{39}Ar/^{40}Ar$ ages range at 74–66 Ma [*Cortés*, 2000]. To the east of the Sierra del Buitre (Figures 3, 4, and 5), the Mesozoic units are overlain by about 500 m of conglomerates, ignimbrites and andesitic lava flows of the Paleocene Cinchado Formation (63–55 Ma) [*Marinovic and García*, 1999]. Locally, the Cinchado Formation is covered by scarce andesitic lava flows and ignimbrites of the Cerro Casado Formation (48–45 Ma). Both units are separated by a smooth angular unconformity.

2.2.2. Regional Structure

[12] The Central Valley is traversed by several NE-NNE striking faults and lineaments (Figures 2, 4, and 5). The most important structural feature is a major lineament parallel to the Antofagasta–Calama road and here termed the Lineamiento Antofagasta–Calama (Figures 2, 4, and 5). To the SE of the Lineamiento Antofagasta–Calama, the Sierra del Buitre is a structurally uplifted block consisting mainly of Mesozoic rocks. The Sierra del Buitre fault (Figure 5), a SE verging imbricate reverse fault lying immediately east of the Sierra del Buitre, places the Quebrada Mala Formation over the Caracoles Group. It probably originated as a normal fault and was later reactivated as an inverse fault during inversion of the Quebrada Mala basin in the latest Cretaceous–early Paleocene [*Marinovic and García*, 1999].

[13] The Mesozoic rocks were deformed in several stages of Cretaceous compression. Deformation in the Caracoles Group is marked by open plunging folds and is especially

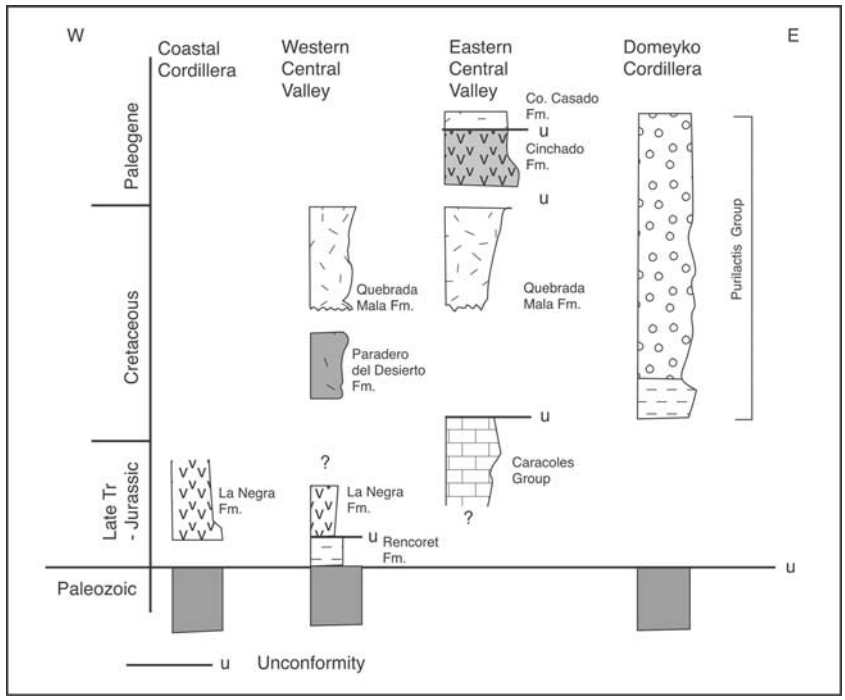

Figure 3. Simplified stratigraphy between Coastal Cordillera and Domeyko Cordillera including the principal names of geological formations described in the text (modified *after* the studies of *Marinovic and García* [1999], *Arriagada et al.* [2000], and *Cortés* [2000].

significant within limestones and evaporites. At least part of the deformation of the Caracoles group predates the accumulation of the Quebrada Mala Formation which is in turn deformed by predominantly symmetrical folds, with subhorizontal axes trending N10°–N50°E. Finally, the Cinchado Formation is deformed only by open folds with amplitudes of several hundred meters. Deformation is not observed everywhere. For example, to the east of Sierra del Buitre (near site CG02), a horizontal volcanic flow of the Cinchado Formation overlies an eroded paleosurface carved in horizontal Jurassic limestones of the Caracoles Group.

2.3. Geology of the Cordillera de Domeyko in the Antofagasta Region

2.3.1. Stratigraphy

[14] The Domeyko range consists mainly of upper Paleozoic plutonic and volcanic rocks, which are devoid of any Mesozoic cover [*Coira et al.*, 1982; *Reutter and Scheuber*, 1988; *Mpodozis et al.*, 1993]. At the eastern edge of the Domeyko range, the Paleozoic basement overthrusts, or is overlain unconformably by, a sequence of red beds and interbedded volcanics, up to 5 km thick, deposited during the Early Cretaceous to Eocene (Figures 2 and 3). They have been described as the Purilactis Group [*Charrier and Reutter*, 1994; *Arriagada et al.*, 2000], and have been interpreted as the infill of a large basin. This basin formed under the modern Salar de Atacama, and was connected, to the east, with the Salta Group rift basins of northwestern Argentina [*Grier et al.*, 1991].

2.3.2. Regional Structure

[15] The Domeyko range is a narrow mountain range lying between the pre–Andean Depression and the Salar de Atacama basin, to the east, and the Central Depression (Central Valley, Figure 2), to the west. The major structural feature in the Domeyko range is the Domeyko Fault System (DFS). Transpressional and left-lateral displacements in the DFS have been documented in the late Eocene and possibly into the early Oligocene to the south of Calama, although offsets probably did not exceed ~2 km [*Mpodozis et al.*, 1993; *Tomlinson et al.*, 1994]. To the north of Calama, however, the Eocene (Incaic) deformation is represented by a set of west and east verging faults, which have uplifted basement blocks and show no significant component of strike-slip [*Tomlinson and Blanco*, 1997a]. By the end of the early Oligocene (after ~31 Ma), a period of left-lateral displacement has been well documented for the area north of Calama (Figure 1), resulting in a net offset of approximately 35 km in the Chuquicamata–El Abra area, ensued up to the middle Miocene (~17 Ma) [*Reutter et al.*, 1996; *Dilles et al.*, 1997; *Tomlinson and Blanco*, 1997b].

[16] In the region west of the Salar de Atacama (Figure 2), the Domeyko range is bounded to the west by the N-S trending Centinela Fault (Figure 5), which has been interpreted as a "master fault" of the DFS [*Mpodozis et al.*, 1993]. Left-lateral strike-slip movements can be inferred from a compressive duplex exposed along the northern part of this fault [*Marinovic and García*, 1999]. To the east of the Centinela Fault, the Cinchado Formation and Caracoles Group are separated from Paleozoic units by the N30°E trending Los Toros Fault. This fault has been interpreted as a secondary structure of the Centinela fault [*Marinovic and García*, 1999].

3. Paleomagnetic Method

3.1. Paleomagnetic Sampling

[17] Paleomagnetic sampling was done during several field trips and a total of 108 sites were sampled. For most sampling, we used a portable gasoline-powered drill with a

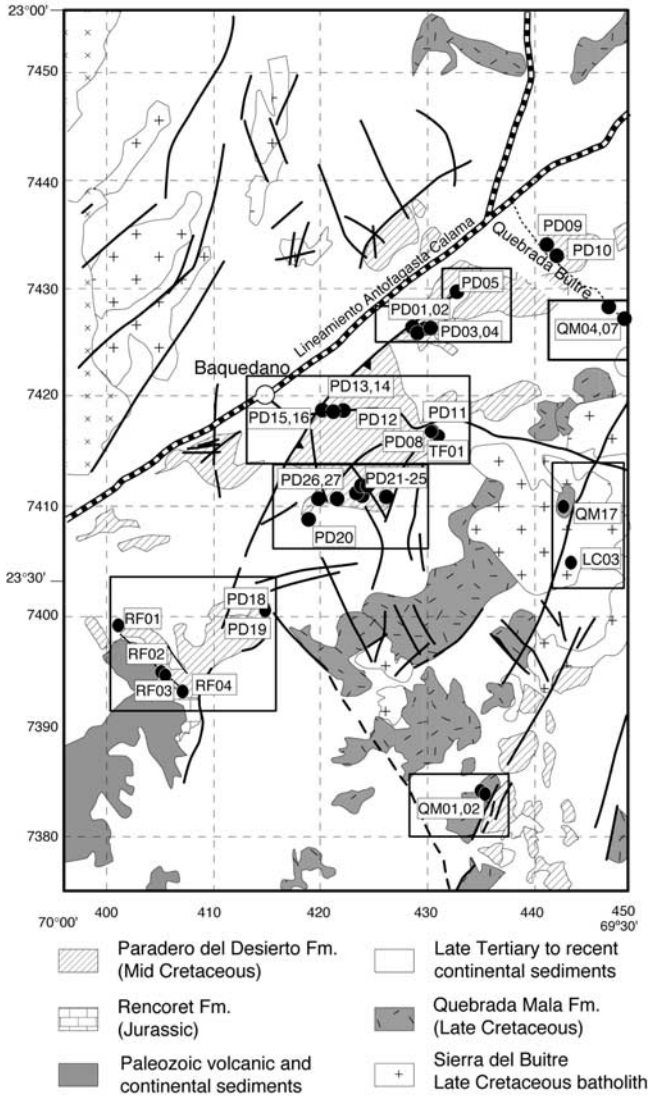

Figure 4. Geology of the Baquedano Area, western Central Valley, and paleomagnetic sites (modified after the studies of *Marinovic and García* [1999] and *Cortés* [2000]).

water-cooling system. For weakly lithified layers, we used an air-cooled system. Samples were oriented using magnetic and solar compasses. The locations of paleomagnetic sites are given in Table 1 and shown in Figures 2, 4, and 5. We sampled the Jurassic La Negra Formation near coastal localities: Tocopilla (13 sites) and Antofagasta (17 sites). Near Antofagasta, the thickness of the sampled section is larger than 3000 m. The sampling is not in a continuous section near Tocopilla.

[18] Within the Central Valley and the Domeyko range most samples are from Cretaceous and Paleocene–Eocene volcanics, whereas a few are from Jurassic marine sediments, Mesozoic sandstones, and Upper Cretaceous to Eocene intrusives. To get an upper constraint on the age of rotations in the forearc, 2 sites in semiconsolidated Oligocene–Miocene continental sediments, and 3 sites in a Miocene ignimbritic flow (Sifón Ignimbrite) were also sampled (Figures 1, 2, and 5).

[19] Sites in volcanic rocks include samples from a single flow, dyke, sill or ignimbrite. Secular variation was thus not averaged at these single-bed sites. In contrast, in sedimentary rocks, sampling included different beds across several meters of stratigraphic section. In such few sites the site-mean paleomagnetic direction should average the secular variation and provide a good estimate of tectonic rotations. Where sediments were not interbedded with volcanics, bedding corrections for volcanic rocks were estimated from general flow attitudes. A few sites were drilled in intrusive rocks. Except at one site (LC02), bedding of the surrounding rocks is almost flat.

3.2. Paleomagnetic Techniques

[20] Samples were analyzed in paleomagnetic laboratories at the University of Chile and the University of Rennes. Remanent magnetization was measured with either a spinner magnetometer (Molspin or AGICO JR5A) or a cryogenic magnetometer (CEA-LETI). Magnetic susceptibility was measured with a Bartington susceptibility meter. To better constrain the magnetic mineralogy, we studied the acquisition of isothermal remanent magnetization (IRM) and the variation of susceptibility during heating (K-T) on characteristic samples. IRM was given with a pulse electromagnet and K-T experiments were done with the AGICO KLY3-CS3 instrument.

[21] For most samples, one specimen was subjected to stepwise thermal demagnetization (10–15 steps) in an

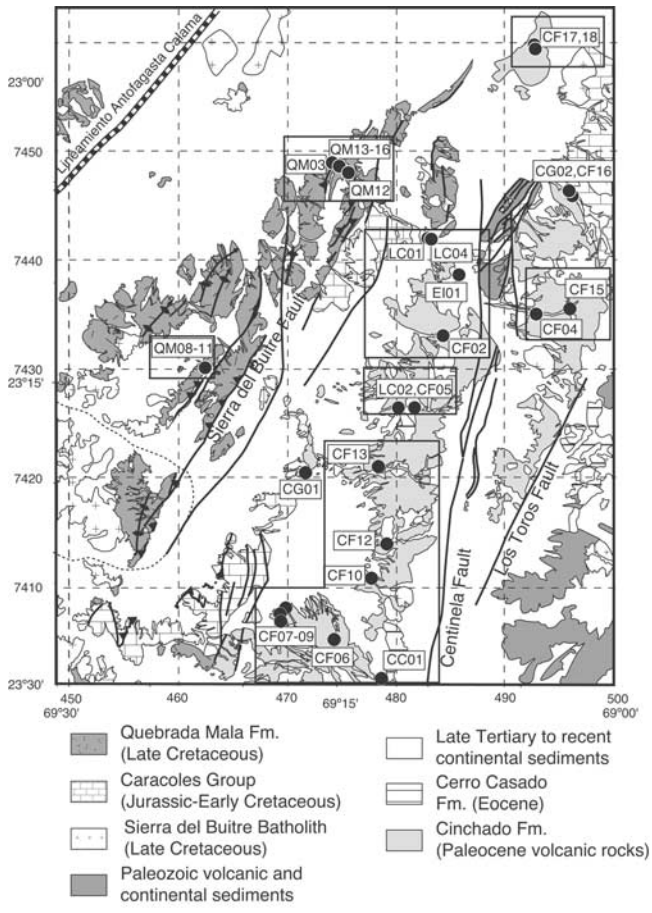

Figure 5. Geology of the Sierra del Buitre Area, eastern Central Valley, and paleomagnetic sites (modified after modified after the study of *Marinovic and García* [1999]).

Table 1. Location of the Paleomagnetic Sampling and Magnetic Properties

Site	Lithology	Latitude (°S)	Longitude (°W)	NRM (A/m)	K (SI)	Strike/Dip
		La Negra Formation (Jurassic) Tocopilla				
LN01	Lava flow	22°11.6	70°13.33	0.42	0.045	0/30
LN02	Lava flow	22°11.52	70°13.48	0.19	0.057	0/30
LN03	Lava flow	22°11.53	70°13.42	0.29	0.052	0/30
LN04	Lava flow	22°9.07	70°13.32	0.47	0.052	0/30
LN05	Lava flow	22°17.52	70°14.45	0.21	0.036	0/30
LN06	Breccia/ oxidized	22°17.52	70°14.50	0.1	0.0013	0/30
LN07	Lava flow	22°17.50	70°14.50	0.25	0.063	0/30
LN08	Lava flow	22°17.50	70°14.50	0.48	0.054	0/30
LN09	Lava flow	22°22.22	70°15.00	0.36	0.069	0/30
LN10	Lava flow	22°22.15	70°14.70	0.39	0.071	0/30
LN11	Lava flow	22°22.1	70°14.57	0.39	0.065	0/30
LN12	Lava flow	22°22.1	70°14.57	0.48	0.069	0/30
LN13	Diorite	22°05.95	70°7.18	0.078	0.022	
		La Negra Formation (Jurassic) Antofagasta				
LN14	Lava flow	23°45.42	70°20.95	0.11	0.022	205/35
LN15	Lava flow	23°45.1	70°21.57	0.17	0.031	160/30
LN16	Lava flow	23°44.83	70°21.39	0.035	0.011	180/30
LN17	Lava flow	23°44.40	70°21.68	0.095	0.023	160/30
LN18	Lava flow	23°43.53	70°21.97	0.15	0.029	180/40
LN19	Sill	23°42.86	70°22.76	0.086	0.015	170/40
LN20	Lava flow	23°41.98	70°23.85	0.061	0.011	170/40
LN21	Ryolite	23°41.97	70°24.63	0.033	0.00023	170/40
LN22	Ryolite	23°41.97	70°24.63	0.011	0.00004	170/40
LN23	Lava flow	23°41.95	70°23.88	0.042	0.0063	170/40
LN24	Lava flow	23°45.75	70°22.3	0.21	0.024	170/40
LN25	Lava flow	23°45.76	70°22.23	0.059	0.0094	170/45
LN26	Lava flow	23°42.94	70°22.58	0.16	0.028	190/45
LN27	Lava flow	23°43.53	70°21.97	0.14	0.035	180/40
LN28	Lava flow	23°43.74	70°21.5	0.36	0.060	190/45
LN29	Lava flow	23°44.83	70°21.39	0.47	0.039	190/45
LN30	Lava flow	23°44.83	70°21.39	0.17	0.016	180/30
		Rencoret Formation (Early Jurassic)				
RF01	Limestone/oxidized	23°31.10	69°57.85	0.00671	0.000115	259.3/24.9
RF02	Limestone/oxidized	23°33.47	69°55.45	0.00387	6.17e−05	292.4/25.2
RF03	Limestone/oxidized	23°33.62	69°55.31	0.00591	0.000108	273.5/11.3
RF04	Limestone/oxidized	23°34.30	69°54.23	0.0178	0.000193	331.1/24
		Caracoles Group (Jurassic)				
CG01	Siltstone/oxidized	23°19.60	69°16.70	0.0366	0.000167	246.4/34.3
CG02	Limestone	23°5.51	69°2.47	0.000889	8.98e−05	243/4
		Paradero del Desierto Formation (mid-Cretaceous)				
PD01	Lava flow	23°16.48	69°41.54	0.136	0.00299	100/30
PD02	Lava flow	23°16.29	69°41.75	0.561	0.00127	100/30
PD03	Lava flow	23°16.34	69°41.10	0.569	0.0329	100/30
PD04	Ignimbritic flow	23°16.24	69°40.74	0.121	0.00111	100/30
PD05	Dyke	23°14.38	69°39.36	0.472	0.00463	Subvert.
PD06	Lava flow	23°42.45	69°38.13	0.133	0.01	250/40
PD07	Lava flow	23°42.84	69°37.49	0.154	0.00171	259.6/36.8
PD08	Lava flow	23°21.62	69°40.51	0.0952	0.000407	Subhoriz.
PD09	Lava flow	23°11.95	69°34.58	0.924	0.0127	Subhoriz.
PD10	Lava flow	23°12.44	69°33.91	0.175	0.0285	Subhoriz.
PD11	Ignimbritic flow	23°21.41	69°40.96	0.379	0.000944	Subhoriz.
PD12	Dyke	23°20.28	69°45.95	0.184	0.0278	145/16
PD13	Lava flow/oxidized	23°20.52	69°46.22	0.0446	0.000329	145/16
PD14	Limestone/oxidized	23°20.23	69°46.57	0.00795	0.000109	138/17
PD15	Lava flow/oxidized	23°20.20	69°46.57	0.0705	0.000595	155/32
PD16	Lava flow/oxidized	23°20.20	69°46.57	0.0546	0.000853	155/32
PD18	Sandstone/breccias	23°30.41	69°49.99	0.0175	0.0004	40/30
PD19	Lava flow	23°30.52	69°49.98	0.033	0.000405	40/30
PD20	Lava flow	23°26.01	69°47.60	0.38	0.00803	327/17
PD21	Lava flow	23°24.05	69°44.48	0.754	0.0256	Subhoriz.
PD22	Lava flow	23°24.06	69°44.78	0.0211	6.39e−05	Subhoriz.
PD23	Lava flow	23°24.45	69°45.05	1.11	0.0251	Subhoriz.
PD24	Lava flow	23°24.67	69°43.45	0.275	0.00132	180/10
PD25	Lava flow	23°24.59	69°44.73	0.54	0.0186	Subhoriz.
PD26	Lava flow	23°24.79	69°46.15	1.77	0.0204	45/5
PD27	Lava flow	23°24.74	69°47.14	0.27	0.0295	45/5

Table 1. (continued)

Site	Lithology	Latitude (°S)	Longitude (°W)	NRM (A/m)	K (SI)	Strike/Dip
			Quebrada Mala Formation (Late Cretaceous)			
QM01	Ignimbritic flow	23°39.57	69°37.87	0.0229	0.000138	76.7/43.1
QM02	Ignimbritic flow	23°39.49	69°38.15	0.631	0.000295	27.2/32.8
QM03	Lava flow	23°4.093	69°15.17	1.45	0.0162	204/63.8
QM04	Lava flow	23°15.25	69°30.89	0.175	0.00136	Subhoriz.
QM05	Lava flow	23°15.02	69°31.43	0.0424	0.00051	222/12
QM06	Ignimbritic flow	23°15.02	69°31.43	0.0318	1.36e−05	222/12
QM07	Lava flow	23°15.69	69°30.33	0.507	0.0127	Subhoriz.
QM08	Ignimbritic flow	23°14.26	69°22.06	0.112	0.00548	216.6/82.6
QM09	Ignimbritic flow	23°14.26	69°22.06	0.256	0.000425	216.6/82.6
QM10	Ignimbritic flow	23°14.26	69°22.06	0.0947	0.0193	216.6/82.6
QM11	Ignimbritic flow	23°14.25	69°22.07	0.343	0.0187	216.6/82.6
QM12	Ignimbritic flow	23°4.57	69°14.28	0.134	0.000304	184.4/87
QM13	Ignimbritic flow	23°4.26	69°14.80	0.265	0.000939	211/74
QM14	Ignimbritic flow	23°4.26	69°14.80	0.0862	0.00047	211/74
QM15	Ignimbritic flow	23°4.26	69°14.80	0.322	0.00129	211/74
QM16	Ignimbritic flow	23°4.26	69°14.80	0.0347	0.000315	211/74
QM17	Tuffaceous sediments	23°25.26	69°33.69	0.455	0.000906	210.8/10
			Late Cretaceous intrusives			
LC01	Diorite	23°7.915	69°9.984	0.0295	0.00506	
LC02	Diorite	23°16.32	69°10.77	0.63	0.00607	
LC03	Diorite	23°28.17	69°33.32	1.17	0.0179	
LC04	Diorite	23°7.983	69°9.865	0.488	0.0166	
			Cinchado Formation (Paleocene)			
CF01	Lava flow	23°7.915	69°9.984	0.275	0.0431	Subhoriz.
CF02	Lava flow	23°12.68	69°9.256	0.137	0.00862	205.7/25.3
CF03	Lava flow	23°13.64	69°6.112	1.24	0.00287	Subhoriz.
CF04	Lava flow/oxidized	23°11.61	69°4.252	1.2	0.0074	156/25
CF05	Ignimbritic flow	23°16.23	69°11.59	0.21	0.00163	240.6/60
CF06	Ignimbritic flow	23°27.96	69°15.15	0.134	0.00186	150.2/41.5
CF07	Ignimbritic flow	23°26.37	69°17.78	0.194	0.00265	148.8/14.6
CF08	Tuffaceous sediments	23°26.67	69°18.10	0.0614	8.57e−05	80/20
CF09	Ignimbritic flow	23°27.04	69°18.06	0.0068	6.13e−05	20/15
CF10	Lava flow	23°24.89	69°13.12	4.72	0.00693	110.4/27.4
CF11	Ignimbritic flow	23°22.43	69°11.46	0.259	0.0129	160/70
CF12	Lava flow	23°23.17	69°12.30	1.23	0.00116	110/15
CF13	Ignimbritic flow	23°19.28	69°12.75	0.621	0.00137	129.3/24.2
CF14	Tuffaceous sediments	23°19.02	69°10.09	1.49	0.000306	145/40
CF15	Lava flow	23°11.37	69°2.352	0.132	0.0224	180/20
CF16	Lava flow	23°5.66	69°2.40	2.0	0.0297	Subhoriz.
CF17	Lava flow	22°58.46	69°4.614	1.34	0.000157	165/15
CF18	Lava flow	22°58.24	69°4.274	0.0779	0.00117	150/30
			Eocene intrusive			
EI01	Diorite	23°9.646	69°8.385	0.519	0.0278	
			Cerro Casado Formation (Eocene)			
CC01	Ignimbritic flow	23°29.95	69°12.52	2.64	0.0108	Subhoriz.
			Tambores Formation or Atacama gravels (Miocene)			
TF01	Sandstone	23°21.41	69°40.91	0.0744	0.00302	Subhoriz.
			El Loa Formation (Oligocene–Miocene)			
LF01	Siltstones	21°37.59	69°32.57	0.0337	0.00198	Subhoriz.
			Sifon ignimbrite (Miocene)			
SI01	Ignimbritic flow	22°56.89	68°26.66	0.193	0.00772	Subhoriz.
SI02	Ignimbritic flow	22°53.45	69°1.111	0.313	0.00115	Subhoriz.
SI03	Ignimbritic flow	22°56.44	68°58.34	0.0493	0.00266	Subhoriz.

Sites coordinates, NRM: Geometric mean intensity of remanent magnetization. K: Geometric mean susceptibility. Strike and dip: Bedding attitude parameters.

ASC Scientific furnace where the residual field was less than 10 nT. Magnetic susceptibility was measured after each thermal demagnetization step, in order to check magnetic mineralogical changes upon heating. To better investigate the origin of the remanent magnetization, stepwise alternating field (AF) demagnetization using the Molspin AF instrument was also performed on some samples. AF demagnetization was preferred to thermal, only where there was evidence of remagnetization by lightning. Magnetization directions were determined with ''least squares lines and planes'' programs according to *Kirschvink* [1980]. Evidence for secondary overprint due to lightning was found at a few sites in volcanic rocks. Statistics combining directions and planes [*McFadden and*

McElhinny, 1988] were used to determine the mean characteristic directions for such sites.

3.3. Reference Poles

[22] The motion of South America since the early Mesozoic has been mostly an E-W displacement with successive small clockwise or counterclockwise rotations. This behavior leads to an APWP positioned close to the present-day geographic axis. Except for the Early Cretaceous (Paraná Volcanics) [*Ernesto et al.*, 1990; *Raposo and Ernesto*, 1995] very precise paleomagnetic reference poles are lacking for the South American plate.

[23] *Roperch and Carlier* [1992] suggested that the best approach for a South American reference curve was to transfer the master curve defined by *Besse and Courtillot* [1991] to the South American plate. *Beck* [1999] criticized this approach and suggested that the APWP variations are small enough for a single pole to be calculated for the whole Mesozoic. *Lamb and Randall* [2001] developed a technique allowing paleomagnetic poles to be calculated from a mixture of declination and inclination data drawn from localities in stable South America and in the Andes. *Lamb and Randall* [2001] also attempted to correct for compaction in sedimentary rocks. The APWP obtained following this interesting approach is not significantly different from the one given by *Roperch and Carlier* [1992] and this demonstrates that an APWP for South America can be determined. *Besse and Courtillot* [2002] have updated several APWPs for most continents. We believe that their new SA APWP (hereafter labeled BC01) is the most reliable APWP and that it should henceforth be used to calculate tectonic rotations. Because of the age uncertainties of the rock formation, we will use the BC01 APWP calculated through a 20 Ma running window.

[24] The lack of geological evidence for large latitudinal displacements in the Andes suggests that our study area has been more or less (within 1°) stable in latitude relative to South America. Comparison of the observed inclinations, in volcanic rocks and remagnetized units (see below), with the expected inclination calculated from the BC01 APWP confirms that no significant latitudinal displacements can be demonstrated.

4. Magnetic Properties and Characteristic Directions

[25] For most samples, except from Jurassic rocks, interpretation of demagnetization data was straightforward and the primary or secondary origin of the characteristic remanent magnetization (ChRM) was well defined for each site. Mostly, the Fisher concentration parameter is higher than 100 and the 95% confidence angle is lower than 5°. The magnetic properties are mainly deduced from progressive thermal or alternating field demagnetizations and measurements of magnetic susceptibility after each step of thermal treatment.

[26] As shown in Table 1, there is a large dispersion in the site-mean values of magnetic susceptibility and intensity of natural remanent magnetization (NRM). NRM intensities are between 0.0008 and 6 A/m while volume magnetic susceptibility varies between 0.00001 and 0.1 SI. These large variations are correlated to changes in lithology. Magnetite and maghemite are the main magnetic carriers of the NRM for sites where magnetic susceptibility is higher than 0.005 SI. Usually, hematite is the main magnetic carrier of the NRM for the highly oxidized rocks. This is especially so for some ignimbrites where oxidation probably occurred during emplacement. At a few localities, field evidence for a late phase of oxidation corroborates paleomagnetic evidence for remagnetization.

4.1. La Negra Formation: Coastal Area

[27] Magnetic susceptibility is mostly high to very high (up to 0.1 SI, Table 1), especially in the Tocopilla area where the Jurassic volcanics are characteristically rich in magnetite. Multidomain magnetite and maghemite are often the main magnetic carriers and secondary magnetizations are widespread. 108 samples were subjected to low temperature demagnetization by cooling in zero field down to liquid nitrogen temperature. This process was efficient in removing part of the secondary overprint associated with multidomain magnetite.

[28] In the Antofagasta area, where low-grade metamorphism is important, normal and reverse polarity magnetizations are often found within the same flow. However, at some sites, samples from the interior part of the lava record a well-defined magnetization, unblocking temperatures being higher than 500°C. In contrast, the brecciated and vesicular part of the lava yield a more complex record of remanent magnetization (Figures 6a and 6b, site LN18).

[29] At some sites, apparent antiparallel magnetizations are observed without clear evidence of significant differences in secondary mineral assemblages (Figures 6c–6e, site LN25). As the volcanics near Antofagasta have the same bedding attitude toward the west, it is not possible to perform a true fold test. The fact that the in situ ChRM directions carried by samples showing low temperature alteration is closer to the tilt-corrected directions of the unaltered samples is an indication that low temperature metamorphism in these rocks is probably later than tilting. Dikes intruding Upper Jurassic plutons in the same area are vertical. This indicates that the plutons, which are younger than La Negra volcanics, are not tilted and could have remagnetized the volcanics after the deformation. Because it is uncertain whether or not a tilt correction should be applied to the secondary magnetization, we will not consider these magnetizations as valid for tectonic purposes.

[30] Two sites were drilled in the upper level of the volcanic pile, one in a red rhyolite overlain by a welded ignimbrite (sites LN21 and LN22, Table 1). In contrast to the magnetic behavior of most of the andesitic lavas of the La Negra Formation, these rocks are highly oxidized and the ChRM is carried by hematite. However, the two successive units show opposite polarities, indicating that oxidation is of primary origin.

[31] The between-site dispersion is high, suggesting high secular variation of the Earth's magnetic field during the Jurassic (Figure 6f). Dispersion decreases slightly upon tilt correction. The mean direction (Table 2) is similar to the expected direction calculated with the 180 Ma pole of the BC01 APWP.

4.2. Rencoret Formation: Central Valley

[32] Samples from oxidized Lower Jurassic limestones (Rencoret locality (RF01-04)) from the Central Valley of the

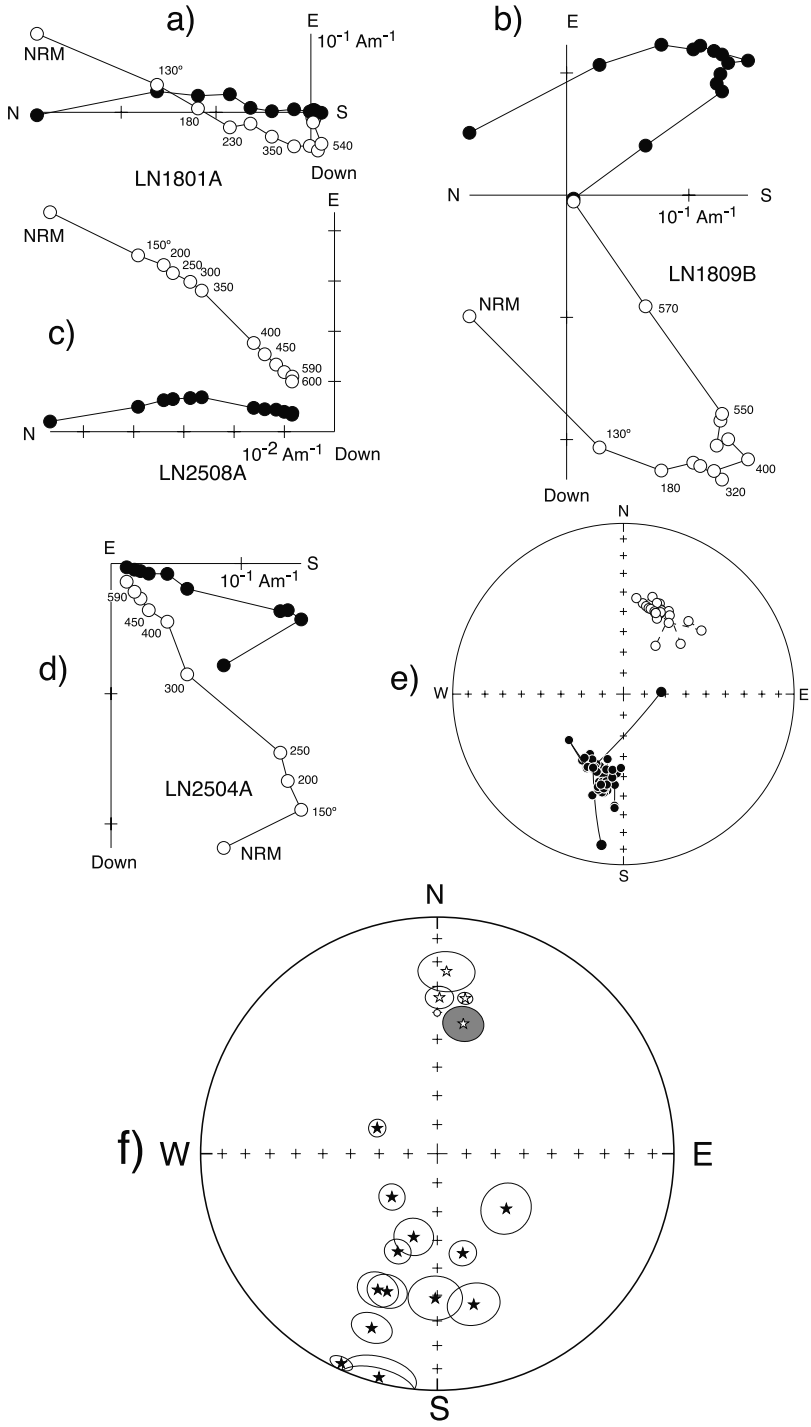

Figure 6. Orthogonal projections (in situ) of thermal demagnetization diagrams for samples in volcanic rocks of La Negra Formation. The reverse component of magnetization with high unblocking temperature observed in sample LN1809B cannot be isolated in the more intensely altered sample LN1801A from the same flow LN18. Both normal (c) and reverse (d) magnetizations are found within the same flow (LN25). (e) In equal-area projection of the demagnetization data for all samples of this site, we can observe antipodal magnetizations. Solid (open) circles correspond to projection into the horizontal (vertical) plane. (f) Equal-area projection of site-mean characteristic directions in tilt corrected coordinates from La Negra Formation (Table 2). The stars with the 95% error angle of confidence indicate the expected direction calculated from the BC01 APWP.

Table 2. Paleomagnetic Results

Site	N/n	In situ Dec	In situ Inc	α95	k	Tilt corrected Dec	Tilt corrected Inc	Locality
Jurassic: La Negra Formation								
Tocopilla								
LN01	14/14	19.6	−29.2	4.3	88	0.8	−34.3	15
LN02	10/11	216.3	23.7	6.3	62	200.0	38.0	15
LN03	7/7	206.5	51.1	4.5	193	165.6	54.2	15
LN05	8/9	195.4	71.1	8.7	41	128.6	59.4	15
LN06	11/11	203.1	−9.1	3.0	239	204.6	2.9	15
LN07	6/9	194.0	−4.7	9.4	63	194.6	2.6	15
LN08	7/10	202.6	32.7	8.4	59	180.8	38.7	15
LN12	9/9	229.1	43.2	6.6	75	195.8	60.0	15
Antofagasta								
LN18	8/12	149.1	48.6	4.4	174	202.0	53.2	16
LN19	9/11	144.1	23.0	8.1	46	166.4	34.7	16
LN21	9/9	341.7	−34.4	2.3	496	10.2	−33.7	16
LN22	6/6	179.3	33.2	6	719	200.6	22.3	16
LN23	5/7	343.7	−25.3	8.2	100	2.9	−23.8	16
LN26	13/13	131.9	53.8	4.5	95	226.3	68.4	16
LN27	10/10	169.2	41.2	6.5	64	203.6	37.3	16
LN28[a]	11/11	89.7	66.7	3.0	252	293.1	67.5	16
mean	15/16	3.9	−36.4	15.3	7			
mean	15/16			**12.0**	**11**	**9.1**	**−39.2**	
Early Jurassic: Rencoret Formation								
RF01	10/10	24.8	−47.8	2.4	405	54.2	−64.2	1
RF02	8/8	33.3	−44.8	3.4	273	44.4	−69.1	1
RF03	10/10	31.3	−50.1	5.3	85			
				10.1	24	19	−58.4	1
RF04	12/16	32.9	−40.6	1.7	646	15.1	−60.1	1
mean		**30.7**	**−45.9**	**5.6**	**270**			
				11.2	68	31.3	−63.9	
Mid-Cretaceous: Paradero del Desierto Formation								
PD18	9/12	53.0	−47.6	7.5	48	20.1	−45.6	1
PD19	7/7	57.4	−42.9	5.7	114	27.8	−44.4	1
PD20	9/9	64.0	−36.7	2.0	702	66.4	−53.5	2
PD21	9/10	47.4	−45.1	5.9	76	47.4	−45.1	2
PD22	10/10	25.9	−21.7	4.3	128	25.9	−21.7	2
PD23	10/10	40.6	−51.5	2.1	536	40.6	−51.5	2
PD24	11/11	23.5	−49.2	3.6	166	32.9	−44.5	2
PD25	13/13	39.9	−50.8	5.4	59	39.9	−50.8	2
PD26	9/9	65.4	−46.8	4.3	146	60.2	−48.4	2
PD27	7/7	59.0	−33.6	8.0	57	55.7	−34.7	2
PD08	6/7	34.4	−38.8	3.5	363	34.4	−38.8	3
PD11	9/9	54.2	−48.0	2.1	588	54.2	−48.0	3
PD12	8/8	41.3	−49.9	2.8	431	44.3	−34.7	3
PD13	10/10	37.4	−61.0	2.3	452	42.9	−45.9	3
PD14	4/5	54.9	−57.8	5.9	330	52.9	−40.6	3
PD15	15/19	53.2	−61.8	1.8	465	58.5	−30.3	3
PD16	13/13	45.5	−68.3	2.2	371	56.0	−37.3	3
PD01	8/8	68.9	−76.7	2.1	699	28.5	−51.6	4
PD02	9/9	60.6	−76.9	1.5	1127	26.0	−50.5	4
PD03	9/10	47.8	−62.9	2.9	313	30.2	−36.2	4
PD04	8/9	88.2	−75.9	3.7	226	34.3	−54.6	4
PD05	8/8	50.7	−56.5	3.6	238	50.7	−56.5	4
mean	22/22	48.4	−53.5	6.4	25			
				5.0	**40**	**42.2**	**−44.6**	
Late Cretaceous: Quebrada Mala Formation and related intrusives								
QM01	6/7	47.3	−55.8	11.6	34	19.1	−24.7	5
QM02	9/12	51.3	−41.9	5.9	78	18.3	−46.7	5
QM17	6/6	3.0	−55.8	5.6	144	17.8	−59.3	6
LC03	7/7	28.2	−54.5	5.1	161	28.2	−54.5	6
QM04	9/12	223.9	50.1	5.8	80	223.9	50.1	7
QM05	7/10	182	11.4	4.4	219	184.5	18.7	7
QM06	9/9	181.0	18.4	9.9	28	184.7	25.7	7
QM07	11/12	13.9	−45.4	3.1	233	13.9	−45.4	7
QM08	5/5	326.4	−2.1	6.1	156	22.7	−69.6	8
QM09	9/9	349.3	16.4	4.1	160	6.9	−41.5	8
QM10	5/5	334.1	21.6	5.4	202	349.0	−50.4	8
QM11	6/8	330.5	24.5	4.0	356	342.0	−50.5	8
QM03	5/5	307.5	−21.0	5.8	172	4.6	−76.1	9
QM12	8/8	338.1	−17.3	3.1	329	22.2	−26.0	9
QM13	9/9	337.2	−19.9	2.7	372	43.7	−55.4	9
QM14	6/6	306.5	−18.2	3.7	325	58.9	−84.2	9
QM15	8/8	314.8	−21.7	3.4	273	58.5	−75.7	9
QM16	8/8	333.1	−3.8	4.2	173	13.9	−56.4	9
mean	18/18	350.1	−26.6	16.5	5			
				9.5	**14**	**15.6**	**−51.9**	
Paleocene: Cinchado Formation and related intrusives								
CF04	4/4	216.9	66.2	4.1	501	230.2	42.8	10
CF15	6/7	208.2	49.1	2.8	987	223.2	36.8	10
CF02	5/5	194.8	38.5	12.0	175	215.6	38.4	11
LC01	8/9	207.6	51.2	10.1	34	207.6	51.2	11
LC04	8/10	29.3	−52.3	5.7	100	29.3	−52.3	11
EI01	6/8	200.2	37.7	11.1	40	200.2	37.7	11
CF06	9/9	14.8	−72.2	6.2	70	43.9	−34.6	12
CF07	5/5	45.5	−56.4	3.9	376	48.6	−42.0	12
CF08	7/9	35.0	−51.3	3.6	275	22.6	−35.8	12
CF09	5/7	36.8	−40.0	11.3	47	23.7	−43.1	12
CF10	6/7	229.7	62.7	5.3	173	216.2	37.4	12
CF12	10/10	230.0	74.6	2.8	308	215.0	60.8	12
CF13	6/8	217.4	55.7	4.4	230	217.6	31.5	12
CC01	5/5	24.8	−46.1	8.1	104	24.8	−46.1	12
CF05	6/11	0.7	25.5	11.1	37	1.9	−29.1	13
LC02	4/6	181.5	40.6	8.5	117	181.5	40.6	13
CF17	6/6	198.8	53.3	4.3	248	211.8	43.5	14
CF18	5/7	193.5	67.1	5.5	298	217.8	41.6	14
CF16	9/10	15.3	−51.0	7.1	64	15.3	−51.0	
mean	19/19	24.5	−51.3	9.4	14			
				5.4	**39**	**29.8**	**−42.7**	
Oligocene–Miocene Tambores Formation								
TF01	9	178.7	33.1	n.d	n.d	178.7	33.1	
Oligocene–Miocene El Loa Formation								
LF01	17/21	352.7	−25.5	5.9	37.8	352.7	−25.5	
Jurassic: Caracoles Group								
CG01	7/8	44.2	−24.2	7.0	80	62.5	−31.4	
CG02	9/13	10.2	−44.5	8.6	37	12.8	−47.6	
Sifon ignimbrite								
SI01	10/10	358.3	17.7	2.9	286	358.3	17.7	
SI02	7/11	6.8	35.8	6.3	106	6.8	35.8	
SI03	9/12	3.8	35.6	16.2	13	3.8	35.6	

N/n: Number of samples used in the calculation of the mean direction/number of demagnetized samples. Dec, Inc: Mean declination and inclination in situ and after tilt correction. α95: Semiangle of 95% of confidence. k: Fisher's precision parameter.

[a]Rejected from the mean calculation.

Antofagasta region, show a well-defined single vector (ChRM) direction observed during thermal demagnetization in the temperature range 150–500°C (Figure 7). Although most of the magnetization is unblocked at temperatures lower than 550°C, low values of magnetic susceptibility (Table 1) and IRM acquisition suggest that magnetite is not plentiful in these rocks. For most samples, alternating field demagnetization up to 100 mT was inefficient in removing the characteristic magnetization. Hematite is thus the likely magnetic carrier of the ChRM.

[33] The characteristic directions are well grouped in in situ coordinates and show an increase in dispersion upon tilt correction (Table 2 and Figure 7e). That magnetic polarity is normal and especially that nearby volcanics belong to the mid-Cretaceous Paradero del Desierto Formation suggest

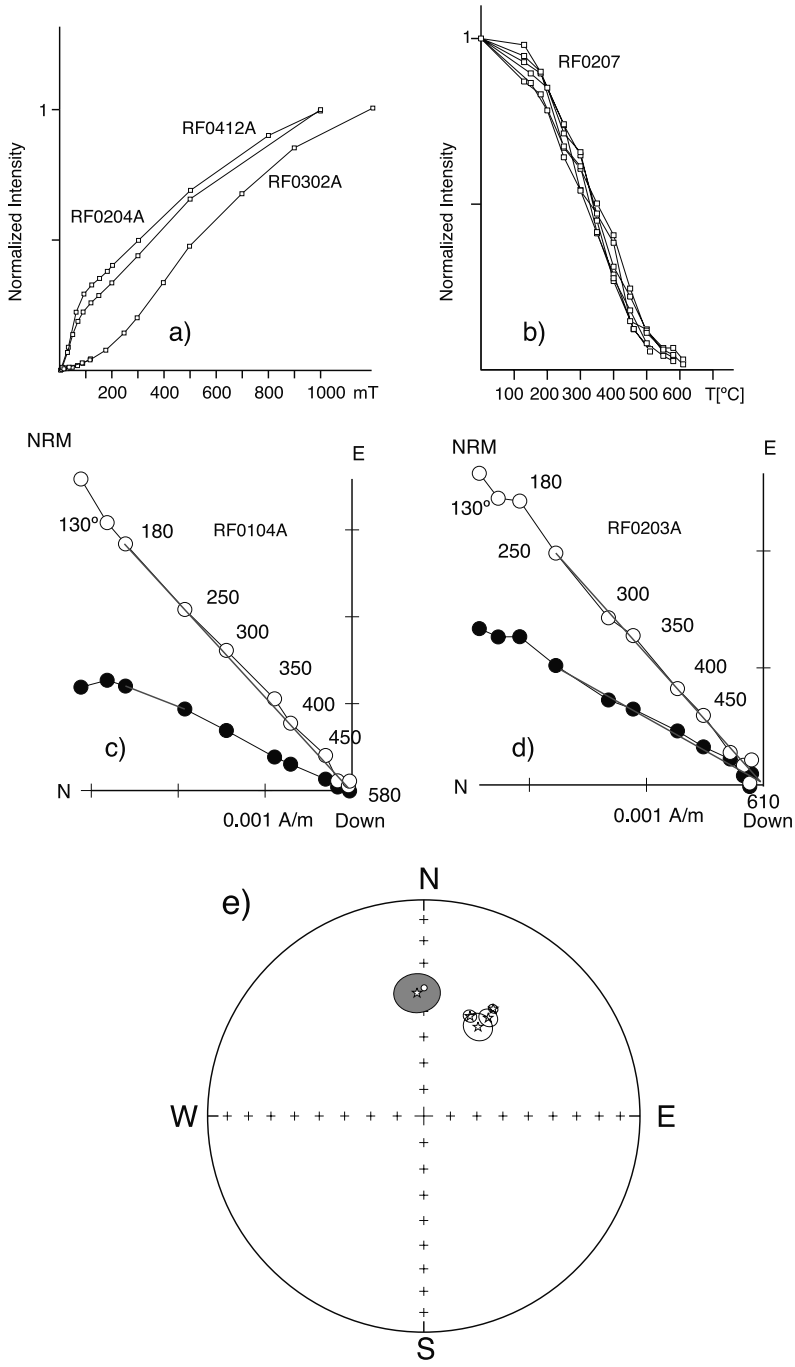

Figure 7. Magnetic properties of remagnetized Jurassic limestones. (a) Normalized isothermal remanent magnetizations (IRM) for three samples of three different sites show the existence of a high coercivity mineral. (b) Variation of the intensity of the NRM during thermal demagnetization for 6 samples of site RF02 demonstrate that the ChRM has unblocking temperatures between 150°C and 500°C. (c and d) Orthogonal projections (in situ) of thermal demagnetization diagrams. (e) Equal-area projection of site-mean characteristic directions in in-situ coordinates from Rencoret Formation (Table 2).

that remagnetization was acquired during emplacement of the Paradero del Desierto volcanics.

4.3. Paradero del Desierto Formation: Central Valley

4.3.1. Remagnetization

[34] East of Baquedano (sites PD13–PD16), a remagnetization is observed at 4 sites with different lithologies (PD13–PD16). These sites are a few hundred meters apart. In all samples a ChRM of normal polarity was observed in the temperature range 150–450°C (Figure 8). However, some samples yielded a reverse polarity component in a limited temperature range (470–610°C). In several samples, a normal polarity component of magnetization, similar to the one observed in the low unblocking temperature range, was observed above 610°C.

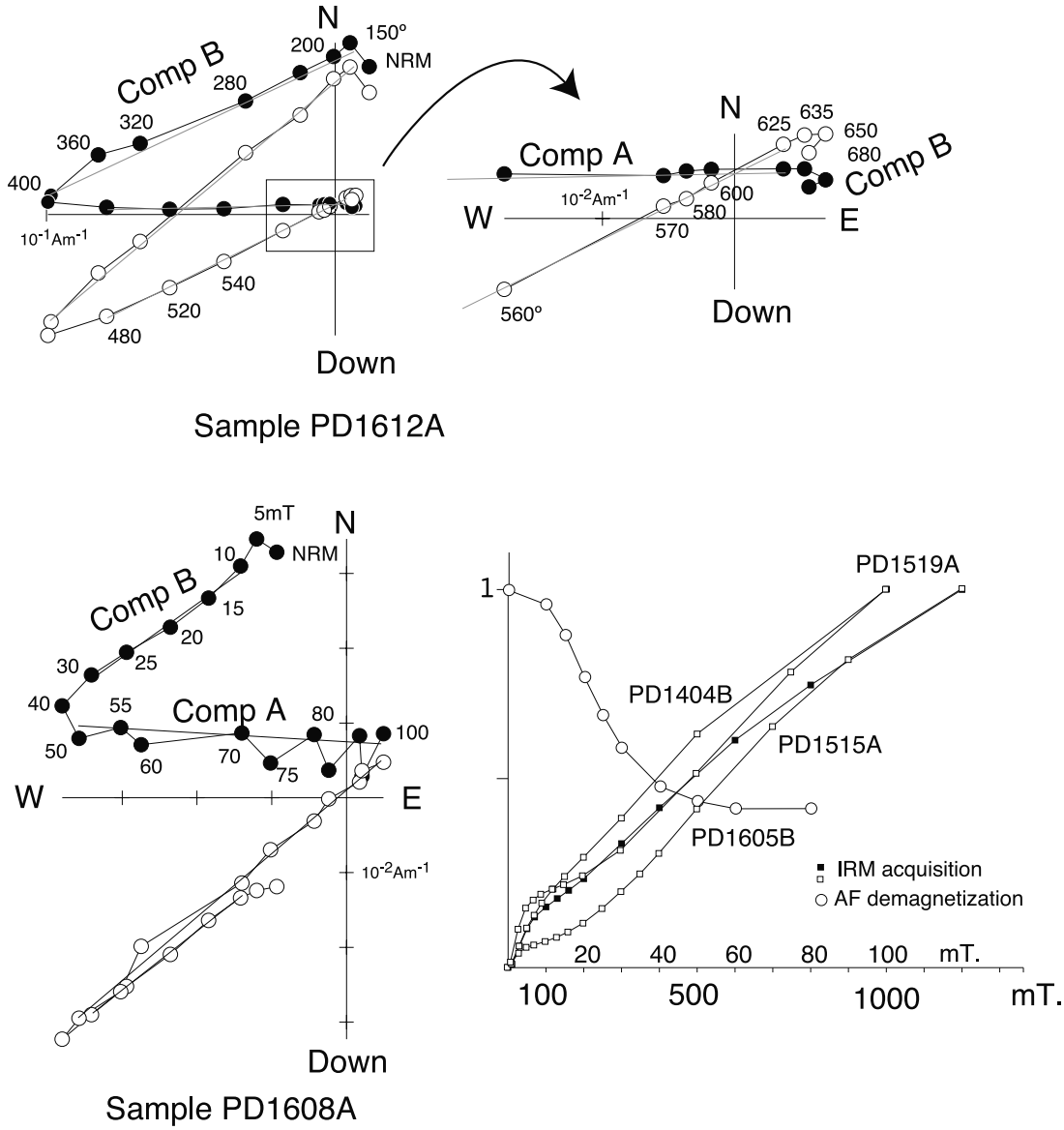

Figure 8. Orthogonal projections (tilt corrected) of thermal or AF demagnetization diagrams for remagnetized samples of Paradero del Desierto Formation. Normalized IRM acquisition and variation of intensity of the remanent magnetization during AF demagnetization (bottom right side). A normal component of magnetization (comp. B) is observed in the temperature range 150–400°C and at high temperatures above 650°C while a reverse component of magnetization (comp. A) is likely carried by magnetite.

[35] There is no evidence for low-grade metamorphism in these rocks but oxidation is widespread. Site PD14 is in lacustrine limestone with fractures filled by hematitic cement. IRM acquisition confirms the existence of hematite but the unblocking temperatures of the characteristic magnetization are widely distributed from 150°C up to 670°C.

[36] The remagnetized component with unblocking temperature higher than 620°C is carried by hematite, in agreement with the IRM acquisition curve (Figure 8). The magnetic carrier of the remagnetization in the temperature range 150–450°C is not well identified. This magnetization (150–450°C) is also partially demagnetized by AF and the carrier could be substituted stable maghemite. We did not encounter this remagnetization in the other sites sampled about 10 km further south. Thus this remagnetization is probably of local rather than regional extent. The steep inclination observed in in situ coordinates (−68° at site PD16) suggests that the remagnetization predates tilting in this area.

4.3.2. Primary Magnetizations

[37] For some sites in Cretaceous units (Paradero del Desierto Formation), a large decrease in susceptibility was observed during thermal demagnetization in the temperature range 250–350°C (Figures 9a and 9b). We attribute this behavior to the instability of maghemite during heating. In most cases, this magnetic phase does not carry a significant remanent magnetization (for example sample PD2105A in Figure 9d). The ChRM was easily recovered at higher temperatures and generally thermal demagnetization proved

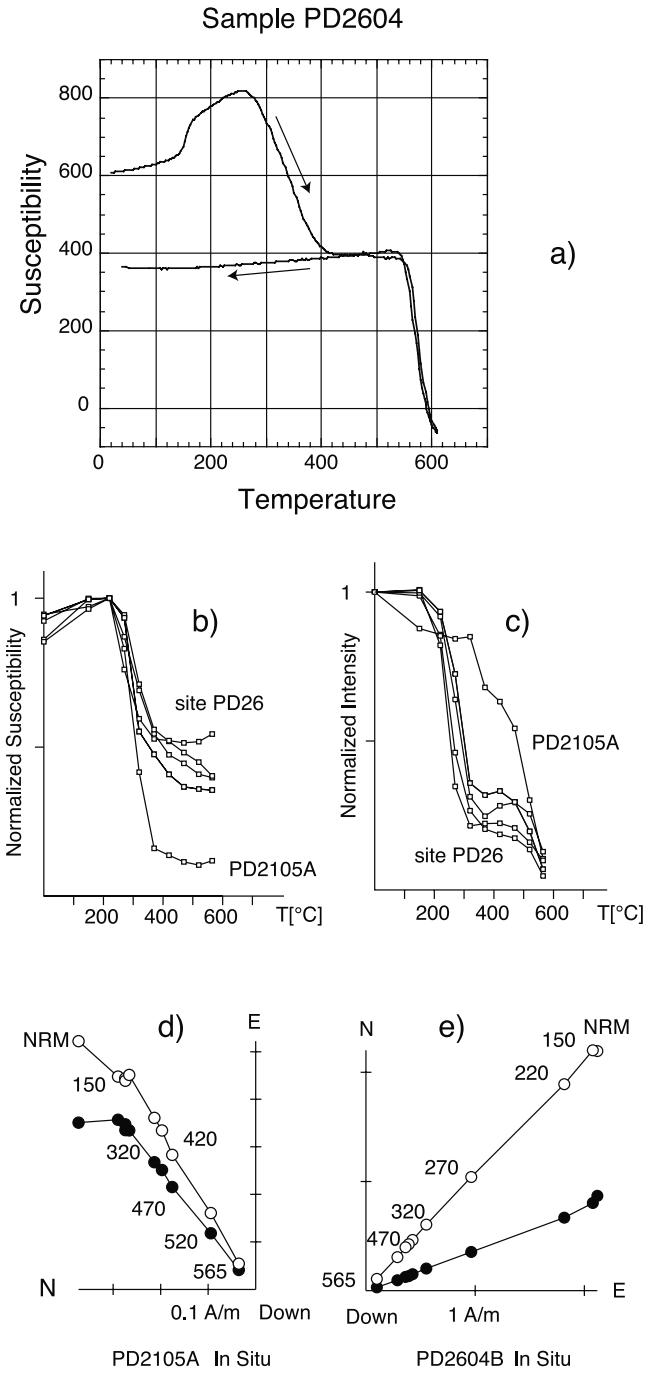

Figure 9. (a) Evidence for maghemite during K-T experiment for one sample of site PD26. During cooling, only magnetite can be identified. Measurements of magnetic susceptibility after each step of thermal demagnetization (b) demonstrate the destruction of a magnetic phase. This behavior is especially well defined for sample PD2105A in the temperature range 250–350°C. (c) The NRM is however not significantly destroyed during demagnetization below 350°C in contrast with the behavior of all samples from site PD26. (d) and (e) Orthogonal diagrams of thermal demagnetization showing well-defined univectorial ChRM.

to be more efficient in isolating ChRM than AF demagnetization. At one site (PD26), about 80% of the characteristic magnetization were unblocked at temperatures lower than 300°C (Figure 9c). Thermomagnetic experiments suggest that the low unblocking magnetic phase is maghemite. Although further magnetic studies are necessary to understand the effect of maghemitization in this site, the magnetization carried by the low temperature magnetic carrier is identical to the magnetization with unblocking temperature above 400°C. This well-defined ChRM (Figure 9e) is unambiguously different from the present-day field and is relevant to our tectonic study and likely pretectonic.

[38] At the other sites, most of the samples show univectorial (single vector) ChRM directions pointing to the

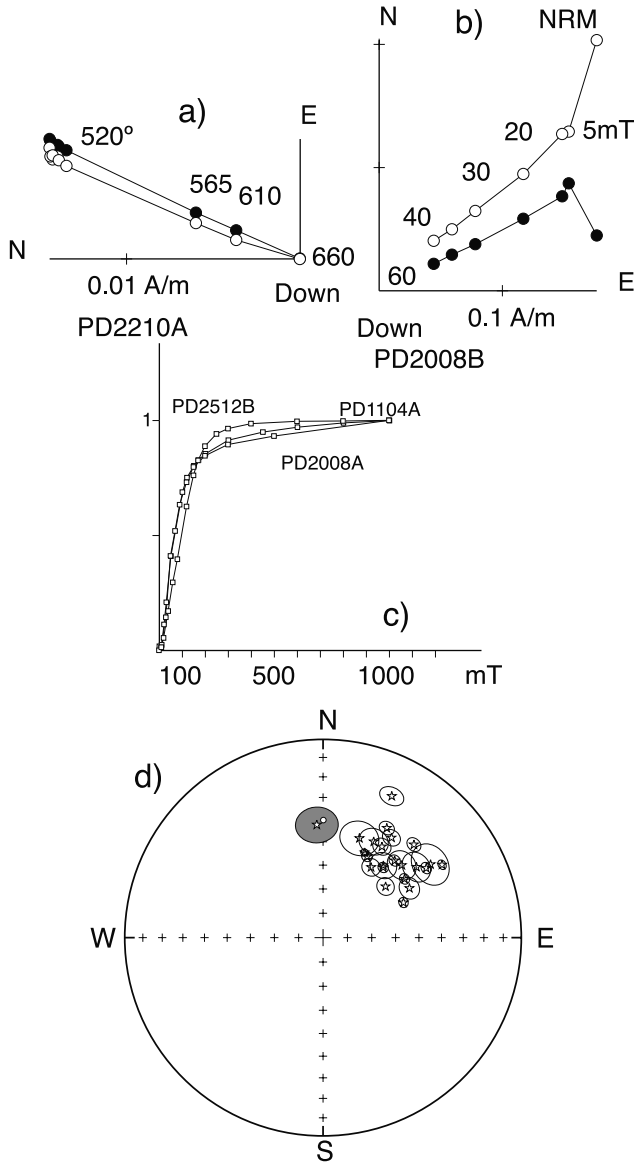

Figure 10. Orthogonal projections (in situ) of thermal (a) or AF (b) demagnetizations for samples of Paradero del Desierto Formation. (c) Normalized isothermal remanent magnetization (IRM). (d) Equal-area projection of site-mean characteristic directions in tilt corrected coordinates from Paradero del Desierto Formation. Same conventions as in Figure 6.

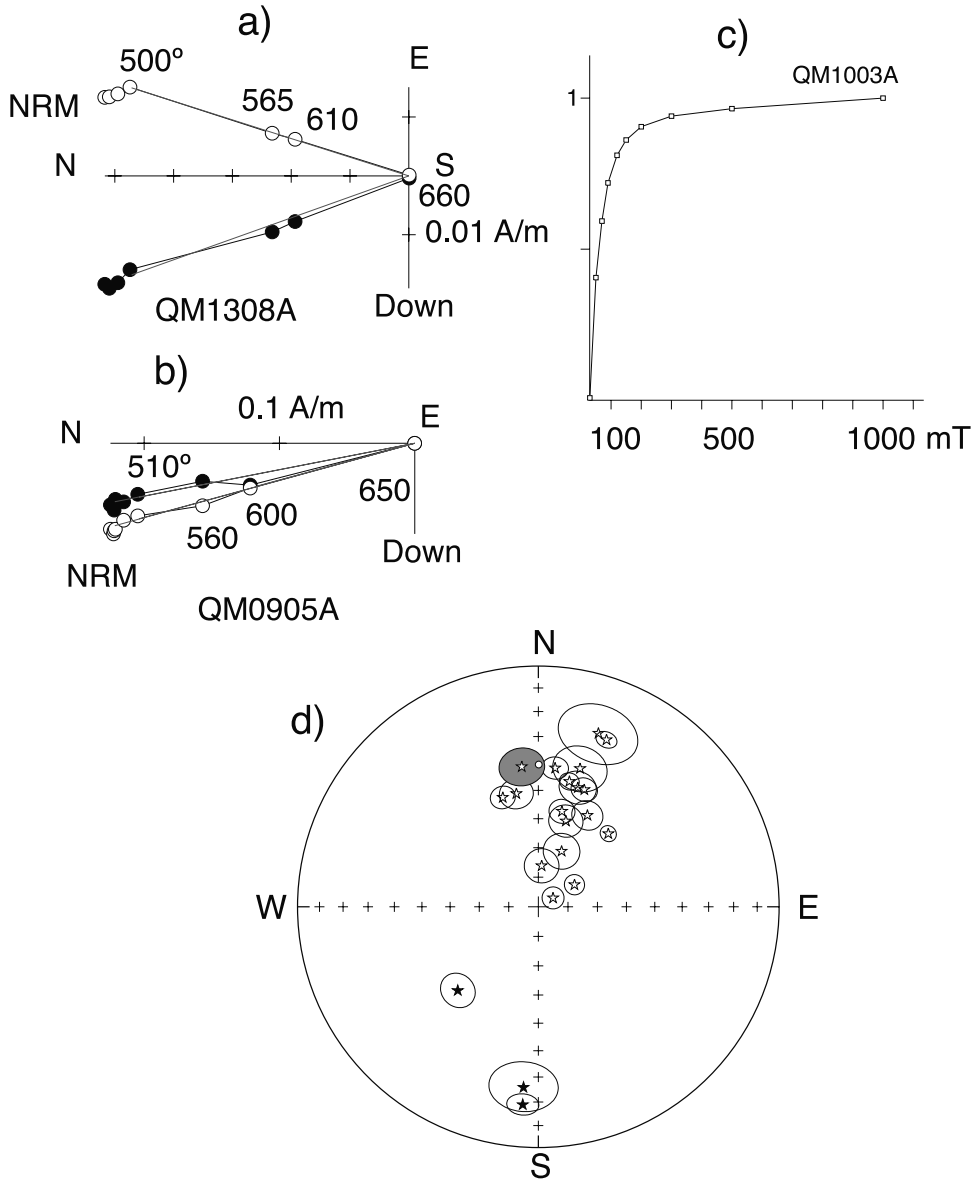

Figure 11. (a and b) Orthogonal projections (in situ) of thermal demagnetizations for samples of Quebrada Mala Formation. (c) Normalized isothermal remanent magnetization (IRM). (d) Equal-area projection of site-mean characteristic directions in tilt corrected coordinates from Quebrada Mala Formation.

origin during demagnetization (Figures 10a and 10b). Hematite and magnetite, in agreement with the IRM acquisition curve (Figures 10a and 10c) carry ChRM directions with unblocking temperatures up to 650°C.

[39] The ChRM directions were determined by least squares fit through the origin using demagnetization data in the temperature range 260–670°C.

[40] There is a slight decrease in dispersion upon tilt correction in the sites from Paradero del Desierto Formation, especially for the inclination (Figure 10d). The characteristic magnetization has a normal polarity in agreement with radiometric dating (unpublished data, SERNAGEOMIN Chile) suggesting that most of these volcanic rocks were emplaced during the long normal Cretaceous superchron.

[41] Sites (PD13–PD16) whose ChRM correspond to a remagnetization have high inclination in in situ coordinates (Table 2) and we believe that the magnetization is pretectonic. These results are included in the mean calculation for the Formation. Dispersion is relatively low (Figure 10d), especially for the inclination, supporting the hypothesis that secular variation of the geomagnetic field was lower during the Cretaceous long normal period [*McFadden et al.*, 1991; *Cronin et al.*, 2001]. The large deviations of the declinations from the expected direction provide evidence for large tectonic rotations.

4.4. Quebrada Mala Formation

[42] Most of the samples have univectorial ChRM directions (Figures 11a and 11b). Hematite and magnetite, in

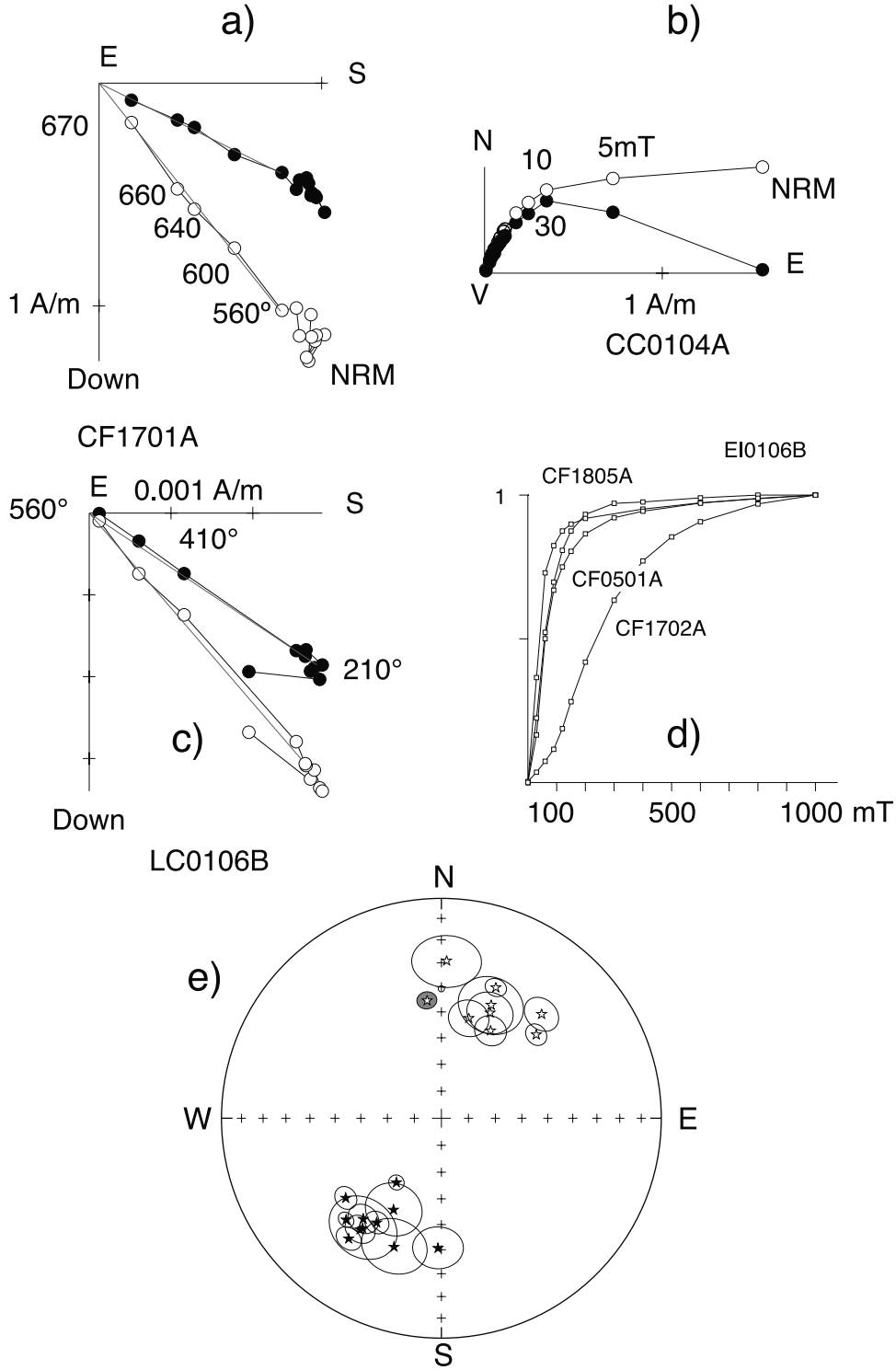

Figure 12. Paleomagnetic results in Paleogene rocks: (a–c) Orthogonal projections (in situ) of thermal or AF demagnetization. (d) Normalized isothermal remanent magnetization (IRM). (e) Equal-area projection of site-mean characteristic directions in tilt corrected coordinates.

agreement with the IRM acquisition curve (Figure 11) carry ChRM directions with unblocking temperatures up to 650°C.

[43] The ChRM directions were determined by least squares fit through the origin using demagnetization data in the temperature range 260–670°C.

[44] In most of volcanic rocks from Quebrada Mala Formation, the magnetizations are interpreted as primary, in agreement with the high dispersion of the characteristic mean-site directions in in situ coordinates (Table 2). Several sites from the Quebrada Mala Formation were taken from the Sierra del Buitre area where bedding attitude is often

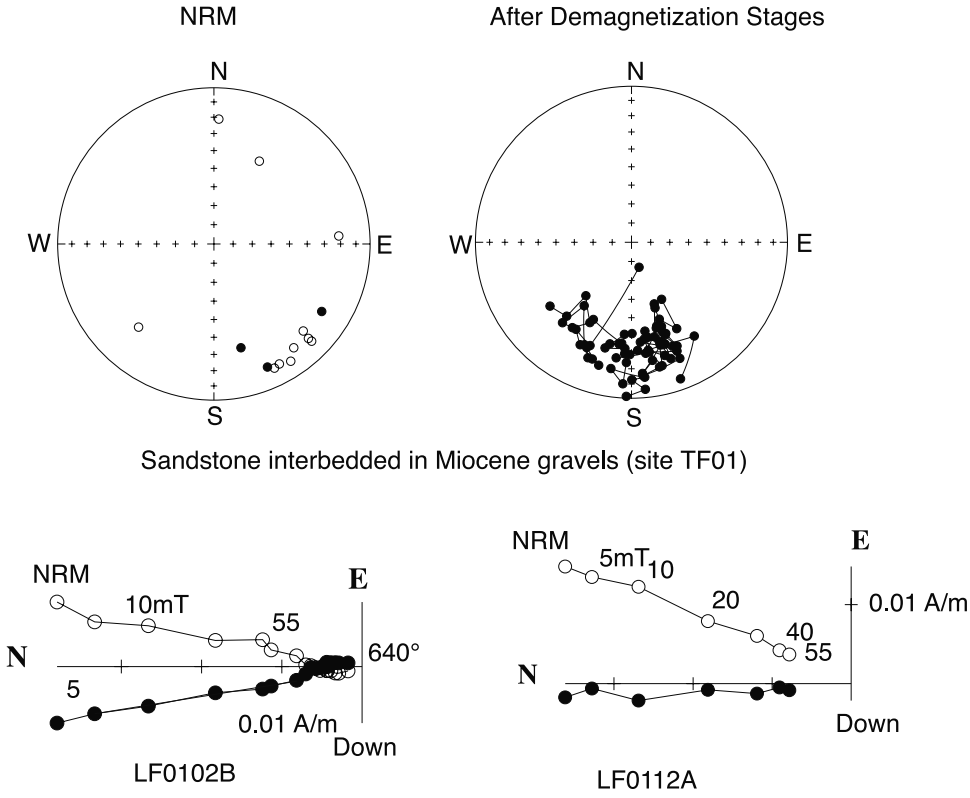

Figure 13. Top: Equal-area projection of NRM for samples of sandstone interbedded in Miocene gravels (left) and directions observed for 9 samples after each step of thermal demagnetization in the temperature range 310–640°C. Bottom: Orthogonal projections (in-situ) of thermal and AF demagnetizations for samples of the El Loa Formation. For sample LF0102B, thermal demagnetization was applied after AF demagnetization at 55 mT.

steep, in contrast with the gently folded area where we sampled the Paradero del Desierto volcanics. Sites with steep magnetic inclinations after bedding correction are in ignimbrites with steep bedding. However, the bedding attitude was determined using interbedded sediments and should not induce inclination errors. Dispersion decreases strongly upon tilt correction, giving a positive fold test (Figure 11d).

4.5. Cinchado Formation

[45] Interpretation of the demagnetization diagrams are in all cases straightforward (Figures 12a–12c). Again magnetite and hematite are the main magnetic carriers of the ChRM (Figure 12d). The reverse magnetization observed in the intrusive rock at site LC02, located nearby site CF05 where bedding dips at 60°, suggests that the intrusive rocks was not affected by the nearby deformation or postdates that deformation. In the Cinchado Formation and related intrusive rocks the observation of normal and reverse polarity magnetizations is in agreement with an Early Tertiary age for these rocks (Figure 12e). The reversal test is statistically positive. Dispersion of paleomagnetic directions decreases upon tilt correction but the fold test is inconclusive because of gentle bedding dips (Table 2 and Figure 12e). Large deviations of the observed declinations from the expected declination again are evidence for clockwise rotations.

4.6. Oligocene–Miocene Sedimentary Rocks

[46] In the Antofagasta region, it is very hard to find fine-grained upper Tertiary sediments. We have collected samples from one site (TF01) where semiconsolidated sediments are interbedded with coarse Atacama gravels (Table 1). Unfortunately, it was not possible to recognize a well-defined ChRM for this site. AF demagnetization up to 30 mT removes a secondary overprint. Thermal demagnetization following AF cleaning yields ChRM directions grouped around a reverse polarity direction (Figure 13).

[47] At the intersection of the El Loa River and the Panamericana road, we have collected 21 samples from subhorizontal, Cenozoic red siltstones of the El Loa Formation (LF01). These samples were first subjected to AF demagnetization and then to thermal demagnetization. A univectorial ChRM direction of normal polarity was observed during demagnetization up to 560°C (Figure 13).

4.7. Upper Miocene Sifón Ignimbrite

[48] Samples of the upper Miocene Sifón ignimbrite were collected at 3 sites (Table 1). The unusual positive inclination (Figure 14) recorded by the Sifón ignimbrite permits

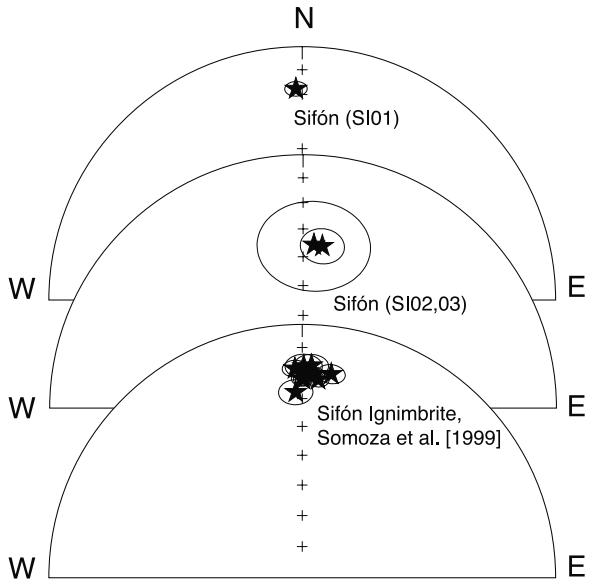

Figure 14. Equal-area projection of site-mean directions for sites of the Sifón Ignimbrite [*Somoza et al.*, 1999; this study].

straightforward paleomagnetic correlation between geographically dispersed sites. This unit is the most extensive ignimbrite in the study area of the Antofagasta region. It results from highly explosive volcanism around 8.3–8.4 Ma [*Naranjo et al.*, 1994; *Somoza et al.*, 1999; *Somoza and Tomlinson*, 2002]. Both AF and thermal demagnetization were successful in isolating a stable ChRM direction. For most of the samples the ChRM direction is univectorial. ChRM were generally demagnetized in the temperature range 210–660°C, or in the range 5–40 mT.

5. Tectonic Rotations Within the Antofagasta Region

[49] Tectonic rotations and inclination anomalies have been calculated from Mesozoic to Cenozoic units, using the estimated age of magnetization and the reference poles provided by *Besse and Courtillot* [2002]. The site-mean directions for each locality and the tectonic rotations and inclination errors are given in Table 3.

[50] Assuming that most sites in a same rock formation belong to a structural block, for which we can calculate a mean tectonic rotation (Table 3), we obtain the following results.

1. Tectonic rotations vary, from almost zero ($-2.2 \pm 13.3°$) in the coastal La Negra Volcanics, to $45.6 \pm 8.1°$ in the Paradero del Desierto volcanics.

2. There are no significant inclination errors, suggesting that changes in latitude cannot be determined paleomagnetically.

3. There is no correlation between age of rock formation and tectonic rotation.

[51] However, sites from the Paradero del Desierto and Cinchado formations show greater variations in declination than in inclination, in contrast to what is expected for the secular variation of the Earth's magnetic field at this latitude. We believe that part of the between-site dispersion is due to relative tectonic rotations. Better to understand spatial variations in tectonic rotations, 16 localities were defined (Table 3 and Figures 4, 5, and 15). Criteria used in defining the localities are (1) sites are within a homogeneous structural block and (2) the magnetization has the same age for all the sites within the locality. The number of sites characterizing the localities is variable and 5 localities out of 16 are defined with only 2 sites (Figures 4 and 5).

[52] In the locality 1 the in situ ChRM direction found at these four sites of the Rencoret Formation is similar to the tilt-corrected direction found at sites PD18 and PD19 of the Paradero del Desierto Formation located about 10 km to the NE of the remagnetized area. The mean direction for the locality corresponds to the four in situ directions in limestone sites and the other two tilt-corrected directions. The ChRM acquisition age probably reflects the mid-Cretaceous age of the Paradero del Desierto Formation. A clockwise rotation of about 32° is inferred for this locality. For localities 2, 3, and 4 the average direction, after tilt correction, shows large clockwise rotations, from about 37° up to about 50° at two localities. As in locality 1, the inclination error is small.

[53] At localities 6–9 of the Quebrada Mala Formation the rotations are not so well defined because of the higher scatter possibly induced by a poor averaging of secular variation. However, rotations are again clockwise, varying from 4.6° to 35.0°.

[54] Clockwise rotations in the localities 10–14 of the Cinchado Formation vary from 8.6° up to 53.3°. However, the smallest rotation is only defined by 2 sites at locality 13. Rotations are larger than 30° at 4 localities out of 5 within the Paleocene arc.

[55] As discussed before, in the volcanics rocks of the La Negra Formation (Localities 15 and 16) high secular variation was inferred from the paleomagnetic data. For this reason, the tectonic parameters have greater uncertainties than those observed at other localities. It is however interesting to note that both localities (Tocopilla and Antofagasta) do not show evidence for significant rotations.

6. Discussion

6.1. Timing of Rotations

[56] The Andes of northern Chile have registered several events of deformation through time since the early Mesozoic. The tectonic rotations observed in the Antofagasta region could be the result of one or several episodes of deformation.

6.1.1. Maximum Age of Rotations

[57] A close inspection of Table 3 and Figure 15 shows that whatever the magnetization age or the sequence ages, rotations in Jurassic and mid-Cretaceous sequences (Rencoret and Paradero del Desierto formations) are not systematically larger than those in Late Cretaceous–Paleocene units. This could suggest that no rotations occurred before Paleocene time. However, Cenozoic and Mesozoic units are in general not found within the same block because of the eastward shift with time of the volcanic arc. Thus we cannot reject the hypothesis that rotations observed in Cretaceous units occurred prior to the emplacement of the Cinchado Formation.

Table 3. Tectonic Rotations

Lat	Long	Decl	Inc	α95	R	ΔR	F	ΔF	Area	Age (Ma)
−22.2	−70.2	9.1	−39.2	12.0	−2.2	13.3	3.0	11.2	La Negra	180
−23.3	−69.8	30.7	−45.9	5.6	34.1	8.7	−3.5	8.4	Rencoret	100
−23.3	−69.8	42.2	−44.6	5.0	45.6	8.1	−2.2	8.1	Paradero	100
−23.2	−69.4	15.6	−51.9	9.5	22.5	13.4	−10.8	9.9	Q. Mala	80
−23.1	−69.2	29.8	−42.7	5.4	36.6	6.4	2.3	5.1	Cinchado	60
−23.6	−69.8	28.4	−45.6	4.0	31.8	7.5	−2.9	7.7	1	100
−23.5	−69.8	45.2	−44.6	10.2	48.6	12.9	−2.0	10.8	2	100
−23.3	−69.8	49.2	−39.7	6.9	52.6	9.3	2.7	9.0	3	100
−23.2	−69.6	33.3	−50.2	9.5	36.6	13.3	−7.9	10.4	4	100
−23.8	−69.6	18.8	−35.7	–	22.1	–	6.8	–	5	80
−23.5	−69.5	23.3	−57.0	–	30.2	–	−15.6	–	6	80
−23.2	−69.5	14.3	−35.9	24.1	21.2	24.8	5.2	20.3	7	80
−23.2	−69.4	357.7	−53.8	17.7	4.6	25.3	−12.7	15.5	8	80
−23.1	−69.2	28.2	−63.6	19.3	35.0	38.8	−22.7	16.7	9	80
−23.2	−69.0	46.5	−39.9	–	53.3	–	5.2	–	10	60
−23.1	−69.2	28.1	−45.0	10.5	34.9	12.2	0.0	8.9	11	60
−23.4	−69.2	34.2	−41.7	8.1	41.1	9.1	3.6	7.0	12	60
−23.2	−69.2	1.7	−34.8	–	8.6	–	10.4	–	13	60
−23.0	−69.0	34.8	−42.6	–	41.6	–	2.3	–	14	60
−22.2	−70.2	5.6	−38.3	20.4	−5.7	21.6	3.9	17.3	15	180
−23.7	−70.4	17.3	−45.9	19.9	5.9	23.9	−1.7	16.8	16	180
−23.7	−70.4	9.0	−25.0	7.0	12.4	6.5	11.4	6.2	[a]	120
−23.7	−70.4	26.0	−34.0	8.0	29.4	8.0	2.4	6.9	[b]	120
−22.7	−68.3	41.0	−36.0	9.0	47.8	10.3	4.5	9.7	[c]	80
−23.3	−69.7	53.2	−37.9	8.3	60.1	8.8	7.3	7.2	a	60
−23.3	−68.8	59.8	−35.3	14.9	66.6	–	10.0	–	b	60
−23.2	−68.6	37.0	−39.8	11.7	43.8	12.5	5.4	9.8	c	60
−23.2	−68.6	36.6	−39.0	10.6	39.9	12.4	3.3	11.0	d	100
−23.2	−68.6	15.6	−41.0	16.7	22.4	18.6	0.1	14.8	e	80
−23.1	−68.5	7.9	−46.2	20.7	14.7	25.1	−5.2	17.7	f	80
−23.0	−68.5	19.6	−38.4	10.5	22.9	12.3	3.7	11.0	g	100
−22.8	−68.2	−3.1	−43.0	12.0	3.7	14.2	−2.3	11.5	h	80
−22.8	−68.5	12.4	−37.0	15.3	19.2	16.3	3.6	13.8	i	80
−22.2	−68.2	359.9	−38.9	6.4	2.1	7.0	6.8	5.8	j	20
−22.4	−68.1	6.2	−38.0	6.7	8.7	7.6	9.1	6.5	k	30
−22.3	−68.3	31.4	−36.9	4.3	34.7	7.3	4.2	8.0	L	100
−23.4	−70.1	41.0	−44.8	7.9	43.4	10.4	−6.0	9.4	M	150

Lat–Long: Position of the localities used in the calculation of the tectonic parameters. R± ΔR, F± ΔF: rotation and flattening parameters and their associated errors [*Demarest*, 1983]. Localities 1–16 [this study]. Localities a–i [*Arriagada et al.*, 2000]. Localities j (El Loa Fm.), k (San Pedro Fm.), and L (Purilactis Fm.) [*Somoza and Tomlinson*, 2002]. Locality M: Mantos Blancos ore body [*Tassara et al.*, 2000]. Age Ma: is the reference pole used to calculate the rotation [*Besse and Courtillot*, 2002]. 20 Ma: 84.7°, 133.8°, α_{95} = 2.7; 30 Ma: 83.7°, 132.6°, α_{95} = 3.8; 60 Ma: 82.9°, 170.4°, α_{95} = 2.8; 80 Ma: 83.7°, 196.2°, α_{95} = 5.9; 100 Ma: 86.7°, 177.9°, α_{95} = 6.7; 120 Ma: 85.3°, 247.1°, α_{95} = 2.3; 150 Ma: 87.3°, 232.7°, α_{95} = 6.2; 180 Ma: 79.4°, 33.9°, α_{95} = 5.4.

[a]Coloso Area [*Tanaka et al.*, 1988].

[b]Coloso Area [*Turner et al.*, 1984].

[c]Purilactis Fm. [*Hartley et al.*, 1992].

[58] If there was only one event of rotation (for all the area), paleomagnetic results obtained in Paleocene volcanic rocks of the Cinchado Formation constrain the maximum possible age of rotation to be Paleocene. This observation is also supported by results obtained along the eastern border of the Domeyko Cordillera in Upper Cretaceous–Paleocene volcanic rocks of the Purilactis Group [*Arriagada et al.*, 2000]. Further south in the Copiapo–Vallenar area, *Gibson et al.* [2001] also found similar large clockwise rotations in Mesozoic coastal intrusives rocks and in lower Tertiary volcanic rocks. This observation suggests that most rotations along the Chilean margin could have occurred during the Early Tertiary.

6.1.2. Minimum Age of Rotation

[59] Unfortunately, most of the Oligocene and Neogene rocks within our study area are conglomerates, which are inappropriate for paleomagnetic studies. Our best result comes from Oligocene to Miocene fine-grained sediments within the Loa basin (Figure 2) where there is no evidence for clockwise rotation (Table 2). The other evidence for lack of rotation was obtained within a 2 m thick sandstone interbedded in Neogene conglomerates but this result can only be seen as tentative, because of the poor paleomagnetic data observed for that site. Our results support the hypothesis of *Somoza and Tomlinson* [2002] that the whole area did not rotate during the Neogene.

[60] Results of *Somoza et al.* [1999] come from Miocene sedimentary rocks from the Calama basin covered by the Sifón Ignimbrite. The ca. 8 Ma Sifón Ignimbrite [*Naranjo et al.*, 1994] recorded an anomalous paleomagnetic direction with a positive inclination probably associated with a polarity transition or excursion of the geomagnetic field. Paleomagnetic correlations between different sites are straightforward because this paleomagnetic direction is most probably associated with a unique volcanic event. Paleomagnetic results from several sites in the Sifón Ignimbrite within the Calama area [*Somoza et al.*, 1999] show no significant relative rotations between sites. We took 3 sites in the same Sifón Ignimbrite, two of them

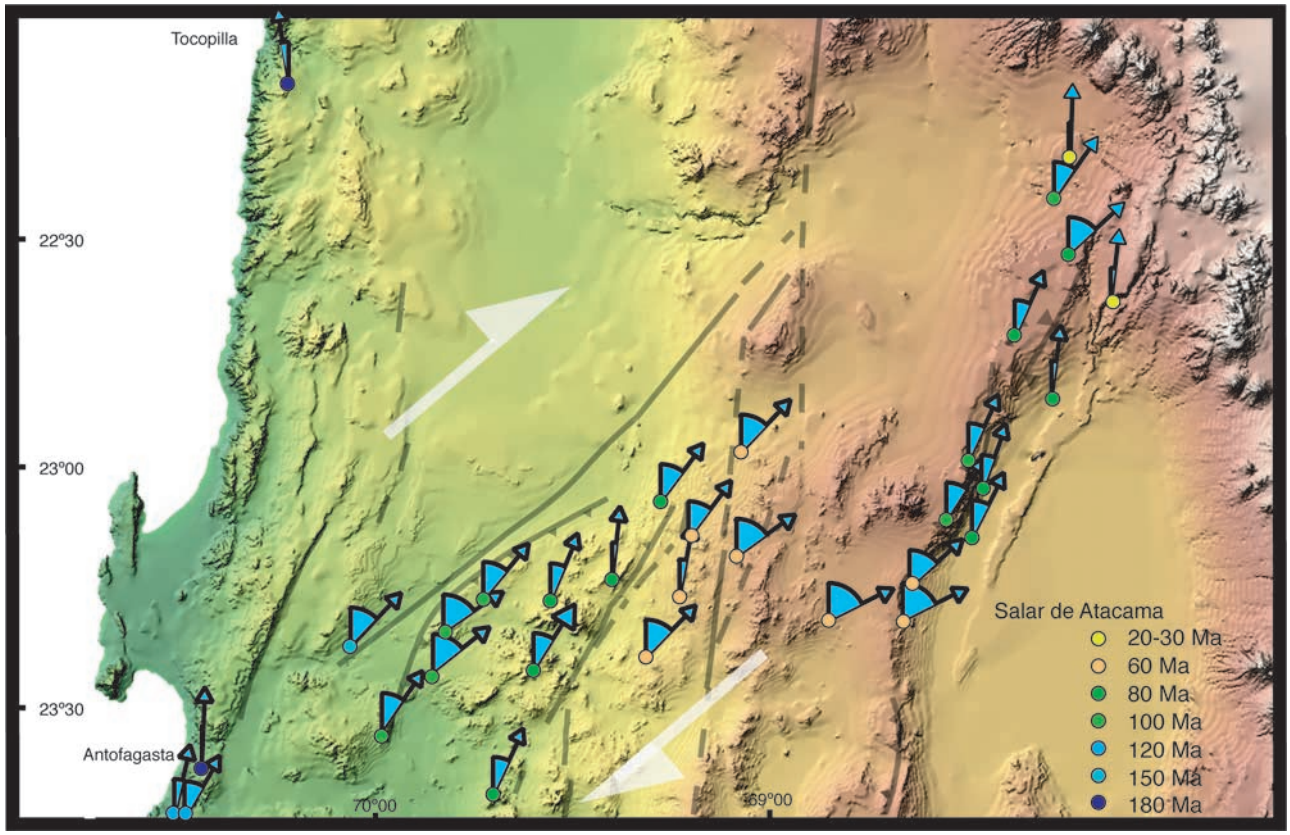

Figure 15. Tectonic rotations (deviations of arrows from a NS direction) and main structural features shown by a digital elevation model for the Antofagasta region. Colored circles are showing the age of the magnetization.

being about 50–80 km to the SW of the area sampled by *Somoza et al.* [1999]. Our results for the Sifón Ignimbrite (sites SI01–SI03, Figure 14) are very close to the direction determined by *Somoza et al.* [1999]. No internal block rotations or deformations occurred in this region of northern Chile since the emplacement of the Sifón Ignimbrite in the late Miocene.

6.2. Relation Between Tectonic Rotations and Regional Structural Pattern

[61] The mean rotation for all localities (including those previously published for the Antofagasta region listed in Table 3) in Mesozoic and Paleocene rocks is 30.8 ± 17.9°, whereas there is no inclination error (Flattening = 0.6 ± 7.6°). As discussed before, the lack of inclination error demonstrates the accuracy of the reference SA APWP used to calculate the tectonic parameters. Also, the low standard deviation associated with inclination error demonstrates that secular variation is roughly canceled at each locality, despite the small number of sites at some places. The variation in magnitude of the rotations from about 0° up to 65° with a standard deviation of about 18° around the mean is thus principally due to local tectonic effects.

[62] The variations in the amount of tectonic rotation indicate that this part of the northern Chilean Andes did not behave as a single rigid block prior to the Neogene and that there is a significant component of in situ block rotations. However, it is not easy to discard the hypothesis that there is a "hidden" component of regional rotation upon which a variable local component is superimposed.

[63] Tectonic rotations along the central Andes form a well-defined pattern of counterclockwise rotations north of the Arica elbow and clockwise rotations farther south. Several authors have suggested that the rotations may be due to oroclinal bending, associated with uplift of the Altiplano–Puna plateau [*Butler et al.*, 1995; *MacFadden et al.*, 1995]. *Coutand et al.* [1999] and *Roperch et al.* [2000] have suggested that rotations in the Altiplano–Puna plateau correlate with the trends of the main tectonic structures and occurred during the Miocene. Our results from Cenozoic semiconsolidated sediments and the Miocene Sifón Ignimbrite, are compatible with previous results from Miocene ignimbrites along the forearc [*Roperch et al.*, 2000] and from Miocene sediments from the Calama basin [*Somoza et al.*, 1999; *Somoza and Tomlinson*, 2002], which show no evidence of rotation. Therefore, any late Neogene bending leading to the development of the Bolivian orocline did not affect the forearc and the formation of the Altiplano–Puna plateau during the Neogene cannot be explained by bending of the whole margin. Instead, we believe that the forearc could have acted as a translating rigid block, which indented the Altiplano during Neogene times without rotating.

[64] A component of oroclinal bending prior to the Neogene possibly occurred in southern Peru [*Roperch and Carlier*, 1992; *Macedo Sanchez et al.*, 1992] but a bending

of the whole Chilean forearc through about 30° seems unrealistic.

[65] Although further paleomagnetic studies are required, to better define the timing and the regional extent of tectonic rotations, the results so far point to a heterogeneous pattern of rotations, where large values concentrate in small areas. This contrasts with the idea of a uniform rotation of the whole northern forearc. According to the plate convergence vectors published by *Pardo-Casas and Molnar* [1987], NNE directed convergence in northern Chile during the Eocene should result in NS dextral transpression along the margin. However, field evidence in the Cordillera de Domeyko is for left-lateral displacements during the Eocene [*Mpodozis et al.*, 1993; *Tomlinson et al.*, 1994]. To explain the strike-slip displacements opposite to the sense predicted by plate convergence models, *Arriagada et al.* [2000] suggested that distributed shear was driven by oblique convergence and that shear traction at the base of the brittle crust played a major role in driving the rotations [*Yañez et al.*, 1994; *Beck*, 1998; *Bourne et al.*, 1998].

[66] Field observations indicate that the strike-slip movements were accompanied by large E-W shortening and regional uplift leading to a rapid unroofing of the Cordillera de Domeyko [*Alpers and Brimhall*, 1988; *Maksaev and Zentilli*, 1999]. A secondary component of oblique strike-slip displacement probably existed in transfer zones, accommodating variations in the amount of EW shortening along the orogen. Within this framework, we suggest that during the Incaic event, due to differential E-W shortening, major NNE-NE shear zones developed. Structures like the ''Lineamiento Antofagasta–Calama,'' Sierra del Buitre Fault, the NNE-SSW curvature of the Atacama Fault Zone, are likely manifestations of this event (see Figures 2, 4, 5, and 15). There is no direct evidence that the postulated major structure ''Lineamiento Antofagasta–Calama'' along the main road between Antofagasta and Calama corresponds to a major dextral shear zone. However, gravity data [*Götze and the Migra Group*, 1996] suggest that the eastern border of the Coastal Cordillera is significantly displaced to the east, north of the ''Lineamiento Antofagasta–Calama.'' We can also observe that the axis of the Cretaceous magmatic arc is also shifted toward the east near Calama. Dextral transpression along the ''Lineamiento Antofagasta–Calama'' could explain the apparent difference in the location of the Mesozoic units north and south of this NE oriented structure and the widespread occurrence of large clockwise rotations. Our interpretation will require checking by means of detailed structural studies, notably of fault displacements and their timing.

7. Conclusions

[67] We have obtained satisfactory paleomagnetic results from a study of 108 sites from sediments, volcanics and intrusive rock of Mesozoic to Cenozoic age, in the forearc of the central Andes in northern Chile.

[68] The average paleomagnetic inclination recorded by upper Mesozoic and lower Tertiary volcanic rocks from the study area are in good agreement with the expected inclination determined from the BC01 APWP. These results indicate that changes in latitude along the Andean forearc are not significant enough to be determined by paleomagnetic techniques. The lack of inclination errors in volcanic rocks and remagnetized sediments contrasts with the large inclination shallowing observed in upper Tertiary red beds from the Altiplano and the Puna [*Coutand et al.*, 1999; *Roperch et al.*, 1999, 2000]. Paleomagnetic results from the Andes, where relative latitudinal displacements are small, demonstrate that inclination shallowing in red beds is strong and was acquired during deposition and further compaction.

[69] Vertical axis rotations, calculated from paleomagnetic declinations, are clockwise and up to 65° in the Antofagasta region. Although the age of the rotations in this area is difficult to constrain accurately, available stratigraphic, radiometric and structural data suggest that deformation and rotations occurred during the Paleogene and probably during the Incaic orogenic event. No evidence for Neogene tectonic rotation can be found in the Chilean forearc (in the study area) suggesting that the development of the Bolivian orocline during the late Neogene and the formation of the Altiplano–Puna plateau cannot be explained by simple bending of the whole margin. We believe that the forearc acted as a translating rigid block during Neogene development of the Altiplano–Puna plateau.

[70] Traditionally, structural studies in the forearc of northern Chile have emphasized motions along major N-S fault systems (i.e., the AFS and the DFS), along which deformation is assumed to be localized. A major result of our paleomagnetic study is that widespread tectonic rotations are not closely related to these faults. Instead Paleogene deformation is much more distributed across the forearc than it was previously thought. Most fold axes and thrusts are not oriented N-S but are significantly trending to the NE (for example, Sierra del Buitre fault, Los Toros fault). We speculate that these structures are indeed rotated.

[71] Large rotations are found not only in our study area but widely spread along the Andean margin. They are clockwise along the Ecuadorian margin [*Roperch et al.*, 1987], the northern Peruvian Andes [*Mourier et al.*, 1988; *Mitouard et al.*, 1992], the Chilean forearc [*Riley et al.*, 1993; *Randall and Taylor*, 1996; *Randall et al.*, 2001; this study] and counterclockwise in central Peru and southern Peru [*Roperch and Carlier*, 1992; *Macedo Sanchez et al.*, 1992]. Tectonic rotations are indeed one of the principal structural characteristics of the Early Tertiary evolution of the Andes.

[72] **Acknowledgments.** The Institut de Recherche pour le Développement (IRD) and CONICYT (FONDECYT projects 1970002 and 199009 and student scholarship to the first author) funded most of this work. The authors thank Mathilde Basso, Pierre Gautier, Nicolas Marinovic, Andres Tassara, and Andy Tomlinson for discussions about the structural evolution of the forearc. Sampling of the La Negra Volcanics was done with the help of Gabriel Carlier and Martine Gérard. Andres Tassara and Luisa Pinto participated in one field trip and in laboratory data acquisition. Part of the paleomagnetic data processing was performed with the excellent ''Paleomac'' software written by Jean-Pascal Cogné. We thank Randall D. Forsythe and Ruben Somoza for constructive reviews.

References

Alpers, C. N., and G. H. Brimhall, Middle Miocene climatic change in the Atacama Desert, northern Chile: Evidence from supergene mineralization at La Escondida with Suppl. Data 88-21, *Geol. Soc. Am. Bull.*, *100*(3), 1640–1656, 1988.

Arriagada, C., P. Roperch, and C. Mpodozis, Clockwise block rotations along the eastern border of the Cordillera de Domeyko, Northern Chile (22°45′–23°30′S), *Tectonophysics*, *326*, 153–171, 2000.

Aubry, L., P. Roperch, M. de Urreiztieta, E. Rosello, and A. Chauvin, Paleomagnetic study along the southeastern edge of the Altiplano–Puna Plateau: Neogene tectonic rotations, *J. Geophys. Res.*, *101*, 17,883–17,899, 1996.

Beck, M. E., Jr., Tectonic rotations on the leading edge of South America: The Bolivian orocline revisited, *Geology*, *15*, 806–808, 1987.

Beck, M. E., Jr., Analysis of Late Jurassic–Recent paleomagnetic data from active plate margins of South America, *J. S. Am. Earth Sci.*, *1*, 39–52, 1988.

Beck, M. E., Jr., On the mechanism of crustal block rotations in the central Andes, *Tectonophysics*, *299*, 75–92, 1998.

Beck, M. E., Jr., Jurassic and Cretaceous apparent polar wander relative to South America: Some tectonic implications, *J. Geophys. Res.*, *104*, 5063–5067, 1999.

Besse, J., and V. Courtillot, Revised and synthetic apparent polar wander paths of the African, Eurasian, North American and Indian plates, and true polar wander since 200 Ma, *J. Geophys. Res.*, *96*, 4029–4050, 1991.

Besse, J., and V. Courtillot, Apparent and true polar wander and the geometry of the Geomagnetic Field in the last 200 million years, *J. Geophys. Res.*, *107*(B11), 2300, doi:10.1029/2000JB000050, 2002.

Boric, R., F. Diaz, and V. Maksaev, Geologia y yacimientos metaliferos de la region de Antofogasta, *Bol. Inst. Invest. Geol. Chile*, *40*(246), 2, 1990.

Bourne, S. J., P. C. England, and B. Parsons, The motion of crustal blocks driven by flow of the lower lithosphere and implications for slip rates of continental strike-slip faults, *Nature*, *391*, 655–659, 1998.

Butler, R. F., D. R. Richards, T. Sempere, and L. G. Marshall, Paleomagnetic determinations of vertical-axis tectonic rotations from Late Cretaceous and Paleocene strata of Bolivia, *Geology*, *23*, 799–802, 1995.

Carey, S. W., A tectonic approach to continental drift, in *Continental Drift: A Symposium*, edited by S. W. Carey, pp. 177–355, Geol. Dep., Univ. of Tasmania, Hobart, 1958.

Charrier, R., and K.-J. Reutter, The Purilactis Group of Northern Chile: Boundary between arc and backarc from Late Cretaceous to Eocene, in *Tectonics of the Southern Central Andes*, edited by K.-J. Reutter et al., pp. 189–201, Springer-Verlag, New York, 1994.

Coira, B., J. Davidson, C. Mpodozis, and V. A. Ramos, Tectonic and magmatic evolution of the Andes of northern Argentina and Chile, *Earth Sci. Rev.*, *18*, 303–332, 1982.

Cornejo, P., R. Tosdal, C. Mpodozis, A. J. Tomlinson, and O. Rivera, El Salvador porphyry copper revisited: Geologic and geochronologic framework, *Int. Geol. Rev.*, *39*, 22–54, 1997.

Cortés, J., *Hoja Palestina, Región de Antofagasta*, Serv. Nac. Geol. Min., Santiago, 2000.

Coutand, I., P. Roperch, A. Chauvin, P. R. Cobbold, and P. Gautier, Vertical axis rotations across the Puna plateau (northwestern Argentina) from paleomagnetic analysis of Cretaceous and Cenozoic rocks, *J. Geophys. Res.*, *104*, 22,965–22,984, 1999.

Cronin, M., L. Tauxe, C. Constable, P. Selkin, and T. Pick, Noise in the quiet zone, *Earth Planet. Sci. Lett.*, *190*, 13–30, 2001.

Demarest, H. H., Error analysis for the determination of tectonic rotation from paleomagnetic data, *J. Geophys. Res.*, *88*, 4321–4328, 1983.

Dilles, J. H., A. J. Tomlinson, M. Martin, and N. Blanco, El Abra and Fortuna Complexes: A porphyry copper batholith sinistrally displaced by the Falla Oeste, in *VIII Congr. Geológico Chileno, Antofagasta*, vol. 3, pp. 1883–1887, 1997.

Ernesto, M., I. G. Pacca, F. Y. Hiodo, and A. J. R. Nardy, Palaeomagnetism of the Mesozoic Serra Geral Formation, southern Brazil, *Phys. Earth Planet. Inter.*, *64*, 153–175, 1990.

Forsythe, R., and L. Chisholm, Paleomagnetic and structural constraints on rotations in the north Chilean coast ranges, *J. S. Am. Earth Sci.*, *7*, 279–294, 1994.

Gibson, M., G. K. Taylor, and J. Grocott, New paleomagnetic results and Ar–Ar geochronology from the Vallenar Region (29°S), N. Chile: Implications for the timing of rotations in the Andean forearc region, *Eos. Trans. AGU*, *82*(47), Fall Meet. Suppl., 2001.

Götze, H.-J., and the Migra Group, Group updates the gravity data base in the central Andes (20–29°S), *EOS Trans. AGU*, 1996. (Available as http://www.agu.org/eos_elec/95189e.html).

Grier, M. E., J. A. Salfity, and R. W. Allmendinger, Andean reactivation of the Cretaceous Salta rift, northwestern Argentina, *J. S. Am. Earth Sci.*, *4*, 351–372, 1991.

Grocott, J., M. Brown, R. D. Dallmeyer, G. K. Taylor, and P. I. Treloar, Mechanisms of continental growth in extensional arcs: An example from the Andean plate-boundary zone, *Geol. Boulder*, *22*, 391–394, 1994.

Hartley, A. J., E. J. Jolley, and P. Turner, Paleomagnetic evidence for rotation in the Precordillera of northern Chile: Structural constraints and implications for the evolution of the Andean forearc: Andean geodynamics, *Tectonophysics*, *205*, 49–64, 1992.

Heki, K., Y. Hamano, H. Kinoshita, A. Taira, and M. Kono, Paleomagnetic study of Cretaceous rocks of Peru, South America: Evidence for rotations of the Andes, *Tectonophysics*, *108*, 267–281, 1984.

Heki, K., Y. Hamano, M. Kono, and U. Tadahide, Palaeomagnetism of Neogene Ocros dyke swarm, the Peruvian Andes: Implication for the Bolivian orocline, *Geophys. J. R. Astron. Soc.*, *80*, 527–534, 1985.

Hervé, M., Movimiento sinistral en el Cretácico Inferior de la Zona de Falla de Atacama, Chile, *Rev. Geol. Chile*, *31*, 37–42, 1987.

Isacks, B. L., Uplift of the central Andean Plateau and bending of the Bolivian orocline, *J. Geophys. Res.*, *93*, 3211–3231, 1988.

Kirschvink, J. L., The least-squares line and plane and the analysis of paleomagnetic data, *Geophys. J. R. Astron. Soc.*, *62*, 699–718, 1980.

Lamb, S. H., and D. E. Randall, Deriving palaeomagnetic poles from independently assessed inclination and declination data: Implications for South American poles since 120 Ma, *Geophys. J. Int.*, *146*, 349–370, 2001.

Macedo Sanchez, O., J. Surmont, C. Kissel, and C. Laj, New temporal constraints on the rotation of the Peruvian central Andes obtained from paleomagnetism, *Geophys. Res. Lett.*, *19*(1), 1875–1878, 1992.

MacFadden, B. J., F. Anaya, and C. C. Swisher III, Neogene paleomagnetism and oroclinal bending of the central Andes of Bolivia, *J. Geophys. Res.*, *100*, 8153–8167, 1995.

Maksaev, V., and M. Zentilli, Fission track thermochronology of the Domeyko Cordillera, northern Chile: Implications for Andean tectonics and porphyry copper metallogenesis, *Explor. Min. Geol.*, *8*, 65–89, 1999.

Marinovic, N., and M. García, *Hoja Pampa Unión, Región de Antofagasta*, Serv. Nac. Geol. Min., Santiago, 1999.

May, S. R., and R. F. Butler, Paleomagnetism of the Puente Piedra Formation, central Peru, *Earth Planet. Sci. Lett.*, *72*, 205–218, 1985.

McFadden, P. L., and M. W. McElhinny, The combined analysis of remagnetization circles and direct observations in paleomagnetism, *Earth Planet. Sci. Lett.*, *87*, 161–172, 1988.

McFadden, P. L., R. T. Merrill, M. W. McElhinny, and S. Lee, Reversals of the Earth's magnetic field and temporal variations of the dynamo families, *J. Geophys. Res.*, *96*, 3923–3933, 1991.

Mitouard, P., C. Laj, T. Mourier, and C. Kissel, Paleomagnetic study of an arcuate fold belt developed on a marginal orogen: The Cajamarca deflection, northern Peru, *Earth Planet. Sci. Lett.*, *112*, 41–52, 1992.

Mourier, T., C. Laj, F. Mégard, P. Roperch, P. Mitouard, and F. Medrano, An accreted continental terrane in northwestern Peru, *Earth Planet. Sci. Lett.*, *88*, 182–192, 1988.

Mpodozis, C., and V. A. Ramos, The Andes of Chile and Argentina, in *Geology of the Andes and Its Relation to Hydrocarbon and Mineral Resources*, edited by G. E. Ericksen et al., pp. 59–90, Circum-Pac. Counc. for Energy and Min. Resour., Houston, Tex., 1990.

Mpodozis, C., N. Marinovic, and I. Smoje, Eocene left lateral strike slip faulting and clockwise block rotations in the Cordillera de Domeyko, west of Salar de Atacama, northern Chile, in *Second ISAG, Oxford, UK*, pp. 225–228, 1993.

Naranjo, J. A., C. F. Ramírez, and R. Paskoff, Morphostratigraphic evolution of the northwestern margin of the Salar de Atacama basin (23°S–68°W), *Rev. Geol. Chile*, *21*, 91–103, 1994.

Pardo-Casas, F., and P. Molnar, Relative motion of the Nazca (Farallon) and South American plates since Late Cretaceous time, *Tectonics*, *6*, 233–248, 1987.

Randall, D. E., and G. K. Taylor, Major crustal rotations in the Andean margin: Paleomagnetic results from the coastal Cordillera of northern Chile, *J. Geophys. Res.*, *101*, 15,783–15,798, 1996.

Randall, D., A. Tomlinson, and G. Taylor, Paleomagnetically defined rotations from the Precordillera of northern Chile: Evidence of localized in situ fault-controlled rotations, *Tectonics*, *20*, 235–254, 2001.

Raposo, M. I. B., and M. Ernesto, An Early Cretaceous paleomagnetic pole from Ponta Grossa dikes (Brazil): Implications for the South American Mesozoic apparent polar wander path, *J. Geophys. Res.*, *100*, 20,095–20,110, 1995.

Reutter, K. J., and E. Scheuber, Relation between tectonics and magmatism in the Andes of northern Chile and adjacent areas between 21° and 25° S, in *I Congr. Geol. Chileno*, vol. 1, pp. 345–363, Dept. de Geol. y Geofisica Univ. de Chile, 1988.

Reutter, K.-J., E. Scheuber, and G. Chong, The Precordilleran fault system of Chuquicamata, northern Chile: Evidence for reversals along arc parallel strike-slip faults, *Tectonophysics*, *259*, 213–228, 1996.

Riley, P. D., M. E. J. Beck, R. F. Burmester, C. Mpodozis, and A. García, Paleomagnetic evidence of vertical axis block rotations from the Mesozoic of northern Chile, *J. Geophys. Res.*, *98*, 8321–8333, 1993.

Roperch, P., F. Megard, L. A. J. Carlo, T. Mourier, T. M. Clube, and C. Noblet, Rotated oceanic blocks in western Ecuador, *Geophys. Res. Lett.*, *14*(1), 558–561, 1987.

Roperch, P., and G. Carlier, Paleomagnetism of Mesozoic rocks from the central Andes of southern Peru: Importance of rotations in the develop-

ment of the Bolivian orocline, *J. Geophys. Res.*, *97*, 17,233–17,249, 1992.

Roperch, P., G. Herail, and M. Fornari, Magnetostratigraphy of the Miocene Corque basin, Bolivia: Implications for the geodynamic evolution of the Altiplano during the late Tertiary, *J. Geophys. Res.*, *104*, 20,415–20,429, 1999.

Roperch, P., M. Fornari, G. Hérail, and G. Parraguez, Tectonic rotations within the Bolivian Altiplano: Implications for the geodynamic evolution of the central Andes during the late Tertiary, *J. Geophys. Res.*, *105*, 795–820, 2000.

Scheuber, E., and P. A. M. Andriessen, The kinematic and geodynamic significance of the Atacama fault zone, northern Chile, *J. Struct. Geol.*, *12*, 243–257, 1990.

Scheuber, E., and G. González, Tectonics of the Jurassic–Early Cretaceous magmatic arc of the north Chilean Coastal Cordillera (22°–26°S): A story of crustal deformation along a convergent plate boundary, *Tectonics*, *18*, 895–910, 1999.

Somoza, R., S. Singer, and A. Tomlinson, Paleomagnetic study of upper Miocene rocks from northern Chile: Implications for the origin of late Miocene–Recent tectonic rotations in the southern central Andes, *J. Geophys. Res.*, *104*, 22,923–22,936, 1999.

Somoza, R., and A. Tomlinson, Paleomagnetism in the Precordillera of northern Chile (22°30′S): implications for the history of tectonic rotations in the Central Andes, *Earth Planet. Sci. Lett.*, *94*, 369–381, 2002.

Tanaka, H., H. Tsunakawa, and K. Amano, Palaeomagnetism of the cretaceous El Way and Coloso Formations from the northern Chilean Andes, *Geophys. J. R. Astron. Soc.*, *95*, 195–203, 1988.

Tassara, A., P. Roperch, and A. Pavez, Paleomagnetismo de los yacimientos Mantos Blancos y Manto Verde: Implicancias tectonicas y cronologicas, in *IX Congr. Geol. Chileno, Puerto Varas*, vol. 2, pp. 166–170, 2000.

Tomlinson, A., C. Mpodozis, P. Cornejo, C. F. Ramírez, and T. Dumitri, El sistema de Fallas Sierra de Castillo-Agua Amarga: Transpresión sinistral eocena en la precordillera de Potrerillos–El Salvador, in *VII Congr. Geol. Chileno, Concepción*, vol. II, pp. 1459–1463, 1994.

Tomlinson, A., and N. Blanco, Structural evolution and displacement history of the West Fault System, Precordillera, Chile, part 1, Synmineral history, in *VIII Congr. Geol. Chileno, Antofagasta*, vol. 3, pp. 1873–1877, 1997a.

Tomlinson, A., and N. Blanco, Structural evolution and displacement history of the West Fault System, Precordillera, Chile, part 2, Postmineral history, in *VIII Congr. Geol. Chileno, Antofagasta*, vol. 3, pp. 1878–1882, 1997b.

Turner, P., H. Clemmey, and S. Flint, Paleomagnetic studies of a Cretaceous molasses sequence in the central Andes (Coloso Formation, northern Chile), *J. Geol. Soc. London*, *141*, 869–876, 1984.

Yañez, G., C. Mpodozis, A. Tomlinson, Eocene dextral oblique convergence and sinistral shear along the Domeyko fault system: A thin viscous sheet approach with asthenospheric drag at the base of the crust, in *VII Congr. Geol. Chileno*, vol. 2, pp. 1478–1482, 1994.

C. Arriagada and P. Roperch, Departamento de Geología, IRD, Universidad de Chile, Santiago, Chile. (cearriag@cec.uchile.cl)

A. Chauvin and P. R. Cobbold, UMR 6118 du CNRS, Géosciences-Rennes, F-35042 Rennes, France.

J. Cortés, Servicio Nacional de Geología y Minería, Santiago, Chile.

G. Dupont-Nivet, Department of Geosciences, University of Arizona, Tucson, AZ 85721, USA.

C. Mpodozis, SIPETROL, Santiago, Chile.

Publication : Rotations horaires de bloc le long du bord oriental de la Cordillère de Domeyko, nord du Chili (22º45'-23º30'S).

Arriagada César, Roperch Pierrick, Mpodozis Constantino

Résumé : Nous apportons de nouveaux résultats paléomagnétiques d'une étude de 38 sites dans des sédiments rouges et des roches volcaniques du Groupe Purilactis, déposées entre le Crétacé et Tertiaire Inférieur, qui affleurent le long du bord occidental du bassin du Salar d'Atacama. Après une démagnétisation thermique détaillée, les directions caractéristiques de 32 sites ont été déterminées. Dans la plupart des cas, les sédiments rouges des membres inférieurs du Groupe Purilactis présentent une magnétisation de polarité normale bien définie, probablement associé à l'hématite, formée comme ciment lors de la diagenèse. Une grande diminution dans la dispersion des directions paléomagnétiques, après la correction de l'inclinaison, démontre que cette magnétisation est une magnétisation prétectonique. Nous interprétons la présence dominante de polarité normale comme preuve d'une acquisition pendant l'anomalie C34 du Crétacé. D'importantes déviations des déclinaisons magnétiques par rapport à celles attendues pour le continent d'Amérique du Sud suggèrent des rotations horaires associées a la déformation Tertiaire dans la Cordillère de Domeyko. Ces données suggère que les rotations tectoniques horaires sont l'une des caractéristiques structurelles les plus importantes des Andes Centrales du nord du Chili. Toutefois, cette étude, montre une variation spatiale dans l'ampleur des rotations, avec des rotations supérieures a 60º dans le secteur de Cerro Totola. Ces rotations se sont simultanément produites durant une déformation décrochante qui a affecté de grands segments de la Cordillère de Domeyko pendant l'Éocène. L'observation systématique de rotations horaires contemporaines de déplacement senestre dans la Cordillère de Domeyko peuvent être expliquées par des cisaillements à la base de la croûte fragile.

Article publié au *Tectonophysics*, v. 326, p. 153-171, 2000

ELSEVIER

Tectonophysics 326 (2000) 153–171

TECTONOPHYSICS

www.elsevier.com/locate/tecto

Clockwise block rotations along the eastern border of the Cordillera de Domeyko, Northern Chile (22°45′–23°30′S)

César Arriagada [a], Pierrick Roperch [b], Constantino Mpodozis [c]

[a] *Departamento de Geología, Universidad de Chile, Santiago, Chile*
[b] *IRD/Departamento de Geología, Universidad de Chile, Santiago, Chile*
[c] *Servicio Nacional de Geología y Minería, Santiago, Chile*

Abstract

We report new paleomagnetic results from a study of 38 sites in Cretaceous to Early Tertiary red beds and volcanic rocks belonging to the Purilactis Group, which outcrop along the western border of the Salar de Atacama Basin. After detailed thermal demagnetization, characteristic directions were determined for 32 units. In most cases, red bed sediments from the lower members of the Purilactis Group have a well-defined normal polarity magnetization probably carried by hematite forming an early diagenetic cement. A large decrease in the dispersion of the paleomagnetic directions upon tilt correction demonstrates that this magnetization is a pre-tectonic magnetization. We interpret the dominant occurrence of the normal polarity direction as evidence for acquisition of the magnetization during the Cretaceous normal polarity superchron. Large deviations of the paleomagnetic declinations from the expected ones for stable South America provides new evidence for clockwise tectonic rotations associated with Tertiary deformation in the Cordillera de Domeyko. These data confirm that clockwise tectonic rotations are one of the most significant structural characteristics of the north Chilean Andes. This study, however, indicates spatial variation in the magnitude of the rotation with rotations $>60^\circ$ in the Cerro Totola area. These rotations have occurred in conjunction with transpressional deformation that affected large tracts of the Cordillera de Domeyko during Eocene deformation. The systematic observation of clockwise rotations contemporaneous with sinistral displacements in the Cordillera de Domeyko can be explained by shear-traction at the base of the brittle crust.

Keywords: Salar de Atacame; paleomagnetism; tectonic rotations; Central Andes

1. Introduction

Several paleomagnetic studies demonstrate that tectonic rotation is one of the major characteristics of the structural evolution of the Central Andes. Counterclockwise rotations with respect to stable South America are found along the Peruvian margin (Heki et al., 1984, 1985; May and Butler, 1985; Roperch and Carlier, 1992) while clockwise rotations characterize the Chilean margin (Forsythe et al., 1987; Hartley et al., 1992b; Riley et al., 1993; Roperch et al., 1997).

The origin of these rotations is, however, still a matter of debate (see recent review by Beck, 1998). In most of the published studies, the lack of structural control and geographically restricted paleomagnetic sampling (few sites) impede a clear understanding of the age of the rotation and the size of the rotating blocks. Until now, rotations

* Corresponding author.
E-mail address: carriaga@quad.dgl.uchile.cl

0040-1951/00/$ - see front matter
PII: S0040-1951(00)00151-7

within the Chilean forearc have been attributed to deformation along the Atacama Fault System during the Early Cretaceous (Forsythe and Chisholm, 1994), the late Cretaceous Central Valley Fault Zone (Randall et al., 1996; Taylor et al., 1998), oroclinal bending of the whole Andes (Heki et al., 1985; Isacks, 1988) or in situ block rotations in response to oblique convergence (Beck et al., 1986).

In this study, we report detailed paleomagnetic results from 38 sites collected along the eastern border of the Cordillera de Domeyko, west of the Salar de Atacama, in northern Chile (Figs. 1 and 2). In situ clockwise block rotations have been proposed to explain the complex structural pattern of the region (Mpodozis et al., 1993a,b). The study area is located at the edge of the Cordillera de Domeyko along the western border of the Salar de Atacama Basin (Fig. 1). Preliminary results from the northern part of the Salar de Atacama region (Barros Arana Syncline, Hartley et al., 1992b), indicating clockwise rotations, were interpreted as a possible consequence of relative motions between thrust sheets. Transpressional deformation played a major role in shaping the tectonic fabric of the Cordillera de Domeyko. Multiple episodes of strike–slip displacements, associated with a complex 'trench-linked' fault system (Domeyko Fault System, DFS, Fig. 1) occurred along the Cordillera de Domeyko axis during the Tertiary. Eocene, Oligocene and Miocene activity, either in sinistral or dextral mode, have been reported (Maksaev, 1990; Reutter and Scheuber, 1991; Mpodozis et al., 1993a,b; Tomlinson and Blanco, 1997).

2. Geological setting

2.1. Stratigraphy

The Cordillera de Domeyko, in the region west of the Salar de Atacama (Fig. 1), comprises Late Paleozoic magmatic complexes, including basaltic to andesitic volcanic rocks, interbedded with lacustrine sediments of Late Carboniferous–Early Permian age (Breitkreutz et al., 1992). They are associated with large outcrops of high silica rhyolitic ignimbrites and domes and granitoid plutons, which have been dated by K–Ar, Rb/Sr and U–Pb (zircon) methods. Most of the ages fall in the range 300–200 Ma (Davidson et al., 1985; Mpodozis et al., 1993a). A major fault zone (Sierra de Varas Fault, Fig. 1) forms the western border of the Cordillera de Domeyko and marks the contact of the Paleozoic basement with Late Triassic to Early Cretaceous marine carbonates, and terrestrial red beds. These sedimentary sequences are covered by basaltic to rhyolitic volcanics of Late Cretaceous to Paleocene age (Quebrada Mala and Cinchado formations), which occupy large areas of the Central Depression of northern Chile (Marinovic et al., 1996).

The eastern border of the Cordillera de Domeyko coincides with the 'El Bordo' Escarpment; a conspicuous 120 km long, NS trending cliff confining the Salar de Atacama Basin (Figs. 1 and 2). Along the escarpment the Paleozoic basement lies in fault contact with or is covered by a 6000 m thick Cretaceous–Oligocene red-bed sequence (Purilactis Group). To the east, this sequence forms the lower section of the Salar de Atacama Basin sedimentary fill (Macellari et al., 1991; Muñoz, et al., 1997).

Numerous authors have described the stratigraphy of the Purilactis Group (Brüggen, 1942; Dingman, 1963; Ramírez and Gardeweg, 1982; Hartley et al., 1992a; Charrier and Reutter, 1995; Mpodozis et al., 1999). The lowermost unit of the Purilactis Group is the Tonel Formation, a sequence of fine-grained red sandstones and evaporites (Fig. 2). A faulted (detached) unconformity marks an upwards transition to the Purilactis Formation which comprises 2800 m of sandstones, red mudstones and minor conglomerates deposited in proximal fluvial, alluvial fan and lacustrine environments (Hartley et al., 1992a). The Tonel and Purilactis formations, of probable Early Cretaceous age, are overlain by a sequence of proximal alluvial fan coarse-grained conglomerates, with volcanic and granitoid clasts up to 1 m in diameter. These conglomerates, (Barros Arana Strata, Fig. 2) cropout at the core of the Barros Arana Syncline (Fig. 2) and attest to a major change in the sedimentary environment. This change could be associated with uplift of the

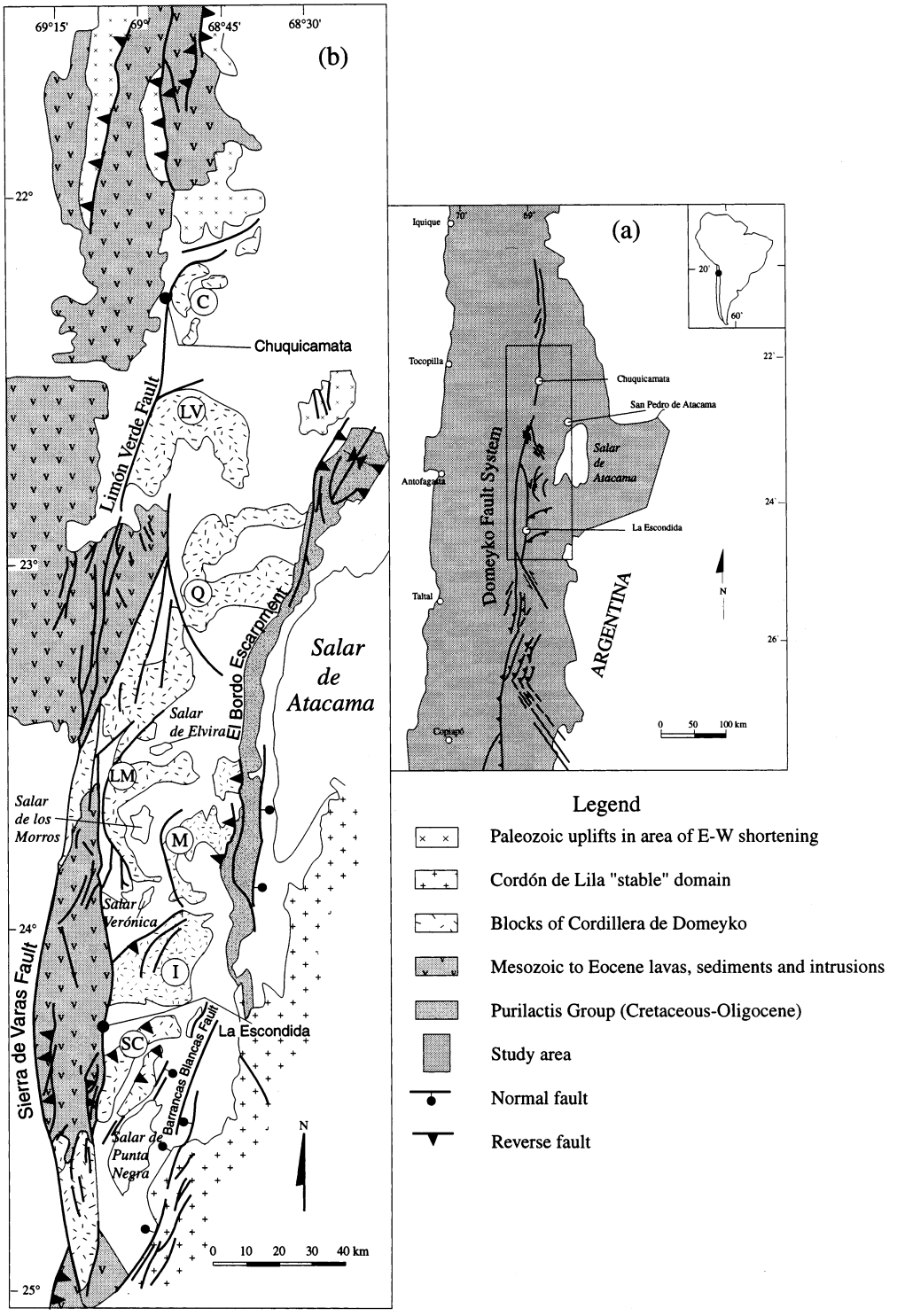

Fig. 1. (a) Main structural features of the Domeyko Fault System in Northern Chile (from Cornejo et al., 1997, modified). (b) Schematic morphostructural map of the Cordillera de Domeyko in the area to the west of the Salar de Atacama. C, Cerros de Chuquicamata; LV, Limón Verde; Q, Quimal; LM, Los Morros; M, Mariposas; I, Imilac; SC, San Carlos basement blocks.

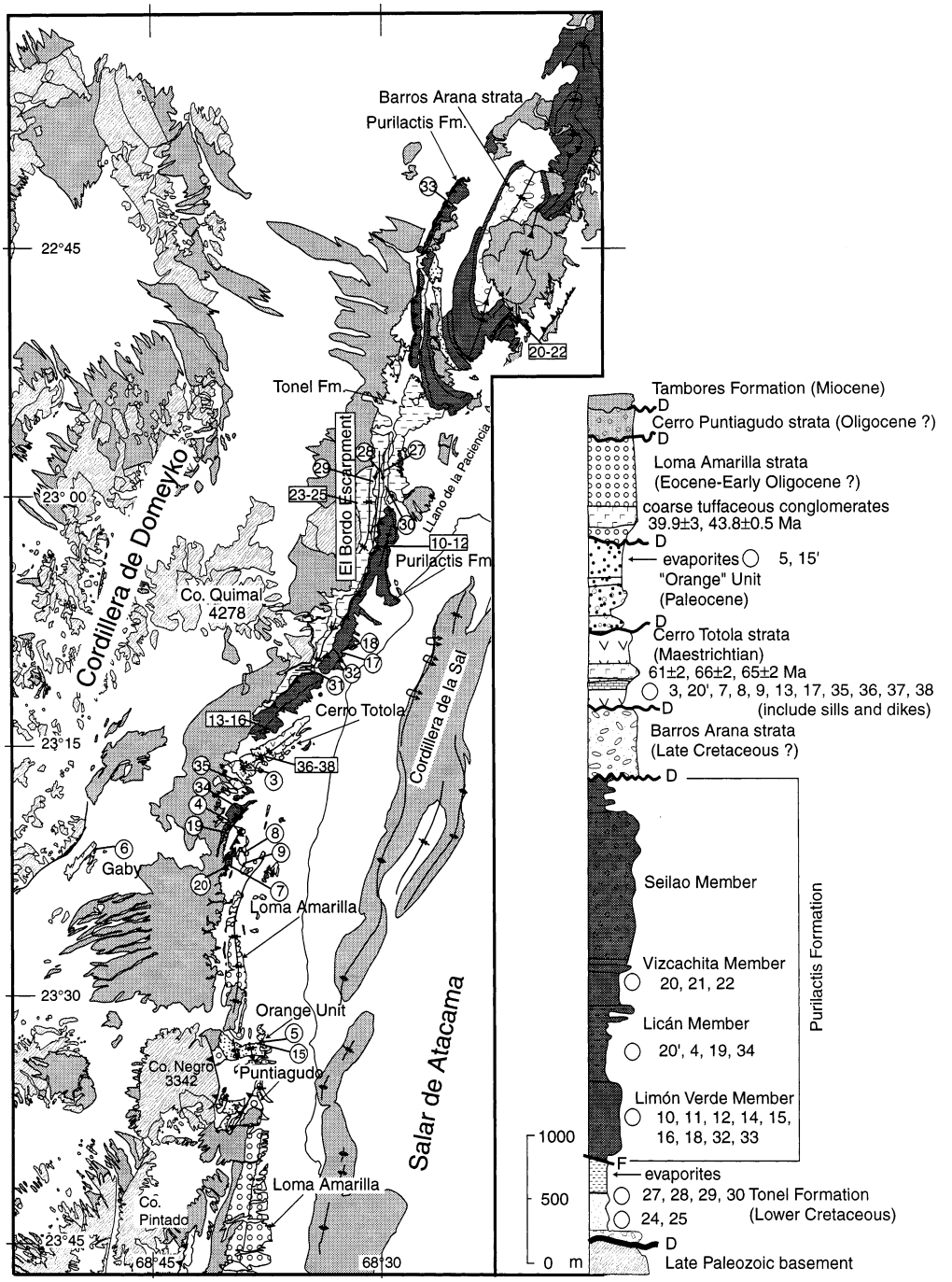

Fig. 2. Simplified geological map and stratigraphic section of the El Bordo Escarpment region with indication of paleomagnetic sampling sites. Lithology is further described in the text. Sites 15′ and 20′ correspond to sites CC15 and CC20 listed in Table 1. All other sites have the header 'CA' in Tables 1 and 2.

adjacent Cordillera de Domeyko during the Late Cretaceous (Mpodozis et al., 1999).

To the south of Cerro Quimal, (Cerro Totola, Cerro Negro, Cerro Pintado, Fig. 2) an 800 m thick sequence of basaltic andesitic lava flows, interbedded with welded rhyolitic ignimbrites and coarse volcaniclastic sediments (Cerro Totola strata) rests unconformably over older Cretaceous units. New K/Ar ages [whole rock, amphibole and biotite, (Arriagada, 1999)] between 65 and 61 Ma indicate a Maestrichtian age. The lavas are unconformably overlain by a Paleocene–Eocene clastic sequence ('Orange Unit', Fig. 2) which begins with 400 m of conglomerates, followed by 500 m of semiconsolidated sandstones alternating with thin evaporite (gypsum) beds. At least 1000 m of Eocene (Oligocene?) conglomerates (Loma Amarilla Strata), overlying the 'Orange Unit' (Fig. 2), represents one of the more regionally important map-scale units of the Purilactis Group. Internal progressive unconformities occur in the basal part of the sequence, where very coarse conglomerates alternate with tuffaceous horizons, dated (K–Ar, $^{40}Ar/^{39}Ar$ methods) between 42 and 39 Ma (Ramírez and Gardeweg, 1982; Hammerschmidt et al., 1992).

2.2. Regional structure

In the area to the west of the Salar de Atacama, the Cordillera de Domeyko comprises a series of discrete basement blocks, which are separated by small, internally draining basins (Salar de Los Morros, Verónica Elvira, Fig. 1). The northwestern faces of the rhomboidal southern blocks (Imilac, San Carlos) are bounded by high-angle reverse faults, while the northernmost blocks (Quimal, Los Morros and Mariposas) are limited to the west and north, by sub-circular, vertical faults. The sense of asymmetry of large scale 'sidewall ripouts' (Swanson, 1989) and displacement of geological contacts indicate left lateral shear along most of the major fault traces (Mpodozis et al., 1993a).

Along their eastern edges, the Imilac, Mariposas and Los Morros basement blocks are thrust over the Purilactis Group sediments exposed along the El Bordo Escarpment (Fig. 1). Deformation in the Purilactis sediments is especially significant when facing the basement blocks, where the red beds present isoclinal to chevron folds with subvertical axial surfaces.

A major change in the structural pattern occurs, however, from Cerro Totola to Barros Arana where basement thrusts disappear (Fig. 2). They are replaced by a large, basement-cored, asymmetrical, overturned to the east, anticline. Purilactis Group sediments unconformably overlie the basement along its subvertical eastern limb. A conspicuous syncline (Barros Arana-El Bordo Syncline) which extends for >80 km along the El Bordo Escarpment between Cerro Totola and Cuesta de Barros Arana occurs to the east. Fold geometry changes from tight-chevron in the south, to open-concentric to the north (cuesta de Barros Arana) while the trend of its axial surface changes form N60°E (Cerro Totola) to NNE (Barros Arana). Secondary west verging, late 'backtrusts' tectonically repeat some of the Purilactis beds in the western limb of the Barros Arana region (Fig. 2).

Mpodozis et al. (1993a,b) interpreted the structural geometry of the Cordillera de Domeyko in the study area as the result of passive northward transport of rigid upper crustal blocks by left-lateral shear during the Eocene Incaic deformation. As they were displaced towards the north, movement of these blocks may have been obstructed by a physical 'buttress' originally thought to be the Limón Verde crystalline massif (Fig. 1). However, new mapping north of Sierra de Limón Verde led Tomlinson and Blanco (1997) to suggest that the buttress was actually located north of Chuquicamata at the Sierra del Medio (Fig. 1) which underwent E–W shortening contemporaneous with the sinistral displacements occurring farther south. According to this model, Mpodozis et al. (1993a,b) and Yañez et al. (1994) suggest that, to overcome the buttress, north directed displacement was transferred towards the east by tectonic escape in the direction of the (Atacama) Purilactis basin. This process may have been associated with extension along the trailing (south and west) edges of the blocks and between the blocks themselves, and thrusting (and folding) along their frontal (east) faces. The model, which implies a significant amount of clockwise in situ block rota-

tions of the individual crustal blocks, agree with the theoretical 'buttress and free face' case of block rotations presented by Beck et al. (1993) and Beck (1998). If true, in this segment of the Cordillera de Domeyko, at least 30–40 km of Eocene northward displacement could have been compensated by 10–20% widening of the original surface area of the Cordillera de Domeyko. The change from sandstones to coarse grained sediments in the Purilactis basin (base of the Loma Amarilla Strata) dated at ca. 44–40 Ma (Ramírez and Gardeweg, 1982, Hammerschmidt et al., 1992), and the 45–42 Ma K–Ar ages of the bimodal, syntectonic intrusives and domes of the Cerro Casado complex in the Quimal block (Mpodozis et al., 1993a), indicate a Middle to Late Eocene age for the beginning of strike–slip deformation.

3. Paleomagnetic sampling

A total of 420 paleomagnetic samples were drilled at 38 sites in the sedimentary sequences, volcanics and intrusives along El Bordo Escarpment where the abrupt topography provides very good outcrops (Fig. 2, Table 1). In the Cerro Totola area, where sediments are intruded by Late Cretaceous dykes, we tried to sample whenever possible, not only the dykes but also the baked sediments within a few centimeters of the dyke borders. In contrast, however, with the El Bordo Escarpment, outcrops of good quality are rare in the Cordillera de Domeyko. At only one site (CA06), was it possible to collect a few samples of red siltstones and a lava flow from a sequence that we consider equivalent to the Cerro Totola Strata.

Sites in volcanic rocks include only samples from a single flow, dyke or ignimbrite. Secular variation was thus not averaged at these single-bed sites. In contrast, in sedimentary rocks, sampling included different beds along several meters of stratigraphic section. In such cases mean-site paleomagnetic results should average the secular variation and provide a good estimate of tectonic rotations at the site. Bedding corrections were applied to all sedimentary and volcanic sites (Table 1). Upper units of the Purilactis Group (Loma Amarilla, Cerro Puntiagudo) did not provide samples suitable for paleomagnetic study.

4. Paleomagnetic methods

Remanent magnetization was measured with Molspin or Agico JR5A spinner magnetometers. Magnetic Susceptibility was measured with a Bartington susceptibilimeter. Magnetic susceptibility was also measured after each thermal demagnetization step in order to check magnetic mineralogical changes upon heating. To better constrain the magnetic mineralogy, isothermal remanent magnetizations (IRM) acquisition and variation of the susceptibility during heating (K–T) were performed for a few samples. IRM were given with a pulse electro-magnet and K–T experiments were done with the AGICO KLY3-CS3 instrument.

In sedimentary rocks, one specimen per minicore was subjected to stepwise thermal demagnetization (10–15 steps) in an ASC furnace where the residual field was <10 nT. For volcanic rocks, we used either thermal cleaning or stepwise alternating field (AF) demagnetization. The magnetization directions have been determined with "least squares lines and planes" programs according to Kirschvink (1980). Evidence for secondary overprint due to lightning was found at a few sites in volcanic rocks. In these cases, statistics combining directions and planes (McFadden and McElhinny, 1988) were used to determine the mean characteristic direction for the site.

5. Magnetic properties

As shown in Fig. 3 and Table 1, there is a large dispersion in the mean-site values of magnetic susceptibility and intensity of natural remanent magnetization. Variation of these magnetic parameters was within the expected range for volcanic rocks, except for the low values found at site CA23, a sill intruding the Tonel Formation. Such behavior is likely related to the alteration and weathering exhibited by the samples collected at the site.

Table 1
Location of the paleomagnetic sampling and mean-site magnetic properties[a]

Site	Lithology	Unit	Longitude	Latitude	NRM(A m^{-1})	K (SI)	Strike	Dip
CC15	Sandstones, siltstones	Orange	−68°37.74′	−23°32.67′	0.0174	0.000409	0	0
CC20	Sill and baked sandstones	Licán	−68°40.06′	−23° 22.25′	0.365	0.0447	11.5	64.1
CC20	Red sandstones	Licán	−68°40.06′	−23° 22.25′	0.0305	0.00052	11.5	64.1
CA03	Andesitics–basaltics lavas	Cerro Totola	−68°37.396′	−23°15.914′	10.3	0.0753	240	65
CA04	Red sandstones	Licán	−68°40.035′	−23°19.630′	0.00421	0.000378	230	66.2
CA05	Orange sandstone	Orange	−68°37.752′	−23°32.312′	0.037	0.00681	213.4	47
CA06	Sandstone, basaltic lava	Cerro Totola	−68°48.841′	−23°21.508′	0.00499	0.000135	202	52.3
CA07	Sill and baked sandstones	Licán	−68°39.724′	−23°22.375′	0.358	0.0213	31.6	61.6
CA08	Andesitics–basaltics lavas	Cerro Totola	−68°38.768°′	−23°21.505′	0.237	0.00422	30	25
CA09	Andesitics–basaltics lavas	Cerro Totola	−68°39.042′	−23°22.305′	0.558	0.0505	0	70
CA10	Sandstone red-brown	Limón Verde	−68°30.173′	−23° 2.987′	0.0178	0.000375	16.8	57.9
CA11	Sandstone red-brown	Limón Verde	−68°30.126′	−23° 2.976′	0.0417	0.00204	18.5	49.7
CA12	Sandstone red-brown	Limón Verde	−68°30.043′	−23° 2.986′	0.0502	0.00432	19	55
CA13	Dike and baked brown sandstone	Limón Verde	−68°37.901′	−23°14.416′	0.867	0.0434	61.8	53.9
CA14	Sandstone red-brown	Limón Verde	−68°38.101′	−23°13.822′	0.0425	0.00646	61.2	42.6
CA15	Sandstone red-brown	Limón Verde	−68°38.067′	−23°13.848′	0.0319	0.0107	70	45
CA16	Dike and baked brown sandstone	Limón Verde	−68°38.067′	−23°13.848′	7.97	0.0488	40.1	70.1
CA17	Dike and baked brown sandstone	Limón Verde	−68°32.615′	−23° 9.223′	0.227	0.000675	49.9	69.3
CA18	Sandstone red-brown	Limón Verde	−68°33.024′	−23° 9.271′	0.0444	0.00199	36.5	69.5
CA19	Sandstone red-brown	Licán	−68°40.866′	−23°20.385′	0.007	0.000462	202.2	68.5
CA20	Andesitic lava	Vizcachita	−68°21.551′	−22°49.054′	0.0767	0.000287	231.4	48.3
CA21	Sandstone, red siltstone	Vizcachita	−68°21.726′	−22°48.578′	0.0072	0.000326	224.8	38.4
CA22	Sandstone, red siltstone	Vizcachita	−68°21.099′	−22°50.044′	0.00529	0.000148	215.8	36.8
CA23	Sill	Tonel	−68°36.853′	−23°15.615′	0.00118	0.000476	0	90
CA24	Red siltstone	Tonel	−68°31.458′	−23° 0.321′	0.0108	0.000145	340.6	42.3
CA25	Red siltstone	Tonel	−68°31.458′	−23° 0.321′	0.00953	0.000145	333.6	37
CA27	Sandstone red-brown	Tonel	−68°29.556′	−22°57.996′	0.0162	0.000932	6.7	49.4
CA28	Sill	Tonel	−68°29.804′	−22°57.964′	0.0465	0.000324	359.5	66.2
CA28	Sandstone red-brown	Tonel	−68°29.804′	−22°57.964′	0.14	0.0363	342.5	20.6
CA29	Red siltstone	Tonel	−68°30.676′	−22°58.953′	0.0127	0.000152	355.9	37.9
CA30	Siltstone, sandstone	Tonel	−68°29.964′	−22°59.366′	0.0125	0.000245	355.9	37.9
CA31	Siltstone	Tonel	−68°34.835′	−23°10.216′	0.00843	0.00018	52.4	56.9
CA31	Sill and baked siltstone	Tonel	−68°34.835′	−23°10.216′	0.132	0.0397	52.4	56.9
CA32	Sandstone red-brown, sill	Limón Verde	−68°33.273′	−23° 9.266′	0.0175	0.000632	25.9	79.4
CA33	Sandstone red-brown	Limón Verde	−68°25.476′	−2242.306′	0.00701	0.000425	32.3	33.5
CA34	Siltstone and sandstone red-brown	Licán	−68°39.556′	−23°18.964′	0.0204	0.00169	229.9	76.8
CA35	Andesitics–basaltics lavas	Cerro Totola	−68°°39.592′	−23°17.568′	1.32	0.0158	240	70
CA36	Ignimbrite	Cerro Totola	−68°37.465′	−23°15.272′	1.63	0.0186	65.2	72.4
CA37	Sill	Cerro Totola	−68°37.465′	−23°15.272′	0.182	0.0108	65.2	72.4
CA38	Andesitics–basaltics lavas	Cerro Totola	−68°37.465′	−23°15.272′	0.854	0.0382	57.5	66.5

[a] NRM is geometric mean intensity of magnetization in A m^{-1}; K is geometric mean susceptibility (SI), strike and dip are bedding corrections.

The lowest magnetic susceptibility values in sedimentary rocks were found in the fine red beds of the Tonel Formation (sites 24, 25, 28, 29, 30, 31). Samples from sediments of the Limón Verde member of the Purilactis Formation (sites 11, 12, 14, 15, 18), present a high magnetic susceptibility which can be attributed to the presence of detrital magnetite. Magnetite was indeed observed in these samples during IRM acquisition and K–T experiments (Figs. 4 and 5). Variation in magnetic susceptibility between the Tonel Formation and the overlying members of the Purilactis Formation suggests a different sedimentary source for both units. We may also speculate that a lower sedi-

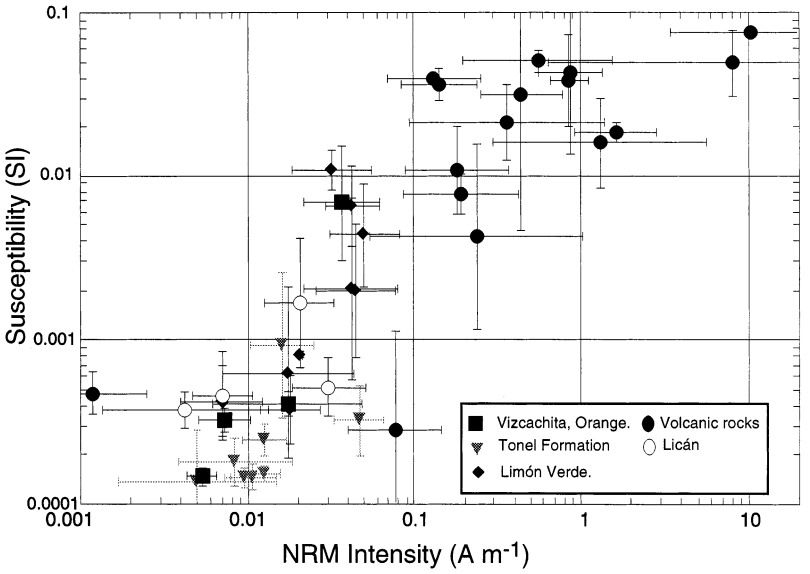

Fig. 3. Log–log plot of the mean-site (geometrical means) intensity of NRM versus the magnetic susceptibility. Magnetic susceptibility is often high in samples from the Purilactis Formation.

mentation rate for the Tonel Formation provided higher oxidation during deposition. Samples with high magnetic susceptibility show a stronger secondary magnetic overprint that was mostly removed during the initial steps of the thermal demagnetization process.

Intensity of NRM is usually <0.05 A m^{-1}. The largest values found at a few sites (CC20, CA17, CA31) are related to remagnetization by nearby dyke or sill intrusions.

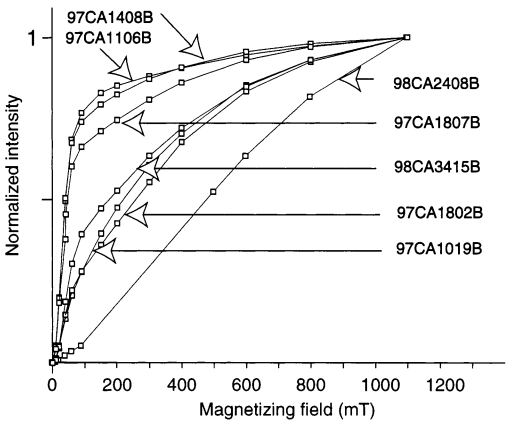

Fig. 4. Isothermal remanent magnetization acquisition for samples from different sedimentary units of the Purilactis Group.

6. Characteristic directions

Interpretation of demagnetization data for volcanic rocks was straightforward in most cases. In contrast, magnetizations observed in red bed sediments are more complex and will be described in more detail.

6.1. El Bordo Escarpment

At most sites sampled along the El Bordo Escarpment both in sedimentary and volcanic rocks, it was possible to determine characteristic magnetizations. Five different types of magnetic behavior, which correlate with the stratigraphic position of the sites within the Purilactis Group, were observed (see below).

6.1.1. Lower Tonel Formation

Samples from the base of the Tonel Formation show low magnetic susceptibility. High unblocking temperatures characterize these samples with a

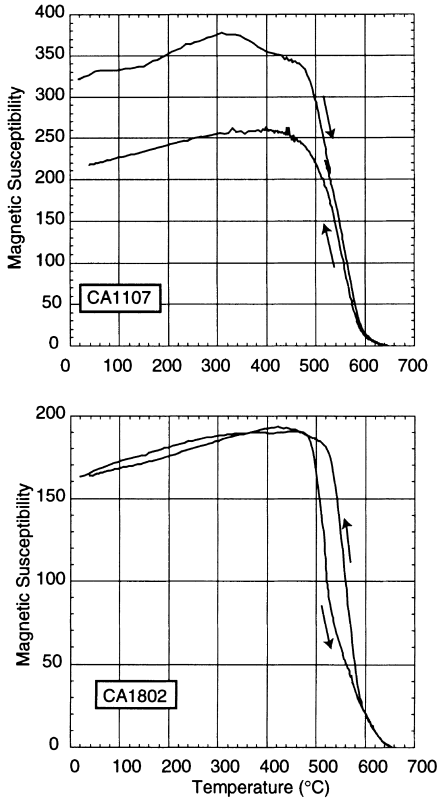

Fig. 5. Thermomagnetic curves showing a Curie temperature characteristic of magnetite in samples from the Limón Verde member of the Purilactis Formation.

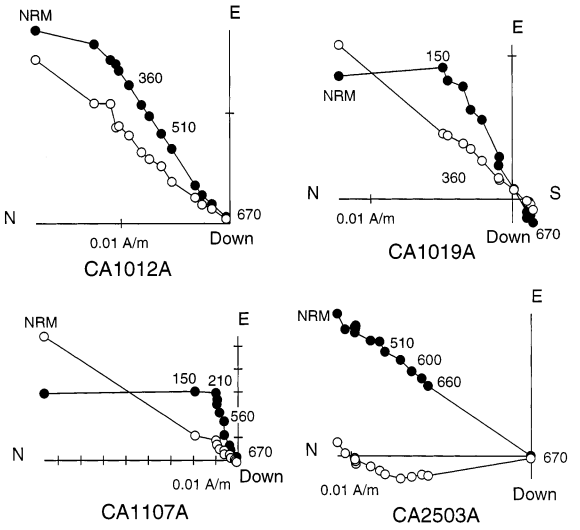

Fig. 6. Typical orthogonal demagnetization diagrams for samples from sedimentary units (in situ coordinates). A soft viscous overprint aligned with the present geomagnetic field is removed during the first step of thermal demagnetization. For samples from the Limón Verde rock type (samples CA1012A, 1019A and 1107A), the characteristic magnetization of normal polarity is observed in the temperature range 150–670°C. Only a few samples show a reverse component of magnetization above 670°C (sample CA1019A). In contrast, samples from the base of the Tonel Formation have higher unblocking temperatures (sample CA2503A). Open circles correspond to the projection onto the vertical plane while solid symbols are the projection onto the horizontal plane. Numbers are temperature in °C.

well-defined magnetization carried by hematite. Medium destructive temperatures (MDT) are >600°C. A univectorial magnetization was observed during demagnetization up to 680°C (Fig. 6).

6.1.2. *Upper Tonel Formation, Limón Verde and Licán members of the Purilactis Formation*

Thermal demagnetization below 250° was usually sufficient to remove a soft overprint aligned with the present geomagnetic field direction. The relative intensity of this overprint was higher in samples showing the highest susceptibility (Fig. 6). Samples drilled in Limón Verde and Licán members show a wide range of unblocking temperatures for the characteristic magnetization (Fig. 7). For most samples MDT was in the range 400–500°C (Fig. 7). The characteristic magnetization is a normal polarity magnetization. Only, in a few cases, did this characteristic magnetization vector not go through the origin during the thermal demagnetization but it was not possible to identify any other characteristic magnetization. Only at site CA10, a few samples show a reverse polarity magnetization above 660°C (Fig. 6). At site CA33, both polarities (nine samples have the normal polarity and three reverse polarity) are also present but in stratigraphic order suggesting a polarity reversal at the time of deposition. The origin of the widespread normal polarity magnetization will be further discussed below.

6.1.3. *Vizcachita member*

A well-defined characteristic magnetization with reverse polarity was identified in sedimentary samples from one site of the Vizcachita member

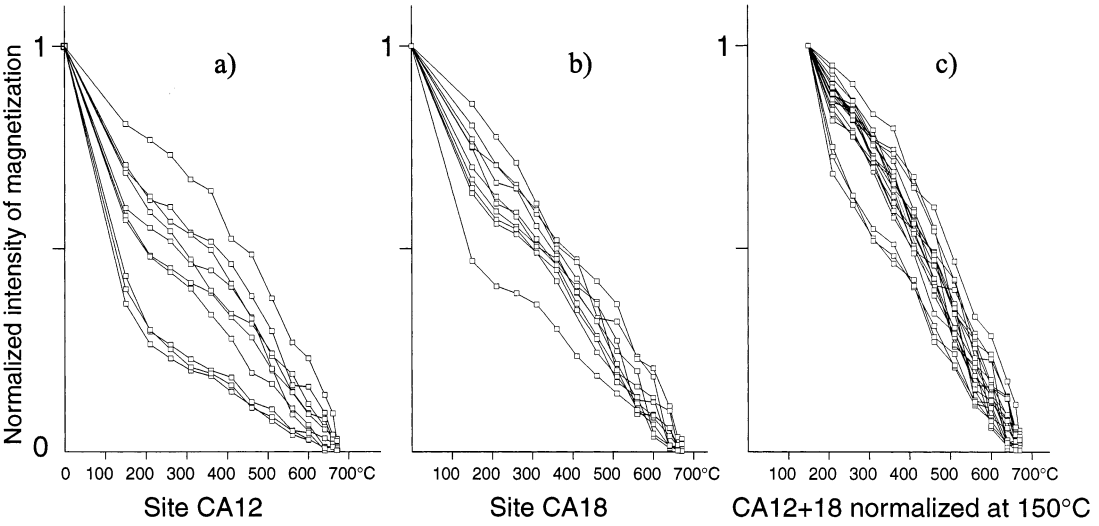

Fig. 7. Variation of the intensity of the remanent magnetization during thermal demagnetization (samples from two sites from the Limón Verde red beds). Apart from a more or less important decrease in intensity after demagnetization at 150°C, unblocking temperatures are linearly distributed from 150 to 670°C.

(CA21). This magnetization was found in the temperature range 150° to 600–640°C while a poorly defined magnetization with normal polarity was observed above 640°C (Fig. 8). This magnetization with reversed polarity has magnetic characteristics similar to the widespread normal magnetization found in samples collected from further south. At site CA22 (Fig. 2), the magnetization is not univectorial but, is dominated by normal polarity component. An overprint, like that observed at site CA21, was not observed at this site (CA22).

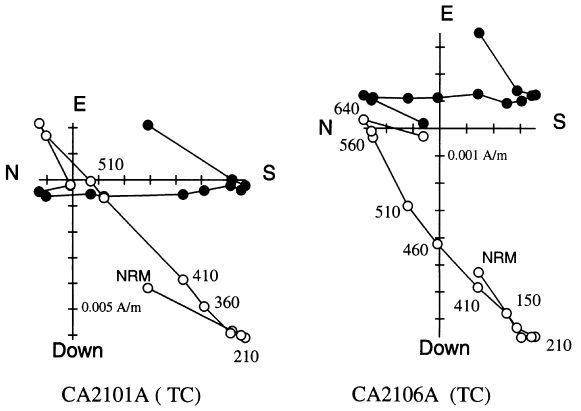

Fig. 8. Orthogonal demagnetization diagrams for two samples from site CA21 (in tilt corrected coordinates). A reverse component of magnetization is observed in the temperature range 210–640°C. A poorly defined magnetization with normal polarity is observed above 640°C. Open circles correspond to the projection onto the vertical plane while solid symbols are the projection onto the horizontal plane.

6.1.4. Cerro Totola and Vizcachita volcanics

South of Cerro Quimal, lava flows and ignimbrites of the Cerro Totola Strata were sampled at eight sites (Fig. 2). A volcanic horizon interbedded in the Vizcachita member was sampled at the eastern limb of the Barros Arana Syncline (Quebrada Seilao). In these samples magnetization is univectorial and goes through the origin during demagnetization (Fig. 9). At a few sites, secondary components, with random orientation and high magnetic intensity, likely to be due to lightning strikes, were, sometimes, difficult to remove entirely. In such cases, great circles were used to determine the mean-site paleomagnetic direction using the method described by McFadden and McElhinny (1988).

Unblocking temperatures, high susceptibility values and rock-magnetic experiments indicate that magnetite is the dominant magnetic carrier in most

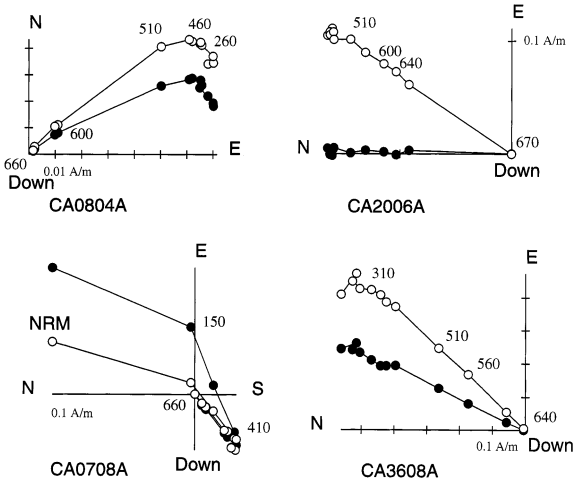

Fig. 9. Typical orthogonal demagnetization diagrams for samples from volcanic rocks (in tilt corrected coordinates). Open circles correspond to the projection onto the vertical plane while solid symbols are the projection onto the horizontal plane.

of these rocks although unblocking temperatures above 600°C indicate that hematite also carries the same magnetization. In this case, hematite is likely to be the oxidation product during emplacement of the lavas and ignimbrites.

Magnetization was often poor in dykes, especially in their inner parts. At a few sites, samples from baked sediments, however, provided very stable magnetizations. They were included in the calculation of the mean-site direction. An important decrease in scatter upon tilt correction ($k=7$ before tilt and $k=28$ after tilt correction) indicates a pre-folding origin for the magnetization Fig. 10). Taking into account the dispersion due to tectonic

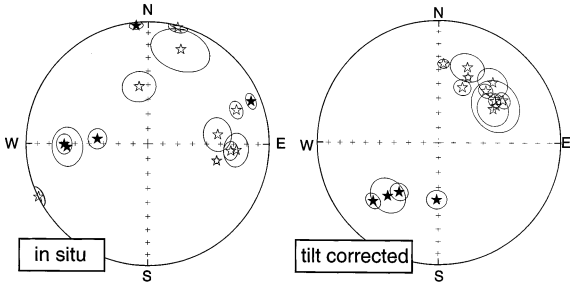

Fig. 10. Equal area projection of mean-site directions in volcanic units. Upon tilt correction, there is a significant decrease in the dispersion of the directions.

rotations within the area, we also performed inclination-only statistics (McFadden and Reid, 1982). The precision parameter is ten times higher after tilt correction ($k=7.9$) than in situ ($k=79$).

6.1.5. Orange Unit

Sediments drilled at two sites in the 'Orange unit' (CC15 and CA05) south of Loma Amarilla (Fig. 2) show a high magnetic susceptibility. Thermal or AF demagnetization did not yield characteristic magnetizations.

6.2. Cordillera de Domeyko

At the only site sampled within the Cordillera de Domeyko (site CA06), (which correspond to a section we consider equivalent to the Cerro Totola Unit), the siltstone beds carry a reverse polarity magnetization while a normal polarity magnetization was found in the overlying lava. The directions of magnetization are not exactly antiparallel probably because secular variation is recorded in the volcanic rocks. The magnetization in the overlying lava is mainly carried by hematite with high unblocking temperatures. In contrast, unblocking temperatures of the magnetization carried by the fine red siltstone sediments are in the range 150–600°C. Further work is needed to fully demonstrate the primary nature of the magnetization within both the lava and the sediment. Indeed, the largest inclination error after tilt correction (Table 2) occurred at this site in the siltstone beds and the reverse magnetization could be a chemical magnetization acquired during emplacement of nearby Eocene intrusions. In this case, the volcanic flow was not affected by remagnetization because of an initial high oxidation state or low permeability.

7. Effects of remagnetization by dyke intrusion

The nature of the magnetization at most sites need to be assessed carefully. The emplacement of volcanic rocks within the Purilactis Group and the intrusion of dykes and sills may have induced possible remagnetization of the sediments. At a few sites, we performed baked contact tests where dykes intruded sediments. While it is obvious that

Table 2
Mean paleomagnetic results[a]

Site	N	D	I	D	I	k	α_{95}	R	ΔR	F	ΔF	Age
		In situ		Tilt corrected								
CC20	10	67.5	8.9	53.4	−42.2	148.6	4.2	65.1	5.5	2.4	4.9	80
CC20	13	69.3	9	55.4	−43.3	141.4	3.5	67.1	5.0	1.4	4.5	60
CA03	6	19.1	−19.1	57.4	−43.4	28	16.6	66	18.9	4.7	13.8	60
CA06	3	203.9	45.3	240.8	24	171.7	9.4	69	9.1	24.2	8.5	60
CA06	6	350.9	−50.7	58.4	−46.5	49	10.7	66.6	13.1	1.7	9.4	60
CA07	7	243.9	−0.2	228.1	28.7	156.7	5	56.3	6	19.5	5.6	60
CA08	9	69	−23	56.7	−37.1	114.1	5.1	64.9	6.4	11.1	5.7	60
CA10	8	59.9	−21.7	18.3	−48.3	244	3.7	30.0	5.4	−3.7	4.6	80
CA11	10	58.4	−27.5	19.4	−48	63	6.1	31.1	7.9	−4.1	6.1	80
CA12	10	42.2	−42.3	348.7	−39.5	62	6.2	−0.4	7.2	5.1	6.1	80
CA13	6	267.7	33.9	223.5	39.3	43	11.6	51.7	12.6	8.8	10.1	60
CA14	10	88.7	−48.1	35.5	−49.9	128.9	4.5	47.2	6.4	−5.3	5.0	80
CA17	9	94.7	−32	23.3	−49.3	87	5.5	31.6	7.8	−0.3	5.8	60
CA18	11	67.6	−23.1	21.2	−36.7	173.4	3.5	33.0	4.7	8.8	4.4	80
CA20	11	354.1	3	3.5	−35.5	182.3	3.4	15.2	4.6	8.3	4.5	80
CA21	13	155.9	16	168.5	50.1	87.6	4.5	0.2	6.4	−6.3	5.1	80
CA24	8	36.2	−5	25.1	−38.7	39	9.2	30.6	11.4	5.0	10.4	100
CA25	8	31.4	3.8	27	−27.5	44	8.6	32.5	10.0	16.1	10.0	100
CA27	10	55.9	−16.4	29.1	−48.2	57	6.6	34.6	10.1	−5.2	9.1	100
CA28	9	27.2	4.5	15.2	−24.2	120.2	4.7	20.7	7.5	18.8	8.3	100
CA29	17	18.4	−29.1	6.2	−39.9	86	3.9	11.7	7.5	3.1	8.0	100
CA30	9	41.6	−27.8	15	−49.9	60	6.7	20.5	10.4	−6.9	9.1	100
CA31	6	71.4	−28.8	35.1	−31	47	9.8	40.6	11.1	12.7	10.7	100
CA31	6	218.4	46.9	269.7	31.8	128.4	5.9	46.6	7.9	1.2	6.1	60
CA31	5	275.4	55.6	181.6	51.3	137.8	6.5	9.8	9.2	−3.2	6.5	60
CA32	16	59.5	−22.5	4.5	−36	7.8	14.1	16.2	14.3	8.5	11.7	80
CA33	12	39.9	−40	12.4	−37	10	15.3	24.1	15.4	6.7	12.5	80
CA34	13	359	−8.8	46.8	−50.4	63	5.3	58.5	7.4	−5.8	5.5	80
CA35	8	14.3	−1.7	42.3	−42.1	166	4.7	50.5	6.4	6.1	5.4	60
CA36	9	103.7	−41.3	24.2	−41	827.3	1.8	32.4	4.3	7.1	4.2	60
CA37	8	93.9	−27.8	42	−34.1	34.5	9.7	50.2	10.1	14	8.7	60
CA38	13	82.3	−41.6	21	−34.4	17	10.3	29.2	10.7	13.7	9.1	60

[a] N, number of samples used in the calculation of the mean direction; D, I, mean declination and inclination in situ (IS) and after tilt correction (TC) k, Fisher's precision parameter; α_{95}, semi-angle of confidence; $R \pm \Delta R$, $F \pm \Delta F$, rotation and flattening parameters and their associated errors (Demarest, 1983). The rotation was calculated using reference poles from Roperch and Carlier (1992). Age is the estimated age of the magnetization chosen in calculating tectonic parameters.

samples taken within 1 m away from the contact should be remagnetized by dyke intrusion, it is not clear how far the thermal or related thermo-chemical overprint could be seen. At site CC20, the magnetization was highly stable in the sediments and recorded characteristic directions similar to those within the dykes (Table 1). However, the intensity of the magnetization found in the sediment several tens of meters away from the dykes (0.03 A m^{-1}) is of the same order of magnitude than the one observed in sediments from the Lican and Limón Verde members. At site CA31 (Fig. 11), dykes and sills intruded during an interval of reverse geomagnetic polarity, allowing the thermo-chemical overprint to be clearly identified. Within one meter, the overprint is almost complete. More than two meters away from the sill, it was possible to isolate normal-polarity primary magnetization. This observation suggests that thermal overprint due to dyke intrusions is

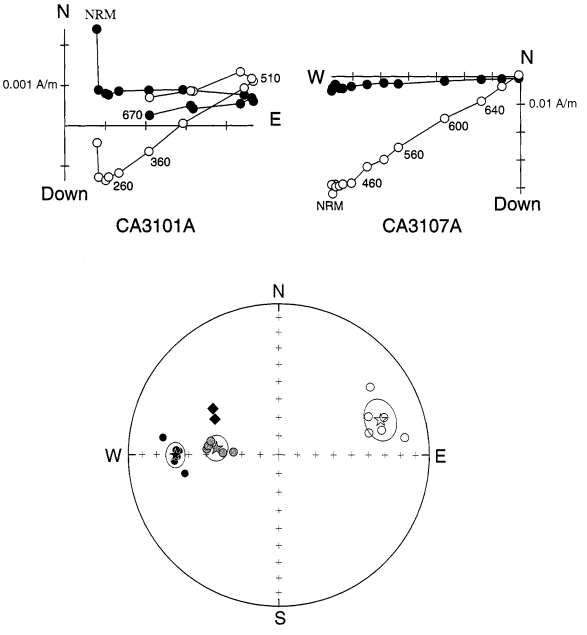

Fig. 11. Orthogonal demagnetization diagrams for samples in sediments nearby sill intrusion (top) in situ coordinates). Sample CA3107A, at <1 m from the sill has a univectorial magnetization while sample CA3101 located >2 m from the sill has both magnetizations. Equal area projection of characteristic directions observed at site CA31 (bottom). Open circles correspond to the primary magnetizations of the red bed sediments (normal polarity) while the magnetizations related to three distinct sills show the reverse polarity. Stars show the mean directions. A mean direction was not calculated for the unit defined by only two samples (lozenges).

not responsible for the well-defined characteristic magnetizations found in the lower members of the Purilactis Formation.

The reverse polarity component observed at site CA21 may be related to dyke or sill intrusion but geological evidence is lacking to support this interpretation.

8. Origin and age of the magnetizations

8.1. Volcanic rocks from the Cerro Totola Unit

A baked contact test, good stability of magnetization during heating, observation of both polarities, and decrease in the dispersion of site-mean directions following tilt correction (Fig. 10) indicate, unambiguously, that the magnetizations are primary and acquired during the emplacement of the volcanic rocks. The presence of both normal and reverse polarities in lavas, dykes and sills is in good agreement with K–Ar dates which indicate Late Cretaceous, possibly Maestrichtian age.

8.2. Red beds from the Tonel and Purilactis Formations

Most sites for which a well-defined paleomagnetic direction is observed are stratigrapically below the Cerro Totola volcanic rocks. Samples from all sites (except site CA21, three samples in the upper part of section at site CA33, and four samples out of 19 drilled at site CA10) have a normal polarity characteristic magnetization. An overprint in the present-day field is easily rejected as an explanation because characteristic magnetization is clearly prefolding as shown by the increase in the concentration of the data after tilt correction ($k=7$; $k=22$ before and after tilt correction, respectively) (Fig. 12). Largest difference is even observed in inclination-only statistics ($k=10$; $k=46$ before and after tilt correction, respectively).

As previously discussed, we also discarded a thermal overprint during dyke intrusion. Moreover both polarities are observed in the intrusive rocks.

At most sites, except in the lowest levels of the Tonel Formation, there is a substantial detrital volcanic content. Optical observations in reflected light show the presence of detrital magnetite and hematitic cement. Petrographic studies of the sediments indicate also that hematite was formed

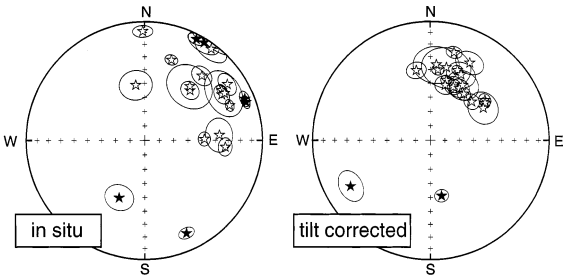

Fig. 12. Equal area projection of site-mean directions in red bed sediments. Upon tilt correction, the site-mean directions are better clustered. The elongated pattern indicates variable amount of tectonic rotations.

during the early phase of diagenesis. Unblocking temperatures of the characteristic normal polarity component are widely distributed between 200 and 660°C (Fig. 7). Samples with high values of magnetic susceptibility contain detrital magnetite. There is, however, strong evidence that magnetite carries a viscous overprint (Figs. 6 and 7), it is thus likely that the diagenetic cement is the main carrier of the characteristic magnetization. The magnetization is thus mainly a chemical magnetization.

Numerous paleomagnetic results obtained in red beds in the Andes (Aubry et al., 1996; Roperch et al., 2000) or elsewhere (Tauxe and Kent, 1984) indicate a significant inclination shallowing in detrital magnetization. It is interesting to note that, on average, inclination shallowing is not statistically significant for most sites from the Limón Verde and Licán members. This observation suggests a chemical origin for the characteristic magnetization found at these sites.

The overwhelming presence of the normal polarity characteristic magnetization in the Tonel, Limón Verde and Licán sediments indicates magnetization during the Cretaceous normal polarity superchron. Only paleomagnetic results from site CA33 and four samples at site CA10 do not support the previous interpretation. Samples with reversed magnetization from site CA21 (Vizcachita) and CA06 (Cerro Totola sediments) were magnetized after the Cretaceous normal polarity superchron.

9. Tectonic rotations

For each site, tectonic rotations and inclination errors were calculated according to the estimated age given to the magnetization and using reference poles provided by Roperch and Carlier (1992). Although refinements in the apparent polar wander path of the South American plate are still needed, there is a good agreement amongst various authors about the Late Cretaceous reference pole (Beck, 1999).

Upon grouping sites into local areas, a mean rotation was calculated for each area (Fig. 13). Tectonic rotations are clockwise and vary significantly in magnitude. There is well-defined spatial variation in the magnitude of the rotations. The largest rotations (45–65°) are observed in the region to the south of Cerro Totola. East of Cerro Quimal, tectonic rotations are ca. 25°. In the area of the Barros Arana Syncline, $<10^{\circ}$ of rotation is observed along the south-eastern border of the syncline while the study by Hartley et al. (1992b) documents larger rotations in the northern sector of the syncline (the recalculated rotation value is $49^{\circ} \pm 9.6$; the lowest value of rotation of $29 \pm 10^{\circ}$ in the original publication was due to an error in the calculation of the rotation).

The paleomagnetic results obtained in the Late Cretaceous volcanic rocks constrain the maximum possible age for the occurrence of rotation to the Paleocene. The minimum age of the rotation is not well constrained but paleomagnetic results, in Middle Miocene rocks from the Calama Basin (Somoza et al., 1999), demonstrate that rotations occurred prior to the Middle Miocene. Hartley et al. (1992b) attempted to obtain paleomagnetic data in coarse-grained sandstones from the Oligocene Paciencia Formation. Unfortunately, dispersion is so high that these results cannot be considered reliable.

10. Discussion

Available data indicate that tectonic rotations along El Bordo Escarpment occurred, at least, after the emplacement of the Maestrichtian Cerro Totola Unit. This rotation possibly occurred during the regionally important Eocene deformation that affected the Cordillera de Domeyko (Maksaev, 1990; Tomlinson et al., 1994).

In the northern Barros Arana Syncline (Fig. 13) results from Hartley et al. (1992b) indicate clockwise rotation of ca. $49 \pm 10^{\circ}$. Our results from the center of the Barros Arana Syncline indicate however that the syncline did not rotate as a single rigid block. The large rotation documented by Hartley et al. (1992b) is related to the strong deformation that characterizes the northern part of the syncline. Further south, east of Cerro Quimal, where tectonic rotation is less significant, the NNE trending syncline axis correlates with the

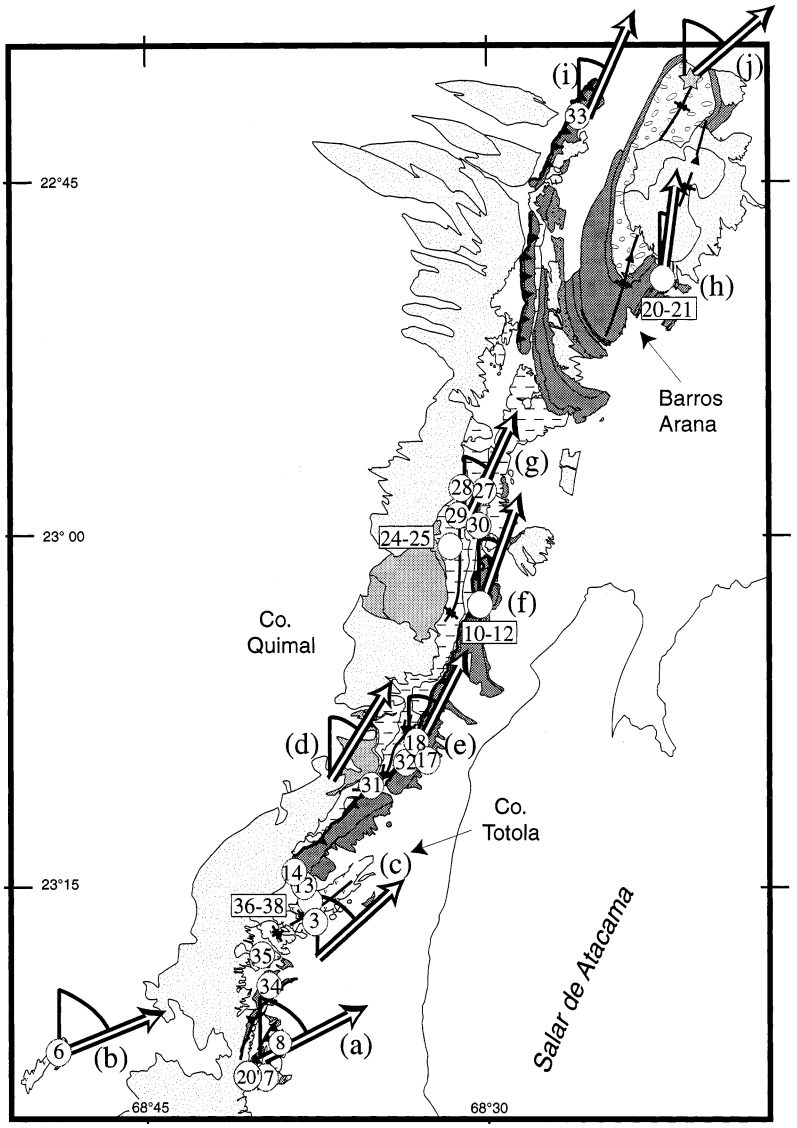

Fig. 13. Simplified geological map showing variation in the magnitude of tectonic rotations. A mean rotation indicated by the large arrow was calculated for each area where paleomagnetic results are available. The largest rotations are observed in the southern area. Rotation seems to be correlated to tectonic structures, especially in the area of Cerro Totola where the fold axes strike northeast. However, the largest rotations are observed farther south where the structures strike north–northeast. Mean rotation values and standard deviation for each locality: a: (CC20a&b, CA7,8) $R=63.3^{\circ}\pm4.8$; b, (CA06a&b) $R=67.8^{\circ}$; c, (CA3,35,36,37,38) $R=47.8^{\circ}\pm14.4$; d, (CA31a,b&c) $R=32.3^{\circ}\pm17.7$; e, (CA17,18,32) $R=26.9^{\circ}\pm9.3$; f, (CA10,11,12) $R=20.2^{\circ}\pm17.8$; g, (CA24,25,27,28,29,30) $R=25.1\pm8.9$; h, (CA20,21) $R=7.7\pm10.6$; i, (CA33) $R=24.1\pm15.4$; j, section from Hartley et al. (1992b) $R=49.0\pm9.6$.

paleomagnetic rotation (20.2°). Larger rotations (48.2°) occur again in the Cerro Totola area, along the southern edge of the Cerro Quimal basement block (Fig. 13) where the frontal syncline axis trends N60°E. The spatial variation in the magnitude of rotations shows, that the syncline did not behave as a rigid block. Instead, along-strike variations in both structure trends and vertical-axis

rotation suggest a causal link between Eocene deformation and rotation.

Much larger rotations were found south of Cerro Totola (63.3°) and within the Cordillera de Domeyko (67.8°) (Fig. 13). South of Cerro Totola, the large rotation does not correlate with local structure since fold axes and thrusts trend NS to NNE near this site. To date, we have not been able to find a mechanism such as strongly dipping fold axes (MacDonald, 1980) to explain these local large rotations. The single result from site 6 must be seen as preliminary and further work is needed to document rotations within the Cordillera de Domeyko.

Several models have been advanced to explain vertical-axis rotation in northern Chile. Our new paleomagnetic results from the eastern border of the Cordillera de Domeyko provide additional evidence that clockwise vertical-axis rotations are characteristic of deformation within the southern Central Andes. Several authors have suggested that tectonic rotations may be related to oroclinal bending associated to the uplift of the Altiplano-Puna plateau (MacFadden et al., 1995; Butler et al., 1995). However, Roperch et al. (2000) and Coutand et al. (1999) suggest that rotations within the Altiplano-Puna occurred during the Miocene while rotation within the fore-arc and the Precordillera of Chile occurred prior to the Miocene. This interpretation is also supported by results in Miocene rocks from the Calama Basin where no significant rotation was observed (Somoza et al., 1999). On the other hand, the significant variation in the magnitude of rotation observed in our study demonstrates that large rotations are related to local deformation rather than to an homogeneous global rotation of the whole northern Precordillera.

An other tectonic mechanism is needed to explain the large rotations. For example Randall et al. (1996) and Forsythe and Chisholm (1994) suggest that tectonic rotation within the Coastal Cordillera are related to sinistral shear along the Atacama Fault System or the Central Valley Fault System during the Cretaceous. In contrast Beck et al. (1986) suggested that oblique convergence inducing dextral shear was responsible for the pattern of clockwise rotation. Such a strain partitioning model (see also Fitch, 1972; Dewey and Lamb, 1992) seems to apply to well-known present-day deformation field like Northwestern America (Wells and Heller, 1988; Beck et al., 1994) or New Zealand (Lamb, 1988) where boundary forces acting on the edge of the plates seem to directly control the deformation.

According to the plate convergence vectors published by Pardo-Casas and Molnar (1987), NNE directed convergence in northern Chile during the Eocene–Early-Oligocene should result in right lateral shear along the Domeyko Fault System (Fig. 1). Evidence for a significant amount of dextral shear in the Cordillera de Domeyko during this period is, however, lacking. Detailed geological mapping and available structural data indicate, on the contrary, sinistral transpression (Mpodozis et al., 1993a,b; Tomlinson et al., 1994; Padilla-Garza, 1998).

Shear traction at the base of the brittle crust (Royden, 1996; Bourne et al., 1998) is the only way to reconcile the observed pattern of rotation with the available structural information. Such a model was proposed by Yañez et al. (1994) to explain the contradiction with the dextral displacements predicted by the application of the rigid block partitioning models. Northward directed flow in the middle to lower crust controlling the deformation field in the brittle upper crust coupled with the local boundary conditions in the Salar de Atacama region, could explain why the sense of rotation is systematically clockwise. It does not however explain the large variation in the magnitude of the rotations. This variation is however better understood if we consider strong rheological heterogeneities in the upper crust and strong lateral shortening gradients along the eastern border of the Cordillera de Domeyko. The largest rotations observed near the Cerro Totola area may correspond to a transfer zone between the Cerro Quimal block and the Cerro Negro block.

11. Conclusions

The paleomagnetic results obtained from the basal units of the Purilactis Group (Tonel Formation and lower members of the Purilactis

Formation) indicate acquisition of the characteristic magnetization during a normal polarity interval. This observation and the Late Cretaceous age of the overlying volcanic rocks (Cerro Totola Strata) suggest that deposition and magnetization of the lowermost units of the Purilactis Group occurred during the Cretaceous normal polarity superchron (119–84 Ma). Although the age of the deformation is difficult to constrain accurately, available stratigraphic and radiometric and the regional structural pattern suggest that deformation occurred during the Eocene. The spatial variation of the rotations indicates that local structures controlled or enhanced the rotations. Previous models for Eocene deformation in the Cordillera de Domeyko (Mpodozis et al., 1993a,b) predicted clockwise rotations associated with sinistral transpression. Our study confirms the existence of clockwise rotations along the eastern margin of the Cordillera de Domeyko. The paleomagnetic results obtained in this study confirm the regional significance of clockwise vertical-axis rotations in the northern Chilean Andes.

Acknowledgements

Funding for this study was provided by Fondecyt Grant No. 1970002 (C. Mpodozis, project's leader). The authors thank Andy Tomlinson for numerous discussions about the structural evolution of the Cordillera de Domeyko and Rubén Somoza for providing preprints of his unpublished paleomagnetic data. This study was also motivated by preliminary results obtained at two sites during a reconnaissance survey with Guillaume Dupont-Nivet and Pierre Gautier from Géosciences Rennes. Fieldwork facilities were provided by Sernageomin.

References

Arriagada, C., 1999. Geología y Paleomagnetismo del Borde Occidental del Salar de Atacama. M.Sc. Thesis, University Chile, Dep. Geol., Santiago.

Aubry, L., Roperch, P., Urreiztieta, M., Rossello, E.A., Chauvin, A., 1996. Paleomagnetic study along the southeastern edge of the Altiplano–Puna plateau: Neogene tectonic rotations. J. Geophys. Res. 101, B8, 17883–17889.

Beck, M.E., 1998. On the mechanism of crustal block rotations in the Central Andes. Tectonophysics 299, 75–92.

Beck, M.E., 1999. Jurassic and Cretaceous apparent polar wander relative to south america: some tectonic implications. J. Geophys. Res. 104, 5063–5068.

Beck, M.E., Drake, R.E., Butler, R.F., 1986. Paleomagnetism of Cretaceous volcanic rocks from central Chile and implications for tectonics of the Andes. Geology 14, 132–136.

Beck, M.E., Rojas, C., Cembrano, J., 1993. On the nature of buttressing in margin-parallel strike–slip fault systems. Geology 21, 755–758.

Beck, M.E., Burmester, R.R., Drake, R.E., Roley, P.D., 1994. A tale of two continents: some tectonic contrasts between the central Andes and the North American Cordillera, as illustrated by their paleomagnetic signatures. Tectonics 13 (1), 215–224.

Bourne, S.J., England, P.C., Parsons, B., 1998. The motion of crustal blocks driven by flow of the lower lithosphere and implications for slip rates of continental strike–slip faults. Nature 391 (12), 655–659.

Breitkreutz, C., Helmdach, F.F., Kohring, R., Mosbruger, V., 1992. Late Carboniferous Intra-arc sediments in the North Chilean Andes. Stratigraphy, Paleogeography and Paleoclimate: Facies 26, 67–80.

Brüggen, J., 1942. Geología de la Puna de San Pedro de Atacama y sus formaciones de areniscas y arcillas rojas Santiago.. Proc., Congr. Pan. Ing. Min. Geol., Santiago 2, 342–367.

Butler, R.F., Richards, D.R., Sempéré, T., Marshall, L.G., 1995. Paleomagnetic determinations of vertical axis tectonic rotations from late Cretaceous and paleocene strata of Bolivia. Geology 23 (9), 799–802.

Charrier, R., Reutter, K.J., 1995. The Purilactis Group of Northern Chile: Boundary between Arc and Backarc from Late Cretaceous to Eocene. In: Reutter, K.J.et al., (Eds.), Tectonics of the Southern Central Andes. Springer Verlag, Berlin, pp. 189–202.

Cornejo, P., Tosdal, R.M., Mpodozis, C., Tomlinson, A., Rivera, O., 1997. El Salvador, Chile, porphyry copper revisited: geologic and geochonologic framework. Int. Geol. Rev. 39, 22–54.

Coutand, I., Roperch, P., Chauvin, A., Cobbold, P., Gautier, P., 1999. Vertical-axis rotations across the Puna plateau (Northwestern Argentina) from paleomagnetic analysis of Cretaceous and Cenozoic rocks. J. Geophys. Res. 104, 22965–22984.

Davidson, J., Ramírez, C.F., Gardeweg, M., Brook, M., Pankhurst, R.J., 1985. Calderas del Paleozoico superior-Triásico inferior y mineralización asociada. Comunicaciones Dep. Geol. Univ. Chile 35, 53–57.

Demarest, H.H.J., 1983. Error analysis for the determination of tectonic rotation from paleomagnetic data. J. Geophys. Res. 88, B5, 4321–4328.

Dewey, J.F., Lamb, S., 1992. Active tectonic of the Andes. Tectonophysics 205, 79–95.

Dingman, R.J., 1963. Cuadrángulo Tulor. Inst. Invest. Geol. Carta Geol. Chile 11 (1:50 000).

Fitch, T.J., 1972. Plate convergence, transcurrent faulting and internal deformation adjacent to Southeast Asia and the Western Pacific. J. Geophys. Res. 77 (23), 4432–4460.

Forsythe, R., Chisholm, L., 1994. Paleomagnetic and structural constraints on rotations in the North Chilean Coast Ranges. J. South Am. Earth Sci. 7, 3/4, 279–295.

Forsythe, R.D., Kent, D., Mpodozis, C., Davidson, J., 1987. Paleomagnetism of Permian and Triassic rocks, central Chilean Andes. In: Elliot et al., (Eds.), Gondwana Six. Structure, Tectonics and Geophysics, AGU Geophys. Monograph 40, 241–252.

Hammerschmidt, K., Döbel, R., Friedrichsen, H., 1992. Implication of 40Ar/39Ar dating of Tertiary volcanics rocks from the north-Chilean Precordillera. Tectonophysics 202, 55–81.

Hartley, A., Flint, S., Turner, P., Jolley, E.J., 1992a. Tectonic controls on the development of a semi-arid aluvial basin as reflected in the stratigraphy of the Purilactis Group (Upper Cretaceous–Eocene) northern Chile. J. South Am. Earth Sci. 5, 275–296.

Hartley, A., Jolley, E., Turner, P., 1992b. Paleomagnetic evidence for rotations in the Precordillera in northern Chile: structural constraints and implications for the evolution of the Andean forearc. Tectonophysics 205, 49–64.

Heki, K., Hamano, Y., Kinoshita, H., Taira, A., Kono, M., 1984. Paleomagnetic studies of Cretaceous rocks of Peru, South America: evidence for rotation of the Andes. Tectonophysics 108, 267–281.

Heki, K., Hamano, Y., Kono, M., 1985. Paleomagnetism of the Neogene Ocros dyke swarm, the Peruvian Andes: implications for the Bolivian orocline. Geophys. J. R. Astron. Soc. 80, 527–534.

Isacks, B.L., 1988. Uplift of the central Andean plateau and bending of the Bolivian orocline. J. Geophys. Res. 93, 3211–3231.

Kirschvink, J.L., 1980. The least-squares line and plane and the analysis of paleomagnetic data. Geophys. J. R. Astron. Soc. 62, 699–718.

Lamb, S.H., 1988. Tectonic rotations about vertical axes during the last 4 Ma in part of the New Zealand plate-boundary zone. J. Struct. Geol. 10 (8), 875–893.

MacDonald, W.D., 1980. Net tectonic rotation, apparent tectonic rotation and the structural tilt correction in paleomagnetic studies. J. Geophys. Res. 85, 3659–3669.

Macellari, C.E., Su, M.J., Townsend, F., 1991. Structure and seismic stratigraphy of the Atacama Basin, Northern Chile. Proc. VI Congr. Geol. Chileno 1, 133–137.

MacFadden, B.J., Anaya, F., Swisher III, C.C., 1995. Neogene paleomagnetism and oroclinal bending of the Central Andes of Bolivia. J. Geophys. Res. 100, B5, 8153–8169.

Maksaev, V., 1990. metallogeny, geological evolution and termochronology of the Chilean Andes between latitudes 21° and 26°S and the origin of major copper depsosits. PdD Thesis, Dalhousie University.

Marinovic, N., Cortés, J., García, M., 1996. Estudio geológico regional de la zona comprendida entre Sierra del Buitre y Pampa San Román. Serv. Nac. Geol. Min. IR 96-8.

May, S.R., Butler, R.F., 1985. Paleomagnetism of the Puente Piedra Formation, central Peru. Earth Planet. Sci. Lett. 72, 205–218.

McFadden, P.L., McElhinny, M.W., 1988. The combined analysis of remagnetization circles and direct observations in paleomagnetism. Earth Planet. Sci. Lett. 87, 161–172.

McFadden, P.L., Reid, A.B., 1982. Analysis of paleomagnetic inclination data. Geophys. J. R. Astron. Soc. 69, 307–319.

Mpodozis, C., Marinovic, C., Smoje, I., 1993a. Estudio geológico-estructural de la Cordillera de Domeyko entre Sierra Limón Verde y Sierra Mariposas Región de Antofagasta. Serv. Nac. Geol. Min. IR 93-04.

Mpodozis, C., Marinovic, C., Smoje, I., 1993b. Eocene left lateral strike–slip faulting and clockwise block rotations in the Cordillera de Domeyko, west of Salar de Atacama, Northern Chile. Proc. II. ORSTOM ISAG, Chile, pp. 195–198.

Mpodozis, C., Arriagada, C., Roperch, P., 1999. Cretaceous to Paleogene Geology of the Salar de Atacama Basin, Northern Chile: A Reaprissal of the Purilactis Group Stratigraphy. Proc. IV IRD ISAG, Chile, pp. 523–526..

Muñoz, N., Charrier, R., Reutter, J.K., 1997. Evolución de la Cuenca del Salar de Atacama: Inversión tectónica y relleno de una cuenca de antepais de retroarco. Proc. VIII Congr. Geol. Chileno 1, 195–199.

Padilla-Garza, R., 1998. Geology of the Escondida porfhyry copper deposit, Antofagasta, Chile, Master of Science, University of Arizona.

Pardo-Casas, F., Molnar, P., 1987. Relative motion of the Nazca (Farallon) and South American plates since Late Cretaceous time. Tectonics 6, 233–248.

Ramírez, C.F., Gardeweg, M., 1982. Hoja Toconao Región de Antofagast. Serv. Nac. Geol. Min. Carta Geol. Chile 58 (1:250 000).

Randall, D.E, Taylor, G.K., Grocott, J., 1996. Major crustal rotations in the Andean margin: paleomagnetic results from the Coastal Cordillera of northern Chile. J. Geophys. Res. 101, B7, 15783–15798.

Reutter, J.K., Scheuber, E., 1991. Structural evidence of orogen-parallel strike, slip displacements in the Precordillera of northern Chile. Geol. Rundsch. 80 (1), 135–153.

Riley, P.D., Beck, M.E., Burmester, R.F., Mpodozis, C., Garcia, A., 1993. Paleomagnetic evidence of vertical-axis block rotation from the Mesozoic of north-central Chile. J. Geophys. Res. 98, B5, 8321–8333.

Roperch, P., Carlier, G., 1992. Paleomagnetism of Mesozoic rocks from the central Andes of Southern Peru: importance of Rotation in the Development of the Bolivian Orocline. J. Geophys. Res. 97, B12, 17233–17249.

Roperch, P., Dupont-Nivet, G., Pinto, L., 1997. Rotaciones Tectónicas en el Norte de Chile. Proc. VIII Cong. Geol. Chileno 1, 241–245.

Roperch, P., Fornari, M., Hérail, G., Parraguez, G., 2000. Tectonic rotations within the Bolivian Altiplano: implications for the geodynamic evolution of the Central Andes during the late Tertiary. J. Geophys. Res. 105, 795–820.

Royden, L., 1996. Coupling and decoupling of crust and mantle in convergent orogens: implications for strain partitioning in the crust. J. Geophys. Res. 101, 17679–17705.

Somoza, R., Singer, S., Tomlinson, A., 1999. Paleomagnetic study of upper Miocene rocks from northern Chile: implications for the origin of late Miocene–Recent tectonic rotations in the Southern Central Andes. J. Geophys. Res. 104, 22923–22936.

Swanson, M.T., 1989. Sidewall ripouts in strike–slip faults. J. Struct. Geol. 11 (8), 933–948.

Tauxe, L., Kent, D.V., 1984. Properties of a detrital remanence carried by hematite from study of modern river deposits and laboratory redeposition experiments. Geophys. J. R. Astr. Soc. 77, 543–561.

Taylor, G.K., Grocott, J., Pope, A., Randall, D.E., 1998. Mesozoic fault systems, deformation and fault block rotation in the Andean forearc: a crustal scale strike–slip duplex in the coastal Cordillera of northern Chile. Tectonophysics 299, 93–110.

Tomlinson, A.J., Blanco, N., 1997. Structural evolution and displacement history of the west fault system, Precordillera. Proc. VIII Congr. Geol. Chileno 3, 1882–1973.

Tomlinson, A.J., Mpodozis, C., Cornejo, P., Ramírez, C.F., Dimitru, T., 1994. El sistema de fallas Sierra Castillo-Agua Amarga: transpresion sinistral eocena en la Precordillera de Potrerillos-El Salvador. Proc. VII Congr. Geol. Chileno 2, 1459–11463.

Wells, R.E., Heller, P.L., 1988. The relative contribution of accretion, shear, and extension to Cenozoic tectonic rotation in the Pacific Northwest. Geol. Soc. Am. Bull. 100, 325–338.

Yañez, G., Mpodozis, C., Tomlinson, A., 1994. Eocene dextral oblique covergence and sinistral shear along the Domeyko Fault System: a thin viscous sheet approach with astenospheric drag at the base of the crust. Proc. VII Congr. Geol. Chileno 2, 1478–1482.

Chapitre IV : Restauration en carte de la déformation et modèles d'évolution de l'Orocline bolivien

Introduction

Les méthodes de restauration de la déformation permettent de reconstruire la géométrie non-déformée d'une région. La différence entre l'état restauré et l'état déformé donne les trajectoires de déplacement fini, déformation, rotations et déplacement des failles, éléments fondamentaux pour analyser et quantifier la cinématique et les relations spatiales de plis et failles. Il est ainsi aussi possible de réviser la cohérence des interprétations géologiques proposées.

Bien que quelques méthodes de restauration de surfaces 3D aient été proposées la plupart ont été développées pour le cas de deux dimensions (sections équilibrées ou en plan). Pour des surfaces 3D, les méthodes de restauration des plis (unfolding) se basent sur la conservation de la surface à restaurer [*Gratier et al*., 1991; *Guillier*, 1991; *Gratier y Guillier*, 1993; *Samson*, 1996; *Williams et al*., 1997] ou sur le déplacement le long de vecteurs avec inclinaison et azimut constant (homegeneous inclined shear) [*Kerr y White*, 1996]. *Rouby et al*. [2000] ont proposé récemment une méthode de restauration 3D. Cette méthode est basée en la restauration des plis et la restauration en plan d'une surface 3D.

Les méthodes de restauration en 2D sont :

(1) Restauration de la déformation (Unstraining) en plan pour régimes de déformation ductile avec déplacement heterogène [*Schwerdtner,* 1977; *Cobbold y Pearcevault*, 1983].

(2) Restauration des plis (Unfolding) de sections équilibrées en conservant la surface [*Dahlstrom,* 1969; *Hossack,* 1979] ou en utilisant des déplacements verticaux ou incliné [*Gibbs,* 1983; *Schultz-Ela*, 1992].

(3) Restauration des failles (Unfaulting) en plan par déplacement et rotation de blocs limités par des failles [*Dokka y Travis*, 1990; *Audibert*, 1991; *Rouby et al*., 1993a; *Bourgeois et al*., 1997].

La restauration de sections équilibrées en 2D est applicable seulement au cas de déformation plane. Des déplacements à l'intérieur ou en dehors de la section ne sont pas permis puisqu'il est nécessaire de conserver la surface. Les méthodes de restauration en plan, contrairement aux méthodes de restauration de sections équilibrées en 2D, peuvent être appliqués à tout type de structures. Celles-ci incluent des régions qui ne présentent pas

une déformation plane. Le déplacement de failles implique le mouvement rigide de blocs. S'il y a une déformation interne dans les blocs (basculement et/ou plissement), cette déformation devrait être décalée avant d'appliquer la restauration en plan. Les procédures de restauration en plan ont été adaptées pour une déformation discontinue et appliquées à des régions dominées par des systèmes décrochants [*Audibert*, 1991], extensifs [*Rouby et al*., 1993a, b, 1996] et compressifs [*de Urreiztieta et al*., 1996; *Bourgeois et al*., 1997].

Les rotations et les déplacements de failles indiquées par ces modèles montrent une bonne corrélation avec les données géologiques (par exemple le bassin du Tajik, *Bourgeois et al*., [1997]). Jusqu'à présent, ces méthodes seulement géométriques n'ont pas considéré, toutefois, une information géologique ainsi que :

(1) Des rotations de blocs
(2) Le sens dans le déplacement de failles

Les données paléomagnétiques des rotations et orientations des failles ont été seulement comparées avec les modèles de restauration. Si la méthode de restauration en plan considérait des données paléomagnétiques ou le sens dans le déplacement de failles la solution devrait être mieux délimitée. Dans le but de considérer les données de rotations paléomagnétiques dans la restauration en plan de la déformation, nous avons modifié les algorithmes de *Audibert*, [1991], *Rouby et al*. [1993] et *Bourgeois et al*. [1997]. Nous avons aussi changé les algorithmes pour modifier la géométrie des blocs pendant la restauration. De cette manière, il est possible de considérer la quantité de raccourcissement tectonique pour certains blocs pendant les itérations. Dans la première partie de ce chapitre, nous présentons la méthode de restauration en mettant particulièrement l'accent sur les modifications que nous avons effectuées. Nous montrons postérieurement des exemples simples de restauration considérant des données de rotation et de raccourcissement tectonique. Finalement, dans le contexte de ce travail de Thèse nous avons essayé de restaurer la déformation de l'Orocline bolivien en utilisant les données de rotations tectoniques et de raccourcissement publiés. De cette manière, un modèle évolutif de l'Orocline des Andes Centrales peut être proposé.

Méthode de Restauration

L'objectif de la méthode est de reconstruire géométriquement l'état original non-déformé d'une surface horizontale qui a été pliée et faillée ou par des failles normales, inverses ou décrochantes. La méthode diminue toutes les séparations ou recouvrements des failles. Si on essaye de restaurer un horizon stratigraphique déterminé les données devraient être acquises à partir des méthodes de *Barr* [1985] y *McCoss* [1988], en utilisant des cartes structurales ou des données de sismique, dans la mesure du possible 3D (Figure IV.1).

L'état actuel déformé d'une surface, pour être restaurée, doit être présenté en plan comme une mosaïque de blocs limités par des failles. Dans cette mosaïque, les blocs peuvent être voisins, séparés par des espaces vides, ou présenter des recouvrements, en accord avec la nature des failles (décrochante, normale ou inverse respectivement) (Figures IV.1&2).

Dans la restauration de surfaces développées dans des régions tectoniques dominées par de l'extension ou de la compression, nous assumons que la surface initiale a été plane, horizontale et continue avant la déformation. Cette hypothèse est raisonnable dans des sédiments marins, où les irrégularités sont généralement petites en comparaison avec l'échelle de travail. Sous ces conditions, la restauration d'une surface stratigraphique considère toute la déformation accumulée depuis la déposition de la couche. Pour le cas compressif, il est nécessaire de déplier chaque bloc séparément [*Bourgeois et al*., 1997]. En général pour des plis non cylindriques il est nécessaire d'utiliser une méthode automatique de déplissement [*Gratier et al*., 1991]. Dans le cas de zones où prédomine le mouvement décrochant, les blocs seront principalement limités par des failles verticales.

Pour avoir un diagramme de blocs totalement limité par des failles, il est nécessaire d'inclure des failles artificielles (Figure IV.1&2). Il est aussi nécessaire d'assumer que les blocs définis sont rigides ou consistent de couches pliées qui seront étirées selon leur direction de raccourcissement pendant la restauration. La supposition que les blocs sont rigides est raisonnable si la déformation à l'intérieur ces blocs est négligeable.

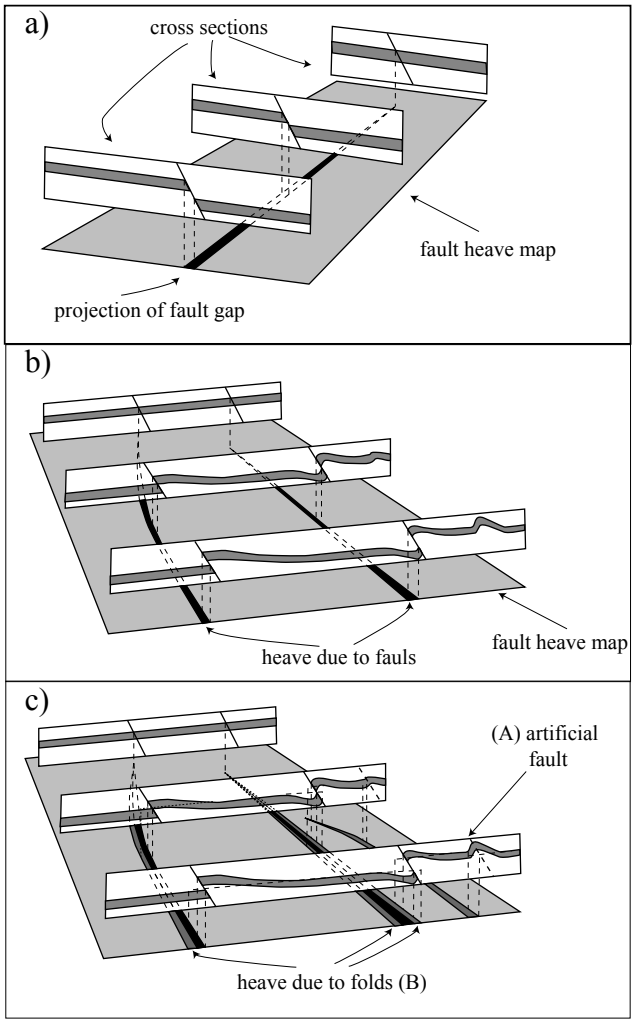

Figure IV.1:Construction of a fault heave map, the surface to be restored is the top of the grey layer visible on sections. (a) extensional tectonics the width of the lens is equal to the heave of the fault (after Rouby et al., 1993a) (b) compressive tectonics, heave map related to reverse faulting (Bourgeois et al., 1997). (c) Unfolding. For a fold of short wavelength and large amplitude (A), an artificial fault is drawn along the axis of the fold. The apparent heave is projected along this artificial fault onto cutoff map. For a fold of long wavelenth and small amplitude (B), the whole block is unfolded and the changes in size and shape are transferred to its external boundaries.

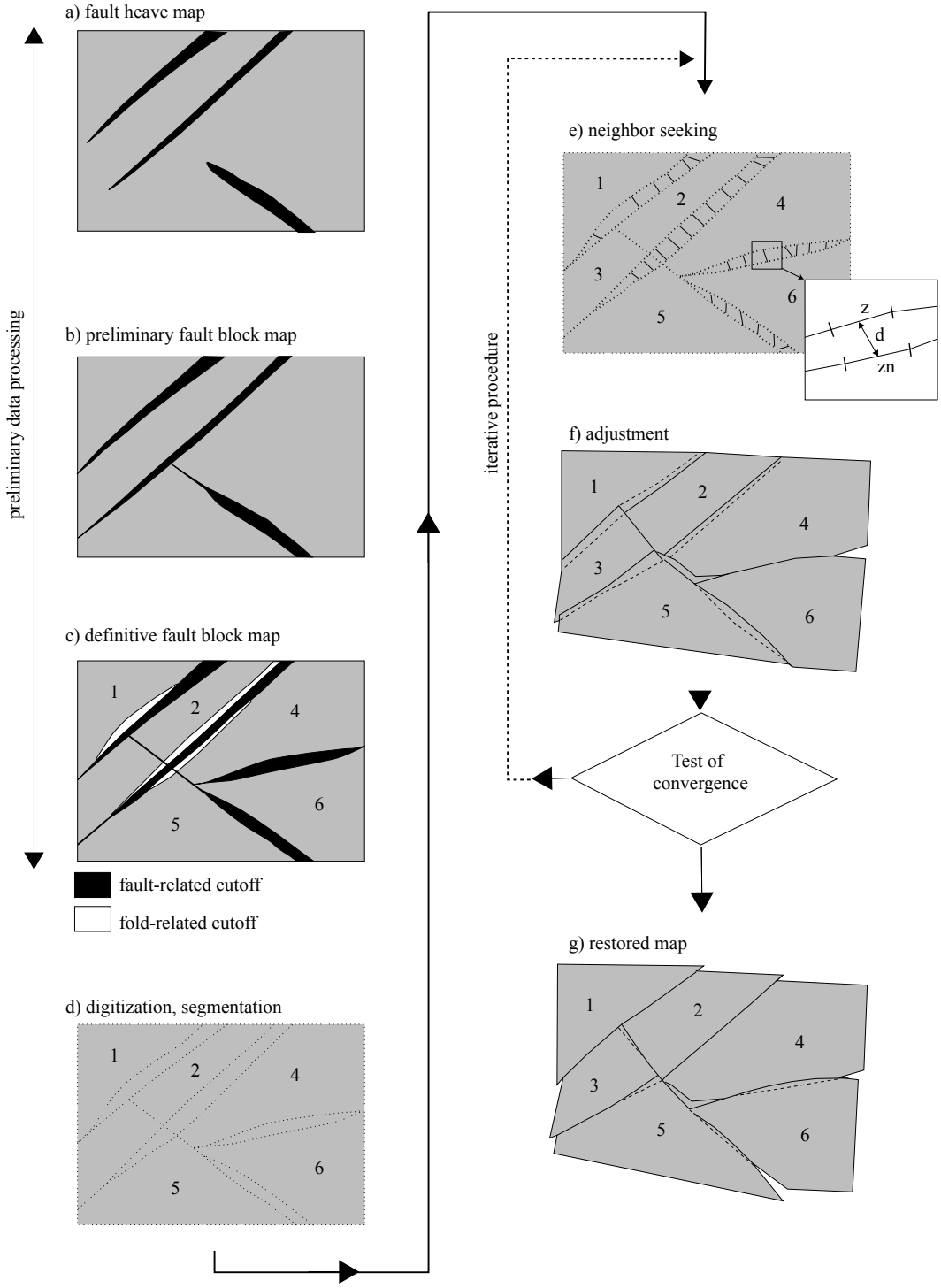

Figure IV.2: Principle of the method of restoration (after Bourgeois et al., 1997). (a) From a structure-contour map and cross sections of the surface to be restored, heaves of the faults are projected onto a preliminary fault heave map. (b) Fault traces are extrapolated to construct fault-bounded blocks. (c) Each block is unfolded and the fault block map is modified accordingly. (d) Bounded of blocks are digitized and their sides are automatically subdivided into line elements of unit length. (e) To each element *z* the program associates a neighboring element *zn* so that *z* and *zn* face each other across a cutoff lens; *d* is the distance between *z* and *zn*. (f) Blocks are then packed by translations and rotations so as to minimize the sum *D* of the squares of all distances *d*. Geological information as paleomagnetic rotations and tectonic shortening can be introduced into the blocks. (g) The neighbor seeking and packing procedures are repeated until *D* becomes stabilized at an acceptably small value.

À partir d'un bloc fixe, la méthode numérique de restauration ordonnera tous les autres blocs (Figure IV.2). Le choix du bloc stationnaire n'affecte pas le résultat de la restauration, toutefois, le déplacement sera calculé à partir du bloc fixe. Pour que les déplacements calculés soient directement comparés avec les données géologiques, le choix du bloc stationnaire doit être approprié.

Procédure Numérique

La figure IV.3 est un diagramme de flux qui résume les pas du programme de restauration et inclut les modifications effectuées pendant ce travail. Les données d'entrée sont les descriptions des blocs où chaque bloc est représenté par son numéro de bloc et les coordonnées de ses points. Le programme découpe automatiquement les côtés de tous les blocs en segments de même dimension (Figure IV.2), dont la longueur est égale au plus petit coté de tous les blocs. Une autre information importante correspond aux valeurs des rotations et erreurs associées acquises à partir des études paléomagnétiques. Des paramètres de déformation (direction et pourcentage de raccourcissement) sont donnés pour certains blocs. Enfin, une information importante est la définition des blocs voisins. Les blocs voisins sont tous ces blocs qui peuvent être en contact avec un bloc déterminé pendant la restauration. La procédure numérique ordonne un bloc dans l'espace existant entre ses blocs voisins en diminuant la somme D des carrés d'un ensemble de distances d. Ces distances sont le module des vecteurs voisins qui séparent le centre de l'élément de ligne voisin avec la hangingwall ou footwall des failles (Figure IV.2). Pour diminuer cette somme, une série des déplacements et des rotations finies se produisent autour du barycentre du chaque bloc.

La minimisation de D donne un système d'équations liées aux déplacements et aux rotations. Pour résoudre les équations, le programme utilise une méthode itérative, semblable à la méthode d'équations linéaires de Gauss-Seidel [*Audibert*, 1991; *Rouby et al*., 1993a]. Une itération correspond à une série d'opérations, qui incluent la recherche des voisins, déplacements des blocs et rotations des blocs. Dans chaque cycle la procédure est répétée en utilisant le même groupe d'éléments voisins jusqu'à ce que les déplacements et les rotations arrivent à une valeur critique pré-définie. Pendant les déplacements et les rotations, la méthode adapte chaque bloc séquentiellement en diminuant les espaces et les recouvrements entre les blocs voisins. Les itérations sont cycliquement répétées jusqu'à ce que les équations convergent. Alors, de nouveaux éléments voisins sont définis et un nouveau cycle commence.

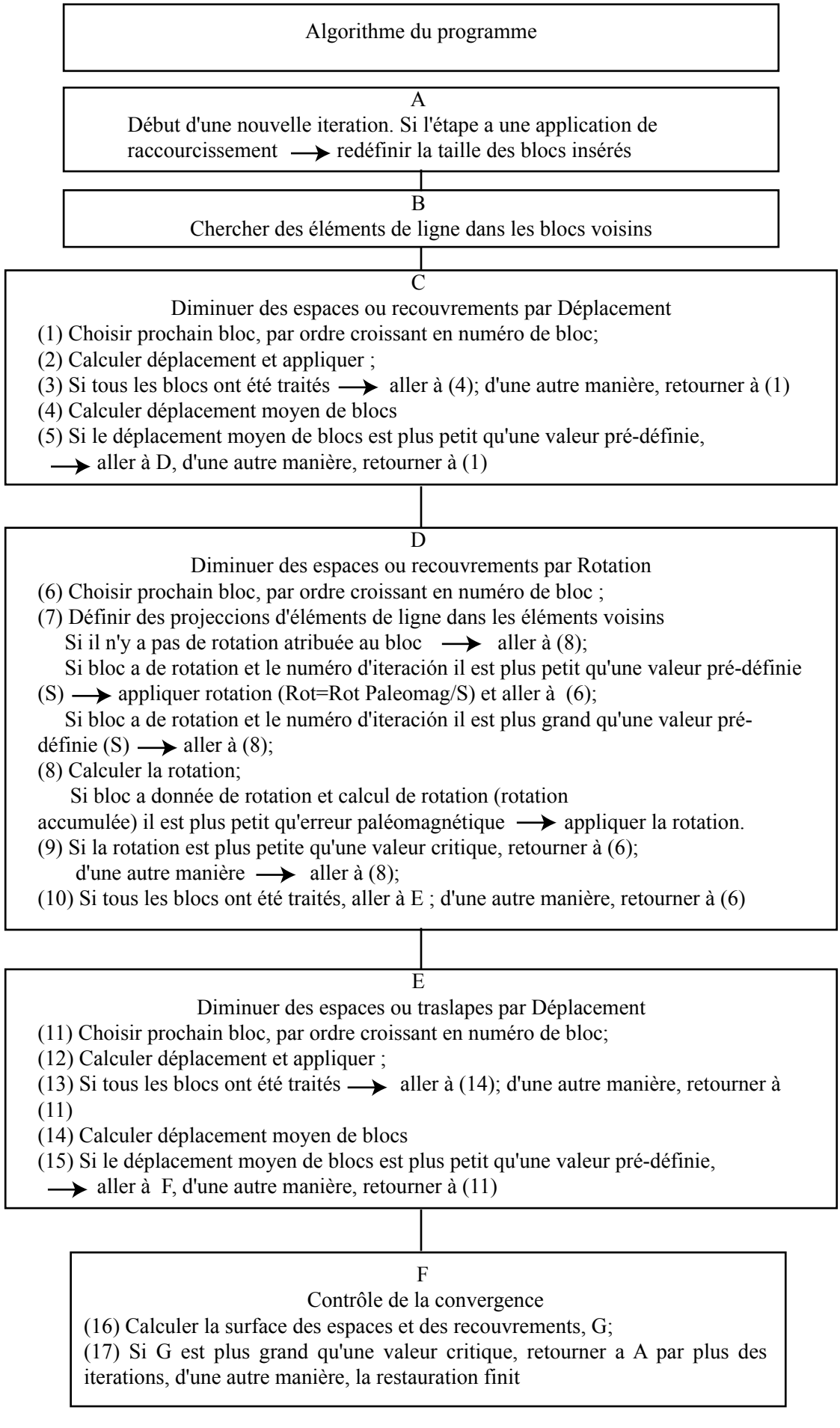

Figure IV.3: Algorithme du programme de restauration

Convergence

Le paramètre qui permet de mesurer la convergence est une valeur sans dimension "G" qui correspond au rapport de la surface totale des espaces et des recouvrements à la surface totale des blocs. La restauration est considérée terminée lorsque G atteint une valeur minimale. La valeur de G est calculée à la fin de chaque itération.

Modifications effectuées aux algorithmes de *Rouby et al.* [1993a] et *Bourgeois et al.* [1997]

Le programme, qui a été modifié, a été écrit principalement par Delphine Rouby. Le programme est en langage C compatible avec le Système Unix sous l'environnement X window. En dehors des implémentations des routines pour prendre en compte les rotations et la déformation des blocs, nous avons aussi modifié la visualisation graphique des restaurations. Un fichier graphique post-script est généré à chaque étape de restauration. Ces fichiers sont ensuite convertis et assemblés pour former une séquence animée au format Quicktime. De cette façon, il est plus facile de suivre l'évolution de la restauration, particulièrement lorsque le modèle comprend un grand nombre de blocs impliquant des temps de calcul importants (> 1 h).

Rotation et Erreur à partir de données paléomagnétiques

Dans les algorithmes développés par *Rouby et al*. [1993a] et *Bourgeois et al*. [1997], les rotations ne sont que des résultats du modèle après la restauration. Ces méthodes, n'ont pas considéré l'information paléomagnétique des rotations de blocs. J'ai modifié les algorithmes afin d'introduire les données de rotation et son erreur dans les calculs. En calculant la rotation d'un bloc le programme cherche automatiquement s'il y a une rotation attribuée au bloc. S'il n'y a pas de donnée, le programme applique les algorithmes déjà définis. Dans le cas contraire, le programme applique la rotation en S itérations que l'utilisateur choisit dans les paramètres du modèle. Si les rotations sont petites nous pouvons incorporer la rotation totale dans les premières itérations (S<10). Lorsque la quantité de rotation est importante, il est cependant nécessaire d'appliquer la rotation par incrément. De cette manière la perturbation produite par la rotation du bloc sera plus petite et permet d'observer une convergence plus rapide lors de la restauration.

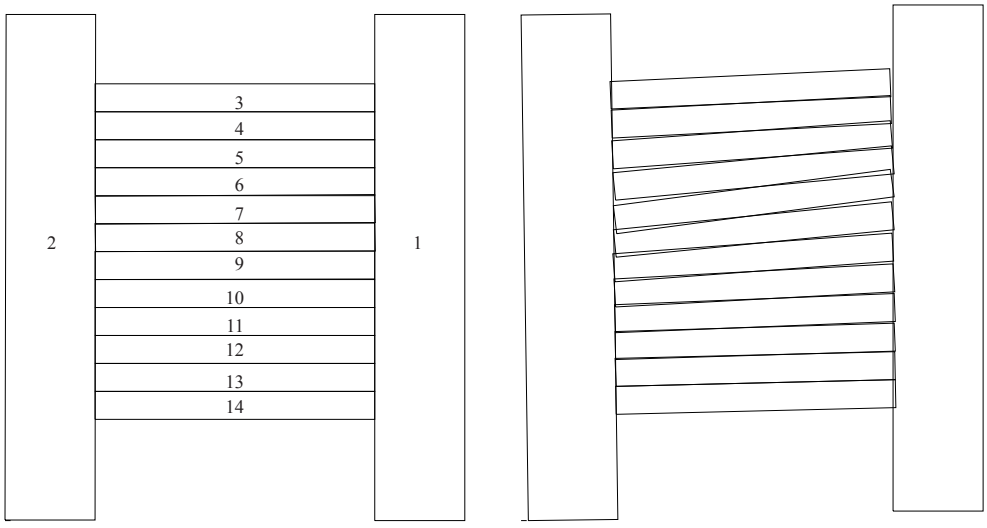

Iteration 0 Iteration 20

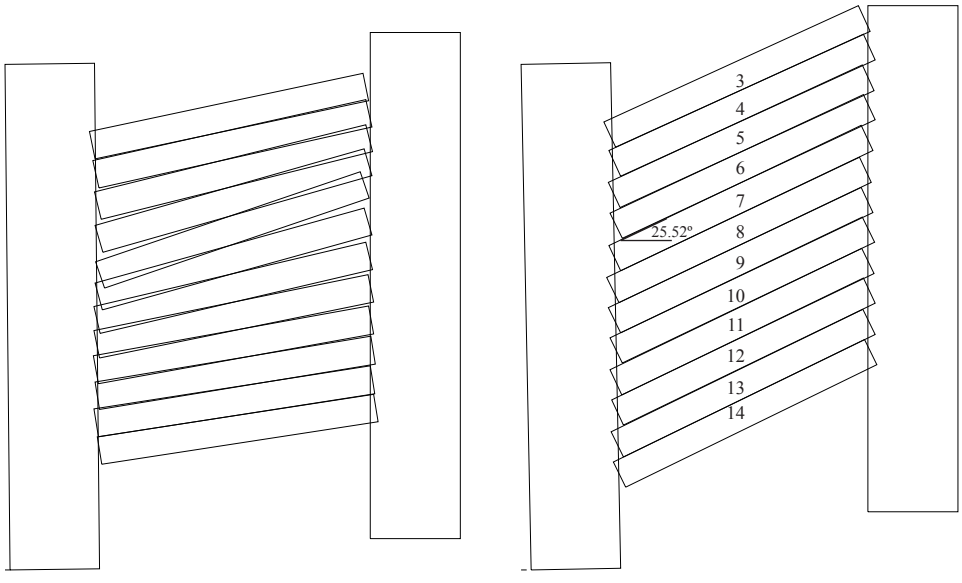

Iteration 50 Iteration 450

Figure IV.4: Example of restoration of a simple domino model. We have only given a rotation of 30º±5º to block 7 in the rotation file. Since we have included an error of 5º in the rotation file, the final rotation was 25.52º for the block 7.

Une fois que le programme a appliqué la rotation paléomagnétique, nous considérons alors l'erreur associée. L'algorithme que nous avons développé permet la rotation d'un bloc seulement dans son intervalle de confiance. Dans les méthodes développées par *Rouby et al*. [1993a] et *Bourgeois et al*. [1997] les rotations étaient produites pendant la minimisation d'espaces et/ou recouvrements. S'il n'y a pas de recouvrements ou d'espaces entre les blocs, le résultat de la restauration est le même que la donnée originale du diagramme de blocs. Dans un modèle à l'origine sans espace ou recouvrement en considérant les rotations paléomagnétiques des recouvrements et/ou des espaces se produisent, qui impliquent une réorganisation du système (Figure IV.4).

Raccourcissement tectonique

Rouby et al. [1993a] et *Bourgeois et al*. [1997] ont proposé la restauration des plis pour des blocs avec déformation interne (unfolding) avant les étapes de restauration. Les études structurales et sismiques effectuées dans la dépression de Tajik [*Bourgeois et al*., 1997] permettent d'avoir un bon contrôle de la structure interne et la géométrie des failles et des plis du bassin. De cette manière, un déplissement des couches pliées avant la restauration en plan a pu être effectuée, et permettant de construire un diagramme de blocs présentant des recouvrements équivalents aux rejets horizontal aux des failles inverses.

Dans les Andes Centrales, des zones comme la chaîne Subandine ou la Cordillère Orientale présentent une structure complexe et un important degré de raccourcissement. Par exemple, si on fait une restauration à l'échelle de la chaîne Subandine, il est difficile de considérer toutes les failles et les plis décrits et de faire une restauration semblable à la dépression de Tajik. Faire une restauration à l'échelle des Andes Centrales en considérant toutes les failles et plis nous obligerait à définir un grand nombre de blocs et recouvrements.

Plusieurs auteurs ont essayé de déterminer le raccourcissement à partir de coupes balancées, particulièrement des les zones subandines. Toutefois les estimations varient d'une étude à un autre pour une même région et seule une valeur moyenne de raccourcissement peut être facilement prise en compte. Ainsi, nous avons développé un algorithme pour restaurer la déformation interne d'un bloc. La méthode considère automatiquement le raccourcissement du bloc et change sa géométrie au fur et à mesure

des itérations. La direction de raccourcissement est aussi progressivement réorientée en fonction des rotations du bloc lors de la restauration

Il n'est pas nécessaire alors de déterminer le recouvrement entre deux blocs (Figure IV.5). De cette manière, différentes modèles tectoniques avec des raccourcissements et directions de raccourcissement différents peuvent rapidement être testés pour un même diagramme de blocs. À chaque itération, la surface des blocs 'étirés' selon la direction de raccourcissement augmente. Il est alors nécessaire de subdiviser à nouveau les côtés des blocs dans des segments de ligne d'égale longueur.

Finalement, puisqu'un même bloc peut souffrir plus d'un événement de déformation avec des directions de raccourcissement différentes, il est possible de tester pour un même bloc divers événements de raccourcissement dans différentes étapes pendant la restauration (voir plus bas).

De cette manière, il est possible d'avoir une représentation 'dans le temps' des différentes étapes de la restauration.

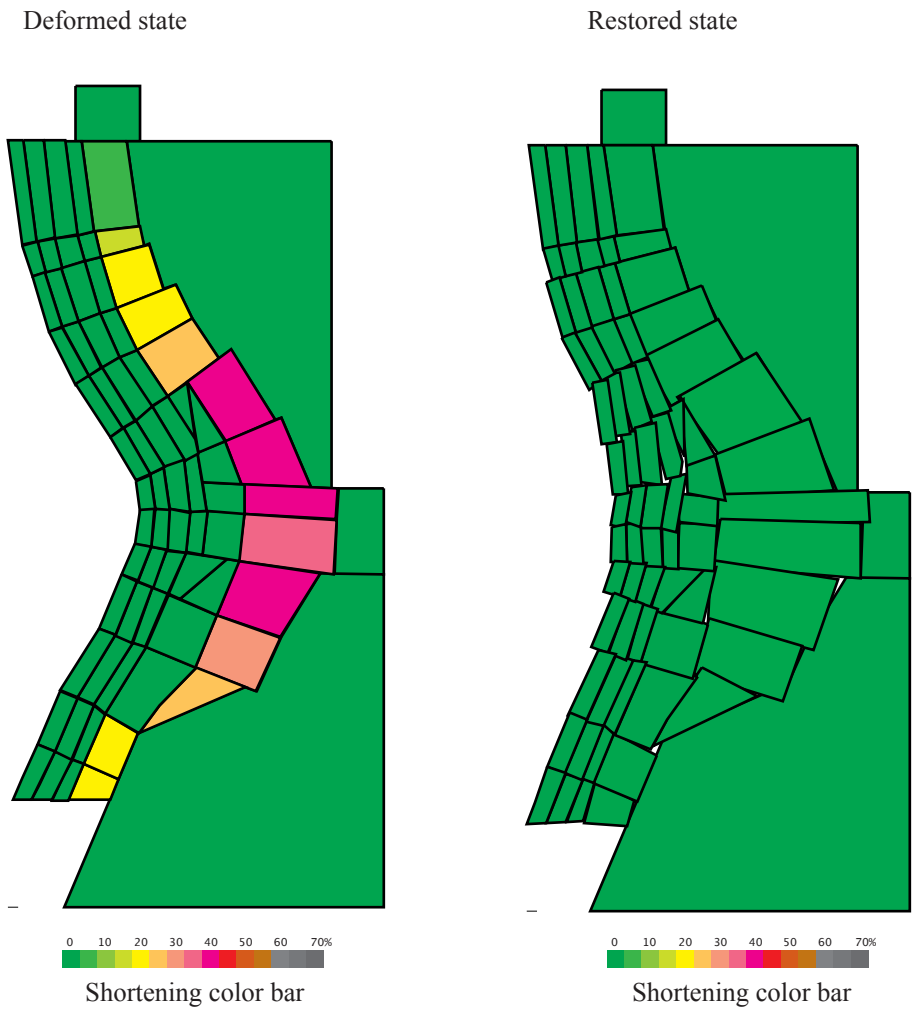

Figure IV.5: Example of restoration using shortening data (Scale of color indicates amount of shortening for each block)

Modèles de restauration de la déformation pour l'Orocline bolivien

Des tentatives de restauration en plan de la déformation dans les Andes Centrales ont été effectuées par *Baby et al*. [1993] et *Kley* [1999]. *Baby et al*. [1993] ont présenté un modèle détaillé de restauration de la zone Subandine à partir de quelques coupes équilibrées. Dans ce modèle, *Baby et al*. [1993] ne considèrent pas de rotations autour d'axes verticaux. *Kley* [1999] a proposé un modèle cinématique simplifié des Andes Centrales entre les 10º à 26ºS. Son modèle utilise principalement le raccourcissement prévu dans les zones Subandine et la Cordillère Orientale mais ses estimations de rotations ne sont pas en accord avec celles qui sont observées dans les études paléomagnétiques. Un modèle cohérent de la restauration de la déformation des Andes Centrales devrait considérer le raccourcissement et la rotation des principaux segments de la chaîne (Cordillère Orientale, Subandine, l'avant arc, etc.) limités par les plus grandes structures. Un modèle plus réaliste devrait aussi considérer les Andes Centrales jusqu'à la déflection de Huancabamba (Figure IV.6&8) [*Mitouard et al*., 1990]. Dans cette région, le raccourcissement documenté dans la zone subandine est seulement de 11 km [*Rodriguez et al*., 2001].

Compilation de données de raccourcissement tectonique

Pendant les dernières années, plusieurs études structurales ont essayé d'estimer la quantité de raccourcissement tectonique pendant le soulèvement des Andes Centrales [par exemple : *Allmendinger et al*., 1983; *Roeder*, 1988; *Sheffels*, 1990; *Baby et al*., 1993,1996,1997; *Dunn* et al., 1995; *Kley*, 1996; *Kley et al*., 1997,1999; *Lamb et Hoke*, 1997; *Kley et Monaldi*, 1998; *Coutand et al*., 2001; *McQuarrie et DeCelles*, 2001; *Rodriguez et al*., 2001; *Müller et al*., 2002]. Les coupes équilibrées faites à partir des données de sismique pétrolière et les informations de terrain permettent d'estimer les raccourcissements pour les zones Subandines et Interandines. Les estimations de raccourcissements sont plus difficiles à établir dans la Cordillère Orientale (Tableau 1). Dans la Cordillère Occidentale et l'avant arc, il n'existe pas d'études détaillées qui permettent pour le moment d'estimer le raccourcissement.

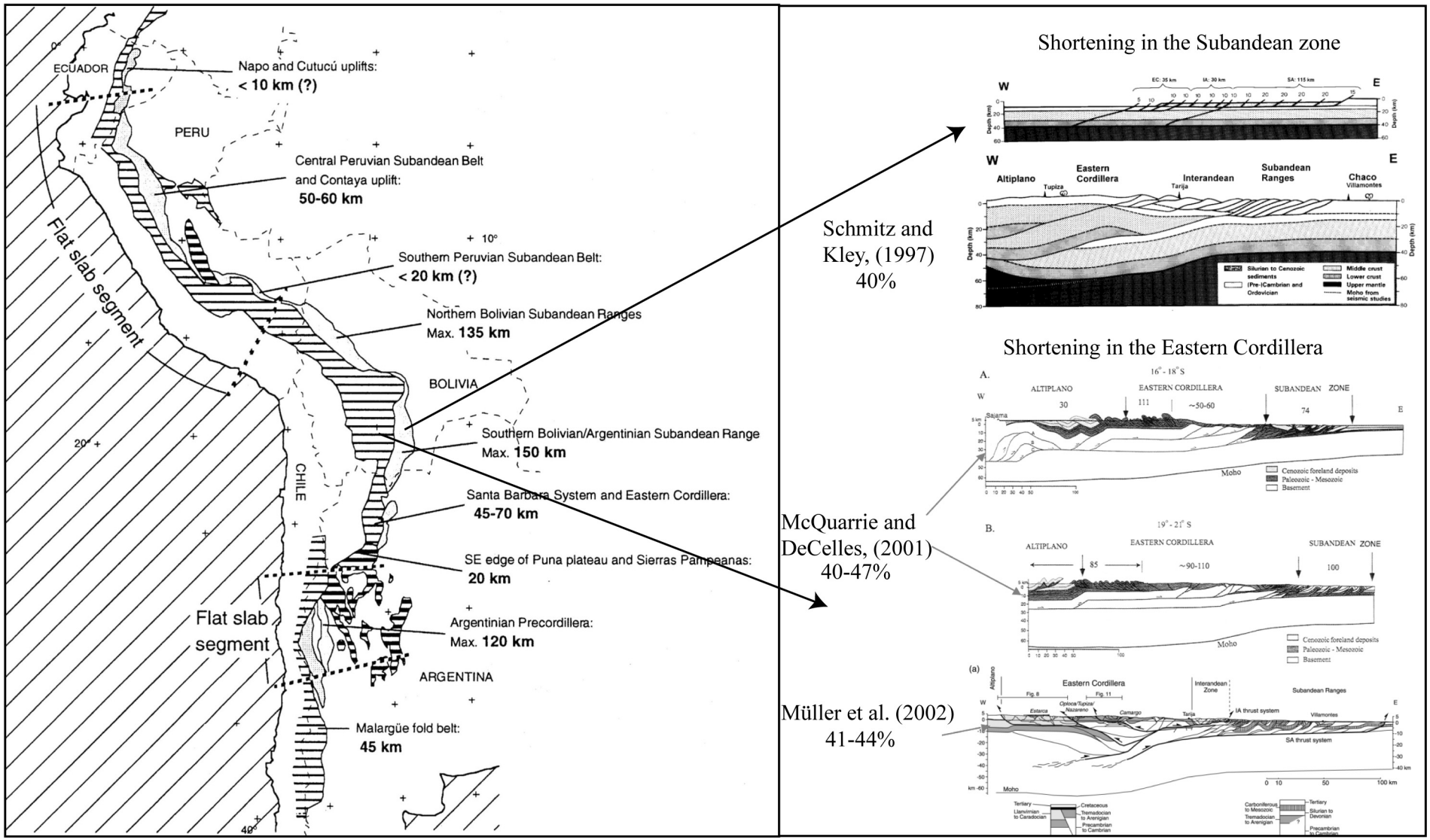

Figure IV.6: Shortening estimations for the Subandean zone and balanced cross sections across the Altiplano (after Schmitz and Kley, 1997; Kley et al., 1999; McQuarrie and DeCelles, 2001 and Müller et al., 2002).

La plupart des études considèrent que le raccourcissement total des Andes Centrales est principalement Néogène dans la Cordillère Orientale et la zone Subandine-Santa Barbara [*Isacks*, 1988; *Sempere et al*., 1990; *Schmitz*, 1994; *Gubbels et al*., 1993; *Allmendinger et al*., 1997; *Baby et al*., 1997; *Lamb et Hoke*, 1997; *Kley et al*., 1999]. La plus jeune de ces unités morpho-tectoniques, est la zone Subandine, une ceinture de chevauchements qui chevauche le bassin d'avant pays légèrement déformé [*Lamb*, 2000]. Selon *Kley et Monaldi* [1998] et *Kley* [1999], le degré de raccourcissement dans la zone Subandine, et dans la large région d'arrière arc a une valeur maximale près du Coude de Santa Cruz (plan de symétrie de *Gephart*, Figure I.2&IV.6) et diminue vers le sud et le nord-ouest. Les estimations de 80-140 kilomètres (~40%) de raccourcissement faites à partir de coupes balancées dans la zone Subandine impliquent un raccourcissement de 8-14 millimètres par an sachant que les déformations se sont produites principalement au cours des dix derniers millions d'années (Figure IV.6). Sur la base de séries sédimentaires syn-orogéniques de l'Oligocène Supérieur et Néogène identifiées dans l'avant pays et l'Altiplano, une valeur maximum du raccourcissement dans les Andes centrales d'environ 200-250 kilomètres est proposée par la plupart des auteurs [*Isacks*, 1988; *Sheffels*, 1990; *Sempere et al*., 1990; *Gubbels et al*., 1993; *Schmitz*, 1994; *Baby et al*., 1997; *Allmendinger et al*., 1997; *Kley et Monaldi*, 1998].

Des études récentes [*McQuarrie et DeCelles*, 2001; *Müller et al*., 2002] basées sur les coupes équilibrées de l'Altiplano et de la Cordillère Orientale, proposent un raccourcissement total minimum de 340 kilomètres (40-47%) dans les Andes centrales (Figure IV.6). Ces nouvelles interprétations structurales suggèrent que l'épaisseur actuelle des Andes centrales puisse être expliquée seulement par l'empilement tectonique, qui s'est produit principalement au niveau de la Cordillère Orientale depuis l'Éocène Supérieur au Miocène Inférieur [*McQuarrie et DeCelles*, 2001; *Müller et al*., 2002; *Husson et Sempere*, 2003].

Tableau IV.1 Estimations de raccourcissement dans les Andes Centrales (4º-25ºS)

Northern Central Andes

North Huancabamba (~4ºS),		Subandean Zone	11 km(13)
North Abancay (~10ºS),		Subandean Zone	101 km(13)
South Abancay (~13ºS),		Subandean Zone	121 km(13)

Bolivian Orocline

	Altiplano-Backthrust Belt	Eastern Fold-Thrust Belt	Foreland	Total
Northern Altiplano (15-17ºS)	141 km (0)	~50-60 km(2) 117 km(2)	135 km(9) 74 km(2)	336-265 km 191 km(2,7)
Central Altiplano (17-20ºS)	189 km(0) 30 km(8)	54 km(11) 210 km(10)	60 km(1) 67 km(11)	303-310 km 240 km(7)
Southern Altiplano (20-24ºS)	85 km(0) 20 km(2) 50 km(6)	~90-110 km(5,6) 80-90 km(5) 145 km(2)	100 km(4) 74 km(3) 86 km(2)	275-295 km 174-184 km 281 km(2)
Puna et Fold-Thrust Belt (~25ºS)				37 km(12)

0, McQuarrie et DeCelles, 2001 ; 1, Baby et al., 1993 ; 2, Baby et al., 1997 ; 3, Dunn et al., 1995 ; 4, Herail et al., 1990 ; 5, Kley, 1996 ; 6, Kley et al., 1997 ; 7, Kley et Monaldi, 1998 ; 8, Lamb et Hoke, 1997 (Altiplano) ; 9, Roeder, 1988 ; 10, Sheffels, 1990 ; 11, Sheffels, 1988 ; 12, Coutand et al., 2001 ; 13, Rodriguez et al., 2001.

Compilation des données paléomagnétiques

Plusieurs études paléomagnétiques ont essayé de décrire le 'pattern' des rotations tectoniques dans les Andes Centrales, une compilation des données paléomagnétiques est donnée dans le tableau IV.2 et représenté sur les Figures IV.7&8. Des rotations horaires sont observées au Chili et des rotations anti-horaires au Pérou. Les rotations sont importantes dans le domaine de l'avant arc, l'Altiplano et la Cordillère Orientale. a tourné dans le sens anti-horaire entre 25º-30°. Les rotations observées dans l'avant arc du sud de Pérou sont interprétées comme la rotation d'un bloc relativement homogène vers la fin de l'Oligocène [*Roperch et al*., 2002a&b]. Les grandes rotations horaires observées le long de la marge du Chili se sont produites probablement au cours du Paléogène [*Randall et al*., 2001; *Somoza et Tomlinson*, 2002; *Taylor et al*., 2001; *Fernández et al.,* 2000; *Cette étude*]. Des fortes rotations sont aussi observées dans la déflection de Abancay (Gilder et al. 2003) et au sud de la déflection de Huancabamba au nord du Pérou (Mitouard et al. 1990). Dans le plateau d'Altiplano-Puna et la Cordillère Orientale, il y a une bonne corrélation entre la déviation de l'orientation des structures principales et la quantité des rotations produites pendant le Néogène [*MacFadden et al*., 1995; *Butler et al*., 1995; *Coutand et al*., 1999; *Roperch et al*., 2000].

N	Reference	Region	Age	Lat	Long		Pole		D	I	A95	D	I	R	DR	F	DF
1	Kono et al. (1985)	Yumagual Fm., Peru	95	-5.9	-78.2	86.2	178.5	6.5	339	-33	5	356.3	-13.3	-17.3	7.1	19.7	10.8
2	Mitouard et al. (1990)	Cajamarca region	50	-6.5	-79.0	82.2	127.7	4.2	333	-21	6	356.4	-25.6	-23.4	6.2	-4.6	7.5
3	Kono et al. (1985)	Pariatambo Fm	110	-7.1	-78.3	85.1	264.2	8.7	308	-21	5	358.5	-4.8	-50.5	8.2	16.2	14.4
4	Kono et al. (1985)	Chulec Fm.	110	-7.1	-78.3	85.1	264.2	8.7	322	-23	10	358.5	-4.8	-36.5	11.1	18.2	16
5	Macedo-Sánchez et al. (1992)	Casma	100	-10.5	-76.0	87.8	29.20	11.5	337.4	-25.4	8.3	2.2	-21.4	-24.8	11.9	4	17.8
6	Macedo-Sánchez et al. (1992)	Intruisve	75	-11	-77.0	83.6	170.6	7.2	334.2	-28	9.1	353.9	-25.4	-19.7	10.2	2.6	12.3
7	Macedo-Sánchez et al. (1992)	Acos	40	-11	-75.0	80.0	139.5	7.3	349.1	-29.8	12.3	354	-34.8	-4.9	12.9	-5	13.2
8	May and Butler (1985)	Puente Piedra Fm.	90	-11.9	-77.1	84.8	175.8	3.6	343	-29	3	354.9	-25.4	-11.9	4	3.6	5.5
9	Roperch and Carlier, (1992)	Surco	25	-12.0	-76.0	84.4	126.1	5.3	346.8	-32	11.7	357.8	-31.7	-11	11.9	0.30	11.5
10	Macedo-Sánchez et al. (1992)	Sediments/volcanics	95	-12.0	-76.9	86.2	178.5	6.5	335	-28	5	356.2	-24.7	-21.2	7	3.3	9.9
11	Rousse et al. (2002)	Ayacucho Fm.	5	-13.1	285.8	86.5	168.0	2.6	-1.3	-22.1	5.4	356.8	-27.7	1.9	5.1	-5.6	5.5
12	Rousse et al. (2002)	Huanta Fm.	10	-13.1	285.6	85.5	139.9	3.1	-14.3	-24.2	7	357.4	-31.1	-11.7	6.7	-6.9	6.9
13	Rousse et al. (2002)	Sallalli Fm.	20	-13.4	285.7	82.1	131.8	4.6	-11.6	-30.2	16.7	356.3	-36.7	-7.9	16	-6.5	14.4
14	Heki et al. (1985)	Ocros Dyke Swarm	15	-13.4	286.2	84.8	136.7	3.2	346	-32	5	357.2	-32.8	-11.2	5.4	-0.80	5.7
15	Macedo-Sánchez et al. (1992)	Nazca	20	-14.8	-74.7	82.1	131.8	4.6	-17	-25	7	356.2	-38.7	-13.2	7.3	-13.7	7.6
16	Roperch et al. (2000)	Sub-andean	10	-15.0	-67.0	85.5	139.9	3.1	-2	-33	21.9	357.8	-34.6	0.20	21.3	-1.6	17.9
17	Roperch and Carlier, (1992)	Chala, Peru	80	-15.8	-74.3	82.3	228.4	6.9	325	-25	4	353.4	-22.2	-28.4	6.6	2.8	10.4
18	Roperch and Carlier, (1992)	Chala, Peru	170	-15.8	-74.3	88.9	41.9	6.8	291	-31	16	1	-30.3	-70	16	0.70	15.5
19	Butler et al. (1995)	Umayo Fm., Bolivia	65	-15.8	-70.1	82.0	193.7	3.6	319	-24	10	351.7	-30.7	-32.7	9.3	-6.7	9.2
20	Roperch and Carlier, (1992)	Chala Remag	100	-15.8	-74.3	87.8	29.20	11.5	324.9	-25.1	4.4	2.2	-30.3	-37.3	10.3	-5.2	15.3
21	Roperch and Carlier, (1992)	Chala Jurassic	170	-15.8	-74.3	88.9	41.9	6.8	290.5	-31.3	16	1	-30.3	-70.5	16.1	1	15.5
22	Roperch et al. (2002)	Moquegua-Arequipa	40	-16.0	-72.0	80.0	139.5	7.3	318.7	-29	17	354.3	-42.3	-35.6	16.9	-13.3	15.6
23	Roperch and Carlier, (1992)	Arequipa, Peru	100	-16.5	-71.8	87.8	29.2	11.5	300	-47	15	2.3	-31.3	-62.3	20.3	15.7	19
24	Roperch et al. (2002)	Arequipa	80	-16.5	-72.0	82.3	228.4	6.9	309.1	-39.2	13.7	353.2	-23.9	-44.1	15.3	15.3	14.6
25	Roperch et al. (2000)	Viacha region	30	-16.8	-68.5	83.5	163.8	5.3	-10.7	-31.6	10.9	354.5	-37.1	-5.2	11.2	-5.5	10.7
26	MacFadden et al. (1990)	Salla, Bolivia	25	-17.2	-67.7	84.4	126.1	5.3	353	-37	5	358.6	-39.8	-5.6	6.8	-2.8	7.1
27	MacFadden et al. (1990)	Micaña, Bolivia	5	-17.5	-67.5	86.5	168.0	2.6	355	-26	6	356.9	-35.2	-1.9	5.8	-9.2	5.7
28	Roperch and Carlier, (1992)	Ilo, Peru	80	-17.5	-71.4	82.3	228.4	6.9	331	-40	9	353.1	-25.8	-22.1	11	14.2	11.9
29	Roperch et al. (2000)	Chuquichambi (N)	30	-17.5	-68.3	83.5	163.8	5.3	329	-27	8	354.5	-38.1	-25.5	8.5	-11.1	8.8
30	Roperch et al. (2000)	Chuquichambi (S)	30	-17.5	-68.3	83.5	163.8	5.3	340	-30	16	354.5	-38.1	-14.5	15.5	-8.1	14.2
31	Roperch et al. (1999)	Totora Fm.	10	-17.5	-68.3	85.5	139.9	3.1	347	-22	3	357.7	-38.2	-10.7	3.7	-16.2	4.3
32	Macedo-Sánchez et al. (1992)	Toquepala	65	-17.5	-71.0	82.0	193.7	3.6	330.8	-37.8	6.7	351.6	-33.1	-20.8	7.4	4.7	7
33	Roperch et al. (2002)	Moquegua 40Ma	40	-17.5	-71.0	80.0	139.5	7.3	326	-33.3	4.8	354.4	-44.3	-28.4	8	-11	8.3
34	Roperch and Carlier, (1992)	Ilo Remag	100	-17.5	-71.4	87.8	29.2	11.5	330.9	-39.9	8.5	2.3	-32.8	-31.4	13.1	7.1	15.9
35	Lamb (2001)	EC Cochabamba	65	-17.6	-66.4	82.0	193.7	3.6	24	-48	12	351.7	-34.2	32.3	14.8	13.8	10.6
36	Roperch et al. (2000)	Chuquichambi region	30	-18.0	-67.8	83.5	163.8	5.3	-27.6	-27.8	6.7	354.5	-38.9	-22.1	7.6	-11.1	8
37	Butler et al. (1995)	Santa Lucia Fm.	60	-18.0	-65.5	82.4	168.5	4.3	347	-38	8	353.4	-39.4	-6.4	8.9	-1.4	8
38	Butler et al. (1995)	Santa Lucia Fm	60	-18.1	-65.8	82.4	168.5	4.3	325	-47	5	353.3	-39.5	-28.3	7	7.5	6.2
39	Roperch and Carlier, (1992)	La Yarada, Peru	80	-18.1	-70.7	82.3	228.4	6.9	331	-38	6	353.1	-26.9	-22.1	8.3	11.1	10.5
40	Roperch et al. (2000)	Arica	20	-18.5	-70.0	82.1	131.8	4.6	357.8	-33.6	8.2	356.7	-44	1.1	8.9	-10.4	8.1
41	Kono et al. (1985)	Camaraca Fm., Chile	175	-18.5	-70.3	79.7	32.2	7.2	352	-38	3	10.7	-36.7	-18.7	6.9	1.3	8.8
42	Palmer et al. (1980)	Camaraca Fm., Chile	155	-18.6	-70.3	87.3	39.6	3.8	339	-37	6	2.7	-35.3	-23.7	6.8	1.7	6.6
43	Heki et al. (1985)	Arica Dyke Swarm	105	-18.6	-70.3	88.0	179.8	24.6	345	-26	3.3	358	-35	-13	21.1	-9	29.8
44	Heki et al. (1985)	Atajaña Sandstone Fm	120	-18.8	-70.3	83.9	238.5	3.1	345	-26	4.1	355.1	-28	-10.1	4.5	-2	5.3
45	Roperch et al. (2002)	Arica	100	-19.0	-70.5	87.8	29.2	11.5	351.2	-38	3	2.3	-35.1	-11.1	10.2	2.9	14
46	Roperch et al. (2002)	Arica	40	-19.0	-70.0	80.0	139.5	7.3	357.5	-47.2	10	354.5	-46.3	3	13.6	0.90	10.7
47	Scanlan and Turner (1992)	Camaraca Fm./Cuya	140	-19.2	-70.3	77.5	238.2	8.1	351	-40	7	350.1	-21.6	0.90	9.9	18.4	12.9
48	Kono et al. (1985)	Cuya Dyke Swarm	130	-19.2	-70.2	82.6	252.6	7.2	346	-21	8	355.4	-25.2	-9.4	9.1	-4.2	11.8
49	Tanaka et al. (1988)	Arica Group	130	-19.2	-70.0	82.6	252.6	7.2	347	-17	15	355.4	-25.2	-8.4	13.9	-8.2	15.6
50	Butler et al. (1995)	El Molino Fm.	70	-19.5	-65.9	82.3	199.0	4.8	33	-42	4	351.8	-36.1	41.2	5.9	5.9	6.5
51	Lamb (2001)	Altiplano-W East Cord.	10	-19.5	-67.5	85.5	139.9	3.1	12	-43	14	357.7	-41	14.3	15.7	2	11.7
52	MacFadden et al. (1993)	Inchasi, Bolivia	5	-19.7	-65.3	86.5	168.0	2.6	355	-30	9	357	-38.6	-2	8.6	-8.6	7.8
53	Lamb (2001)	SubAndean	25	-20.0	-63.9	84.4	126.1	5.3	4	-30	12	358.9	-43.6	5.1	12.1	-13.6	11
54	Roperch et al. (2000)	North Uyuni	20	-20.0	-67.0	82.1	131.8	4.6	-1.6	-41.1	16.7	357.1	-46.1	1.3	18.4	-5	14.1
55	Lamb (2001)	Altiplano-W East Cord	15	-20.0	-68.0	84.8	136.7	3.2	10	-42	10	357.6	-42.6	12.4	11.2	-0.60	8.7
56	Lamb (2001)	EC Otavi Syncline	80	-20.0	-65.3	82.3	228.4	6.9	-10	-48	15	352.6	-31.1	-2.6	19.1	16.9	14.9
57	MacFadden et al. (1995)	Quehua, Bolivia	10	-20.0	-67.0	85.5	139.9	3.1	15	-38	9	357.8	-41.7	17.2	9.6	-3.7	7.9
58	Lamb (2001)	Subandean	25	-20.5	-63.9	84.4	126.1	5.3	7	-31	9	358.9	-44.2	8.1	9.6	-13.2	9
59	Lamb (2001)	Subandean	25	-20.5	-64.0	84.4	126.1	5.3	5	-32	7	358.9	-44.3	6.1	8.1	-12.3	7.8
60	Lamb (2001)	Camarco Syncline	65	-20.6	-65.2	82.0	193.7	3.6	9	-49	14	351.5	-38.8	17.5	17.6	10.2	11.9
61	Lamb (2001)	Subandean	25	-20.7	-63.8	84.4	126.1	5.3	10	-33	22	358.9	-44.6	11.1	21.7	-11.6	18.4
62	MacFadden et al. (1995)	Cerdas	15	-20.8	-66.3	84.8	136.7	3.2	10	-39	7	357.8	-43.7	12.2	7.8	-4.7	6.5
63	Lamb (2001)	Camarco Syncline	65	-21.0	-65.2	82.0	193.7	3.6	16	-42	11	351.5	-39.4	24.5	12.3	2.6	9.7
64	Lamb (2001)	Camarco Syncline	15	-21.5	-65.2	84.8	136.7	3.2	2	-42	4	357.8	-44.7	4.2	5.2	-2.7	4.5

65	Roperch et al. (2000)	Lipez region	20	-21.8	-66.5	82.1	131.8	4.6	37.5	-38.6	10.8	357.2	-48.3	40.3	11.9	-9.7	9.6
66	Roperch et al. (2000)	Lipez region	20	-21.8	-66.5	82.1	131.8	4.6	8	-44.7	14.9	357.2	-48.3	10.8	17.5	-3.6	12.7
67	MacFadden et al. (1995)	Cerdas, Bolivia	15	-21.8	-66.7	84.8	136.7	3.2	10	-39	7	357.7	-45	12.3	7.8	-6	6.4
68	MacFadden et al. (1990)	Quebrada Honda	10	-22.0	-65.5	85.5	139.9	3.1	18	-41	4	357.9	-44.4	20.1	5.1	-3.4	4.5
69	Coutand et al. (1999)	Yavi	80	-22.2	-65.5	82.3	228.4	6.9	22	-22	12	352.6	-34.4	29.4	11.9	-12.4	12.7
70	Arriagada et al. (2003)	Tocopilla	180	-22.2	-70.2	78.4	26.6	7.6	5.6	-38.3	20.4	12.5	-40.5	-6.9	22.1	-2.2	18.3
71	Somoza and Tomlinson, (2002)	El Loa	20	-22.2	-68.2	82.1	131.8	4.6	359.9	-38.9	6.4	356.9	-48.6	3	7.8	-9.7	6.7
72	Somoza et al. (1999)	El Loa	10	-22.3	-68.6	85.5	139.9	3.1	1	-46	7	357.6	-44.6	3.4	8.5	1.4	6.4
73	Somoza and Tomlinson, (2002)	Purilactis Fm.	100	-22.3	-68.3	87.8	29.2	11.5	31.4	-36.9	4.3	2.4	-39.7	29	10.9	-2.8	13.2
74	Lamb (2001)	Subandean	25	-22.4	-64.5	84.4	126.1	5.3	35	-44	19	358.8	-46.6	36.2	22.1	-2.6	16
75	Somoza and Tomlinson, (2002)	San Pedro Fm.	30	-22.4	-68.1	83.5	163.8	5.3	6.2	-38	6.7	354.3	-44.7	11.9	8.3	-6.7	7.6
76	Somoza et al. (1996)	Lipiyoc, Argentina	10	-22.5	-67.0	85.5	139.9	3.1	358	-34	8	357.7	-44.9	0.30	8.2	-10.9	7.1
77	Somoza et al. (1996)	Granada	10	-22.6	-66.5	85.5	139.9	3.1	1	-31	7	357.8	-45.1	3.2	7.1	-14.1	6.4
78	Hartley et al. (1992)	Paciencia Group	20	-22.6	-68.3	82.1	131.8	4.6	20	-27	14	356.9	-49.1	23.1	13.3	-22.1	12
79	Hartley et al. (1992)	Purilactis Fm.	80	-22.8	-68.4	82.3	228.4	6.9	41	-36	9	352.7	-34.8	48.3	10.7	1.2	11
80	Coutand et al. (1999)	Abra Pampa	80	-22.8	-65.7	82.3	228.4	6.9	42	-48	19	352.5	-35.3	49.5	24	12.7	17.3
81	Arriagada et al. (2000)	Purilactis Group	80	-22.8	-68.2	82.3	228.4	6.9	-3.1	-43	12	352.7	-34.8	4.2	14.4	8.2	12.7
82	Arriagada et al. (2000)	Purilactis Group	80	-22.8	-68.5	82.3	228.4	6.9	12.4	-37	15.3	352.7	-34.8	19.7	16.5	2.2	14.8
83	Turner et al. (1984)	Coloso Fm., Chile	120	-23.0	-71.0	83.9	238.5	3.1	26	-34	8	355	-34.6	31	8.2	-0.60	7.4
84	Arriagada et al. (2003)	Cinchado Fm.	60	-23.0	-69.0	82.4	168.5	4.3	34.8	-42.6	2	352.8	-45.4	42	4.4	-2.8	4.5
85	Arriagada et al. (2000)	Purilactis Group	100	-23.0	-68.5	87.8	29.2	11.5	19.6	-38.4	10.5	2.4	-40.7	17.2	14.7	-2.3	15.1
86	Arriagada et al. (2003)	Quebrada Mala Fm.	80	-23.1	-69.2	82.3	228.4	6.9	28.2	-63.6	19.3	352.8	-35.1	35.4	38.9	28.5	17.5
87	Arriagada et al. (2003)	Cinchado Fm.	60	-23.1	-69.2	82.4	168.5	4.3	28.1	-45	10.5	352.8	-45.5	35.3	12.6	-0.50	9.4
88	Arriagada et al. (2000)	Purilactis Group	80	-23.1	-68.5	82.3	228.4	6.9	7.9	-46.2	20.7	352.7	-35.2	15.2	25.3	11	18.5
89	Arriagada et al. (2003)	Paradero del Desierto	100	-23.2	-69.6	87.8	29.2	11.5	33.3	-50.2	9.5	2.4	-41	30.9	15.6	9.2	14.6
90	Arriagada et al. (2003)	Quebrada Mala Fm.	80	-23.2	-69.5	82.3	228.4	6.9	14.3	-35.9	24.1	352.8	-35.2	21.5	24.9	0.70	21
91	Arriagada et al. (2003)	Quebrada Mala Fm.	80	-23.2	-69.4	82.3	228.4	6.9	357.7	-53.8	17.7	352.8	-35.2	4.9	25.5	18.6	16.4
92	Arriagada et al. (2003)	Cinchado Fm.	60	-23.2	-69.0	82.4	168.5	4.3	46.5	-39.9	2	352.8	-45.7	53.7	4.4	-5.8	4.5
93	Arriagada et al. (2003)	Cinchado Fm.	60	-23.2	-69.2	82.4	168.5	4.3	1.7	-34.8	2	352.8	-45.7	8.9	4.3	-10.9	4.5
94	Arriagada et al. (2000)	Cinchado Fm.	60	-23.2	-68.6	82.4	168.5	4.3	37	-39.8	11.7	352.8	-45.7	44.2	12.8	-5.9	10.3
95	Arriagada et al. (2000)	Purilactis Group	100	-23.2	-68.6	87.8	29.2	11.5	36.6	-39	10.6	2.4	-41	34.2	14.9	-2	15.1
96	Arriagada et al. (2000)	Purilactis Group	80	-23.2	-68.6	82.3	228.4	6.9	15.6	-41	16.7	352.7	-35.4	22.9	18.8	5.6	15.7
97	Arriagada et al. (2003)	Paradero del Desierto	100	-23.3	-69.8	87.8	29.2	11.5	49.2	-39.7	6.9	2.4	-41.2	46.8	12.4	-1.5	13.6
98	Arriagada et al. (2000)	Purilactis Group	60	-23.3	-69.7	82.4	168.5	4.3	53.2	-37.9	8.3	352.7	-45.7	60.5	9.3	-7.8	7.9
99	Arriagada et al. (2000)	Purilactis Group	60	-23.3	-68.8	82.4	168.5	4.3	59.8	-35.3	14.9	352.8	-45.8	67	15.2	-10.5	12.6
100	Arriagada et al. (2003)	Cinchado Fm.	60	-23.4	-69.2	82.4	168.5	4.3	34.2	-41.7	8.1	352.8	-45.9	41.4	9.5	-4.2	7.7
101	Tassara et al. (2000)	Mantos Blancos Mine	150	-23.4	-70.1	85.8	61.6	6.3	41	-44.8	7.9	3.5	-44.5	37.5	10.6	0.30	9
102	Arriagada et al. (2003)	Paradero del Desierto	100	-23.5	-69.8	87.8	29.2	11.5	45.2	-44.6	10.2	2.4	-41.5	42.8	15.3	3.1	14.8
103	Arriagada et al. (2003)	Quebrada Mala Fm.	80	-23.5	-69.5	82.3	228.4	6.9	23.3	-57	2	352.8	-35.7	30.5	6.6	21.3	8.4
104	Arriagada et al. (2003)	Paradero del Desierto	100	-23.6	-69.8	87.8	29.2	11.5	28.4	-45.6	4	2.4	-41.6	26	11.1	4	12.7
105	Tanaka et al. (1988)	La Negra Fm.	180	-23.7	-70.4	78.4	26.6	7.6	10	-28	6	12.7	-42.5	-2.7	8.6	-14.5	9.3
106	Arriagada et al. (2003)	Antofagasta	180	-23.7	-70.4	78.4	26.6	7.6	17.3	-45.9	19.9	12.7	-42.5	4.6	24.4	3.4	17.8
107	Tanaka et al. (1988)	Coloso Area	120	-23.7	-70.4	83.9	238.5	3.1	9	-25	7	355	-35.7	14	6.7	-10.7	6.7
108	Turner et al. (1984)	Coloso Area	120	-23.7	-70.4	83.9	238.5	3.1	26	-34	8	355	-35.7	31	8.2	-1.7	7.4
109	Tanaka et al. (1988)	Coloso and El Way Fm	120	-23.8	-70.4	83.9	238.5	3.1	9	-25	7	355	-35.9	14	6.7	-10.9	6.7
110	Arriagada et al. (2003)	Quebrada Mala Fm.	80	-23.8	-69.6	82.3	228.4	6.9	18.8	-35.7	2	352.8	-36.1	26	6.2	-0.40	8.3
111	Hartley et al. (1988)	Coastal Cordillera	150	-24.0	-70.0	85.8	61.6	6.3	27	-29	8	3.5	-45.2	23.5	9.2	-16.2	9
112	Forsythe and Chisholm (1994)	Coastal Cordillera	145	-24.5	-70.5	74.7	227.2	11.9	28	-34	11	345.9	-31.1	42.1	14.6	2.9	17.6
113	Prezzi et al. (1996)	Puna Salteña	15	-24.6	-67.1	84.8	136.7	3.2	14	-41	5	357.6	-48.3	16.4	6.1	-7.3	5
114	Prezzi et al. (1996)	Puna Salteña	15	-24.6	-67.1	84.8	136.7	3.2	12	-41	8	357.6	-48.3	14.4	9	-7.3	7.1
115	Coutand et al. (1999)	Salar de Arizaro 1	30	-24.6	-67.3	83.5	163.8	5.3	1	-35	8	354.2	-47.4	6.8	9.2	-12.4	8.1
116	Coutand et al. (1999)	Salar de Arizaro 2	10	-24.6	-67.2	85.5	139.9	3.1	12	-39	3	357.7	-47.5	14.3	4.2	-8.5	3.8
117	Roperch et al. in prep.	Catalina	60	-25.0	-69.7	82.4	168.5	4.3	30.4	-49.6	7.4	352.6	-47.7	37.8	10	1.9	7.2
118	Forsythe et al. (1987)	Cifuncho Fm.	100	-25.6	-70.6	87.8	29.2	11.5	40	-54	15	2.4	-44.2	37.6	23.3	9.8	16.7
119	Roperch et al. in prep.	Juncal	60	-25.8	-69.5	82.4	168.5	4.3	20.5	-48.4	9.1	352.6	-48.6	27.9	11.7	-0.20	8.3
120	Roperch et al. in prep.	Aeropuerto	140	-25.9	-69.9	77.5	238.2	8.1	26.4	-42.3	12.1	349.7	-32.8	36.7	14.8	9.5	14
121	Randall et al. (1996)	La Negra Fm.	180	-26.0	-70.4	78.4	26.6	7.6	42	-36	10	12.9	-45.3	29.1	12	-9.3	11
122	Randall et al. (1996)	Vetado Pluton/Dykes,	195	-26.3	-70.5	83.7	41.6	4.9	49	-50	12	6.6	-47.4	42.4	15.7	2.6	10.7
123	Randall et al. (1996)	Las Animas Pluton/Dykes	155	-26.3	-70.3	87.3	39.6	3.8	44	-49	11	2.9	-45.8	41.1	14	3.2	9.6
124	Randall et al. (2001)	Qda Vicuñita Central	160	-26.4	-69.5	88.2	189.6	7.1	27.5	-44.7	9.1	358	-45.1	29.5	12.1	-0.40	10.1
125	Randall et al. (2001)	Qda Monardes Fm.	130	-26.5	-69.5	82.6	252.6	7.2	326.6	-36.2	11.6	355.2	-36.9	-28.6	13.1	-0.70	12.5
126	Randall et al. (1996)	Flamenco Pluton/Dykes	155	-26.5	-70.6	87.3	39.6	3.8	46	-43	9	2.9	-46	43.1	10.5	-3	8.1
127	Randall et al. (1996)	Las Tazas Pluton/Dykes	130	-26.5	-70.3	82.6	252.6	7.2	39	-42	12	355.2	-36.8	43.8	14.4	5.2	12.8
128	Aubry et al. (1996)	Pirgua Group	95	-26.5	-66.0	86.2	178.5	6.5	4	-45	6	356.1	-46.9	7.9	9	-1.9	7.9
129	Randall et al. (2001)	Cerro Valiente	60	-26.5	-69.5	82.4	168.5	4.3	40.1	-38.5	12.1	352.5	-49.5	47.6	13.1	-11	10.4
130	Fernandez in prep.	West Falla Amarga	70	-26.5	-69.8	82.3	199.0	4.8	21.2	-57.4	8.6	351.4	-44.8	29.8	13.6	12.6	8.4

131	Randall et al. (2001)	Qda Monardes Fm	130	-26.5	-69.5	82.6	252.6	7.2	358.5	-47.8	8.3	355.2	-36.9	3.3	11.7	10.9	10.7
132	Randall et al. (2001)	Qda Monardes Fm	130	-26.5	-69.5	82.6	252.6	7.2	1	-38.3	10.6	355.2	-36.9	5.8	12.5	1.4	11.9
133	Fernandez in prep.	Remag. Falla Amarga	50	-26.6	-69.4	82.2	127.7	4.2	1.1	-54.3	6.3	357.2	-53.5	3.9	9.6	0.80	6.1
134	Randall et al. (1996)	Remolino Pluton Dyke	125	-26.7	-70.2	83.4	233.0	3.4	37	-39	12	354	-40.3	43	12.8	-1.3	10.3
135	Fernandez in prep.	Qda Monardes Fm.	130	-26.7	-69.2	82.6	252.6	7.2	-2.2	-49.9	26.5	355.1	-37.2	2.7	35.6	12.7	22.8
136	Randall et al. (2001)	Qda Monardes Fm.	130	-26.8	-69.5	82.6	252.6	7.2	27.8	-39.5	11.6	355.1	-37.3	32.7	13.6	2.2	12.5
137	Randall et al. (2001)	Qda Vicuñita	160	-26.8	-69.5	88.2	189.6	7.1	12.4	-48.8	11.6	358	-45.7	14.4	15.6	3.1	11.6
138	Fernandez in prep.	Cerro Valiente	60	-26.9	-69.4	82.4	168.5	4.3	16.9	-70	14.7	352.5	-49.9	24.4	38.5	20.1	12.4
139	Aubry et al. (1996)	Hualfín-Santa María	15	-27.0	-66.5	84.8	136.7	3.2	15	-37	11	357.6	-51.1	17.4	11.5	-14.1	9.2
140	Taylor et al. (1996)	Caldera Gabbro	190	-27.1	-71.0	82.5	37.0	5.5	35	-30	15	8.2	-48.2	26.8	14.8	-18.2	13.1
141	Taylor et al. (1996)	Sierra La Dichosa	70	-27.2	-70.1	82.3	199.0	4.8	29	-42	8	351.3	-45.6	37.7	9.7	-3.6	8
142	Riley et al. (1993)	Qda Monardes Fm.	130	-27.6	-69.4	82.6	252.6	7.2	23.7	-40.9	20.5	355.1	-38.5	28.6	22.9	2.4	18.3
143	Riley et al. (1993)	Cerrillos Fm. Remag,	60	-27.6	-70.1	82.4	168.5	4.3	46.8	-45	5.2	352.4	-50.6	54.4	7.1	-5.6	5.6
144	Riley et al. (1993)	Dichosa.	80	-27.6	-69.6	82.3	228.4	6.9	21.6	-48.5	22.9	352.6	-41.4	29	29.4	7.1	19.8
145	Riley et al. (1993)	Quebrada Monardes Fm	130	-27.6	-69.5	82.6	252.6	7.2	24	-41	14	355.1	-38.5	28.9	16.2	2.5	13.9
146	Riley et al. (1993)	Ternera Fm.	200	-27.7	-69.5	78.8	70.6	5.7	33.1	-51.1	7.8	8.9	-55.5	24.2	11.5	-4.4	7.7
147	Aubry et al. (1996)	Tinogasta, Argentina	15	-28.1	-67.3	84.8	136.7	3.2	6	-37	9	357.5	-52.2	8.5	9.5	-15.2	7.7

Table IV.2: Synthesis of paleomagnetic rotations for the Central Andes. N, Lat-Long: Location shown in Figures IV.6,7; Age, is the reference pole used to calculate the rotation [*Bess*
Courtillot, 2002]. R±DR, F±DF: Rotation and flatening parameters and their associated errors [*Demarest*, 1983].

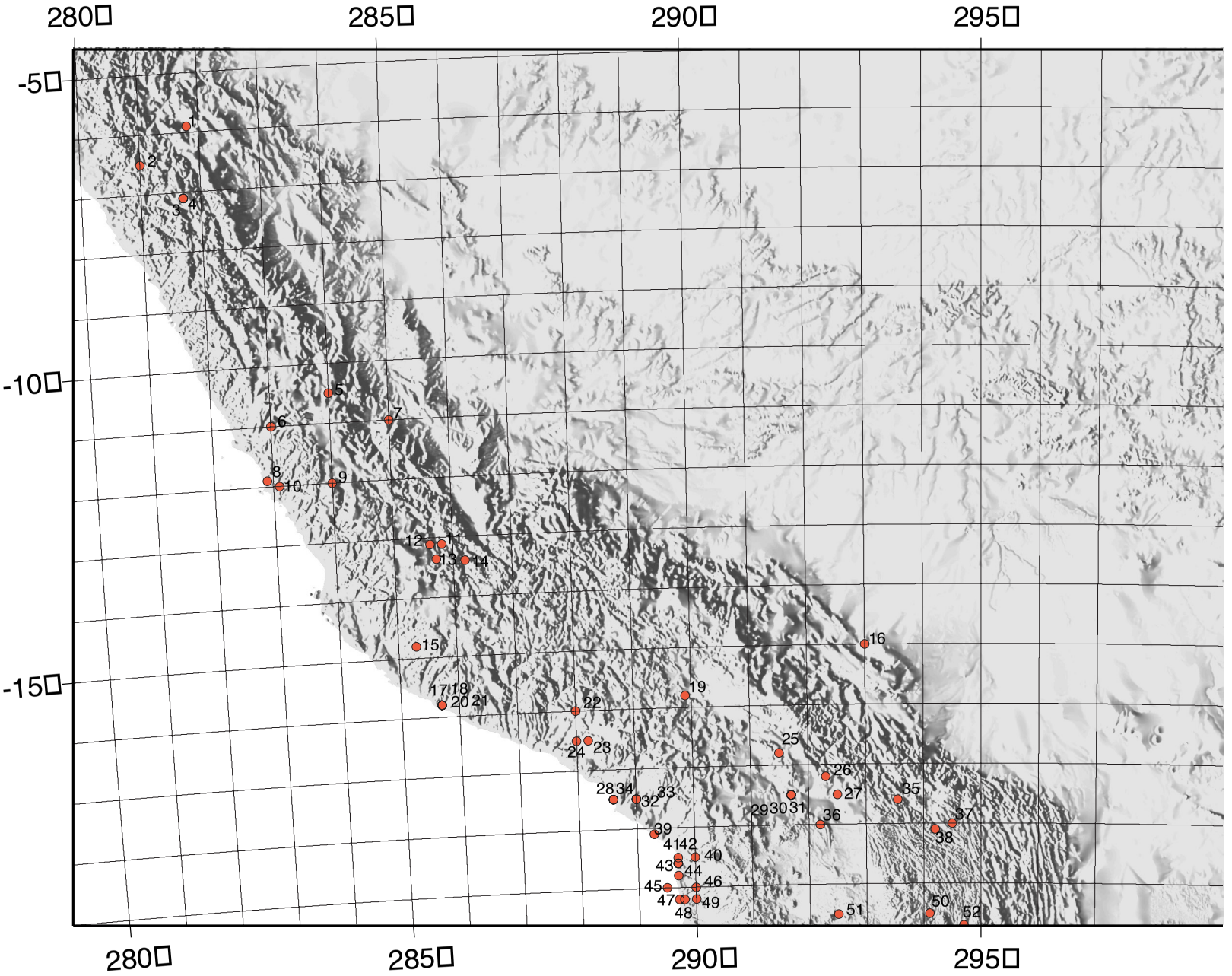

Figure IV.7a: Location of the paleomagnetic studies conducted in the Central Andes between 5º-19ºS (see table IV.2 for details).

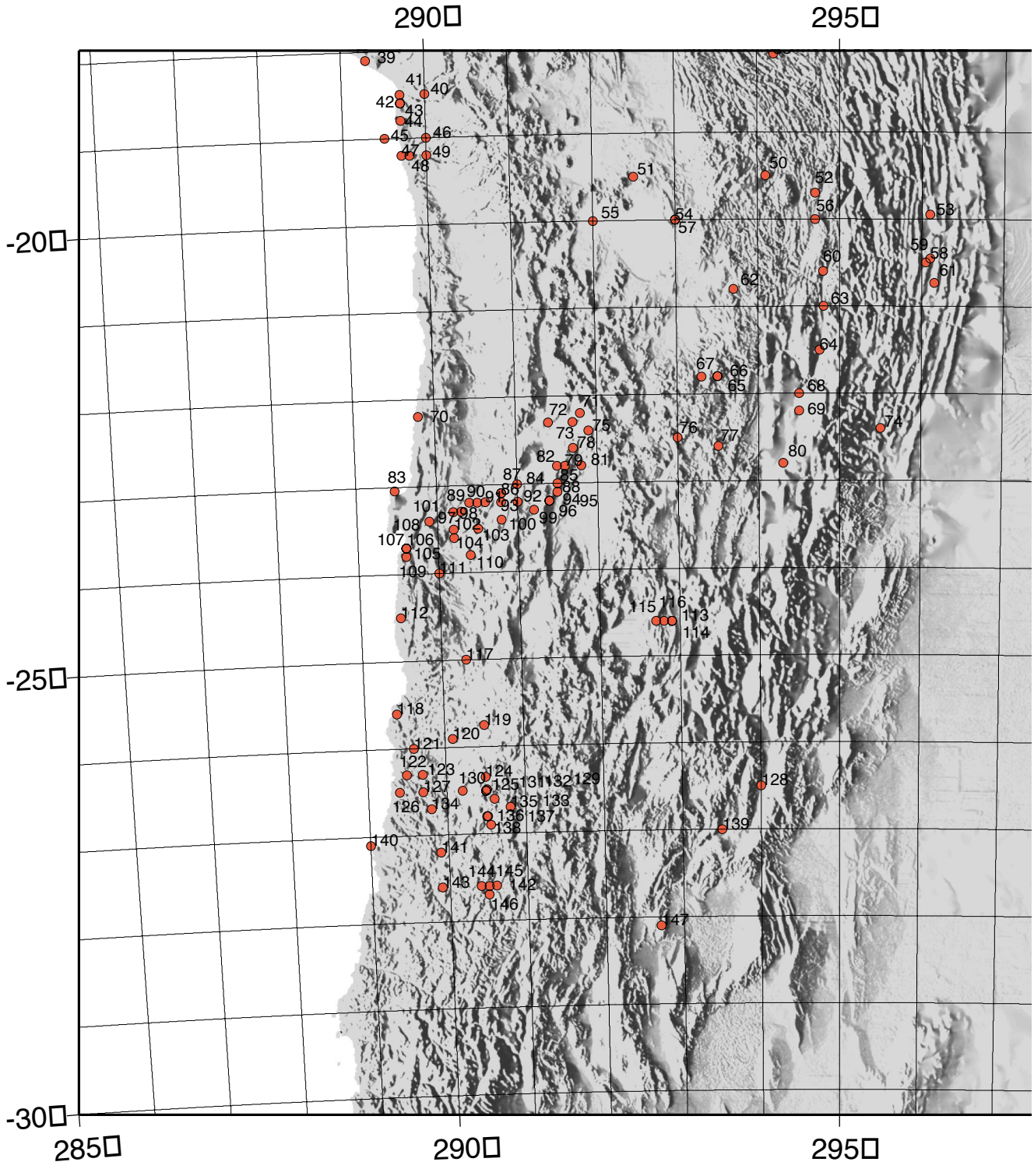

Figure IV.7b: Location of the paleomagnetic studies conducted in the Central Andes between 18º-28ºS (see table IV.2 for details).

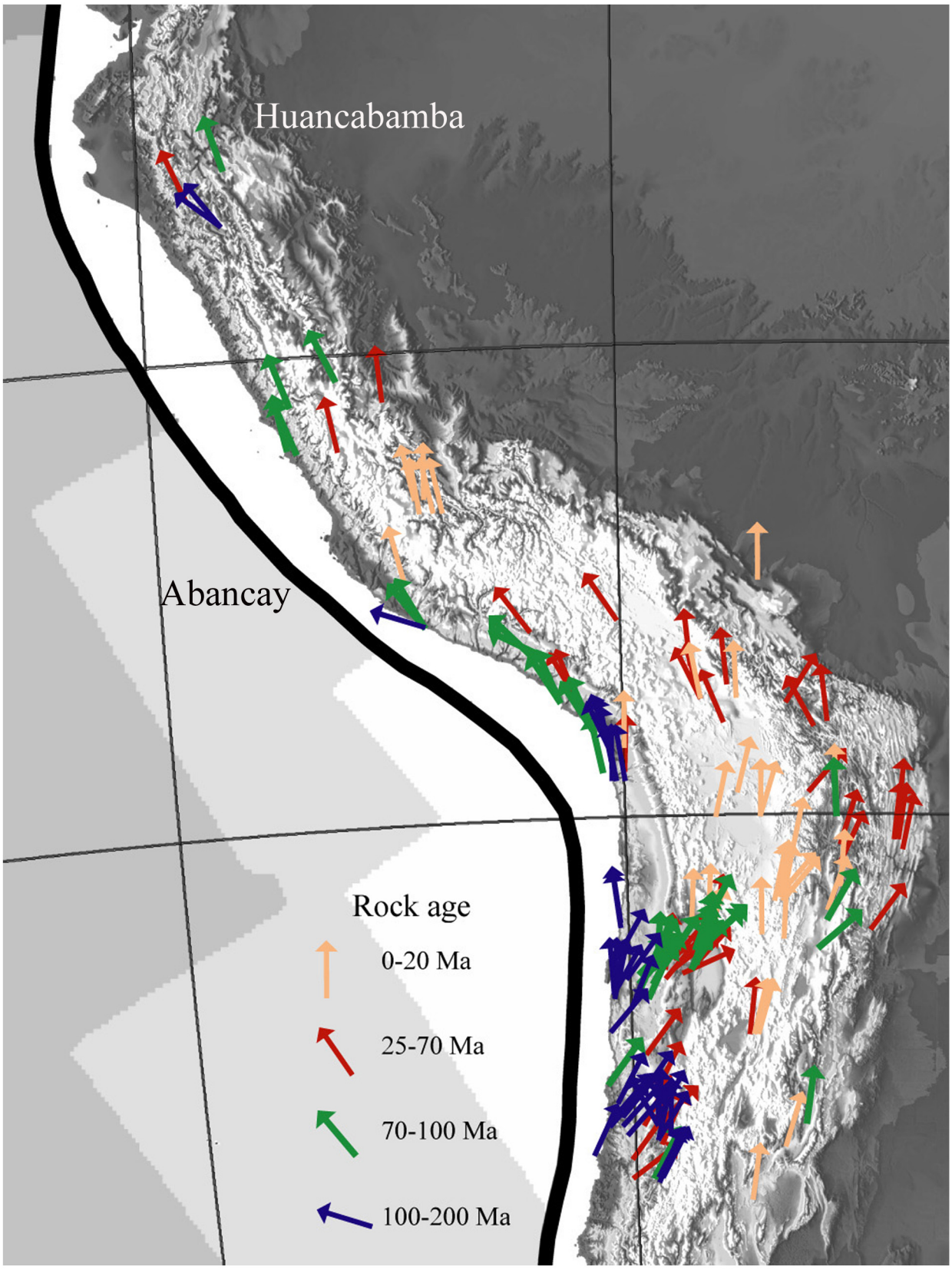

Figure IV.8: Tectonic rotations in the Central Andes (see Table IV.2 for details).

Modèle Simplifié

Dans une première étape nous avons développé un modèle simplifié des Andes Centrales. La figure IV.9 montre la construction du diagramme de blocs. Les blocs fixes correspondent à toute la zone non-déformée à l'Est de la chaîne Subandine et un bloc fixe dans la zone de Huancabamba. À partir de la topographie des Andes Centrales, en projection d'égale surface et selon le plan de symétrie de *Gephart*, [1994], nous avons divisé les Andes selon des segments simples depuis la zone de subduction jusqu'à la chaîne subandine. Les limites des blocs coïncident avec les caractéristiques topographiques les plus importantes (Zone de subduction, l'avant arc, Cordillère Occidentale, Cordillère Orientale, limite Altiplano-Puna, etc.). L'avant arc a été divisé en suivant les structures principales parallèles à la zone de subduction (Zone de Faille d'Atacama, Système de Faille de Domeyko). L'avant arc a été divisé avec des coupes perpendiculaires à la marge pour permettre une déformation interne.

La figure IV.10 montre l'état déformé et l'état non-déformé après avoir appliqué la restauration en utilisant des valeurs de rotation et raccourcissement. Nous avons restauré le même modèle mais dans ce cas sans utiliser des données de rotation (Figure IV.10e). Le modèle avec des données de rotation (Figure IV.10b) montre une meilleure continuité des blocs pour l'avant arc. En contraste, le modèle sans données de rotation (Figure IV.10e) montre des discontinuités des blocs de l'avant arc entre le sud du Pérou et le nord du Chili (~16-20ºS). Ces différences entre les deux modèles montrent l'importance d'assigner des données de rotation à l'algorithme pour obtenir des résultats plus cohérents.

Les deux modèles montrent l'importance du raccourcissement des zones subandine et de la Cordillère Orientale pour produire les rotations observées dans l'avant arc (Figure IV.10). Un déplacement important de la marge vers le cœur de l'orocline est observé pendant le développement de l'orocline (Figure IV.10d). Le déplacement vers le nord de l'avant arc du nord du Chili est en accord avec la subduction oblique dextre pendant le Paléogène [*Pardo Casas et Molnar*, 1987] et implique une déformation décrochante dextre dans les systèmes des failles nord-sud du nord du Chili. Ce modèle suggère aussi une extension NS de la marge pendant la formation de l'orocline.

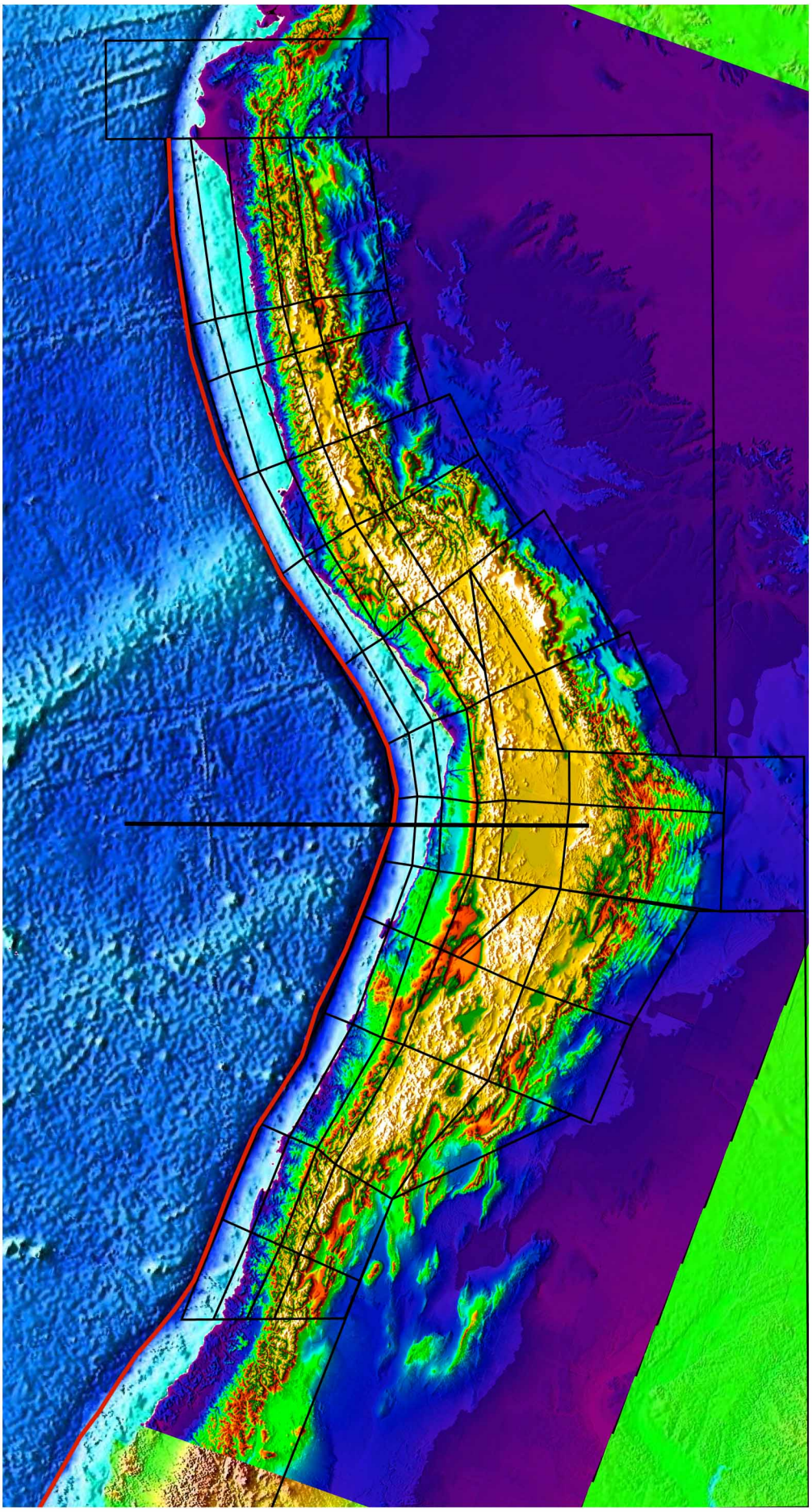

Figure IV.9: Sinple block model for the central Andes (the Andes are rotated using the Gephart's symmetry plane).

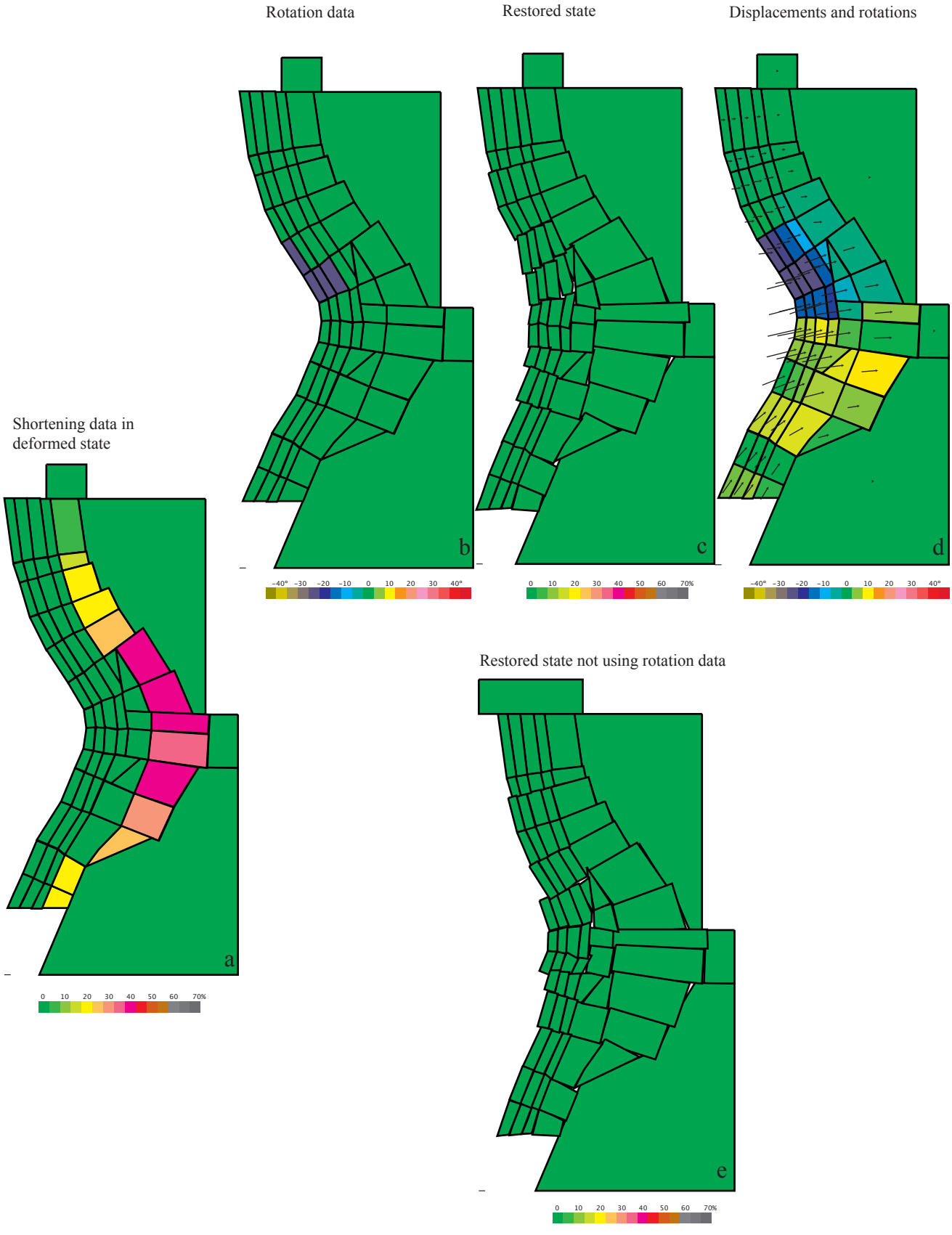

Figure IV.10: Deformed and restored state for a simple block model for de Central Andes, showing parameters of shortening and rotation used during restoration (see discussion in text).

Modèle Final

Étant donné la complexité d'un modèle cinématique à l'échelle de l'orocline à partir de données géologiques, il est nécessaire de simplifier les structures observées, par des limites plus simples mais encore représentatives. La plupart des études tectoniques effectuées dans les Andes Centrales se concentrent dans des secteurs spécifiques et ne présentent pas un schéma tectonique de toute la région. A partir de cartes et des modèles tectoniques publiées (Figure IV.6&11), outre l'analyse d'images de satellite, la topographie numérique, nous avons considéré les principales structures de la région pour représenter les Andes Centrales comme un ensemble de blocs limités par des failles (Figure IV.12). Dans certaines zones comme le plateau et l'avant arc nous avons divisé arbitrairement certains blocs dans lesquels il pourrait y avoir une déformation interne. Finalement, nous avons obtenu un modèle de 179 blocs entre la zone de subduction et la chaîne Subandine.

La figure IV.13a montre le modèle de blocs développé pour les Andes Centrales dans l'état actuel. Les données de raccourcissement tectonique obtenues à partir des études publiées sont essentiellement concentrées dans la zone Subandine et la Cordillère Orientale (Figure IV.13a droite [~40-50%]).

À partir des études paléomagnétiques publiées, nous avons attribué une rotation tectonique et son erreur pour certains blocs (Figure IV.13a gauche). Pour le cas du Pérou, les rotations sont environ -30º au sud de la déflection d'Abancay et environ –15º au nord d'Abancay. Pour le cas de l'avant arc du nord du Chili, et après avoir fait plusieurs tests, nous avons trouvé qu'il est nécessaire de considérer une rotation moyenne entre 15-25º (Figure IV.13a gauche). Si on considère la rotation obtenue à partir des études publiées (par exemple entre 40-60º pour quelques blocs dans la région d'Antofagasta) on obtienne un résultat qui n'est pas cohérent. Les fortes rotations observées dans l'avant arc du nord du Chili sont probablement la somme de rotations locales et d'une rotation globale plus caractéristique de la déformation oroclinale.

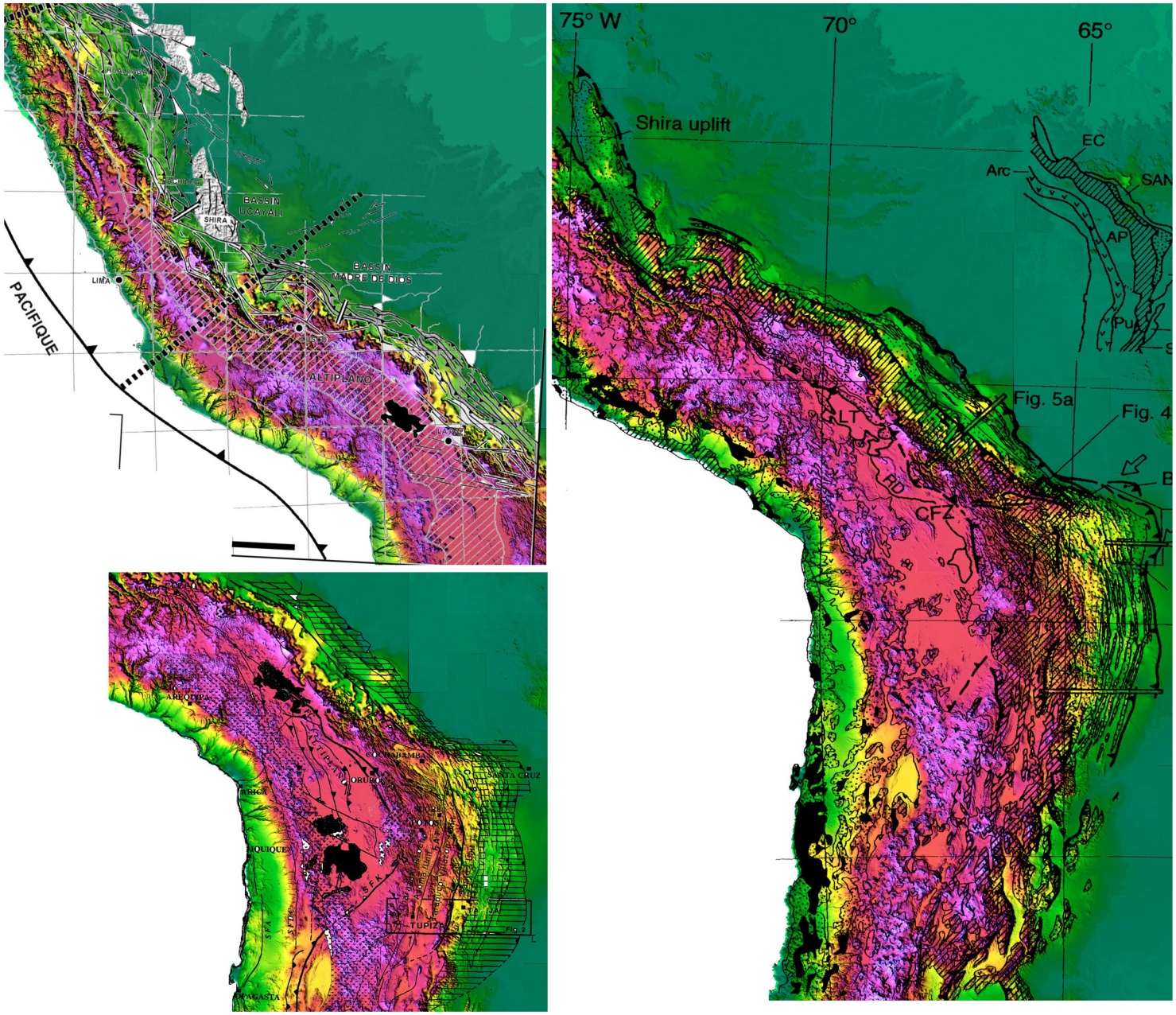

Figure IV.11: Topography and geologic maps of the Central Andes showing main tectonic features (after Hérail et al., 1996; Kley, 1999 and Rodriguez et al., 2001).

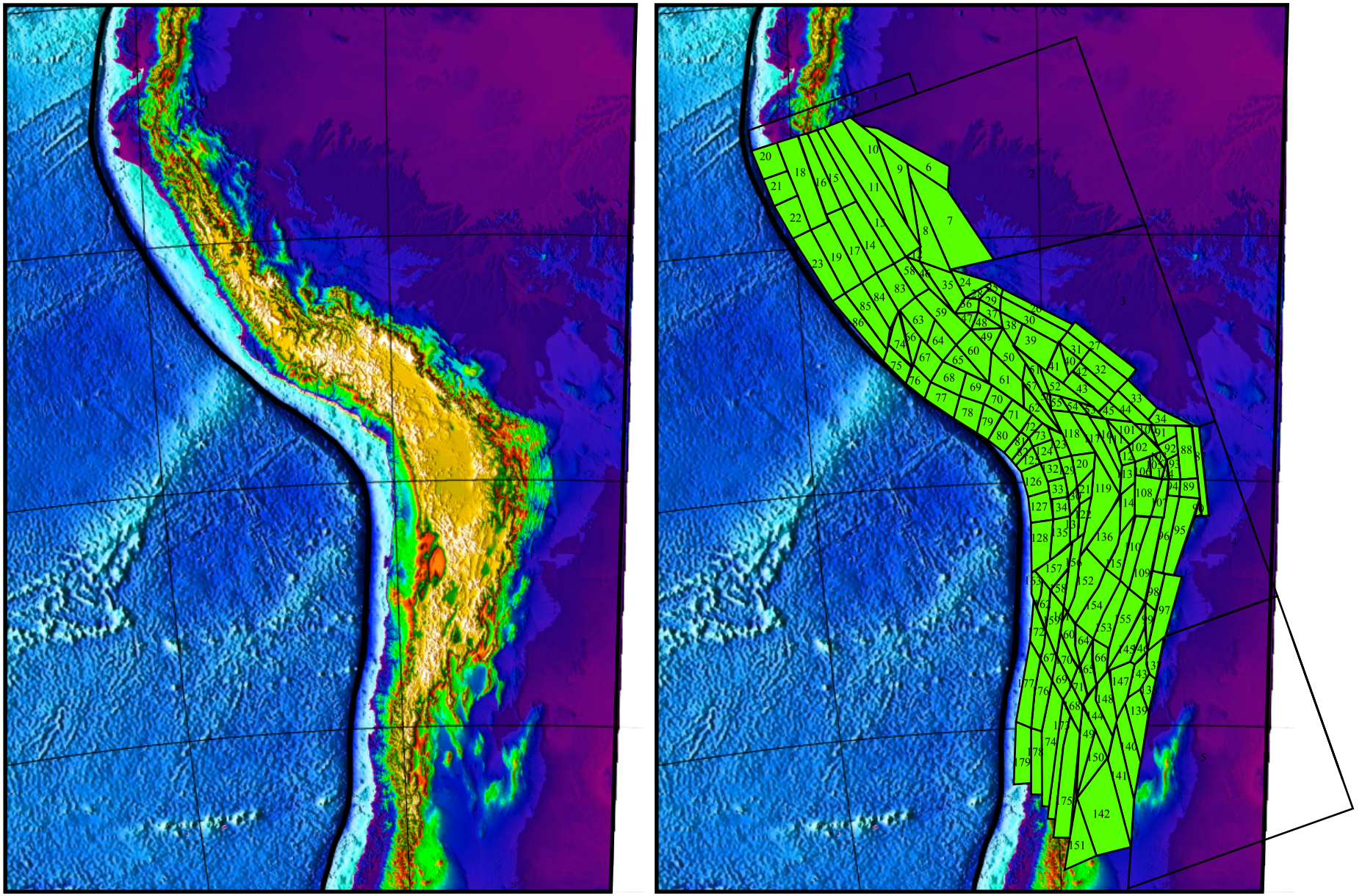

Figure IV.12: Block model for the Central Andes using published geologic map, Landsat image/DEM interpretation and our own observations.

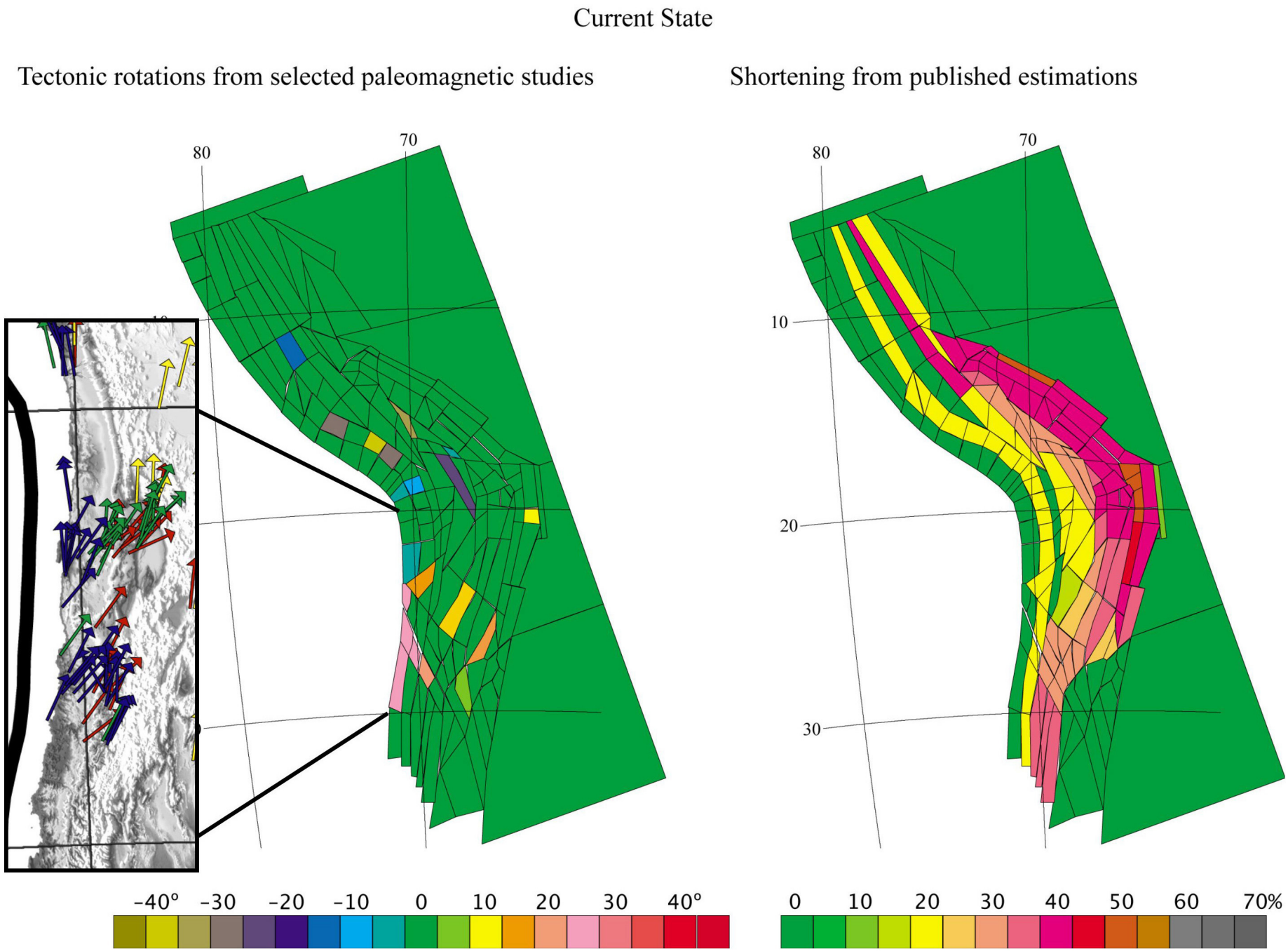

Figure IV.13a: Block model of the Central Andes in the current state. Rotation and shortening data used in the restoration are shown. In the current state the green color (0º) for a given block mean that no paleomagnetic data is available for the block. The rotation data considered for the forearc of northern Chile in the block model are smaller than published paleomagnetic data (see discussion in the text).

Les figures IV.13b,c,d montrent les déplacements et les rotations produites dans différentes étapes pendant la restauration. Au cours des premières itérations, on considère le raccourcissement de la zone Subandine (Miocène Supérieur-Pliocène) (Figure IV.13b), ensuite la déformation plus ancienne de la Cordillère Orientale (Éocène à l'Oligocène) (Figure IV.13c&d) et finalement la déformation Crétacé Supérieur-Paléogène de l'avant arc. (Figure IV.13d). Sachant que l'estimation des raccourcissements pré-Néogène dans la plupart des segments de l'avant arc reste incertaine, nous avons attribué une valeur arbitraire de 20%.

Résultats

Après les premières étapes de restauration et considérant seulement le raccourcissement concentré dans la ceinture Subandine (Miocène Supérieur–Pliocène, Itération 100, Figure IV.13 b) on n'observe pas une variation significative dans la géométrie de la marge. Un raccourcissement total à la latitude de Arica entre 70-90 km entraine des rotations inférieures à 10º (-10º) dans la région de l'avant arc du Chili (du Pérou).

Après avoir restauré (déplié) toute la déformation de la chaîne Subandine, la restauration d'une partie de la déformation dans la Cordillère Orientale, déformation Oligo-Miocène (Itération 200, Figure IV.13c) entraine une variation de la géométrie de la marge et un raccourcissement total du 180-190 km à la latitude de Arica-Santa Cruz. A l'itération 300, toute la déformation Éocène-Oligocène, essentiellement concentrée dans la Cordillère Orientale, est restaurée. À la latitude d'Arica Santa Cruz, ce modèle correspond à un raccourcissement total entre 300-310 km. Cette quantité de raccourcissement estimé à partir de la restauration en carte est cohérente avec les dernières estimations entre 310-340 km de raccourcissement publiées par *McQuarrie et DeCelles* [2001] et *Müller et al*. [2002].

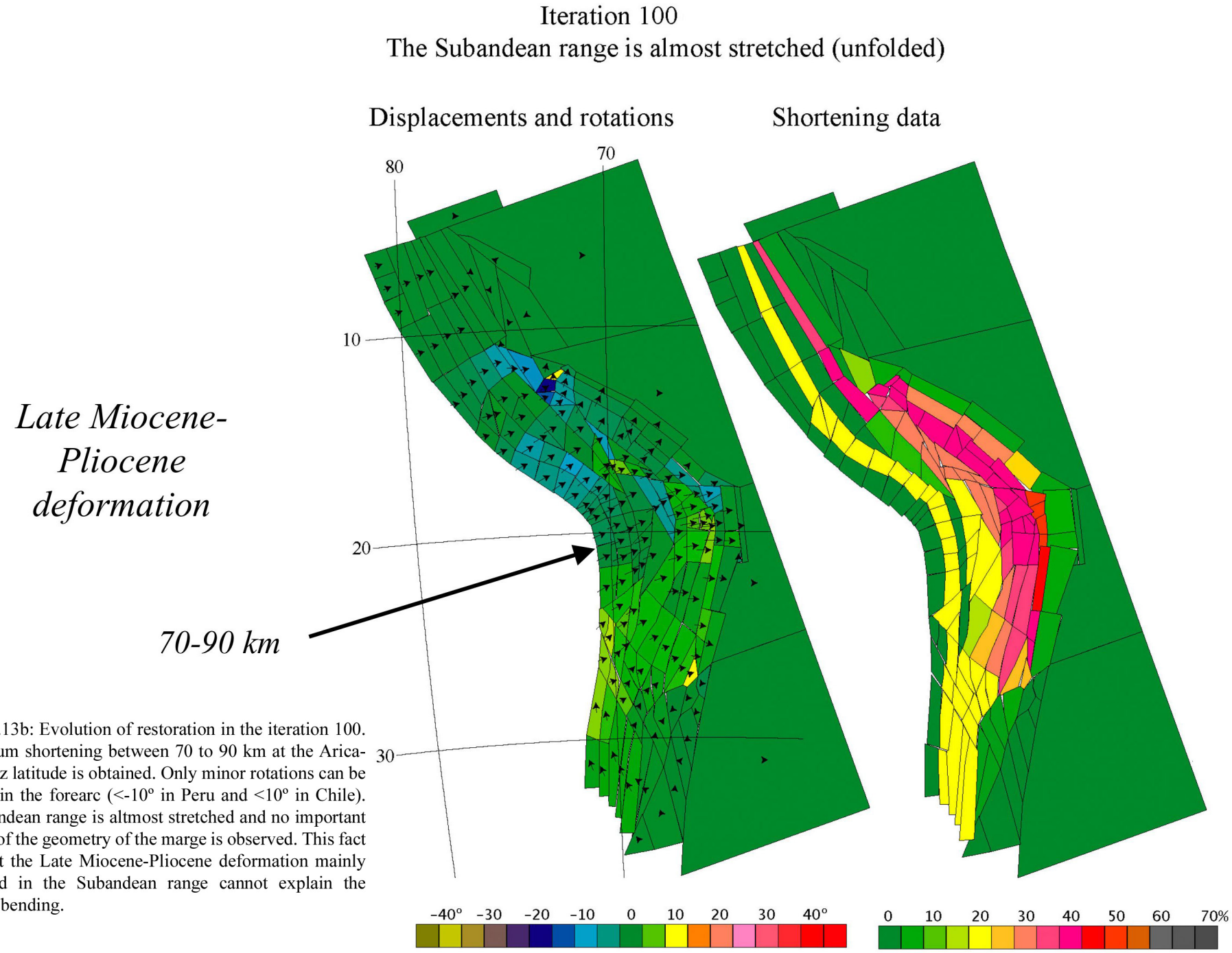

Figure IV.13b: Evolution of restoration in the iteration 100. A maximum shortening between 70 to 90 km at the Arica-Santa Cruz latitude is obtained. Only minor rotations can be observed in the forearc (<-10° in Peru and <10° in Chile). The Subandean range is altmost stretched and no important variation of the geometry of the marge is observed. This fact imply that the Late Miocene-Pliocene deformation mainly concentred in the Subandean range cannot explain the Oroclinal bending.

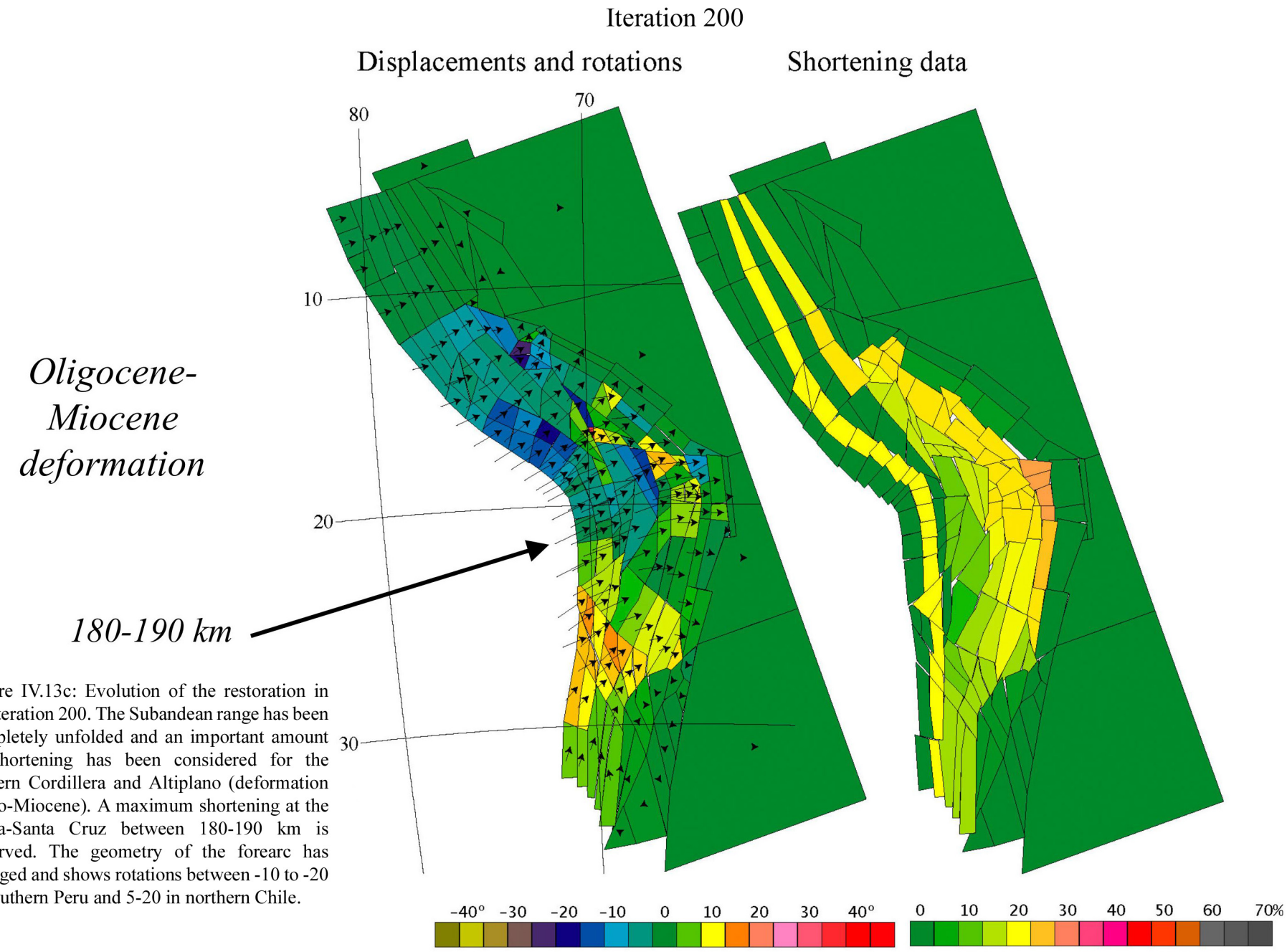

Figure IV.13c: Evolution of the restoration in the iteration 200. The Subandean range has been completely unfolded and an important amount of shortening has been considered for the Eastern Cordillera and Altiplano (deformation Oligo-Miocene). A maximum shortening at the Arica-Santa Cruz between 180-190 km is observed. The geometry of the forearc has changed and shows rotations between -10 to -20 in southern Peru and 5-20 in northern Chile.

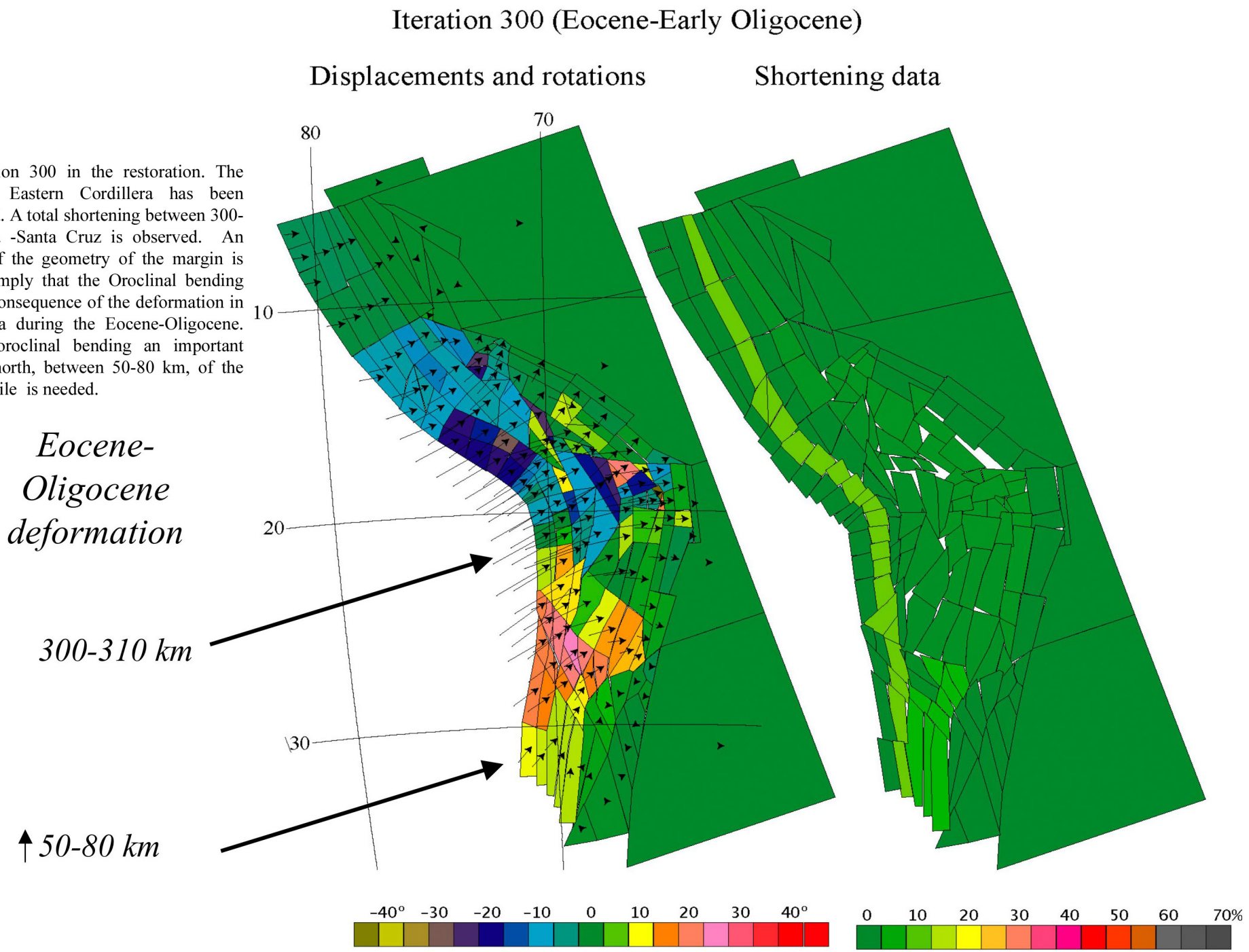

Figure IV.13d: Iteration 300 in the restoration. The deformation in the Eastern Cordillera has been completely considered. A total shortening between 300-310 km at the Arica -Santa Cruz is observed. An important variation of the geometry of the margin is observed. This fact imply that the Oroclinal bending mainly resulted as a consequence of the deformation in the Eastern Cordillera during the Eocene-Oligocene. Also, to form the oroclinal bending an important displacement to the north, between 50-80 km, of the forearc of northern Chile is needed.

Tout comme dans le modèle simplifié (Figure IV.10) on observe un important déplacement de l'ordre de 50 à 80 km vers le nord pour l'avant arc du nord du Chili.

Ce qui précède suggère que les rotations observées dans la marge ne peuvent pas être expliquées par une rotation globale de la marge pendant le Miocène-Pliocène. Au contraire, la courbure de la marge semble plus contemporaine avec la formation de la Cordillère Orientale essentiellement durant l'Éocène Oligocène.

Erreurs dans le modèle

La figure IV.14 montre les recouvrements et les vides produits pendant la restauration. Ces erreurs ont principalement pour origine la forme des blocs et les changements de forme associés aux étirements suivant des directions données. Au cours des premières itérations, il n'existe pas de grands recouvrements (itération 100 dans la figure IV.14), mais ils augmentent dans les itérations postérieures en considérant le raccourcissement de la Cordillère Orientale (itération 300). Les recouvrements et les vides sont observés principalement dans la région de l'Altiplano. Un meilleur contrôle structural permettrait peut-être une meilleure modélisation. Étant donné l'échelle du problème et la complexité de la tectonique, le modèle proposé n'est certainement pas unique. Il permet cependant d'apporter des informations de premier ordre permettant une meilleure interprétation des données de rotation dans les Andes.

Figure IV.14: Restoration in stages 100 and 300 with transparency of a 50% to show overlaps of blocks (see discussion in text).

Chapitre V : Synthèse des résultats, discussion et conclusions.

L'approche pluridisciplinaire adoptée pour cette étude, nous a permis (1) de caractériser la tectonique du bassin du Salar de Atacama et ses implications pour le développement de l'avant arc Crétacé au Paléogène, (2) de mieux comprendre l'organisation et le développement du champ de rotation à travers la chaîne andine au nord du Chili (3) de reconsidérer l'importance de la tectonique pré Néogène dans la construction des Andes Centrales et (4) d'argumenter le développement de l'orocline bolivien dans l'espace et dans le temps.

Caractérisation du bassin du Salar de Atacama

La plus grande quantité d'information sur le développement de l'avant arc dans la région d'Antofagasta se trouve dans le bassin du Salar d'Atacama. Ce profond dépôcentre montre un remplissage sédimentaire Mésozoïque-Cénozoïque bien préservé qui enregistre les événements tectoniques précoces qui ont mené à la formation des Andes Centrales. Les données de terrain, sismiques, paléomagnétiques et âges géochronologiques, ont permis de construire un système stratigraphique qui rend compte de l'histoire précoce du bassin représenté dans le Groupe Purilactis et des séquences clastiques du Paléogène.

Les styles structuraux et l´occurrence des strates de croissance suggèrent que la partie inférieure du Groupe Purilactis s'est accumulée dans un contexte compressif contrôlé par un système de failles inverses a vergence Est, enracinés dans la proto Cordillère de Domeyko. Des épisodes successifs de soulèvement en relation avec le raccourcissement dans la Cordillère de Domeyko ont participé à l'accumulation de sédiments syntectoniques des formations Purilactis et Barros Arana pendant le Crétacé Supérieur. Pendant ce même intervalle, volcanisme et sédimentation se sont produit dans des bassins de pull-apart le long de l'arc actif dans la partie centrale de la région d'Antofagasta (Formation Quebrada Mala). Au même temps, au nord de la latitude de Calama, une sédimentation syntectonique contrôlée par des chevauchements de vergence ouest s'est aussi produite dans des bassins à l'ouest de la proto Cordillère de Domeyko (Formation Tambillos).

Des laves alcalines, ignimbrites et des strates rouges continentales d'âge Maastrichtien (Formation Totola) ont été déposées dans le bassin d'Atacama en même temps que les formations marines, Molino et Yacoraite, ont couvert de grands secteurs de l'Altiplano-

Puna. Des niveaux calcaires intercalés avec les niveaux volcaniques de la Formation Totola indiquent que cette transgression marine a avancé vers l'Ouest jusqu'au bord Est de la proto Cordillère de Domeyko.

Des âges de traces de fission de l'intrusif du Cerro Quimal indiquent un soulèvement rapide de la Cordillère de Domeyko autour des 63 Ma. Ce soulèvement est cohérant avec l'occurrence des faciès alluviaux Paléocènes-Éocènes de la Formation Naranja (Orange Formation) dans le basin d'Atacama. Cette unité montre une grande croissance vers le centre du bassin, contrôlée par des mouvements dans de la Faille du Salar, structure associée au soulèvement du bloc de bassement du Cordón de Lila. L'événement tectonique principal dans la région correspond à la phase Incaïque de l'Éocène Supérieur, lorsque plus de 1000 m de faciès alluviaux proximaux (Formation Loma Amarilla) sont déposés, associés à un important soulèvement de la Cordillère de Domeyko et du Cordón de Lila. Pendant cet événement compressif se produisent d'importantes rotations horaires dans l'avant arc (voir plus bas).

La tectonique Crétacé-Paléogène représentée dans les faciès du bassin d'Atacama, a aussi probablement affecté d'autres régions plus a sud de l'actuelle dépression pré andine du nord du Chili. Ceci est suggéré par la similitude des faciès du Crétacé - Paléocène observées plus au sud dans le bassins de Pedernales - Maricunga, au latitude 27°S. En même temps, le bassin d'Atacama est le dépôcentre le plus occidental du système de basins formées sur l'Altiplano-Puna pendant le Crétacé au Paléogène. Les événements enregistrés dans le remplissage du bassin d'Atacama sont cohérents avec le debut de la contraction plus ancien des secteurs distaux du nord-ouest de l'Argentine et sud-est de la Bolivie. Toutefois le système de rift de Salta dans le nord-ouest de l'Argentine a été formé pendant la période d'extension généralisée du Crétacé Inférieur, aussi enregistré en Bolivie (Groupe Puca Inférieur) et le long de la marge Chilienne. Des effets associés a l'inversion Crétacé Supérieur précoce du bassin d'arrière arc du nord du Chili et le soulèvement initial de la Cordillère de Domeyko ont été reconnus au sud du plateau Bolivien et du système de rift de Salta.

En conclusion, et comme d'autres études ont suggéré [*Charrier et Reutter*, 1994; *Muñoz et al*., 1997, 2002] nous considérons que le Bassin d'Atacama ne s'est pas formé dans un

contexte extensif, ni non plus comme un bassin d'avant-pays associé à une flexure de la lithosphère. Ce bassin s'est formé pendant le Crétacé Supérieur précoce comme une conséquence de l'inversion des bassins extensionnels d'arrière arc du Crétacé Inférieur du nord du Chili. Pendant cet inversion a commencé à être soulevé la mince ceinture du socle de la proto Cordillère de Domeyko.

Étant donné les petites dimensions du bassin d'Atacama, la création d'espace et la longue vie du dépôcentre ne peuvent pas seulement être expliquées par la flexure et la subsidence induite par charge tectonique de la mince Cordillère de Domeyko. Des études récentes ont indiqué la présence d'une anomalie positive dans le domaine de gravité résiduelle isostatique [*Götze et Krause*, 2002] qui est bien lié avec la faible topographie des bassins d'Atacama et Arizaro (nord-ouest d'Argentina). Plus encore des données de tomographie sismique sous le Salar d'Atacama montrent un manteau de lithosphère anormalement froid qui peut-être mécaniquement lié avec la plaque de Nazca [*Yuan et al*., 2002]. Des ophiolites rémanentes ou corps ultrabasiques de haute densité de l'Ordovicien ou la racine d'un arc magmatique Cambrien-Ordovicien (exposées en surface au Cordón de Lila) pourraient causer l'anomalie observée, et avoir induit, dynamiquement la subsidence du bassin d'Atacama [*Yuan et al*., 2002].

Rotations tectoniques dans l'avant arc du nord du Chili

Pendant le Crétacé Supérieur et Paléogène, une importante partie de la déformation de la marge andine, a été absorbée par des rotations horaires de blocs, allant jusqu'à 65º. Bien que quelques auteurs aient suggéré que ces rotations soient en rapport avec la formation de l'Orocline Bolivien pendant le Néogène, notre étude et des études récentes indiquent qu'une importante partie des rotations se sont produites principalement pendant l'Éocène-Oligocène (Phase Incaïque).

La vaste distribution de ces rotations dans le Nord du Chili implique que la déformation Incaïque est un événement tectonique d'importance régionale et non seulement local, lié à la déformation dans la Précordillère ou Cordillère de Domeyko comme l'indiquent des travaux publiés à ce sujet.

L'âge minimal des rotations dans l'avant arc du nord du Chili n'est pas connu du fait du manque de séquences Oligocènes favorables aux études paléomagnétiques. Cependant les résultats de *Somoza et Tomlinson* [2002] indiquent que les rotations de l'avant arc Chilien sont pré - Néogènes. Dans le sud du Pérou des rotations antihoraires (25º à 30°) on été enregistrées sur des roches sédimentaires d'âge Éocène – Oligocène [*Roperch et al*., 2000 ; *Roperch et al*., 2002 a,b]. Dans le nord du Chili et le sud du Pérou, les ignimbrites du Miocène Inférieur ne présentent pas d'évidences de rotation [*Roperch et al*., 2002a,b]**.** À partir de ces faits, nous ne pouvons pas écarter l'hypothèse que les rotations aient été simultanées au Pérou et au Chili, ce que impliquerait que l'Orocline Bolivien s'est formé principalement durant l'Oligocène. Si c'en est le cas, des rotations plus jeunes observées à l'Est, dans l'Altiplano, Cordillère Orientale et Zone Subandine, peuvent être une conséquence du déplacement généralisée vers l'Est de l'avant-arc précédemment courbé pendant le Néogène lequel pourrait avoir avancé comme un bloc rigide vers le craton [*Roperch et al*., 2000]. Il faut cependant noter que *Rousse et al*. [2002] ont suggéré que les rotations observées dans le nord du Pérou correspondent essentiellement à des événements tectoniques très limités dans le temps au cours du Miocène Supérieur et sans relation avec les processus tectoniques donnant naissance à l'Orocline des Andes Centrales.

Bien que durant ces dernières années, de meilleures données aient été obtenues sur l'âge et la magnitude des rotations tectoniques dans les Andes Centrales, jusqu'à présent il n'y a pas de modèle géologique capable d'intégrer les données paléomagnétiques et les études structurales. En opposition avec la situation au sud du Pérou, où les données semblent en faveur d'une rotation générale de la marge, le Nord du Chili enregistre un ajustement complexe de rotations sur des petits blocs. Une composante de rotation globale Oligocène de 10-20º ne peut pas cependant être complètement écartée si les données du Nord du Chili sont comparés à celles du Pérou. Toutefois, la grande variabilité spatiale de l'ampleur des rotations suggère un contrôle tectonique sur les rotations locales et non seulement à l'échelle de tout l'avant arc.

Quel modèle tectonique pour expliquer des rotations systématiquement horaires dans le nord du Chili ?

La convergence oblique de la plaque de Nazca et aussi, l'occurrence des structures anciennes affectant la croûte au niveau de la marge ont été utilisée pour expliquer les rotation tectoniques dans le Nord du Chili. Les mouvements au long de failles obliques à la marge a souvent été avancé pour expliquer l'existence des rotations [*Randal et al*., 1996; *Taylor et al*., 1998; *Abels et Bischoff*, 1999]. A cet égard, notre étude suggère qu'une importante zone de cisaillement transpressif dextre d'orientation NE-NNE a contrôlé l'ampleur des rotations dans la Vallée Centrale au Nord Est d'Antofagasta, où les rotation probablement dependent des différences dans la quantité de raccourcissement EW le long de la marge pendant l'événement tectonique Incaïque**.**

Plus au sud, dans la région de Copiapó, un système complexe de rotations horaires a été aussi observé [*Riley et al*., 1993 ; *Randall et al*., 1996 ; *Taylor et al*., 1998 ; *Randall et al*., 2001 ; *Fernández et al*., 2000 ; *Fernández et al*., 2002]. Le réseau structural principal de cette région inclut des systèmes de failles NW et NNE obliques à l'orogène [*Mpodozis et al*., 1995]. *Abels et Bishoff*, [1999] en utilisant les données de rotations publiées de la région de Copiapó et l'interprétation de linéaments d'images satellites, ont proposé un mécanisme de déformation qui expliquerait les rotations horaires de ce segment de la zone d'avant-arc. Ce modèle simple, considère que des structures préandines, d'orientation NW ont été réactivés en failles sénestres pendant l'Éocène (model domino). Toutefois, ce modèle n'est pas cohérent avec les études géologiques de terrain, où on ne reconnaît pas clairement de 'structures réactivées' [*Cornejo et al*., 1993 ; *Tomlinson et al*., 1994]. Cette idée que la tectonique du nord du Chili ait été influencée par des structures préandines d'orientation NW n'est pas nouvelle [voir *Salfity*, 1985], mais jusqu'à présent il n'y a pas de preuves concrètes de terrain qui permettent de suggérer l'existence 'réelle' de ces 'linéaments'.

Développement de l'orocline bolivien dans l'espace et dans le temps.

Bien que notre travail et d'autres études récentes aient permis de mieux définir l'âge des rotations et d'en connaître leur distribution spatiale et magnitude, le mécanisme et l'origine de ces rotations ne sont pas encore bien compris. Les modifications que nous avons effectuées aux algorithmes de *Rouby et al*. [1993a] et *Bourgeois et al*. [1997] ont permis de

considérer les données de raccourcissement et rotation tectonique disponibles des Andes Centrales pour établir des modèles tectoniques de l' évolution de l'Orocline Bolivien. Bien que les modèles présentés doivent être considérés comme préliminaires, quelques idées sur les processus de premier ordre qui contribuent au développement de l'orocline peuvent être mentionnées.

Dans tous les modèles effectués on observe une relation directe entre la quantité de raccourcissement dans l'orogène et la quantité de rotation observée dans la marge. Néanmoins, si on considère, seulement le raccourcissement Miocène Supérieur-Pliocène dans la Zone Subandine il n'y a pas une modification importante de la géométrie de la marge. Ainsi, les rotations observées dans la marge ne peuvent pas être expliquées considérant seulement la déformation plus jeune ou plus lointaine, ou de thin-skin qui affecte (principalement) la zone Subandine. Au contraire, si on considère le raccourcissement dans la Cordillère Orientale, dû à déformation thick-skin et d'une partie de l´Altiplano-Puna on observe une importante variation dans la géométrie de la marge. Les rotations observées après la restauration sont cohérentes avec les données paléomagnétiques dans l'avant arc du Pérou, mais, pour l'avant arc du nord du Chili on obtien, seulement, une rotation horaire maximum entre 10-20º. Cette rotation est inférieure aux données paléomagnétiques publiées et démontre une contribution locale significative.

La variabilité spatiale et la grande magnitude des rotations dans la marge Chilienne suggèrent la contribution de deux processus superposés.

(1) Pendant le Paléogène (phase Incaïque) se seraient produit des rotations horaires entre 20-30º, contrôlées principalement par la tectonique locale de la marge (par exemple : l'activité des failles d'orientation NE décrites dans la région d'Antofagasta).

(2) Postérieurement (ou simultanément), durant la déformation qui a donné naissance à la Cordillère Orientale s'est produit la rotation globale de toute la marge. De cette manière les rotations locales ont été augmentées de 15-25º.

L'important déplacement vers le nord de ~50 km de la marge du Chili observé dans les modèles de restauration est cohérent avec la direction de convergence oblique dextre documentée pendant le Paléogène. La cinématique de la déformation dans les limites des

plaques est principalement contrôlée par la direction et magnitude du vecteur de déplacement relative en rapport à la direction de la limite des plaques [*McKenzie et Jackson*, 1986; *Tikoff et Teyssier*, 1994; *Braun et Beaumont*, 1995; *Saint Blanquet et al*., 1998; *Burbridge et Braun*, 1998]. Une haute vitesse relative et un angle de convergence oblique entre les plaques de Nazca et sud-américaine [*Pilger*, 1984; *Pardo-Casas et Molnar*, 1987] ont résulté en mouvement décrochant dans le système de Failles de Domeyko pendant l'Éocène Supérieur [*Scheuber et Reutter*, 1992; *Reutter et al*., 1991,1993,1996; *Scheuber et al*., 1994]. La convergence oblique pendant l'Éocène Oligocène aura pu être divisé dans une composante normal à l'arc, qui a produit raccourcissement et épaississement à travers des failles inverses et une composant parallèle à l'arc, qui a causé le déplacement dextre parallèle au système de Domeyko. Raccourcissement et épaississement a porté à la hausse du Système de Domeyko et à une érosion d'au moins de 4 à 5 km [*Maksaev et Zentilli*, 1999].

L'étude de la déformation ductile des intrusives minéralisés de Chuquicamata, indiquent que leur mise en place c'est produite en étroite relation avec des failles décrochantes du système de failles de Domeyko (Faille Ouest) durant l'Éocène Oligocène. *Lindsay et al*., [1995], *Lindsay*, [1998] et *Maksaev*, [1990] ont proposé que, à Chuquicamata, un régime dextre a persisté pendant l'Éocène-Oligocène. Cependant, *Tomlinson et Blanco* [1997a,b] ont suggéré que l'épisode dextre a été un événement de courte durée, et que le mouvement senestre a prédominé depuis l'Oligocène. Des déplacements senestres de 25 kilomètres [*Reutter et al*., 1996] à 35 kilomètres [*Dilles et al*., 1997; *Tomlinson et Blanco*, 1997a,b] et 40 kilomètres [*Ambrus*, 1979] ont été estimés pour la Faille Ouest dans la région de Chuquicamata. Peut-être si on considère que la déformation a été non seulement concentrée dans la Cordillère de Domeyko, si non dans tout l'avant arc et on considère aussi les rotations horaires, comme le montre notre étude, les déplacements senestres dans la Cordillère de Domeyko peuvent être conciliés dans un contexte de subduction oblique dextre.

Conclusions

L'étude géologique du bassin d'Atacama montre que la déformation compressive dans les Andes Centrales a commencé depuis le début du Crétacé Supérieur. La compression dans

l'arrière arc Crétacé Supérieur - Paléogène a favorisé l'inversion des bassins d'arrière-arc formés pendant le Jurassique-Crétacé Inférieur et l'accumulation de dépôts syntectoniques dans le bassin d'Atacama. Durant le Paléogène s'est produit un important soulèvement de la Cordillère de Domeyko associé a des rotations horaires dans la Cordillère de Domeyko et la Vallée Centrale de la région d'Antofagasta. Les données paléomagnétiques obtenues montrent des rotations horaires systématiques jusqu'à 65º dont la magnitude est indépendante de l'âge des séries étudiées. Notre étude suggère qu'une importante zone de cisaillement transpressif dextre d'orientation NE-NNE a contrôlé l'ampleur des rotations à l´est d'Antofagasta. La relation apparente entre les rotations tectoniques et l'orientation des structures (failles) régionaux suggère que les rotations se sont probablement produite dû a des différences dans la quantité de raccourcissement EW le long de la marge chilienne pendant la phase Incaïque a l'Éocène - Oligocène Inférieur. La large distribution de ces rotations dans le Nord du Chili implique que la déformation Incaïque est un événement tectonique d'importance régionale et non seulement local, lié à la déformation dans la Cordillère de Domeyko.

Les modèles de restauration en carte de l'Orocline Bolivien sont cohérents avec des études récentes qui montrent que durant l'Oligocène la déformation était concentré dans la Cordillère Orientale et montre que les rotations observées dans la marge ne peuvent pas s'expliquer en considérant seulement la déformation Miocène qui affecte surtout la Zone Subandine. La courbure oroclinale implique une rotation globale horaire de l'avant arc du nord du Chili de 10-20º mais la plus grande quantité des rotations observées dans l'avant arc du nord du Chili par rapport au Pérou peut être expliquée comme la somme de une composante associée a la tectonique locale du Paléogène et une rotation globale de toute la marge pendant l'Oligocène. En conclusion, le raccourcissement pré Néogène est sans doute significatif dans l'avant arc et doit être pris en compte dans les modèles tectoniques qui essayent d'expliquer l'actuelle épaisseur de la croûte continentale des Andes Centrales.

Références bibliographiques

Allmendinger, R. W., Jordan, T. E., Kay, S. M., Isacks, B.L., 1997. The evolution of the Altiplano-Puna Plateau of the Central Andes. An. Rev. Earth Planet. Sci. 25, 139-174.
Allmendinger, R. W., Ramos, V., Jordan, T., Palma, M., Isacks, B. 1983. Paleogeography and Andean structural geometry, northwest Argentina. Tectonics, v.2, p.1-16.
Ambrus, J. 1979. Emplazamiento y Mineralización de los Pórfidos Cupríferos de Chile. Ph.D. thesis, Universidad de Salamanca, Spain, 3149.
Andriessen, P. A. M and K-J. Reutter. 1994. K-Ar and fission track mineral age determinations of igneous rocks related to multiple magmatic arc systems along the 23ºS Latitude of Chile and Argentina. In Tectonics of the Southern Central Andes. (Reutter, K-J.; Scheuber, E.; Wigger, P,; editors). Springer-Verlag, p. 141-154. Berlin.
Arriagada, C. 1999. Geología y Paleomagnetismo del Borde Occidental del Salar de Atacama. M.Sc. Thesis, University Chile, Dep. Geol., Santiago.
Arriagada, C., Cobbold, P., Mpodozis, C., Roperch, P. 2002. Cretaceous to Paleogene compressional tectonics during deposition of the Purilactis Group, Salar de Atacama. Fifth International Symposium on Andean Geodynamics, Toulouse, Extended abstracts, Ed. IRD.
Arriagada, C., P. Roperch, and C. Mpodozis. 2000. Clockwise block rotations along the eastern border of the Cordillera de Domeyko, northern Chile, Tectonophysics, 326, 153-171.
Arriagada, C., Roperch, P., Mpodozis, C., Dupont-Nivet, G., Cobbold, P.R., Chauvin, A., Cortés, J. 2003. Paleogene clockwise tectonic rotations in the fore-arc of Central Andes, Antofagasta Region, Northern Chile. Journal of Geophysical Research.
Aspden, J.A., McCourt, W.J. 1986Mesozoic oceanic terrane in the Central Andes of Colombia. Geology, 14, 415-418.
Astini, R.A., Benedetto, J.L., Vaccari, N-E., 1995. The Early Paleozoic evolution of the Argentine Precordillera as a Laurentian rifted, drifted, and collided terrane: a geodynamic model. Geological Society of America Bulletin 107, 253-273.
Audibert, M. 1991. Déformation Discontinue et Rotations de Blocs, Méthodes Numériques de Restauration, Mém. Doc. Cent. Armoricain Etud. Struc. Socles, vol, 40, 239 pp., Géosci, Rennes, Rennes, France.
Babeyko, A.; Sobolev, S.; Trumbull, R.; Oncken, O.; lavier, L. 2002. Numerical models of curstal scale convection and partial melting beneath the Altiplano – Puna plateau. Earth and Planetary Sciences Letters, V 199, p. 373 – 388.
Baby, P., Guillier, B., Oller, J., Montemurro, G. 1993. Modèle cinématique de la zone Subandine du Coude de Santa Cruz (entre 16ºS and 19º S. Bolivie) déduit de la construction de cartes équilibrées C. R. Acad Sci., Ser. II, 317, 1477-1483.
Baby, P., P. Rochat, G. Hérail, G. Mascle, and A. Paul, 1996. Neogene thrust geometry and crustal balancing in the northern and southern branches of the Bolivian orocline (Central Andes), paper presented at 3rd International Symposium on Andean Geodynamics, St. Malo, France.
Baby, P., P. Rochat, G. Mascle, and G. Herail, 1997. Neogene shortening contribution to crustal thickening in the back arc of the central Andes, Geology, 25, 883–886.
Baeza, L. and Pichowiak, S. 1988. Ancient crystalline basement provinces in the North Chilean Central Andes - relics of continental crust development since the Mid-Proterozoic. In: Bahlburg, H., Breitlcreuz, C. and Giese, P. (eds.): The Southern Central Andes, Lecture Notes in Earth Sciences, 17: 3-24.
Bahlburg, H., Hervé, F., 1997. Geodynamic evolution and tectonostratigraphic terranes of northwestern Argentina and Northern Chile. Geological Society of America Bulletin 109, 869-884.
Barazangi, M. and Isacks, B. L. 1979. Subduction of the Nazca plate beneath Peru: evidence from spatial distribution of earthquakes. Geophys, J. R. Astron. Soc. 57, 537-55.
Barazangi, M., and B. Isacks, Spatial distribution of earthquakes and subduction of the Nazca plate beneath South America, Geology, 4, 686-692, 1977.
Barr, D. 1985. 3-D Palinspastic restoration of normal faults in the Inner Moray Firth: implications for extensional basin development. Earth Planet. Sci. Lett., 75, 191-203.
Beck, M.E., Burmester, R.R., Drake, R.E., and Riley, P.D., 1994. A tale of two continentes: Some tectonic contrasts between the central Andes and the North American Cordillera, as illustrated by their paleomagnetic signatures, Tectonics, 13, 215-224.
Beck, M.E., Jr., 1988. Analysis of Late Jurassic-Recent paleomagnetic data from active plate margins of South America, Journal of South American Earth Sciences., 1, 39-52.
Beck, S., Zandt, G., Myers, S., Wallace, T., Silver., R., Drake, L. 1996. Crustal-thckness variations in the central Andes. Geology 24, 407-410.
Bevis, M., and B. L. Isacks. 1984. Hypocentral trend surface analysis: Probing the geometry of Benioff zones, J. Geophys. Res., 89, 6153-6170
Bevis, M., E. Kendrick, R. Smalley, T. Herring, J. Godoy, and F. Galban. 1999. Crustal motion north and south of the Arica deflection: Comparing recent geodetic results from the Central Andes, Geochem. Geophys. Geosyst., 1.

Bevis, M.; Kendrick, E.; Smalley Jr, R.; Brooks, B. A.; Allmendinger, R. W.; Isacks, B. L. 2001. On the strength of interplate coupling and the rate of back arc convergence in the central Andes: An analysis of the interseismic velocity field. Geochem. Geophys. Geosyst., 2, 2001GC000198.
Bogdanic, T. 1990. Kontinentale sedimentation der Kreide und des Alttertiärs im Umfeld des subduktionsbedingten magmatismus in der chilenischen Präkordillere. Berliner Geowiss. Abh. A123, pp. 117.
Boric, R., F. Diaz, and V. Maksaev. 1990. Geologia y yacimientos metaliferos de la region de Antofogasta, Bol. Inst. Invest. Geol. Chile, (40), 246 p.; 2.
Bourgeous, O., Cobbold, P.R., Rouby, D., Thomas, J.C., 1997. Least squares restaration of Tertiary thrust sheets in map view, Tadjik depression, Central Asia. Journal of Geophysical Research 102, 27553-27573.
Braun, J., Beauont, C. 1995. Three-dimensional numerical experiments of strain partitioning at oblique plate boundaries : Implications for contrasting tectonic styles in the southern Coast ranges, California, and the central South Island, New Zealand, Jounal of Geophysical Research, 100, p. 18,059-18,074.
Breitkreuz, C., and W. Zeil, 1994. The late Carboniferous to Triassic volcanic belt in northern Chile, in Tectonics of the Southern Central Andes, edited by K.-J. Reutter, E. Scheuber, and P. Wigger, pp. 277–292, Springer-Verlag, New York.
Breitkreuz, C., Bahlburg, H., Delakowitz, B., Pichowiak, S. 1989. Volcanic events in the Paleozoic Central Andes. Journal of South American Earth Sciences 2, 171-189.
Burbridge, D. Braun, J. 1998. Analogue models of convergent continental plate boundaries. Journal of Geophysical Research, 103, p. 15.221-15.237.
Butler, R.F., D.R. Richards, T. Sempere, and L.G. Marshall. 1995. Paleomagnetic determinations of vertical-axis tectonic rotations from Late Cretaceous and Paleocene strata of Bolivia, Geology, 23, 799-802.
Cahill, T; Isacks, B. 1992. Seismicity and shape of the subducted Nazca plate. Journal of Geophysical Research, Vol 97, No B12, p. 17503 - 17529.
Carey, S.W. 1958. A tectonic approach to continental drift, in Continental drift. A symposium., edited by S.W. Carey, pp. 177-355, Hobart, Tasmania
Charrier, R. and Reutter, K.J. 1994. The Purilactis Group of Northern Chile: Boundary between Arc and Backarc from Late Cretaceous to Eocene. in Tectonics of the Southern Central Andes edited by K.-J. Reutter, E. Scheuber, and P. Wigger, pp. 277–292, Springer-Verlag, New York, pp. 189-202.
Charrier, R., Chavez, A., Elgueta, S., Herail, G., Flynn, J., Croft, D., Wyss A. and Garcia M., 2002. Rapid tectonic and paleogeographic evolution: the Chucal anticline, altiplano of Arica, northern Chile Proc. V. ORSTOM ISAG Toulouse, pp. 137-140.
Chong, G. 1977. Contributions to the knowledge of the Domeyko Range in the Andes of northern Chile. Geologische Rundschau 66, 374-404.
Chong, G., and K.J. Reutter. 1985. Fenómenos de tectónica compresiva en las Sierras de Varas y de Argomedo, Precordillera Chilena, en ámbito del Paralelo 25º sur, IV Congreso Geológico Chileno, Actas, 2, 219-238.
Cobbold, P.R. Pearcevault, M.N. 1983. Spatial integration of strain using finite elements. In: S.H. Treagus, P.R. Cobbold and W.M. Schwerdtner (Editors), Strain Patterns in Rocks. J. Struct. Geol., 5: 299-305.
Coira, B., J. Davidson, C. Mpodozis, and V.A. Ramos, 1982. Tectonic and magmatic evolution of the Andes of northern Argentina and Chile, Earth Sci. Rev., 18, 303-332.
Cornejo, P., R. Tosdal, C. Mpodozis, A.J. Tomlinson, O. Rivera, and Fanning. 1997. El salvador Porphyry Copper revisited: Geologic and geochronologic Framework, International Geology Review, 39, 22-54.
Cortés, J., Hoja Palestina, 2000. Región de Antofagasta., Serv. Nac. Geol. Min., Santiago.
Coutand, I., Cobbold, P.R., de Urreiztieta, M., Gautier, P., Chuvin, A., Gapais, D., Rossello, E., and O.L., Gamundi. 2001. Style and history of Andean deformation, Puna plateau, northwestern Argentina. Tectonics, Vol. 20, 2,pp. 210-234.
Coutand, I., P. Roperch, A. Chauvin, P.R. Cobbold, and P. Gautier. 1999. Vertical axis rotations across the Puna plateau (northwestern Argentina) from paleomagnetic analysis of Cretaceous and Cenozoic rocks, J. Geophys. Res., 104, 22,965-22,984
Cross, T. A., and Pilger, R. H. 1982. Controls of subduction geometry, location of magmatic arcs, and tectonics of arc and back-arc regions. Bull. Geol. Soc. Am. 93, 545-62.
Dahlstrom, C. 1969. Balanced cross-section. Can. J. Earth Sci., 6: 743-757.
Dalziel, I.W.D., 1997. Neoproterozoic-Paleozoic geography and tectonics: review, hypothesis, environmental speculation. Geological Society of America Bulletin 109, 16-42.
Dalziel, I.W.D., Dalla Salda, L.H., Gahagan, L.M., 1994. Paleozoic Laurentia-Gondwana interaction and the origin of the Appalachian-Andean mountain system. Geological Society of America Bulletin 106, 243-252.
Damm, K.-W. and Pichowiak, S. 1981. Geodynamik und Magmengenese in der Küstenkordillere Nordchiles zwischen Taltal und Chañaral. Geotektonische Forschungen, 61: 1-166.
Damm, K.W., Harmon, R.S., Kelley, S. 1994. Some isotope and geochemical constraints on the origin and evolution of the Central Andean basement (19º-24ºS). In: Reutter, K.J., Scheuber, E., Wigger, P.J. (Eds.). Tectonics of the Southern Central Andes. Springer, Heidelberg, Germany, pp. 263-275.

Damm, K.W., Pichowiak, S., Harmon, R.S., Todt, W., Kelley, S., Omarini, R., Niemeyer, H. 1990. Pre-Mesozoic evolution of the Central Andes: the basement revisited. Geological Society of America Special Paper 241, 101-126.
Damm, K.-W., S. Pichowiak, C. Breitkreuz, R. S. Harmon, W. Todt, and M. Buchelt. 1991. The Cordon de Lila Complex, central Andes, northern Chile: An Ordovician continental volcanic province, in Andean Magmatism and Its Tectonic Setting, edited by R. S. Harmon and C. W. Rapela, Geol. Soc. Am. Spec. Pap, 265, 1–309.
Delouis, B., Philip, H., Dorbath, L. and Cisternas, A. 1998. Recent crustal deformation in the Antofagasta region (northern Chile) and the subduction process, Geophys. J. Int., 132, 302-338.
DeMets, C., R. G. Gordon, D. F. Argus, and S. Stein. 1994. Effect of recent revisions to the geomagnetic reversal time scale on estimates of current plate motions, Geophys. Res. Lett., 21, 2191–2194
Diaz, M., Cordani, U.G., Kawashita, K., Baeza, L., Venegas, R., Herve, F. and Munizaga, F. 1985. Preliminary radiometric ages from the Mejillones Peninsula, Northern Chile. Comunicaciones, 35..59-67. Santiago.
Dilles, J.H., A.J. Tomlinson, M. Martin, and N. Blanco. 1997. El Abra and Fortuna Complexes: A porphyry copper batholith sinistrally displaced by the Falla Oeste., in VIII Congr. Geológico Chileno, vol. 3, pp. 1883-1887, Antofagasta.
Dingman, R.J., 1963. Cuadrángulo Tulor. Inst. Invest. Geol. Carta Geol. Chile 11 (1:50 000).
Dokka, R. K., Travis, C. J. 1990. Late Cenozoic strike slip faulting in the Mojave Desert, California, Tectonics, 9, 311-340.
Dunn, J.F., Hartshorn, K.G., Hartshorn, P.W. 1995. Structural styles and hydrocarbon potencial of the Subandean thrust belt of southern Bolivia, in Petroleum Basins of South America, edited by A.J. Tankard, R. Suarez, and H.J. Welsink, AAPG Mem., 62, 523-543.
Ferraris, F. and Di Biase, F. 1978. Hoja Antofagasta, Carta geol. Chile, 1:250.000, Inst. Invest. Geol., Santiago.
Flint, S., P. Turner, E. J. Jolley, and A. J. Hartley. 1993. Extensional tectonics in convergent margin basins: An example from the Salar de Atacama, Chilean Andes, Geol. Soc. Am. Bull., 105, 603–617.
Forsythe, R., and L. Chisholm. 1994. Paleomagnetic and Structural Constraints on Rotations in the North Chilean Coast Ranges, J. S. Am. Earth Sci., 7, 279-294
Gansser, A. 1973. Facts and theories on the Andes. Journal geological Society London, 129, 93-131.
García, M.; Hérail, G.; Charrier, R. 1999. Age and structure of the Oxaya Anticline, a major feature of the Miocene
García, M.; Herail, G.; Charrier, R.; Mascle, G.; Fornari, M.; Perez de Arce, C. 2002. Oligocene – Neogene tectonic evolution of northern Chile (18° - 19°S). In Fifth International Symposium of Andean Geodynamics, Toulusse, France, p. 235 – 237.
Gephart, J., 1994. Topography and subduction geometry in the central Andes: Clues to the mechanics of a non collisional orogen, J. Geophys. Res., 99, 12279-12288.
Gibbs, A. 1983. Balanced cross-section construction from seismic sections in areas of extensional tectonics. J. Struct. Geol., 5: 153-160.
Götze, H-J., Krause, S. 2002. The Central Andean gravity high, a relic of an old subduction complex?. Journal of South American Earth Sciences 14, 799 – 811.
Götze, H-J., Lahmeyer, B., Schmidt, S., Strunk, S. 1994. The lithospheric structure of the Central Andes (20°-26°S) as inferred from interpretation of regional gravity. In Tectonics of the Southern Central Andes, Reutter, K., Scheuber, E., Wigger, P. (Eds), Springer-Verlag, Berlin, Germany.
Götze, H-J.; Kirchner, A. 1997. Interpretation of Gravity and Geoid in the Central Andes between 20° and 29°S. Journal of South American Earth Sciences, V10, No 2, p. 179 – 188.
Gratier, J.P. Guillier, B. 1993. Compatibility constraints on folded and faulted strata and calculation of total desplacement using computational restaration (UNFOLD program). J. Struct. Geol., 15. 391-402.
Gratier, J.P., Guillier, B., Delorme, A., Odonne, F. 1991. Restoration and balance of a folded and faulted surface by best-fitting of finite elements: principle and applications. J. Struc. Geol., 13: 111-115.
Grier, M.E., J.A. Salfity, and R.W. 1991. Allmendinger, Andean reactivation of the Cretaceous Salta rift, northwestern Argentina, J. S. Am. Earth Sci., 4, 351-372.
Grocott, J., B. Michael, D.R. David, T.G. K, and T.P. J. 1994. Mechanisms of continental growth in extensional arcs; an example from the Andean plate-boundary zone, Geol. Boulder, 22, 391-394.
Gubbels, T., B. Isacks, and E. Farrar, High-level surfaces, plateau uplift, and foreland development, Bolivian Central Andes, Geology, 21, 695-698, 1993.
Guillier, B. 1991. Dépliage automatique de strates plissées et faillées: Application à l'équilibrage de structures naturelles, Ph.D. thesis, Univ. Grenoble, Grenoble, France.
Gutscher, M., Spakman, W., Bijwaard, H., Engdahl, E. 2000. Geodynamics of flat subduction: Seismicity and tomographic constraints from the Andean margin. Tectonics, V. 19, 5. 814-833.
Hammerschmidt, K., Döbel, R., Friedrichsen, H. 1992. Implication of 40Ar/39Ar dating of Tertiary volcanics rocks from the north-Chilean Precordillera. Tectonophysics 202, 55–81.

Harley, A.J., Flint, S., Turner, P., Jolley, E. J. 1992. Tectonic controls on the development of a semiarid, alluvial basin as reflected in the Stratigraphy of the Purilactis Group (upper Cretaceous-Eocene), northern Chile. J. S. Am. Earth Sci. 5, 275-296.
Hartley, A.J. and Jolley, E.J. 1995. Tectonic implications of Late Cenozoic sedimentation from the Coastal Cordillera of northern Chile (22–24°S). Journal of the Geological Society, vol. 152, no. 1, pp. 51-63(13).
Hartley, A.J., Jolley, E. J., Turner, P. 1992. Paleomagnetic evidence for rotation in the Precordillera of northern Chile: structural constraints and implications for the evolution of the Andean fore-arc. Tectonophysics 205, 49-64.
Heki, K., Y. Hamano, H. Kinoshita, A. Taira, and M. Kono. 1984. Paleomagnetic study of Cretaceous rocks of Peru, South America: evidence for rotations of the Andes, Tectonophysics, 108, 267-281
Heki, K., Y. Hamano, M. Kono, and U. Tadahide. 1985. Palaeomagnetism of Neogene Ocros dyke swarm, the Peruvian Andes: implication for the Bolivian orocline, Geophys. J. R. Astron. Soc., 80, 527-534
Hérail, G., Baby, P., López, M, Oller, J., López, O., Salinas, R., Sempere, T., Beccar, G., Toledo, H. 1990. Structure and kinematic evolution Subandean thrust system of Bolivia, paper presented at International Symposium on Andean Geodynamics, ORSTOM, Paris.
Hervé, M. 1987. Movimiento sinistral en el Cretácico Inferior de la Zona de Falla de Atacama, Chile., Rev. Geol. Chile, 31, 37-42.
Hervé, M. and Marinovic, N. 1989. Geocronología y evolución del batolito Vicuña Mackena, Cordillera del la Costa, Sur de Antofagasta (24-25 deg. S). Revista Geológica de Chile, 16: 31-49.
Horton, B.K., DeCelles, P.G. 1997. The modern foreland basin system adjacent to the Central Andes. Geology 25, 895-898.
Hossack, J.R. 1979. The use of balanced cross sections in the calculation of orogenic contraction, a review. J. Geol. Soc. London, 136, 705-711.
Husson, L., Sempere, T. In press. Thickening the Altiplano crust by gravity-driven crustal channel flow. Geophysical Research Letters.
Isacks, B. 1988. Uplift of the Central Andes plateau and bending of the Bolivian Orocline. Jour. Geophys. Res., Vol 93, p. 3211 – 3231.
J. Chmielowski, G. Zandt and C. Haberland. 1999. The Central Andean Altiplano-Puna magma body. Geophys. Res. Lett. 26, pp. 783 786.
Jaillard, E. Soler, P. 1996. The Cretaceous to Early Paleogene tectonic evolution of the northern Central Andes and its relations to geodynamidcs. Tectonophysics, 259, 41-53.
James, D. 1971. Andean Crustal and Upper Mantle Structure, J. Geophys. Res, 76/14
Jolley, E. J., P. Turner, G. D. Williams, A. J. Hartley, and S. Flint. 1990. Sedimentological response of an alluvial system of Neogene thrust tectonics, Atacama Desert, northern Chile, J. Geol. Soc. London, 147, 769–784.
Jordan, T., B. Isacks, R. Allmendinger, J. Brewer, V. Ramos, and C. Ando. 1983. Andean tectonics related to geometry of the subducted Nazca plate, Geol. Soc. Am. Bull., 94, 341-361, 1983.
Kerr, H., White, N. 1996. Application of an inverse method for calculating three dimensional fault geometries and slip vectors, Nun River field, Nigeria. American Association of Petroleum Geologist Bulletin 80, 432-444.
Kind, R. et al. 1996. Evidence from earthquake data for a partially molten crustal layer in southern Tibet.
Kley, J. 1996. Transition from basement involved to thin-skinned thrusting in the Cordillera Oriental of southern Bolivia, Tectonics, 15, 763-775.
Kley, J. 1999. Geologic and geometric constraints on a kinematic model of the Bolivian orocline. J. South Am. Earth Sci. 12, 221-235.
Kley, J., and C. Monaldi. 1998. Tectonic shortening and crustal thickening in the Central Andes: How good is the correlation?, Geology, 26, 723-726.
Kley, J., Müller, J., Tawackoli, S., Jacobshagen, V., Manutsoglu, E. 1997. Pre-Andean and Andean age deformation in the Eastern Cordillera of southern Bolivia, J. S. Am. Earth Sci., 10, 1-19.
Kley, J; Monaldi, C; Salfity, J. 1999. Along-strike segmentation of the Andean foreland; causes and consequences. Tectonophysics, Vol 301, p. 75 - 94.
Klotz, J.; Khazaradze, G.; Angermann, D.; Reigber, R.; Perdomo, R.; Cifuentes, O. 2001. Earthquake cycle dominates contemporary crustal deformation in the Central and southern Andes. Earth and Planet. Sci. Lett. V 193, p. 437 – 446.
Kono, M., Heki, K., and Hamano, Y. 1985. Paleomagnetic study of the central Andes: Counterclockwise rotation of the Peruvian block, Journal of Geodynamics, 2, 193-209.
Lamb, S. 2000. Active deformation in the Bolivian Andes, South America. Journal Geoph. Res. 105, B11, 25627 – 2653.
Lamb, S. 2001. Vertical axis rotation in the Bolivian orocline, South America 1. Paleomagnetic analysis of Cretaceous and Cenozoic rocks. Journal of Geophysical Research, Vol. 106, n B11, 26.605-26.632.
Lamb, S., Hoke, L., Kennan, L., Dewey, J. 1997. The Cenozoic evolution of the Central Andes in Bolivia and northern Chile, in Orogeny through time, edited by J-P Burg and M. Ford, Geol. Soc., Spec. Publ., 121, 237-264.

Lamb, S.; Hoke, L. 1997. Origin of the high plateau in the Central Andes, Bolivia, South America. Tectonics 16, 623 – 649.
Lindsay, D. 1998. Structural Control and Anisotropy of Mineralization within the Chuquicamata Porphyry Copper Deposit, Northern Chile. Ph.D. thesis, Dalhouse University, Halifax, 381 p.
Lindsay, D., Zentilli, M., Rojas, J. 1995. Évolution of an active ductile to brittle shear system controlling mineralization at the Chuquicamata porphyry copper deposit, northern Chile. International Geology Reviews, 37, p. 945-958.
Lucassen, F., Becchio R., Wilke, H.G., Franz, G., Thirlwall, M.F., Viramonte, J. Wemmer, K. 2000. Proterozoic-Paleozoic development of the basement of the Central Andes (18-26ºS) – a mobile belt of the South American craton. Journal of South American Earth Sciences 13, 697-715.
Lucassen, F., Franz, G., Laber, A. 1999. Permian high pressure rocks the basement of Sierra de Limón Verde in N. Chile. Journal of South American Earth Sciences 12, 183-199.
Macedo Sanchez, O., J. Surmont, C. Kissel, and C. Laj. 1992. New temporal constraints on the rotation of the Peruvian Central Andes obtained from paleomagnetism, Geophys. Res. Lett, 19, 1875-1878; 1.
Macellari, C. E., M. J. Su, and F. Townsend. 1991. Structure and seismic stratigraphy of the Atacama Basin, northern Chile, paper presented at the VI Congreso Geológico Chileno, Vina del Mar.
MacFadden, B.J., F. Anaya, and C.C. Swisher III, 1995. Neogene paleomagnetism and oroclinal bending of the central Andes of Bolivia., J. Geophys. Res., 100, 8153-8167
Maksaev, V. 1979. Las Fases tectónicas Incaica y Quechua en la Cordillera de los Andes del Norte Grande de Chile. Actas, II Congreso Geológico Chileno, 1. p. B63-B77.
Maksaev, V. Zentilli, M. 1988. Marco metalogénico regional de los megadepósitos de tipo pórfido cuprífero del norte de Chile. Actas, 5th Congreso Geológico Chileno, 1, p. B181-B212.
Maksaev, V., and M. Zentilli. 1999. Fission Track Thermochronology of the Domeyko Cordillera, Northern Chile: Implications for Andean Tectonics and Porphyry Copper Metallogenesis, Explor. Mining Geol., 8, 65-89.
Marinovic, N., and M. García. 1999. Hoja Pampa Unión. Región de Antofagasta., Serv. Nac. Geol. Min., Santiago.
May, S.R., and R.F. Butler, 1985. Paleomagnetism of the Puente Piedra Formation, central Peru. , Earth Planet. Sci. Lett., 72, 205-218.
McCoss, A.M. 1988. Restoration of transpression/transtension by generating the three-dimensional segmented helical loci of deformed lines across structure cotours maps. J. Struct. Geol., 10: 109-120.
McKencie, D. Jackson, J. 1986. A block model of distributed deformation by faulting. Journal of the Geological Society of London, 143, p. 349-353.
McQuarrie, N., and DeCelles, P.G. 2001. Geometry and Structural Evolution of the Central Andean Backthrust Belt, Bolivia. Tectonics 17, 203-220
Miller, H., Toselli, A.J., Rossi de Toselli, J., Aceñolaza, F.G. 1994. Regional and geochronological development of the metamorphic basement in Northwest Argentina. Zentralblatt Geologie Paläontologie 1 (1/2), 263-273.
Mitouard, P., Kissel, C., Laj, C. 1990. Post-Oligocene rotations in southern Ecuador and northern Peru and the formation of the Huancabamba deflection in the Andean Cordillera. Earth Planetary Science Letters, 98, 329-339.
Mpodozis, C., and V.A. Ramos. 1990. The Andes of Chile and Argentina, in Geology of the Andes and Its Relation to Hydrocarbon and Mineral Resources, edited by G.E. Ericksen, M.T. Cañas Pinochet, and J.A. Reinemud, pp. 59-90, Circum-Pac. Counc. for Energy and Min. Resour., Houston, Tex.
Mpodozis, C., Arriagada, C., Roperch, P. 1999. Cretaceous to Paleogene geology of the Salar de Atacama basin, northern Chile: A reappraisal of the Purilactis Group stratigraphy. Proc. III. (ORSTOM) ISAG Göttingen, pp. 523-526.
Mpodozis, C., N. Marinovic, and I. Smoje. 1993. Eocene left-lateral strike slip faulting and clockwise block rotations in the Cordillera de Domeyko, west of Salar de Atacama, northern Chile, paper presented at Symposium International Géodynamique Andine ISAG 93, Inst. Fr. de Rech. Sci. pour le Dév. en Coop. (ORSTOM), Oxford, UK.
Müller, J. P., Kley, J.; Jacobshagen, 2002. V. Structure and Cenozoic kinematics of the Eastern Cordillera, southern Bolivia (21°S). Tectonics, VOL. 21, NO. 5,
Muñoz, N., Charrier, R. and Pichowiak. S. 1989. Cretácico superior volcánico-sedimentario (Formación Quebrada Mala) en la región de Antofagasta, Chile, y su significado geotectónico. Contrib. Simposios Cretacico de America Latina, A.. Eventos y registro Sedimentario, 113-148, Spalletti Buenos Aires.
Muñoz, N., Charrier, R. y Reutter, J.K. 1997. Evolución de la Cuenca del Salar de Atacama: Inversión tectónica y relleno de una cuenca de antepaís de retroarco. Proc. VIII Congreso Geológico Chileno, 1: pp. 195-199.
Muñoz, N., Charrier, R., y Jordan, T. 2002. Interactions between basement and cover during the evolution of the Salar de Atacama Basin, northern Chile. Rev. geol. Chile, vol.29, no.1, p.55-80.
Nelson, K. D. et al. 1996. Partially molten middle crust beneath southern Tibet: Synthesis of projec INDEPTH results. Science 274, 1684-1688

Niemeyer, H. 1984. La megafalla Tucucaro en el extremo sur del Salar de Atacama: Una antigua zona de cizalle reactivada en el Cenozoico, Comun. Dep. Geol., 34, pp. 37–45, Univ. de Chile, Santiago.
Norambuena, E., Leffer-Griffin, L., Mao, A., Dixon, T., Stein, S., Sacks, S., Ocola, L., Ellis, M. 1998. Space geodetic observations of Nazca-South America convergence across the Central Andes. Science 279, 358-362.
Oncken O.; Luschen E.; Mechie J.; Sobolev S.; Schulze A.; Gaedicke C.; Grunewald S.; Bribach J.; Asch G.; Giese P.; Wigger P.; Schmitz M.; Lueth S.; Scheuber E.; Haberland C.; Rietbrock A.; Gotze H.-J.; Brasse H.; Patzwahl R.; Chong G.; Wilke H.-G.; Gonzalez G.; Jensen A.; Araneda M.; Vieytes H.; Behn G.; Martinez E.; Rossling R.; Amador J.; Ricaldi E.; Chumacero H.; Luterstein R. Seismic reflection image revealing offset of Andean subduction-zone earthquake, Nature, Volume 397, Issue 6717, 28 January 1999, Pages 341-344
Pardo-Casas, F; Molnar, P. 1987. Relative motion of the Nazca (Farallon) and South American plates from Late Cretaceous time. Tectonics, Vol 6, No 3, p. 233 - 248.
Pilger, R. 1984. Cenozoic plate kinematics, subduction and magmatism : South American Andes. Journal of the Geological Society of London, 141, p. 793-802.
Ramírez, C. F., and M. Gardeweg. 1982. Hoja Toconao, Región de Antofagasta-Carta Geológica de Chile, 121 pp., scale 1:250,000, Serv. Nac. de Geol. y Minera de Chile, Santiago.
Ramos, V.A. 1988. Late Proterozoic-Early Paleozoic of South America a collisional history. Episodes 11, 168-174.
Ramos, V.A., 1995. Sudamerica: un mosaico de continentes y oceanos. Ciencia hoy 6 (32), 24-29.
Ramos. V. A., Alemán, A., 2000. Tectonic Evolution of the Andes. Tectonic Evolution of South America. 31th Int. Geol. Cong. (Rio de Janeiro), 635-685.
Randall, D., A. Tomlinson, and G. Taylor, 2001. Paleomagnetically defined rotations from the Precordillera of northern Chile: Evidence of localized in situ fault-controlled rotations, Tectonics, 20, 235–254.
Randall, D.E., and G.K. Taylor, 1996. Major crustal rotations in the Andean margin: Paleomagnetic results from the Coastal Cordillera of northern Chile, J. Geophys. Res., 101, 15,783-15,798.
Rapela, C.W., Toselli, A.J., Heaman, L., Saavedra, J., 1990. Granite plutonism of the Sierras Pampeanas; An inner cordilleran Paleozoic arc in the southern Andes. Geological Society of America Special Paper 241, 77-90.
Reutter, K., Scheuber, E., Helmcke, D. 1991. Structural evidence of origin-parallel strike-slip displacements in the North Chilean Precordillera. Geologishe Rundschau, 80, p. 135-153.
Reutter, K., Chong, G., Scheuber, E. 1993. The West Fissure and the Precordilleran fault System of Northern Chile. Andean Geodynamics, Second International Symposium of Andean Geodynamics 1993, ORSTOM/Oxford University, p. 237-240.
Reutter, K.J., and E. Scheuber. 1988. Relation between tectonics and magmatism in the Andes of northern Chile and adjacent areas between 21° and 25° S, in I Congr. Geol. Chileno, vol. 1, pp. 345-363, Departamento de Geología y Geofisica Universidad de Chile.
Reutter, K.-J., E. Scheuber, and G. Chong. 1996. The Precordilleran fault system of Chuquicamata, northern Chile: Evidence for reversals along arc parallel strike-slip faults, Tectonophysics, 259, 213-228.
Riley, P.D., M.E.J. Beck, R.F. Burmester, C. Mpodozis, and A. García. 1993. Paleomagnetic evidence of vertical axis block rotations from the mesozoic of northern Chile, J. Geophys. Res., 98, 8321-8333.
Rodriguez, W., Baby, P., Ballard, J.F. 2001. Structure et controlôle paléogéographique de la zone subandine péruvienne. C. R. Acad. Sci., Ser. II, 333, 741-748.
Roeder, D. 1988. Andean-age structure of Eastern Cordillera (province of La Paz, Bolivia), Tectonics, 7,23-29.
Roperch, P., and G. Carlier, Paleomagnetism of Mesozoic Rocks From the Central Andes of Southern Peru: Importance of Rotations in the Development of the Bolivian Orocline, J. Geophys. Res., 97, 17233-17249, 1992.
Roperch, P., F. Megard, L.A.J. Carlo, T. Mourier, T.M. Clube, and C. Noblet, 1987. Rotated oceanic blocks in western Ecuador, Geophys. Res. Lett., 14, 558-561; 1.
Roperch, P., G. Herail, and M. Fornari. 1999. Magnetostratigraphy of the Miocene Corque basin, Bolivia: Implications for the geodynamic evolution of the Altiplano during the late Tertiary, J. Geophys. Res., 104, 20415-20429; 3.
Roperch, P., Sempere, T., Arriagada, C., Fornari, M., Macedo-Sanchez, O., Tapia, C. 2002a. New paleomagnetic constraints on the formation of the Bolivian Orocline. EGS XXVII General Assembly, Nice, France, April, EGS02-A-05121;SE2.05-1TU5P-031.
Roperch, P., Sempere, T., Macedo, O., Arriagada, C. and Fornari, M. 2002b. Counterclockwise rotation of the south Peruvian forearc and implications for the formation of the Bolivian orocline. Proc. V. ORSTOM ISAG Toulouse, pp. 545-546.
Roperch, P., Sempere, T., Macedo, O., Arriagada, C., Fornari, M. 2002. Counterclockwise rotation of the southern Peruvian forearc and implications for the formation of the Bolivian orocline. V International Symposium on Andean Geodynamics, Toulusse, France, 545-548.

Roperch, P., Sempere, T., Macedo, O., Arriagada, C., Fornari, M. 2002. Counterclockwise rotation of the southern Peruvian forearc and implications for the formation of the Bolivian orocline. V International Symposium on Andean Geodynamics, Toulusse, France, 545-548.
Roperch, P; M. Fornari, G. Herail, G. Parraguez. 2000. Tectonic rotations within the Bolivian Altiplano: Implications for the geodynamic evolution of the central Andes during the late Tertiary. J. Geophys. Res., 105. 795 – 820.
Rössling, R. 1988. Petrologie in einem tiefen Stockwerk des jurassischen magmatischen Bogens in der nordchilenischen Küstenkordillere südlich von Antofagasta. Berliner Geowiss. Abh., A112, 73 pp.
Rouby, D., Cobbold, P.R., Szatmari, P., Demercian, D., Coelho, D., Rici, J.A., 1993a. Least-squares palinspastic restoration of regions of normal faulting. Application to the Campos basin (Brazil). Tectonophysics 221, 439-452.
Rouby, D., Cobbold, P.R., Szatmari, P., Demercian, S., Coelho, D., Rici, J.A. 1993b. Restoration in plan view of faulted Upper Cretaceous and Oligocene horizons and its bearing on the history of salt tectonics in the Campos Basin (Brazil). Tectonophysics 228, 435-445.
Rouby, D., Fossen, H., Cobbold, P.R. 1996. Extension, displacement and block rotation in the Larger Gullfakc area, northern north Sea: Determined from map view restoration, AAPG Bull., 80, 875-890.
Rouby, D., Suppe, J., Xiao, H., 2000. 3-D restoration of complexly faulted and folded surfaces using multiple unfolding mechanisms. American Association of Petroleum Geologist Bulletin 84, 805-829.
Rousse, S., Gilder, S., Farber, D., Brendan, Mc., Torres, V. 2002. Paleomagnetic evidence for rapid vertical-axis rotation in the Peruvian Cordillera ca. 8 Ma. Geology, v.30; 1; pp 75- 78.
Rutland, R. 1971. Andean orogeny and sea floor spreading. Nature. 233: 252-255.
Saint Blanquet, M., Tikoff, B., Teyssier, C. Vigneresse, J. 1998. Transpressional kinematics and magmatic arcs. In Continental Transpression and Transtenssional tectonics. Edited by R. Holdsworth, R. Strachan and J. Dewey. Geological society of london, special publication, 135, p. 327-340.
Samson, P. 1996. Equilibrage de structures géologiques 3-D dans le cadre du projet GOCAD. Ph.D. thesis, Institut National Polytechnique de Lorraine.
Scheuber, E., Bogdanic, T., Jensen, A. Reutter, K. 1994. Tectonic development of the North Chilean Andes in relation to plate convergence and magmatic since the Jurassic. In tectonics of the Southern Central Andes : Structure and Évolution of an Active Continental Margin. Edited by K-J. Reutter, E. Scheuber and P. Wigger. Springer-Verlag, Berlin, p. 121-139.
Scheuber, E., and G. González. 1999. Tectonics of the Jurassic-Early Cretaceous magmatic arc of the north Chilean Coastal Cordillera (22º-26ºS): A story of crustal deformation along a convergent plata boundary, Tectonics, 18, 895-910.
Scheuber, E., and K.-J. Reutter. 1992. Magmatic arc tectonics in the central Andes between 21° and 25°, Tectonophysics, 205, 127–140.
Scheuber, E., and P.A.M. Andriessen. 1990. The kinematic and geodynamic significance of the Atacama fault zone, northern Chile. , J. Struc. Geol., 12, 243-257.
Schmitz, M., 1994 A balanced model of the southern central Andes, Tectonics, 13, 484–492,
Schmitz, M., Heinsohn, W-D., Schilling, F., 1997. Seismic, gravity and petrological indications for partial melting beneath the thickened Central Andean crust 21º-23ºS. Tectonophysics 270, 313-326.
Schultz-Ela, D. 1988. Application of a three-dimensional finite-element method to strain field analyses. J. Struct. Geol., 10: 263-272.
Schultz-Ela, D. 1992. Restoration of cross-sections to constrain deformation processes of extensional terranes. Mar. Pet. Geol., 9: 372-388.
Schwerdtner, W. 1977. Geometric interpretation of regional strain analyses. Tectonophysics, 39: 515-531.
Science 274, 1692-1694.
Sempere, T., Butler, R.F., Richards, D.R., Marshal, L.G., Sharp, W., Swisher, C.C., 1997. Stratigraphy and chronology of late Cretaceous-early Paleogene strata in Bolivia and northern Argentina. Geol. Soc. Am. Bull. 109, 709-727.
Sempere, T., Hérail, G., Oller, J., Bonhomme, M.G., 1990. Late Oligocene-early Miocene major tectonic crisis and related basins in Bolivia. Geology 18, 946-949.
Sheffels, B. M. 1990 Lower bound on the amount of crustal shortening in the central Bolivian Andes, Geology, 18, 812–815,
Sheffels, B.M. 1988. Structural constraints on structural shortening in the Bolivian Andes, Ph. D. thesis, 167 pp., Mass Inst. Of Technol., Cambridge.
Somoza, R., 1998 Updated Nazca (Farallon) - South America relative motions during the last 40 My: Implications for mountain building in the central Andean region, J. South Am. Earth Sci., 11, 211-215,.
Somoza, R., and A. Tomlinson, 2002 Paleomagnetism in the Precordillera of northern Chile (22°30S): implications for the history of tectonic rotations in the Central Andes, Earth Planet. Sci. Lett., 94, 369–381
Somoza, R., S. Singer, and A. Tomlinson, 1999 Paleomagnetic study of upper Miocene rocks from northern Chile: Implications for the origin of late Miocene–Recent tectonic rotations in the southern central Andes, J. Geophys. Res., 104, 22,923–22,936,.
Steinmamm, G., 1929. Geologie von Peru, 448 pp., C. Winters, Heidelberg, Germany.

Suarez, M., Bell, C.M. 1992. Triassic rift related sedimentary basins in northern Chile (24-29 S). Journal of South American Earth Sciences 6, 109-121.
Tanaka, H., H. Tsunakawa, and K. Amano, Palaeomagnetism of the cretaceous El Way and Coloso Formations from the northern Chilean Andes, Geophys. J. Roy. Astr. Soc., 95, 195-203, 1988.
Tassara, A. 2002. Nazca-south America interaction: Review of a 2D flexural analysis along the central Andean Forearc. Proc. V. ORSTOM ISAG Toulouse, pp. 625-628.
Taylor, G. K., Groccot, J., Pope, A., and Randall, D.E., 1998. Mesozoic fault systems, deformation and fault block rotation in the Andean forearc: A crustal scale strike-slip duplex in the Coastal Cordillera of northern Chile, Tectonophysics, 299, 93-109.
Taylor, G.K., Grocott, J., Gipson, M.J., 2001. Vertical Axes Rotations in Northern Chile in Relation to Deformation. Eos Trans. AGU, Fall Meet. Suppl., Abstract 82(47).
Thorpe, R. S., Francis, P. W., and Harmon, R. S. 1981. Andean andesites and crustal growth. Phil Trans R. Soc. Lond. A301, 305-20.
Tikoff, B. Teyssier, C. 1994. Strain modelling of displacement field partioning in transpressional orogens. Journal of Structural Geology, 16, p. 1575-1588.
Tomlinson, A., and N. Blanco. 1997a. Structural evolution and displacement history of the West Fault System, Precordillera, Chile: Part 1, synmineral history., in VIII Congr. Geol. Chileno, vol. 3, pp. 1873-1877, Antofagasta.
Tomlinson, A., and N. Blanco. 1997b. Structural evolution and displacement history of the West Fault System, Precordillera, Chile: Part 2, postmineral history., in VIII Congr. Geol. Chileno, vol. 3, pp. 1878-1882, Antofagasta.
Tomlinson, A., C. Mpodozis, P. Cornejo, C.F. Ramírez, and T. Dumitri. 1994. El sistema de Fallas Sierra de Castillo-Agua Amarga: transpresión sinistral eocena en la precordillera de Potrerillos-El Salvador, in VII Congr. Geol. Chileno, vol. II, pp. 1459-1463, Concepción.
Tosdal, R.M. 1996. The Amazon-Laurentian connection as viewed from the Middle Proterozoic rocks in the Central Andes, western Peru and Northern Chile. Tectonics 15, 827-842.
Unrug, R., 1996. The assembly of Gondwanaland. Episodes 19, 11-20.
Urreiztieta, M. de, Gapais, D., Le Corre, C., Cobbold, P.R., Rossello, E., 1996. Cenozoic dextral transpression and basin development at the southern edge of the Puna Plateau, northwes-tern Argentina. Tectonophysics 254, 17±39.
Van Thournout, F., Hertogen, J. and Quebedo, L. 1992. Allochtonous terranes in northwestern Ecuador. Tectonophysics, 205, 205-221.
Viramonte, J.G., Becchio, R., Coira, B., Aramayo, C., Omarini, R., Garcia Cacho, A. 1993. Aspectos petrológicos y geoquímicos del basamento preordovícico del borde oriental de la Puna Austral, Argentina. XII Congreso Geológico Argentino, Actas 4, pp. 307-318.
Von Huene, R., Ranero, C. 2003. Subduction erosion and basal friction along the sediment-starved convergent margin off Antofagasta, Chile. J. Geophys. Res. V. 108, B2.
Wasteneys, H.A., Clark, A.H., Farrar, E., Lagridge, R.J. 1995. Grenvillian granulite-facies metamorphism in the Arequipa Massif, Peru: a Laurentia-Gondwana link. Earth and Planetary Science Letters 132, 63-73.
Wdowinski, S., R. O'Connell, and P. England, A continuum model of continental deformation above subduction zones: Application to the Andes and the Aegean, J. Geophys. Res., 94, 10,331-10,346, 1989.
Wigger, P., M. Schmitz, M. Araneda, G. Asch, S. Baldzuhn, P. Giese, W.D. Heinsohn, E. Martinez, E. Ricaldi, P. 1994. Rower, and J. Viramonte, Variation in the crustal structure of the southern Central Andes deduced from seismic refraction investigations, in *Tectonics of the Southern Central Andes*, edited by K.J. Reutter, E. Scheuber, and P. & Wigger, pp. 23-48, Springer, Berlin.
Wilkes, E. and Görler, K. 1994. Sedimentary and Structural Evolution of the Salar de Atacama Depression. In: Reutter, K.-J., Scheuber, E. & Wigger, P.: Tectonics of the Southern Central Andes. Springer-Verlag Berlin.
Williams, G., Kane, S., Buddin, T., Richards, A. 1997. Restoration and balance of complex folded and faulted rock volumes: flexural flattening, jigsaw fitting and decompaction in 3-D. Tectonophysics 273, 203-218.
Yañez, Gonzalo A. ; Ranero, César R. ; von Huene, Roland ; Díaz, Juan. 2001. Magnetic anomaly interpretation across the southern central Andes (32º - 34ºS): The role of the Juan Fernández Ridge in the late Tertiary evolution of the margin, J. Geophys. Res. Vol. 106 , No. B4
Yuan, X.; Sobolev, S.; Kind, R. 2002. Moho topography in the central Andes and its geodynamic implications. Earth and Planetary Sciences Letters, V 199, p. 389 – 402.
Yuan, X.; Sobolev, S.; Kind, R.; Oncken, O. y 18 more. 2000. Subduction and collision processes in the Central Andes constrained by converted seismic phases. Nature, V 408, 21/28 Diciembre, p. 958 – 961.
Zandt, G.; Velasco, L.; Beck, S. 1994. Composition and thickness of the southern Altiplano crust, Bolivia. Geology, V 22, p. 1003 – 1006.